

产品综述

概述

ABAQUS/CAE 是一个完整的对 ABAQUS 分析任务进行建模、管理、监控,同时又可以对 ABAQUS 分析结果进行可视化后处理的环境。ABAQUS/CAE 的后处理功能也可以构成 ABAQUS 的另一个单独的产品 - ABAQUS/Viewer。

产品目标

- 提供完善的建模和分析解决方案

ABAQUS/CAE 将建模、分析、任务管理、结果后处理等无缝的集成在一起。这些功能分别在不同的模块中实现,在每个模块包括着详细的逻辑子集以实现全部功能。CAE 系统的每个模块的用户交互界面保持相同的风格,新用户非常容易入手。ABAQUS/CAE 使用类似的组合概念,如:分析步,接触,截面,集合,材料,构成直观的图形用户交互界面。

- 完整全面的 CAD 系统以及其他建模工具

ABAQUS/CAE 建模基于零件和装配概念,与流行的 CAD 软件相一致。零件可以在 ABAQUS/CAE 中创建,或从 CAD 中导入几何模型,然后在 CAE 中划分网格。

- 高效率处理大模型

ABAQUS/CAE 的设计越来越多的考虑到应用大模型。

- 包含交互环境,可以用于用户自主开发应用

提高生成率的关键之一是提供特殊用途的 ABAQUS/CAE 的用户接口。ABAQUS 中嵌入 Python 程序语言 (www.python.org),在 ABAQUS/CAE 中作为用户图形交互界面的扩展工具。

特 征

用户界面

ABAQUS/CAE 用户界面由菜单、按钮以及表格构成。ABAQUS/CAE 的设计考虑了新老用户的不同需求。菜单中提供了实现所有功能的选项。按钮则是上述常用功能的快捷方式。

主要的表层构件为：

- **多重视图以及无限大画板**

视图由于显示模型或分析结果，画板是一个无限大的屏幕或者公告板，在这上面用户可以放置视图或者添加注释。几个模型计算得到的结果可以同时处理。视图的背景颜色可以从列表中选择。

- **菜单条**

显示所有可用下拉菜单。

- **工具条和工具箱**

加速实现菜单中的功能

- **文本敏感帮助**

文本敏感帮助可以调用任何用户截面上的帮助内容。

- **帮助菜单**

包含文本敏感帮助和 on-line 的帮助文件。

- **文本工具条**

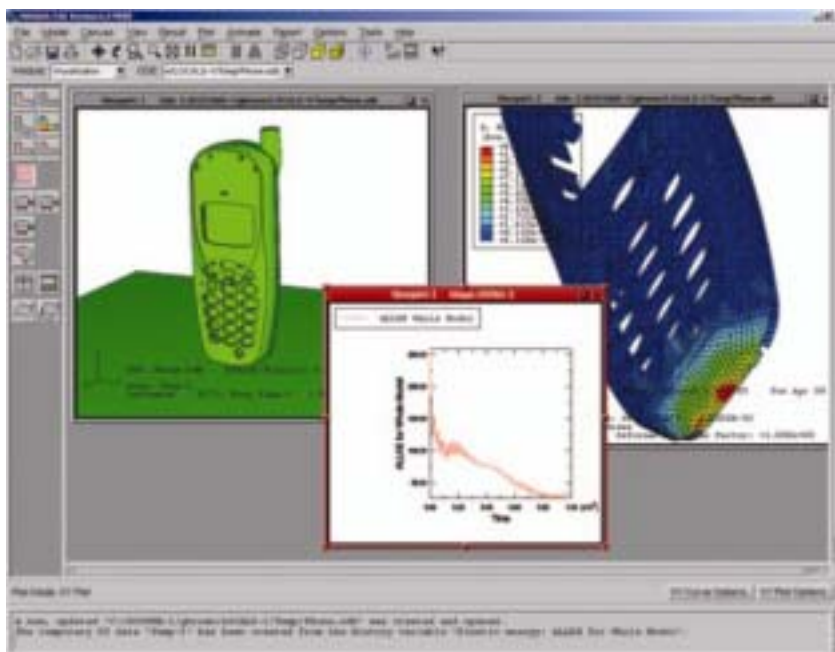
用于指示和改变当前视图中的模型和输出数据库。

- **注释**

文本和箭头可以在画板上任意放置。

- **查询**

提供快速的查询模型信息的工具，如：探针工具。



多重视图和动态操作显示给出分析结果的细节。

ABAQUS/CAE 的模块

视图和显示

模型可以被旋转、拖动和任意地缩放，用户定义的视角可以和标准的视角一起储存在视角工具框中。

模型可以以下列风格显示：

- 填充图
- 线框图（隐藏内部线）
- 阴影
- 线框图

可以同时使用多个视图用不同的显示风格显示模型。而且每一个视图中的模型可以被任意的动态缩放以及放置在显示区的任意方便的位置上。显示区可以根据需要无限的被放大——可以根据用户需要把显示区的大小调节到超过显示器的尺寸。

除“分析任务”模块以外的中的在任何模块中都有显示组工具存在，在与零件和装配有关的模块中，用户可以定义显示的集合，如显示几何结构（如面、边），或者单元集合、节点集合、表面集合等。

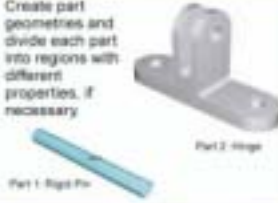




另外规定条件、约束和接触等也可以在 CAE 中显示。

打印

ABAQUS/CAE 可以以 PostScript、PNG 和 TIFF 格式打印图形信息，图像可以直接送至打印机，也可以存储到文件以便拷贝和再次打印。图形可以是彩色的、黑白的、灰度的等形式。用户可以控制图形的分辨率和大小。

模块

CAE 的全部功能被划分到 10 个模块中，每个模块是其功能的一个逻辑子集。用户在模块的下拉菜单中选择并激活模块。

| Part | Property | Assembly |
|---|---|---|
| <ul style="list-style-type: none">• Create part geometries and divide each part into regions with different properties, if necessary.  | <ul style="list-style-type: none">• Define materials.• Define and assign section properties to parts or regions. | <ul style="list-style-type: none">• Position parts in the initial configuration.  |
| Step | Interaction | Load |
| <ul style="list-style-type: none">• Define analysis steps.• Define output requests. | <ul style="list-style-type: none">• Define contact and other interactions on regions or named sets and assign them to steps in the analysis history. | <ul style="list-style-type: none">• Apply loads, BCs, and fields to regions or named sets and assign them to steps in the analysis history.  |
| Mesh | Job | Visualization |
| <ul style="list-style-type: none">• Split parts into meshable regions and mesh them.  | <ul style="list-style-type: none">• Submit analysis jobs to run locally or remotely on another computer on the network.• Monitor and manage analysis jobs. | <ul style="list-style-type: none">• Examine results.  |

特征管理器

特征管理器允许操作和查询所有的模型的特征。同时可以显示这些特征的继承关系（哪个是父特征哪个是子特征）。

几何模型

零件和装配

在 ABAQUS/CAE 中，模型是基于零件和装配的概念，与流行的 CAD 软件一致。零件型可以用下面三种途径得到：

- 从其他模型中导入几何模型
 - 从其他模型中导入模型网格
 - 使用 ABAQUS/CAE 直接创建模型
- 对零件进行装配，即可以创建用于 ABAQUS 的模型。

零件

ABAQUS/CAE 中的零件可以是二维的、轴对称的或者三维的。每个零件可以包括实体、曲面、曲线等特征。零件可以是变形体也可以是刚体。

零件管理器可以显示模型中所有的零件，并且允许对这些零件拷贝、删除、重命名和编辑。同时可以方便的查询零件的材料特性和几何特征（如体积、惯性矩、任意两点距离）。

几何模型的导入和导出

零件可以从其他模型中导入。ABAQUS/CAE 可以对导入的零件加入附加特征,比如开孔、切割等。ABAQUS/CAE 使用 ACIS 三维几何引擎。也就是,导入任何其他基于 ACIS 引擎的几何模型都不会改变模型的精度。

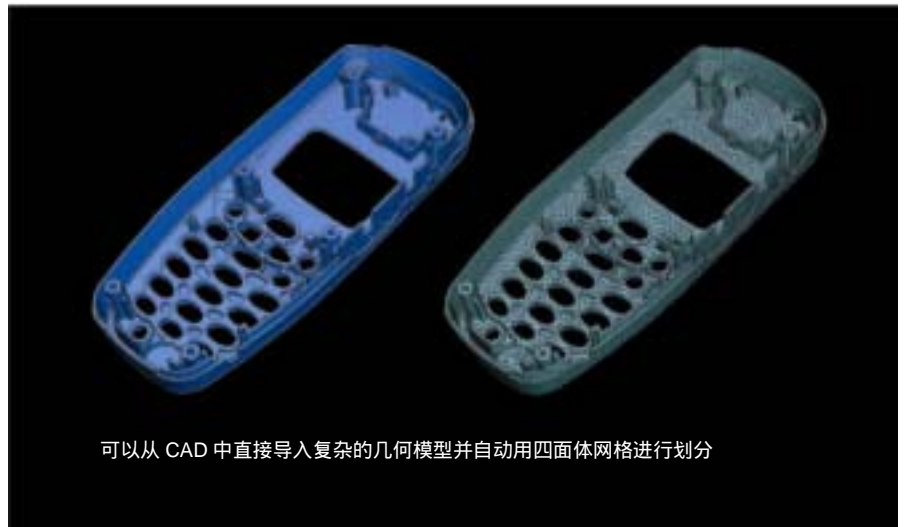
ABAQUS/CAE 支持 SAT, IGES, STEP 和 DXF 格式的二维图形导入,支持 SAT, IGES, STEP 和 VDA-FS 格式的三维图形导入和导出。另外二维的图形可以以 SAT, IGES, STEP 格式导出。

ABAQUS/CAE 提供自动和手动的修复几何模型的工具。自动“修复”功能用于将原始 CAD 模型的容错度和 ABAQUS/CAE 的规定公差调节一致。另外的修复工具用于删除原来模型中的点、线和面,或者添加面或单元到此模型中。诊断工具用于识别过于微小和尖锐的不利于划分网格的结构。

导入网格

零件还可以以有限元网格的形式从 ABAQUS 输入文件和 ABAQUS 输出文件中导入。原模型中的节点集和单元集能同时都被导入,并且可以改变这些节点/单元集的属性,例如材料特性、荷载和边界条件。如果被修改过的网格又被导入,这些修改的节点/单元集的属性都将被保留。

在导入的网格中可以另外定义节点/单元集,同样可以另外定义和修改这些节点/单元集的属性。ABAQUS/CAE 提供了方便的选择导入网格的节点/单元的工具。例如,要选择一个复杂的表面,只需要选择一个单元的表面,CAE 可以自动选择与该表面相邻的表面,直到两个相邻



可以从 CAD 中直接导入复杂的几何模型并自动用四面体网格进行划分

表面的夹角超过用户定义的角度。网格编辑工具可以编辑导入的网格。用户可以删除、创建节点和单元,改变节点坐标,翻转壳单元的法向,可以将一次单元转换成二次单元,反之亦然。

参量化几何模型

零件 (Part) 模块是一个参数化、基于特征的造型系统。他提供的工具可以构建复杂的几何模型。

零件 (Part) 是由特征组成。可以通过修改这些参数特征来改变零件的形状。特征也可以被删除,特征还可以暂时被隐藏,可以根据用户的需求随时恢复。

ABAQUS/CAE 提供下列基本的特征构建零件:

- 切割特征
 - 延伸
 - 旋转
 - 延曲线延伸
 - 圆孔
- 导角特征
 - 圆角
 - 直角

- 立体特征

- 沿平面的法线直线延伸一个二维的图形 (通过定义截面形状实现);
- 绕轴旋转一个二维的图形 (通过定义截面形状实现);
- 二维图形沿曲线运动,扫过轨迹为生成的几何体 (通过定义截面形状实现);

- 表面特征

- 延平面的法线延伸直线或曲线构造表面;
- 绕轴旋转直线或曲线构造表面;
- 直线或曲线沿规定曲线运动,形成表面;
- 选择实体的表面;

- 线特征

- 平面内的直线或曲线;
- 连接两点构造直线;

下面的功能同样可以方便的构造复杂的零件：

- **辅助几何构形**

辅助几何是用来辅助创建或者切割零件的，辅助几何构形不是零件的组成部分。辅助坐标系，辅助轴、辅助点、辅助面可以用多种方法来创建。不同种类的辅助几何构形可以任意的添加和删除。

- **切分工具**

一个零件可以被分割成多个区域。这些区域可以被定义为不同的材料，荷载、边界条件。切分的功能对于划分网格是非常重要的。边、表面、实体都可以用多种方法分割。

绘图器

ABAQUS/CAE 使用平面绘图器来定义二维零件的二维几何构形，定义三维构件的特征，用来切割零件以便方便的划分网格或者定义零件的材料特征。创建草图时，一般先绘制大概的草图形状，标注草图特征，最后修改标注完成精确的草图的创建。创建过程中，草图特征

的标注有可能包含过度约束或者约束不足的现象。也就是说，草图的特征不必完全标注。草图可以包括点、线、圆、圆弧或曲线等特征，每个特征都可以用多种方式创建。一个或多个特征可以被拷贝、移动、旋转；圆角可以定义在两个曲线之间；辅助线或者辅助圆可以用来辅助创建草图。另外，绘制草图的坐标网格可以根据草图来调整以方便过程定位。

装配

所有零件创建结束后（通过 ABAQUS/CAE 创建或者从其他模型中导入），装配模块用来装配零件以形成一个完整的解析的模型，在装配模块中不同的零件可以被定位工具方便的连接在一起。

一个零件可以在一个模型中多次引用。例如，一个模型中会包括很多个完全相同的螺栓。在这种情况下只需创建一个螺栓，装配模块可以重复引用，放置在相应的多个位置上。ABAQUS/CAE 的每个模型只包括一种装配方案。每个零件

的映像可以被任意移动（通过给出移动的矢量方向或者在视图选择两点来确定位移）或旋转。下面的几种约束方法用来确定两个零件的位置：

- **接触**

调节一些表面和其他表面接触。

- **平行面**

约束两个平面平行。

- **面对面**

控制两个平行的面的距离。

- **平行线**

约束两条边平行。

- **边对边**

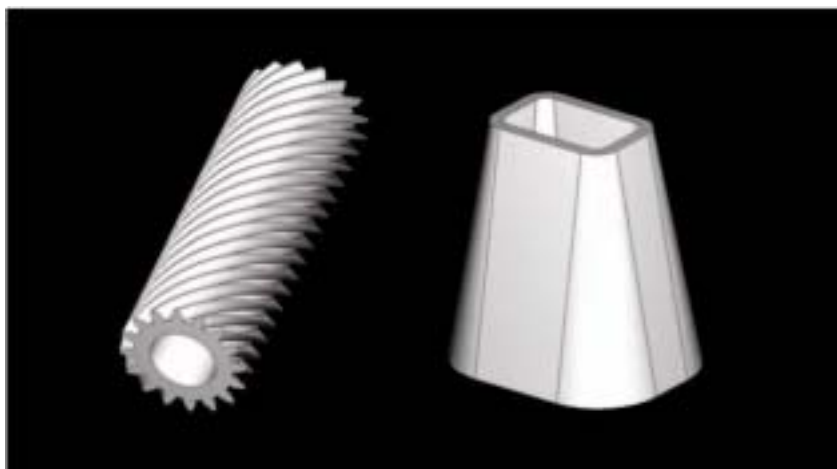
控制两条平行的线的距离。

- **同轴**

约束两个圆或圆柱面使得它们同心或共轴

另外一种定位零件的方法是给出零件的绝对位置。

零件的映像和装配的约束都是模型的特征。如果零件的几何形状发生改变，装配模块中将会自动反映出最近更新的零件特征。



ABAQUS/CAE 创建的轴套和齿轮的参数化模型。

分析属性

ABAQUS/CAE 允许用户直观的定义 ABAQUS/Standard 和 ABAQUS/Explicit 的分析属性，如材料特性、加载历史、分析类型等。

所有的属性都定义在几何模型上，提交分析任务时将会把这些属性映射到有限元网格上。如，某零件的某个特征被修改，该零件重新生成后所有属性将会重新分配到这个修改过的零件上。

ABAQUS/CAE 中可以定义集合，几何可以是零件或零件的部分，也可以是通过网格导入的模型的节点或者单元。生成

分析任务或者写入 ABAQUS 的输入文件时，在零件上定义的集合将自动转换为相应的节点集或单元集。

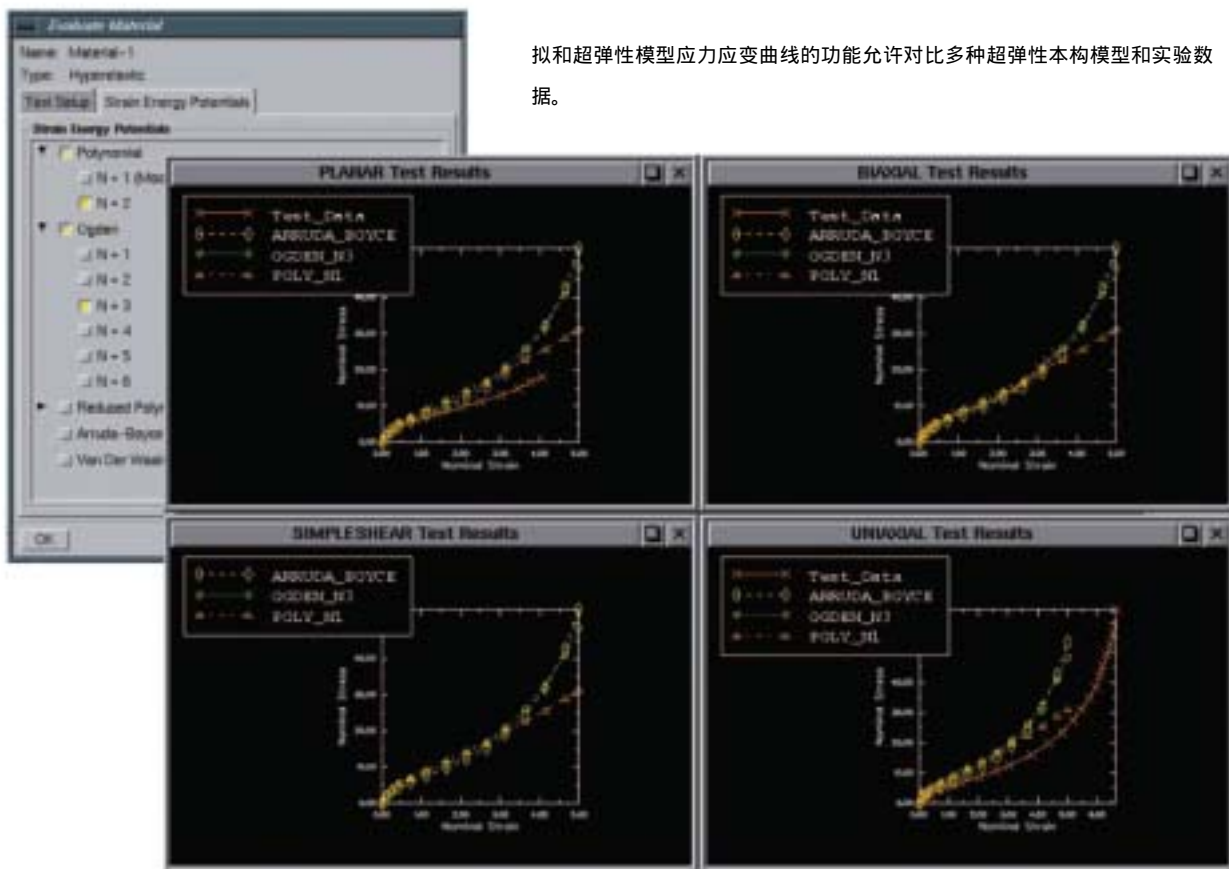
特性模块

材料特性和截面特性在特性模块中被定义并且被分配到零件上。材料特性按照传统的方式定义：通过定义材料库和创建包含材料属性和其他特性（比如壳单元需要的壳的厚度）的截面特性。在特性模块中可以定义材料和梁单元的性质。然后截面特性被分配到零件上。

- **材料** 材料管理器用来创建、修改、拷贝、删除、重新命名材料。

ABAQUS 中材料模型可以包括下列属性：

- **一般特性** 密度、热膨胀系数、阻尼等；
- **弹性** 线弹性（包括平面应力，面内各向同性，材料失效选项），多孔材料弹性，超弹性（包含通过实验数据输入定义材料参数），亚弹性，弹性泡沫，粘弹性等。
- **电学电导率** 电介质，压电特性
- **塑性** Mises 屈服准则包括各向同性硬化，运动硬化，Johnson-Cook 硬化或用户自定义硬化；Hill 各向异性



拟和超弹性模型应力应变曲线的功能允许对比多种超弹性本构模型和实验数据。

屈服准则；多孔金属塑性；韧性断裂；蠕变；体积膨胀；扩展的 Drucker-Prager 模型；修正的 Drucker-Prager 模型；混凝土损伤塑性；Mohr-Coulomb 塑性；灰铸铁塑性；双层粘塑性；剑桥黏土模型；可褶皱泡沫模型；应变率相关塑性；混凝土模型；形变塑性（Ramberg-Osgood 塑性）；ORNL 模型等。

- 质量扩散

扩散率，溶解率

- 孔隙渗流特性

Gel, moisture swelling, 渗透性，孔隙流体膨胀，多孔体积模量，吸附作用

- 热力学性质

热传导系数、比热、潜热、热产、非弹性热部分、焦耳热部分

- 垫圈

延厚度方向特性、横向剪切模量、垫圈膜弹性

- 声学介质

体积模量、体积阻力系数

- 状态方程材料（EOS）

- 用户定义材料

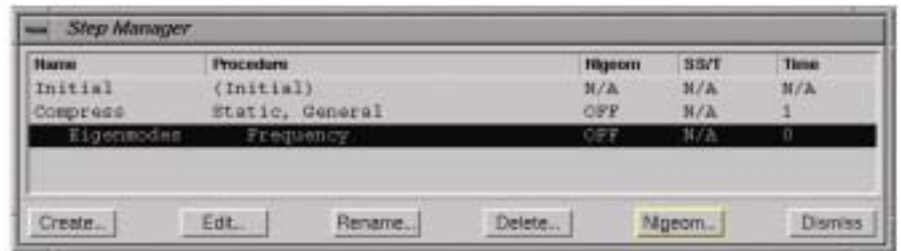
截面 截面管理器中提供创建，修改，拷贝，重命名或删除截面属性。可以创建实体、壳、梁、杆、垫圈、膜这些种类的单元的截面特性。对于刚体给出集中质量、转动惯量的参考点。

• 轮廓

轮廓管理器中创建梁截面的形状。可以进行拷贝、修改、重命名或删除。

• 夹层

可以在三维零件内部定义面，面可以被定义位壳或者膜的截面特性，面与三维的零件共用节点。同样可以在二维零件中定义边，共用二维零件的节点。夹层管理器可以创建，修改，重命名或者删除夹层。



材料特性的 X-Y 曲线图会在测试数据中分层次显示出来并且整个过程均是互动的

• 材料特性评估

对于超弹性材料，有些情况如：有实验数据而没有应变能系数，材料特性评估这个功可以帮助选择哪组应变能参数。ABAQUS 可以对实验数据进行曲线拟和。可以给出多种应变能对应的二维超弹性材料的应力应变曲线。

分析流程

在分析流程模块中定义分析流程。用户可以根据需要将整个的加载历史定义为多个分析步骤。每个分析步骤都有相应的边界条件、加载情况、接触条件和计算结果输出要求。

流程管理器

流程管理器按顺序列出定义的分析步骤。允许创建分析步骤。以下是 ABAQUS 中提供的分析：

• 非线性通用分析

- 孔隙渗流 - 应力耦合
- 温度位移耦合分析
- 热电耦合分析
- 显式分析（ABAQUS/Explicit）
- 土压应力状态分析
- 传热分析
- 隐式动态分析
- 质量扩散分析

- 静态应力/位移分析

- 粘弹性粘塑性相应分析

• 线性扰动分析

- 特征值屈曲
- 线形应力/位移分析
- 自振频率提取
- 随机相应分析
- 响应频谱分析

在分析流程模块中定义计算结果输出请求。用户可以要求输出结果到 ODB 文件（用于 ABAQUS/CAE 后处理）中，也可以请求输出结果到 res 文件中（用于再启动分析）。输出的要求自动从前一分析步输出请求中继承。如需要改动结果输出请求可以使用输出管理器来实现。分析任务诊断信息输出到 msg 文件中，同时还可以定义监控对象，输出监控对象的信息到 msg 文件中。

连接模块

在连接模块中定义零件之间的接触和约束。ABAQUS 中支持下面的连接种类。

• 接触

- 通用接触（ABAQUS/Explicit）
- 面对面的接触
- 自接触

• 弹性地基

• 热力学

- 对流
- 边界辐射

• 连接单元

ABAQUS 中提供下列约束：

- TIE 连接
- 约束方程
- 显示构件（仅用于前后处理）
- 变形体内的刚体和等温体
- 耦合连接

接触中可以定义力学和热力学的特性。力学特性的定义包括接触面切向的摩擦，接触面法向行为特性，与间隙相关的粘性阻尼。热力学接触特性包括接触表面之间的热传导，对流和热辐射。连接管理器可以显示模型的每个分析步骤中定义的所有连接特性。

载荷、约束和初始条件

载荷(Load)模块可以生成作用于模型的初始条件以及载荷和边界条件。在 ABAQUS/CAE 上，每个分析步中上述预设条件是否被激活可以显示出来。通过载荷器(Load Manager)、边界条件管理器(BC Manager)和域管理器(Field Manager)可以看到被定义的预设条件及其在一分析步的状态。进而，可以生成、复制、重命名以及删除这些预设条件。

ABAQUS/CAE 支持绝大多数分析流程中的载荷和边界条件。

• 载荷

可以预设模型上的集中力、面力、体力等，也可以定义螺栓力载荷。对热传导问题，还可以定义模型的热通量。载荷随时间的变化可以通过生成和指定对应的幅值曲线来实现

• 边界条件

可以预设模型任意节点上的平动和转动位移。对常用的边界条件如固支、对称边界等可以用快捷方式定义。对动力学问题，边界条件还可以是速度。温度也可以作为边界条件施加到体和面结构上。边界条件随时间的变化也可以通过生成和指定对应的幅值曲线来实现。

• 域

可以预设作用到结构模型任意区域的初始速度和初始温度等。

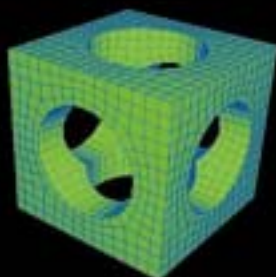
网格划分

ABAQUS/CAE 包含了一维、二维和三维区域网格划分的各种方法。ABAQUS/CAE 要保证同一部件不同区域的相容性，如果不相容，ABAQUS/CAE 将自动生成面连接(Tie)协调这两个区域。不同的部件(Part)的网格之间不需要协调。

网格种子

网格密度是由网格种子来控制的。可以为整个部件指定一个单元典型尺寸。对局部的边则可以指定典型单元尺寸或单元的个数。单元种子可以是均匀分布也可以沿某个边呈线性梯度变化。网格种子通常是实际网格分布的一个标志，我们可以强制规定网格单调增加或必须与网格种子完全一致。

结构网格



上图的结构是将部件划分成 8 个对称部分之后再划分网格

表面网格



该部件是在找到网格种子之后系统自动进行的网格划分

实体网格



该部件包含整个的四面体网格

结构化网格划分

一维曲线区域可以划分成一维单元网格
被三条或四条曲线围成的二维区域可以划分成四边形(Quadrilateral)单元网格。
拓扑结构上的立方体或可划分成立方体的三维区域可以划分成六面体(Hexahedral)单元网格。

面网格

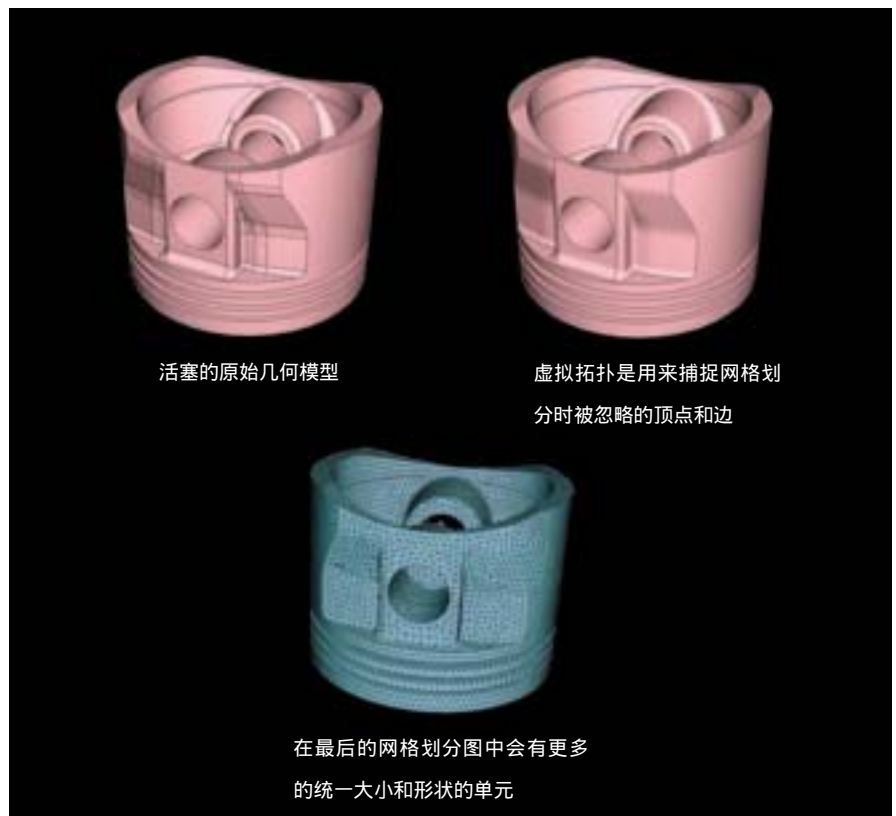
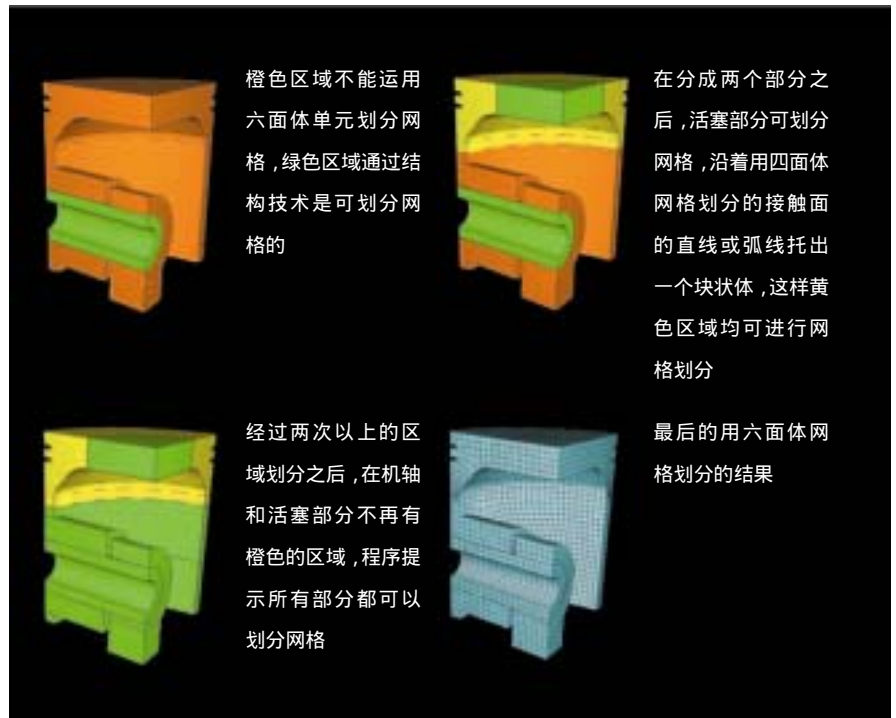
任意二维表面区域可以通过中心轴方法(Medial Axis Method)自动化分成四边形(Quadrilateral)单元。
对相同区域也可以自动生成三角形(Triangular)单元网格。

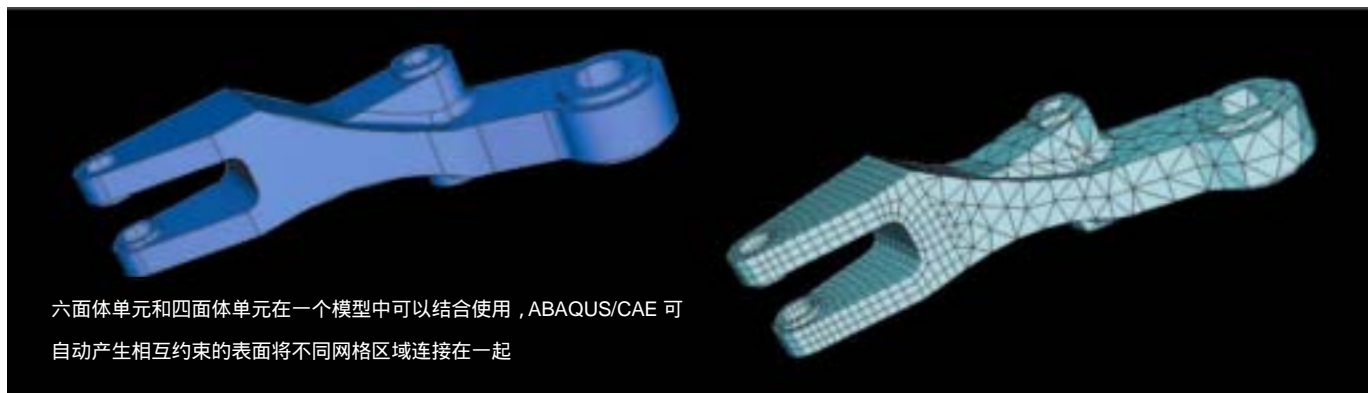
实体网格

对任意三维实体区域，四面体(Tetrahedral)单元网格划分是可以自动实现的。对四面体(Tetrahedral)网格，可以实现边界网格预览。这样，在网格生成之前，用户就可以预先判断网格的质量。网格划分失败的面将突出显示，以便用户通过网格细化等方法进行修正。
对六面体网格，几何切分工具允许用户将几何切分成可进行网格划分的区域。这些区域可以用结构化或循环复制方法进行网格划分。ABAQUS/CAE 可以通过颜色不同显示出可以进行网格划分的区域，如右图的活塞、连杆和曲轴结构所示。

虚拟拓扑

虚拟拓扑允许用户指定一个不重要的几何实体，用来划分四面体网格。多个细小面（边）可以组合成一个完整的面，这样可以得到一个更简洁质量更高的网格划分结果。





单元选择

对部件的各个区域可以指定单元的种类。绝大多数 ABAQUS/Standard、ABAQUS/Explicit 提供的单元类型, ABAQUS/CAE 都支持, 如:

- 梁单元
- 连接单元
- 三维实体单元
 - 轴对称或广义轴对称单元
 - 平面应变或广义平面应变单元
 - 平面应力单元
- 关节单元
- 薄膜单元
- 管单元
- 壳单元
 - 三维壳单元
 - 轴对称壳单元
- 杆单元
- 垫片单元

对上述单元, 下列分析流程可供用户选择:

- 声学分析
- 热传导分析
- 压电分析
- 渗流/应力分析
- 应力分析
- 热变形分析
- 热电耦合

作业管理

作业提交

根据存储的模型可以生成作业。作业进而可以提交到网络上装有求解器的计算机上进行求解, ABAQUS 自动在计算机间传输所需要的文件。不提交作业, ABAQUS/CAE 也可以生成求解器输入文件。

作业管理器可以报告作业的状态, 作业可以被提交也可以被停止。此外, 作业还可以被生成、编辑、复制、更名及删除。

过去作业在用户指定的分析步和增量可以被再启动。

作业监控

正在运行的作业与 ABAQUS/CAE 之间的信息传递使用户可以在 ABAQUS/CAE 上随时监测作业的运行状态。每个作业的监测对话框显示作业的提交及运行的详细情况。它也可以显示作业产生的错误及警告信息, 这些信息随着作业的运行实时更新。通过监测对话框, 用户可以随时停止作业的运行。如果用户指定了一个监测变量, 在作业

运行过程中, ABAQUS/CAE 可以绘制并随时更新该变量的 X-Y 曲线。这使用户可以随时掌握作业的运行情况和过程。

求解器输入文件编辑器

ABAQUS/CAE 支持绝大部分 ABAQUS 求解器的选项。为了处理那些目前还不支持的选项, ABAQUS/CAE 提供了求解器输入文件编辑器, 它可以在作业提交前根据需要对 ABAQUS/CAE 生成的输入文件进行修改。

这些修改被存储在数据库和数据库的记录文件(Journal File)里, 如果模型随后在 ABAQUS/CAE 中修改(例如修改了某一部件的维数), 并重新生成, ABAQUS/CAE 将自动将这些修改应用到新的输入文件中。

后处理

不论分析模型是否是由 ABAQUS/CAE 生成,分析结果都可以在 ABAQUS/CAE 中进行结果仿真。大规模模型分析结果已经成为结构设计的一个重要目标, ABAQUS/CAE 提供了一个便捷的利用计算机进行结果仿真的途径(应用图形加速器)。

ABAQUS/CAE 可以绘制结构的模型图、变形图、结果云图、矢量图、路径图、多层视图、X-Y 曲线图等,也可以进行结果提取和结果动画仿真等。在作业运行的过程中,可以观察阶段性结果。多个作业的结果可以在同一个 ABAQUS/CAE 窗口中显示,极大地方便了结果的对比分析。

观看和显示

ABAQUS/CAE 为各种绘图模式如模型图、变形图、云图、矢量图、X-Y 曲线图等提供了着色显示和其他显示方式。例如,变形图可以用隐藏边界线、填充着色和云图等组合方式显示。

ABAQUS/CAE 中有下列着色方式可供选择:

- 填充图
- 框架(隐藏内部线)
- 阴影
- 框架

用户还可以控制显示单元的颜色和标号,以及单元的边界,以便于判断模型的几何特征如孔、边角等。模型可以设置成半透明的,也可以将各个单元收缩到质心点来表示。轴对称或平面模型可以通过拉伸和旋转等方式用三维图形表示。

也可以绘制接触面以及二维或三维刚体表面。模型也可以仅仅显示指定的单元集、节点集或表面集。显示组也可以在操作窗口指定或以输出结果为判据来指定。

用户还可以通过多窗口方式同时显示不同的模型、显示方式、观察角度等。窗口可以在画板上可以动态地移动、伸缩。画板可以根据需要伸缩,直至充满整个屏幕。

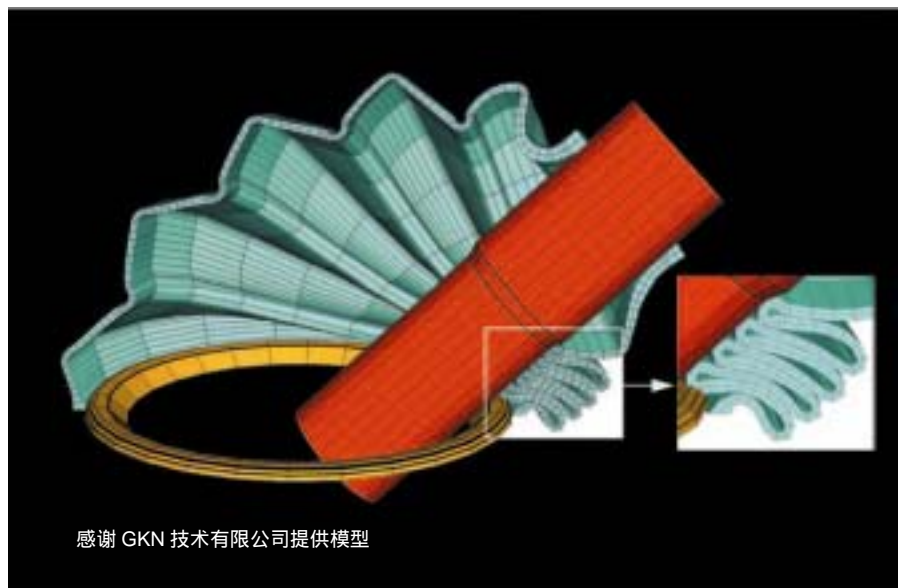
模型和变形图

ABAQUS/CAE 可以显示全部或部分模型变形后的几何形状。模型图可以重叠显示到变形图上,变形的放大因子可以自动或手动控制。以矢量表示的材料方向特性可以在模型图或变形图上表示。

云图

单元输出量如应力、应变等,节点输出量如位移、温度等,面输出量如接触压力等可以用模型图或变形图基础上的云图来显示。云图可以绘制到三维单元的各个表面、板壳结构的各个层、梁单元的各个截面点。多个接触面的接触应力可以同时绘制到一张云图上。

单元输出量如应力和应变,是通过积分点数值插值到节点得到的,为得到连续的场输出变量还需进一步将这些数值平均。有若干种选择可以控制节点变量平均的方式。程序可以自动检测材料和截面的不连续,默认情况下,不对这些边界节点的输出量进行平均。另外,插值



橡胶密封件的方针计算

感谢 GKN 技术有限公司提供模型

结果的不连续性也可以通过云图显示出来，这可以用于判断模型的不精确性和指出需要网格细化的区域。

标线图(Tick Mark Contour)提供了一种替代的方法来表示梁或其他一维单元的输分布情况。标尺图在一系列垂直实际单元的标线上联接成反映输出变化的曲线。

用户可以控制云图的范围，图例的位置、形式及其显示特性。

除了输出文件的结果外，用户还可以绘制过去计算数据数值操作后结果的云图。例如，用户可以绘制线性分析中不同载荷情况对比结果的云图，也可以绘制非线性分析不同状态对比结果的云图等。

符号图

矢量和张量可以用符号形式显示在模型或变形图上。位移、速度、加速度等可以用云图显示其各个分量，也可以用矢量图来表示出他们的幅值和方向。张量的主值的幅值和方向可以用张量图表示。

薄膜单元的纤维加强结构材料方向也可以用符号图表示出来。

X-Y 曲线图

用户可以绘制输出量随时间变化或两个变量之间相对变化的 X-Y 曲线图。

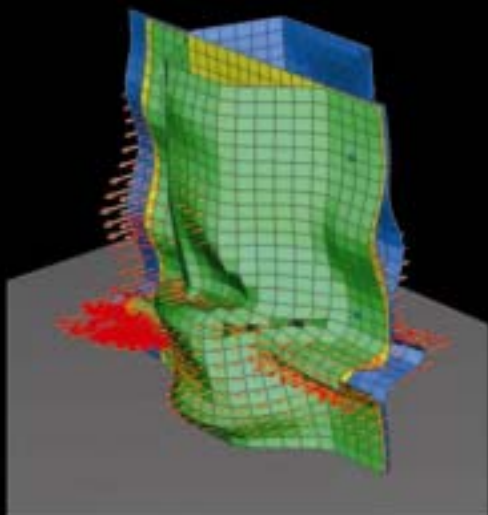
外部的 X-Y 数据如实验数据可以直接或通过文件输入并显示。每一条 X-Y 曲线

都可以被指定一个名字储存起来已用于以后的绘图。多组 X-Y 数据可以在同一张图中显示出来。X-Y 曲线也可以存储到当前的或另一个新的数据文件中以便于以后应用。

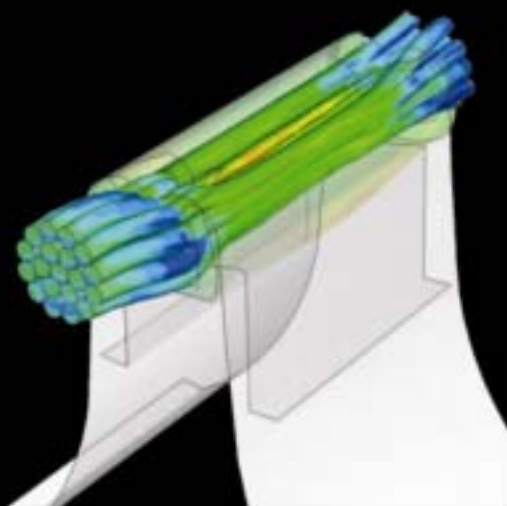
沿模型某一路径输出结果的变化也可以用 X-Y 曲线表示出来。路径可以通过在模型上指定一系列的点实现。

通过图形操作可以从当前的图形对象得到另外的图形对象。这些操作包括：数值运算、数值过滤、积分、微分、坐标轴互换、附加图形对相等。

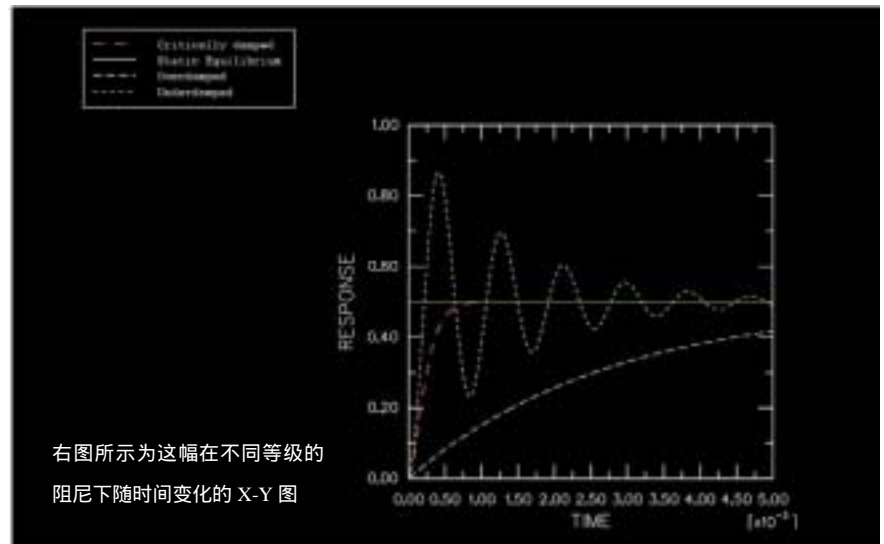
用户可以控制图形的界面，如标题和图例、对数或线性坐标轴、标线、坐标轴尺度、数据点的符号、线性等。



采用符号图的横向位移功能观看一个点焊接模型模拟挤压



用于云图功能观看金属线包裹模拟试验



重叠绘图

重叠绘图功能可以使多个单独的图形（例如，模型图、云图、X-Y 曲线图等）在同一个窗口显示。每一个图形作为一个“层”存储在数据库中，多个层可以根据位置和顺序不同复合显示。

数值提取

用户可以数值提取(Probe)工具来实时查询计算结果、模型信息和 X-Y 数据等。当数值信息提取功能被激活后，用户在界面上移动鼠标位置，信息提取对话框马上可以显示所需要的信息。这些信息也可以写入到数据文件中。

应力线性化

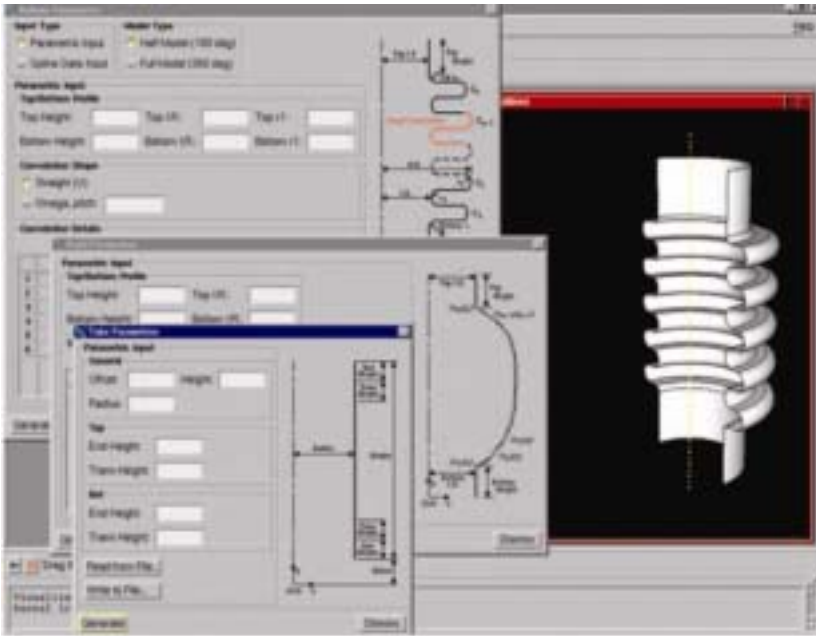
所谓应力线性化是指将截面的结构应力分离成薄膜应力和弯曲应力。ABAQUS/Viewer 执行应力线性化并通过 X-Y 曲线将结果显示出来。

动画

ABAQUS/Viewer 提供时间历程和比例系数两种动画方式。时间历程动画用来显示计算输出量变化过程，比例系数动画在线性设动分析（如屈曲、固有频率提取等）中将计算输出量变化按比例显示。对于复动力学问题的计算结果，对指定的频率可以显示整个相位区间 ($0 \sim 2\pi$) 计算输出量变化历程。

动画可以应用基于对象或基于图形的技术来显示。基于对象的技术在动画的过程中可以调整对象的显示特性，例如在动画过程中，用户可以动态旋转模型。尽管如此，对于较大模型，上述方法会遇到困难。基于图像的方法可以回放过去抓取得一系列图像。只要图像被抓取和存储起来，模型的大小就不会对回放速度造成影响，但显示和图像就不能再调整了。基于图像的动画可以存储成 AVI 或 QuickTime 格式，在 ABAQUS/CAE 的内部或外部都可以放映。

一个专门为铰链分析而设定的用户界面
面的简单例子



数据库和脚本

数据库

数据库所有模型的信息都储存在模型数据库中，一个数据库可以包含多个模型。ABAQUS 求解器计算出的数据结果将被储存在输出数据库(.odb)中，用于后处理。这些数据库高效率地使用磁盘空间，数据库使用与计算机类型无关的二进制存储格式。因此他们可以在不同机器中拷贝而不需要做任何翻译。另外，用户可以通过 C++或 Python API 直接访问数据库。

日志和重新启动文件

所有恢复一个数据库文件必须的命令都存储在日志文件中。日志文件在 ABAQUS/CAE 使用模型数据库的过程中会一直存在。

数据库前一次保存开始的所有执行的命令都保存在一个 .rec 文件中。如果 ABAQUS/CAE 因为某些原因异常关闭，.rec 文件将会用来恢复数据库保存之前做过的所有修改。独立进程在重新启动文件中保存。这些文件记录了所有用户交互信息，包括视图的改变等。（日志文件仅包括重新创建数据库的内容）重新启动文件可以用于执行一系列普通用户命令的书写程序的基础。例如，创建一个特殊的后处理的图形。同样，用户可以用这一系列动作定义为宏，而在后续的扩充和重现时可以直接启动宏而实现这一系列动作。可以将命令储存在一个启动文件中。在 ABAQUS/CAE 启动的时候会自动执行。例如，用户可以创建一系列标准材料模型库或者自定义视图显示的选项。

脚本

ABAQUS/CAE 嵌入 Python(参考 www.python.org) ,python 是一个完全的特征化，面向对象的脚本语言。使用 Python，多数的 ABAQUS/CAE 用户界面都可以被修改，包括菜单和工具条。甚至也可以建立新的对话框。Python 和改变界面能力的综合为用户化，应用化提供了强大的工具。

硬件和性能

ABAQUS/CAE 在多种的桌面工作站上都可以运行。计算机应该有 OpenGL 硬件图形加速器。推荐最少使用 256M 内存。如果有更多的内存将会提高 ABAQUS 的性能和有利于显示大模型。ABAQUS/CAE 在下列平台上可以运行。

- **HP**
- **IBM**
- **SGI**
- **Inter Pentium**
 - **Windows NT/2000/XP**
 - **LINUX**
- **Sun**

ABAQUS 网站上有详细的 ABAQUS 支持的平台的详细内容。www.abaqus.com ABAQUS 未限制模型的大小，绘图功能对大模型依然使用，并且 OpenGL 绘图工具使用于任何情况。

用户配置图形设置使得用户可以调节程序使得硬件和需求协调。

文档

ABAQUS/CAE 包含便于理解得在线文档和书面文档。入门手册可以让初学者很快的熟悉软件。软件设计的非常直观。因此，入门后，手册只会在特殊的条件下使用。

培训和支持

HKS 公司及其代理处对 ABAQUS 软件提供全面支持。培训班定期举办，同时可以在用户单位进行培训。

ABAQUS/CAE 在线用户手册



ABAQUS/CAE 的优势

受益于 ABAQUS/CAE 提供了一个完整的集成建模，分析，监控，诊断、查看结果的环境。

提供了一个流行的用户界面，用户可以容易、直观的使用。

扩展的 CAD 概念，如零件，装配，特征重生和高级的非线性分析。

完善了其他的模型包。零件的可以以几何构形和网格的形式导入 ABAQUS。不同来源的零件可以被放在同一个模型中。

于其他基于特征的参数化模型协调的配合。可以从其他 CAD 软件中导入平面图或者平面图。

高效率的处理大模型。

比任意建模器支持更多的 ABAQUS 功能求解器。

允许多重分析，并且可以通过网络进行管理。

允许在运行时显示分析的结果。

支持 ABAQUS 特殊的特性的显示，比如接触表面的力和刚体。

使用 Python，提供强大的脚本和面向对象的编程语言。

提供用户自定义截面的方法接口以产生针对应用的截面。

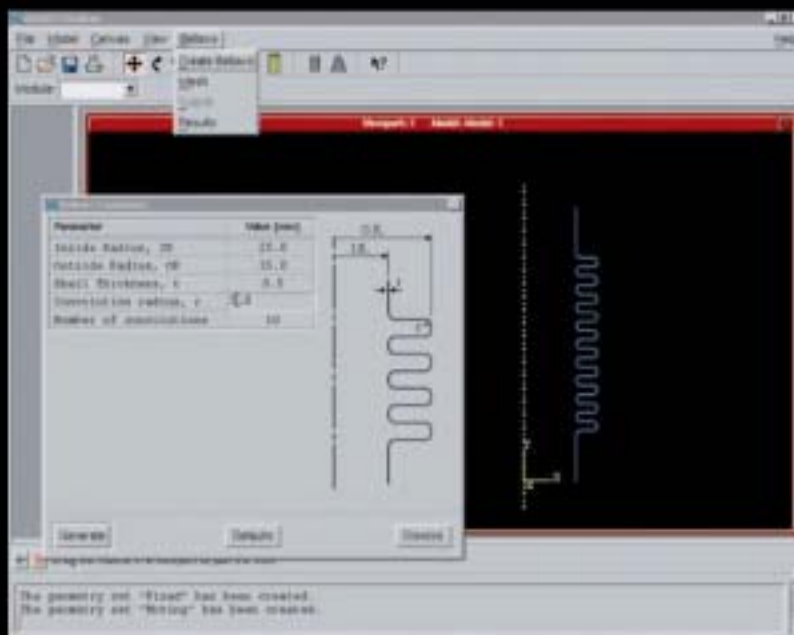
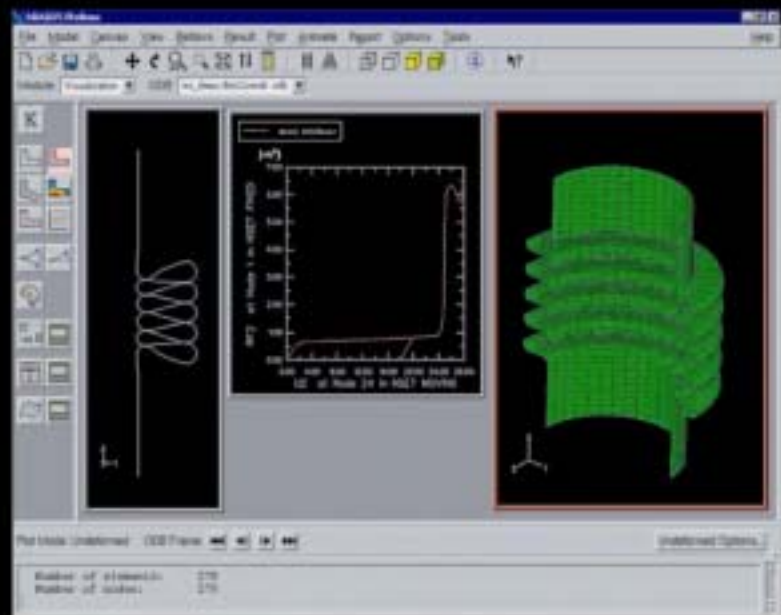
提供压缩的与操作平台无关的二进制数据库。

使用面向对象的结构化的 C++ 编写，便于产品的迅速的后继开发。

提供全面的截面文档支持和详尽的用户手册和培训教程。

符合 ISO 9001 和 ANSI/ASME NQA-1 质量认证要求。

包括遍及世界各地的 ABAQUS 办公处和代表处的技术支持。



用户设计应用

产 品 综 述

简 介

ABAQUS/Explicit 是一种适用于高度非线性连续介质结构分析的高级有限元程序。同时它对高度非线性的瞬时动态现象和一些非线性准静态模拟也有较好的适用性。它是直接针对于产品分析的目的而设计的，因而它的整个体系结构具有易于使用、可靠性高、适用性好、效率高等特点。ABAQUS/Explicit 能在各种计算机系统中运行，从使用 Windows NT 或 UNIX 的台式机或工作站到各级服务器和超级计算机。经过优化的代码提高了程序的性能，是数据管理系统更为简洁、高效。

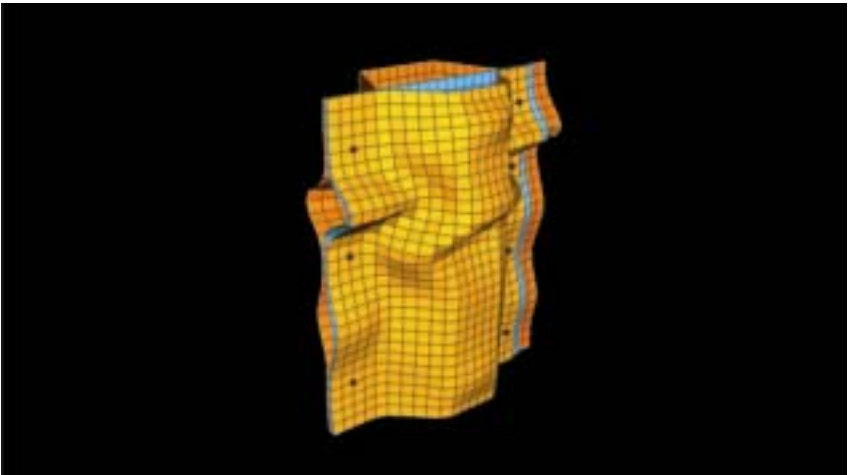
分析能力

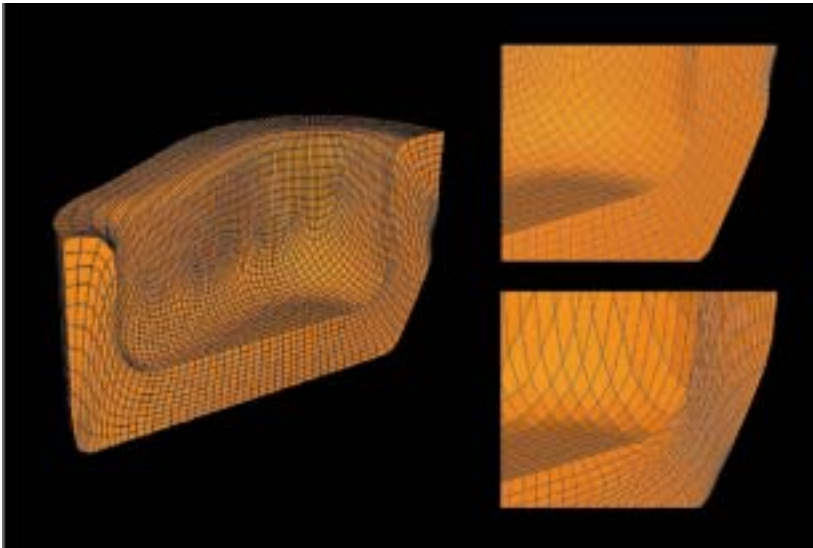
ABAQUS/Explicit 对时间步采用显式时间积分，它包括以下几种分析类型：

- 有无绝热效应的显式动态响应；
- 完全耦合的瞬时动态温度-位移分析对力学量和热量的响应都使用显式算法；
- 多步骤成型和退火过程模拟；
- 噪声及噪声结构耦合分析；
- 对多步骤成型退火过程的模拟；
- 对于波在声学介质中，如振动载荷在水下结构中的传播等声学 and 声学结构耦合的传播仿真分析。

自适应的网格功能对高度非线性问题提供了稳定可靠的解答。

网格独立的焊点定义与广义接触定义相结合可以简化建模过程可以有效模拟焊接结构的大变形。





锻造仿真模型：图左所示的锻造部件采用了自适应网格化的分析技术，图右上所示为采用了自适应网格化分析技术的放大图以及图右下所示没有使用自适应网格化技术的放大图。以上两图在最初都是使用了相同的网格划分。

材料

对金属、橡胶、塑料、复合物、混凝土、土壤以及具有回弹和可挤压性质的泡沫等材料都提供了模型。上述模型可以影响和热效应。可提供两种状态方程对水动水压材料和爆炸进行模拟。用户还可以通过一个通用的界面自定义材料的行为和特性。

几何模型

对多种结构和连续体都可以建立模型。提供了一维、二维和三维的连续介质单元以及壳单元、薄膜单元、梁单元和桁架单元。ABAQUS/Explicit 是一种模块化的程序：任何具有适当材料模型的单元组合都可以用在同一分析过程中。

运动学特性

ABAQUS/Explicit 里的所有单元(不包括一些特殊用途的单元) 能够为任意大小的位移、旋转和应变提供准确的模拟。

规定条件

边界条件包括指定的运动学条件 (单点约束)，例如指定位移、速度和加速度历史。载荷条件包括集中力和分布载荷，例如压力，离心力和重力。另外，还提供了热力选项。

相互作用

提供了模拟物体之间相互作用的能力，包括面-面接触和多点约束。

其它分析技术和建模方法

- ABAQUS/Standard 的中断继续分析功能
- 继续分析过程的结果传递
- 中断点的再启动分析
- 未结束分析过程的恢复
- 自动质量系数
- 线性动量
- 自动网格
- 子模型
- 参数化及参数化研究
- 几何的自动摄动
- 结构加强
- 肘单元
- 多坐标系统输入
- 局部自由度
- 流体静力学单元
- 用户子程序

特 征

分析

多步骤分析能够在 ABAQUS/Explicit 里直接进行。用户可以仅仅基于自己方便的基础上把加载历史分成若干个步骤。每一加载步都是总的加载历史的一个典型阶段。每一步的初始状态是上一步的最终状态，它提供了一种方便的方法来跟随复杂的加载历史，例如一个制造过程。

- **非线性动力学/位移分析**

提供了基于中心差分方法的全自动显式积分。既能够用于小位移模拟也可用于大位移模拟。

对于在材料受力产生变形时，产生热量由于变形过程太快导致热量无法在材料中传播的情况下可以引入绝热效应。

- **充分耦合的瞬时动态温度-位移温度**

引入了全自动显式积分来解释力学和热学响应问题。给这种分析提供了一种一阶减缩积分耦合连续体单元族。

- **准静态分析**

显式积分分析方法能够用来进行准静态分析。自动质量比例缩放能保证这种分析有效地执行。

- **退火**

对结构发生非弹性变形时的退火也能进行模拟。所有相应的状态变量都调到零，包括应力、应变、塑性应变、速度以及任何用户自定义的状态变量。

- **声学分析**

提供了声学分析和声学结构耦合分析

功能，可以实现对声学介质中的波传播的仿真，例如振动载荷在水下结构中的传播。

材料定义

提供了众多的材料模型。大多数材料参数依赖于温度和预定的场变量，例如多相材料中某些特定相的密度。还提供了一个选项可以允许在网格中定义材料的局部方向以方便材料特性的输入和应力/应变分量的输出。这一选项在构造层合复合材料和其他各向异性材料的模型时很有用处。

弹性

- **线弹性**

弹性模量可以是各向同性的，也可以是正交的各向异性的。

- **平面应力正交破坏**

在线弹性中引入了破坏理论。这可以用在后处理中输出结果，比较典型地用在复合材料壳的分析中。

- **超弹性**

这些模型用于研究橡胶一类材料的大应变弹性响应。包括了以下五种超弹性模型：普通多项式应变能量函数（包括 neo-Hookean 和 Mooney-Rivlin）、Ogden 模型、仅包含第一不变量的缩减多项式模型（包括 Yeoh 模型）、Arruda-Boyce 模型以及 Vander Waals 模型。也含有用于模拟高回弹性的泡沫材料的模型。所有大应变弹性模型的材料常数都可以直接给定，或者从用户提供的测试数据中计算得到。

• 粘弹性

对于小应变及有限应变问题提供了时域粘弹性。它使用了一个普朗尼 (Prony) 序列表示法, 其常数是根据用户指定的测试数据由 ABAQUS/Explicit 计算得出的。粘弹性材料可以通过 Williams-Landel-Ferry 关系具体化为热流变量简化形式 (TRS)。

塑性

• 金属塑性

对各向同性塑性问题采用 Mises 屈服准则, 对各向异性问题采用 Hill 屈服准则。在经典的金属塑性模型中也包括理想塑性和各向同性硬化。此外还具有 Gurson 塑性模型, 它用于模拟具有孔隙成核作用的多孔型金属以及填充材料的应变硬化。

• 延性失效

延性失效模型提供了一种基于等效塑性应变之上的简单失效准则, 它允许由于结构的裂开而导致的单元在网格上的稳定移除。

• 扩展的 Drucker-Prager 模型

这种模型提供了一个压力相关型的屈服面, 包括应变硬化软化, 率相

关以及颗粒材料的非关联流动, 例如沙土, 还有在拉伸和压缩方向具有不同的屈服行为的材料, 例如聚合物和铸铁。

• Capped Drucker-Prager 模型

这个模型中把临界状态模型和扩展的 Drucker-Prager 模型结合在一起。这种模型适用于地质工艺专业, 例如隧道挖掘。

• 可挤压型泡沫

这种模型适合于模拟可高度挤压的材料, 例如消费品的包装以及车辆的安全装置中的一些材料。

• 混凝土

提供了两种描述混凝土结构的本构关系模型: 脆性断裂模型和塑性破坏模型。两种模型都可以用来定义混凝土本身或钢筋加强混凝土, 结构形式既可以是梁、杆、板, 也可以是三维实体。

• **应变率相关塑性** 所有金属塑性模型、extended Drucker-Prager 模型以及可挤压泡沫模型中的硬化可以是率无关也可以是率相关 (粘塑性)。Johnson-Cook 模型可以模拟金属和其他材料在大应变率情况下的变形。

• 大应变率失效

带有大应变率拉伸和剪切失效模型可以与 Mises 或 Johnson-Cook 塑性功能一起去除的单元。

其它材料特性

• 热膨胀

各项同性或正交各向异性热膨胀系数可以定义为温度相关或指定的场变量相关。

• 热传导性

可以定义温度和场变量相关的各向同性、正交或完全各向异性的热传导性质。

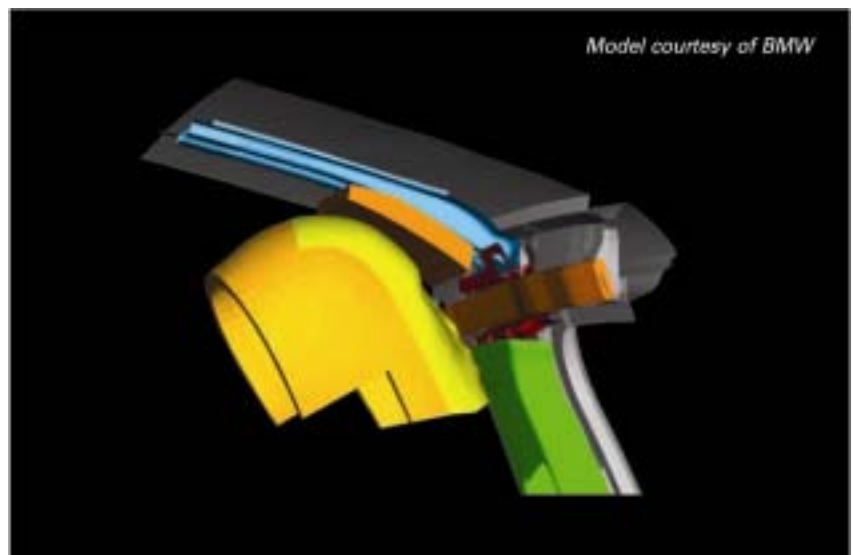
• 比热

可以定义温度相关和场变量相关型的比热。

• 状态方程

包括了模拟爆炸和手动水压材料时的 JWL 和线性与 Hugoniot 状态方程。同时也包括理想气体状态方程。状态方程仅仅支配着体积的响应。可以用线性各项同性或牛顿粘型模型来定义偏量行为。

在聚合泡沫材料和热塑性材料的高级建模中, 有效的结合了通用接触和集成功能, 使 ABAQUS/Explicit 成为解决安全和冲击方针问题的有效工具



- **密度**

这个性质用于变形材料的质量矩阵。

- **材料阻尼**

可以指定质量和刚度比例阻尼。

- **用户自定义材料**

用户子程序 VUMAT 可以执行用户自定义的材料模型。子程序接口以矢量数据块的形式传递数据，因此用户在编 VUMAT 程序代码是可以利用矢量化的便利。

单元库

单元可按不同方式分类：根据基本原因的不同（实体单元、壳单元、梁单元、桁架单元等）；根据维数或应力表示法的不同（一维的、二维的、平面应变、平面应力、轴对称或三维的）；根据积分方式不同（完全积分或减缩积分）。所有的单元的公式都适用于任意大小的位移、旋转和变形，并且所有单元都具有集中质量矩阵。用户可以选择不同的单元表达式来满足费用或精确度的要求。非默认单元控制差不多可以减少 40% 的分析时间（视问题本身决定）。

实体单元

对于平面问题，包括平面应力和平面应变问题，提供 3 节点三角形，6 节点三角形单元，和 4 节点四边形单元。对于轴对称问题，提供 3 节点三角形，6 节点三角形和节点四边形单元。在三维问题中提供了 4 节点四面体，10 节点四面体，6 节点五面体和 8 节点六面体单元实体单元。二阶三角形（6 节点）和四面体（10 节点）单元能够很好地解决设计及接触和应力波传播的问题。

壳单元

ABAQUS/Explicit 提供了 3 节点三角形和 4 节点四边形的一般壳单元以及 2 节点轴对称壳单元。壳的截面可以式均匀的，也可以是分层的（用于复合材料层合系统分析）。初始厚度可以在其中一个单元或节点基础上指定。既提供了小应变壳，也提供了有限应变壳。通过节点位置定义的单元参考面可以在壳的厚度方向的任何位置。

薄膜单元

ABAQUS/Explicit 提供了 3 节点三角形和 4 节点四边形薄膜单元。其初始厚度可以在其中一个单元和节点基础上制定。

梁单元和桁架单元

- **梁单元**

提供了平面和空间的 2 节点梁单元，并带有相关的截面定义库。

- **桁架**

提供了 2 节点桁架/杆单元。

惯性、刚体和容量单元

- **质点和转动惯量**

可以指定集中质量和转动惯量。

- **刚性单元**

具有二维或三维的单元来模拟刚体的接触作用。刚性单元也可以附加于变形体上。

- **容量单元**

点热容量单元允许在上一个点上传入集中的热容量。

刚体和等温体

- **刚体**

刚体常常用于其变形相对于模型中其它部分可以忽略不记的场合，例如一

个坚硬的结构挤压一块柔软的橡皮密封垫。一个刚体可以用以下几种方式来定义：指定它的几何形状；应用刚体单元；或者把任何梁、连续体、薄膜、壳、桁架等单元指定为刚性。节点集也被视为刚体的组成部分，通过它可以很方便的定义确切的约束条件。刚体的重心，质心和转动惯量可以直接指定，也可以在已知材料密度和几何形状的基础上自动的计算出来。

- **显示体**

显示体类似于刚体，但它只应用于显示。显示体的单元和节点不参与计算，但参与后处理过程。显示体尤其适用于机构或多体动力学分析问题，在这些问题中，刚体部件通过连接件相互作用。这种情况下，一个部件可以用简单的刚体来代表，但可以用更复杂的显示体来显示。

- **等温体**

等温体是指热量相等的刚性体。在温度-位移耦合作用的分析过程中，它能用来模拟温度均匀但可随时间变化的物体。

连接单元

- **连接单元**

连接单元可以模拟节点之间不连续的物理连接，能用于含有弹性或刚性部分的任何实际问题中；相关的例子由运动约束（比如槽形或回转形约束），单一部件非线性材料响应和单向接触约束。此外，连接单元在具有有效的相对运动分量（没有被约束的相对自由度）时是允许被驱动的。在驱动连接中，例如齿轮驱动的伸展臂或液压活塞，相对运动分量作为一个已知的位移或驱动力历史被给定。

• 线性或非线性弹簧和阻尼器

弹簧和阻尼器可以置于节点之间，分别把一个力耦合为相对的位移和速度。弹簧刚度和阻尼系数依赖于温度和预定的场变量。

规定条件

• 幅值曲线

被命名的幅值曲线可以用离散的数据、傅立叶级数和其它的函数描述。然后这些名字就可以被引用来说明任何载荷或边界条件的变化。对于准静态分析，幅值的定义是以载荷和边界条件的平滑变化为条件的。

• 初始条件

初始条件可以在多类区域上定义。数据可以以表格的形式输入，也可以从其它 ABAQUS 分析中传入。

• 边界条件

位移、速度或加速度边界条件可以定义在模型上任何有效的自由度上。

• 载荷

任何载荷可以即刻应用，也可以指定为任意的幅值曲线，例如一个复杂的压力脉冲历史。分布载荷可以直接应用在单元或面上。非均匀分布载荷可以直接通过用户子程序来定义。能够应用的载荷类型有集中力和弯矩，包括随动力；温度；场变量；非零的位移，转角，速度或加速度和离心力；以及 Coriolis 力。在适当的地方也可以有随动力效应。对于热量模型提供了分布流和集中流以及薄膜环境。

• 规定场

这些温度以外的场，而材料特性也许会依赖于他们。

相互作用

模型内的区域能以多种方式互相作用：

- 通过接触
- 通过某一运动约束
- 通过对点焊接的定义

ABAQUS/Explicit 在模型接触和表面相互作用的问题上有强大的解决能力。

接触定义

ABAQUS/Explicit 提供了定义接触作用的有效方法，根据接触局部行为的特点，用户可以从不同的接触定义方法中选择一种，也可以选择多种方法进行组合。

在这些方法中，一个非常有效的方法是定义广义接触，即认为模型的每个部位都有接触的可能。ABAQUS/Explicit 进而决定进入接触的面，并据此求解。广义接触可以扩展到复杂的形式，这样接触的局部特性如摩擦等可以方便地定义。

接触定义可以根据运算步不同而发生改变，也可以在作业再启动过程中实现。

接触相互作用

ABAQUS/Explicit 具有多项能力来解决模型的接触和表面相互作用的问题。

- 能模拟变形体之间以及变形体和刚体之间的接触。无论在二维还是三维的情况下都能对微小或有限的滑移进行模拟。在小滑移接触时，表面之间的间隙能精确地指定。
- 接触可以发生在三维壳、薄膜和刚体单元的任何边上。也可以发生在这些单元地外表面或参考面上。
- 一种自接触的算法能够模拟一个表面和它自己的接触。
- 接触可以定义在节点和表面之间，这是模拟穿透问题的一种有效方法。

- 边—边接触可以模拟梁或杆结构的周线等几何特征的接触情况。
- 可以模拟静态摩擦和动态摩擦。摩擦系数依赖于局部滑移速度，接触压力，温度和其他用户定义的变量。用户子程序 VFRIC 允许组合成复杂的摩擦模型。
- 对于完全耦合问题，接触相互作用包括接触表面之间的热传导和热辐射，并考虑接触应力和间隙对它们的影响。由于摩擦滑移所引起的生热也可以进行模拟。
- 表面可以定义为粘合的，这给二维和三维问题提供了一种简单的网格划分精化技术。
- 提供两种接触列式：运动学列式和罚函数列式。运动学接触或“硬”接触迫使完全地接触，因此不存在过封闭的情况。罚函数接触或“软”接触是和运动学接触相对的，它提供了接触体之间的局部弹性响应。罚函数刚度是自动计算的。另外，还可以把压力和间隙的关系定义成指数关系或表格方式，以此来模拟特殊的预期局部接触行为。也可以指定粘性接触阻尼。相互接触的表面的定义在每一步都可以改变，直至分析的重新开始。

运动约束

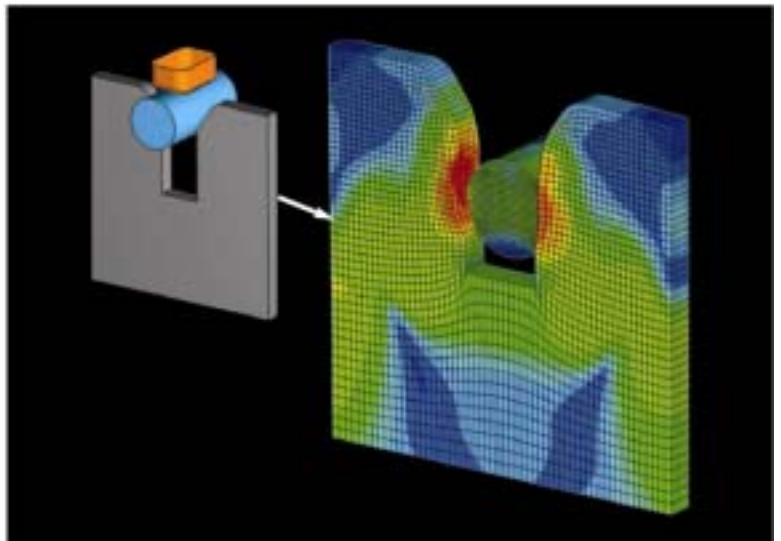
提供了线性和非线性的多点约束 (MPCs)，像刚性连接，刚性梁，壳-实体连接。刚体也可以用来模拟某些运动约束。

基于面的耦合约束提供了一种灵活的控制部件间耦合关系的方法，这种约束也可以用来确定面和体之间的连接。

• 焊点连接

焊点连接定义可以确定两个和多个部件间的连接关系。独立与网格的焊点连接可以定义在部件的任意位置，而不用考

具有大的塑性变形的三维结构部件间的接触模拟仿真是 ABAQUS/Explicit 的一个重要功能。这个例子是说明了导线压入连接卡座的准静态模拟过程,由于大应变导致的网格变形奇异可以通过 ALE 网格自适应方法调整。



考虑该位置的网格情况。此外,点对点连接提供了定义可分离焊点连接的方法。

其它分析技术

• 输入

运行结果可以在 ABAQUS /Standard 和 ABAQUS/Explicit 之间通过二进制文件的形式相互传递。这项功能完全可以在 ABAQUS/Standard 下继续完成 ABAQUS/Explicit 里的模拟,或者在 ABAQUS/Explicit 分析之前使用 ABAQUS/Standard 对模型的初始状态进行定义。

这方面应用的实例有:在使用 ABAQUS/Explicit 进行一个冲击问题的分析之前,使用 ABAQUS /Standard 对装配好的模型施加预应力;在 ABAQUS/Explicit 进行成型模拟之后,使用 ABAQUS/Standard 来确定快速成型后的回弹和固定频率。

• 重启

重启能力允许用户定期地保存整个分析状态,使分析过程可以从这些保存点开始在附加额外的加载历史重新启动。

• 恢复

由于计算机系统故障,例如 CPU 的超载和磁盘空间的不足,而使程序提前终止时,通过恢复功能可以使分析任务完成。

• 自动质量比例缩放

这项特性提供了一种方法来增加稳定时间增量,从而减少了准静态和动态分析的计算花费。

• 线性运动

这项功能能够确保解决小位移问题,波传播问题和其他小应变问题时,比用大位移公式更精确有效。

• 适应性的网格化

设计适应性的网格化方法来保持高质量的网格,即使是网格所属的材料发生严重变形的情况。ABAQUS/Explicit 使用了 ALE(任意 Lagrangian-Eulerian)技术,网格的移动独立于其所属的材料,从而在整个分析过程中保持一致的网格拓扑结构;单元既 not 生成也不剔除,单元的连接也不改变。这个方法是完全自动的。

• 欧拉网格适应域

欧拉网格适应域这一方法用于模拟材料在网格中的流动。这一方法对于稳态成型问题特别有效,例如挤压成型。欧拉边界区域用于处理模拟材料流进或流出网格。

• 跟踪点

跟踪点可以用于获取材料上指定点处的输出,而这个点在使用了适应性网格后可能不是对应于网格上的固定位置。在分析过程中跟踪点不管网格如何运动而始终跟随材料的运动,这使它们可以理想的再现材料某点的运动,绘制这一点的应力、应变等随时间的变化图。加强件在连续体单元中可以附加多层的加强筋来模拟复合的材料,比如钢筋混凝土,或者是橡胶加强件,如轮胎。

• 子模型

子模型方法允许用户根据原始的整体模型计算结果,应用细化的网格分析局部结构。子模型作为独立的模型进行分析计算。它与原始模型之间的唯一联系就是子模型边界节点的各个变量及它们的插值。子模型边界不需要和原始模型吻合,子模型也可以用来将 ABAQUS/Standard 和 ABAQUS /Explicit 混合计算。

- **数据参数化及参数化研究**

参数化研究功能使用户可以生成、执行及后处理参数值发生改变的多重分析作业。

- **自动几何摄动**

ABAQUS/Standard 特征屈曲分析的结果可以作为初始几何叠加到后屈曲分析过程中。同样地，任何分析地变形数据都可以作为初始几何附加到另外的分析过程中去。

- **加强结构**

在连续体、膜和板单元内部还可以定义纤维加强层，以便于模拟复合材料、钢筋混凝土、以及轮胎等橡胶部件。纤维加强结构定义可以独立于宿主单元的网格。

- **静压流腔**

充满流体的容腔可以模拟成二维或三维的形式。从静压的数学描述中可知在任何时候流腔中导入或导出，也有一种一维的连接单元来模拟流体在流腔之间的流动。有关这方面的应用有：液压引擎装置，空气减震器，液压传动装置等。

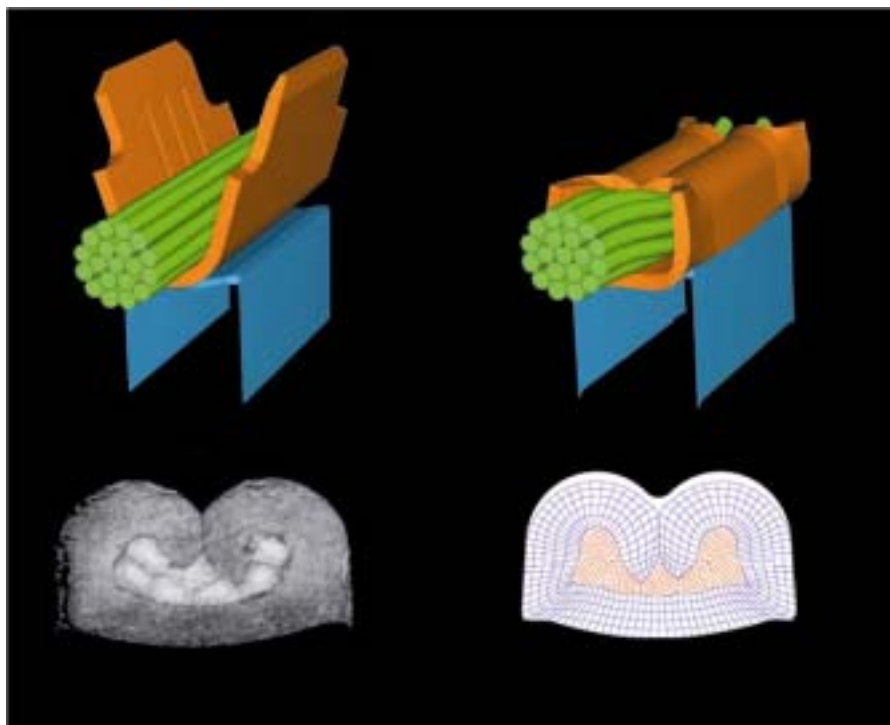
- **局部自由度**

任何节点处的自由度都可以转换到笛卡尔坐标系、圆柱坐标系或球坐标系。

- **用户子程序**

ABAQUS/Explicit 允许用户通过用户子程序以代码的形式扩展程序的功能。并给用户提供了一些接口，方便用户定义材料模型和一般的加载条件。

导线卡子的机械特性会影响它的电可靠性。导线产生较大的塑性应变从而破坏其表面的氧化层，导线卡子在导线和导电支座间成型并递电流。



输入输出文件

输入

ABAQUS/Explicit 的输入文件是文本文件，通常由 ABAQUS/CAE 或其它前处理器以交互的方式产生。在执行分析之间通常要对输入的数据进行多方面的检查。

- **关键字**

输入文件由直观的关键词以及相关的数据组成。关键词表明了所选的选项，数据为自由输入格式。

- **集的概念**

可以把节点和单元组合成“集”，每个集由用户指定一个名称。集可以是嵌套的。这种集的概念给材料、载荷、约束的定义、输出的编辑等提供了一种简单易懂的引用方法。这个概念尤其对大型复杂的模型更有价值，他在分析模型的开发过程中简化了数据的处理。

- **简单的网格生成选项**

输入文件允许单元沿直线或曲线方向的增量填充，区域的填充以及对节点块的等参映射。

- **多坐标系**

具备笛卡尔坐标系、圆柱坐标系和球坐标系。对于节点位置、自由度方向以及材料方位可以指定独立的坐标系。

- **部件及装配**

ABAQUS 提供把有限元模型定义成各个零散部件的选项，随后在将这些部

件装配在一起。这个方案允许多次使用同一部件的定义来产生大的模型，也允许在模型里相互分离的部件中重复使用节点和单元的编号。

输出

- **交互式的图形后处理**

ABAQUS/Viewer(包含在 ABAQUS/Explicit 的使用许可中)提供了网格图、结果的等值线图、动画、时程变化图、矢量图、X-Y 图。还提供“点击”查询结果的功能。

- **外部文件输出**

分析结果可以选择性的写入输出数据库和结果文件中。存储在输出数据库中的数据可以被 ABAQUS/Viewer 读取，以此进行后处理。结果文件是标准的第三方后处理包进行交流的基础。

- **重启动输出**

重启动输出可以将所处理的问题分成方便的几个部分进行输出，以防止意想不到的程序终止。它的用途广泛，使用起来非常容易方便。

- **出错信息**

ABAQUS/Explicit 对出错的信息进行了描述，包括对出错的解释和建议。并且提供了一个含有时间积分细节的特殊诊断文件。

硬件和性能

硬件兼容性

ABAQUS/Explicit 是使用 FORTRAN、C 及 C++ 语言编写的，保持着多个版本，并被大多数的工程计算机所支持。ABAQUS/Viewer 支持标准的图形和绘图设备。

ABAQUS/Standard 及其界面产品在下列计算机平台上均可使用：

- **Compaq Alpha**
- **HP**
- **IBM**
- **SGI**
- **Intel Pentium**
 - Windows NT/2000/XP
 - LINUX
- **Intel Itanium**
 - HP-UX
 - LINUX
- **Sun**

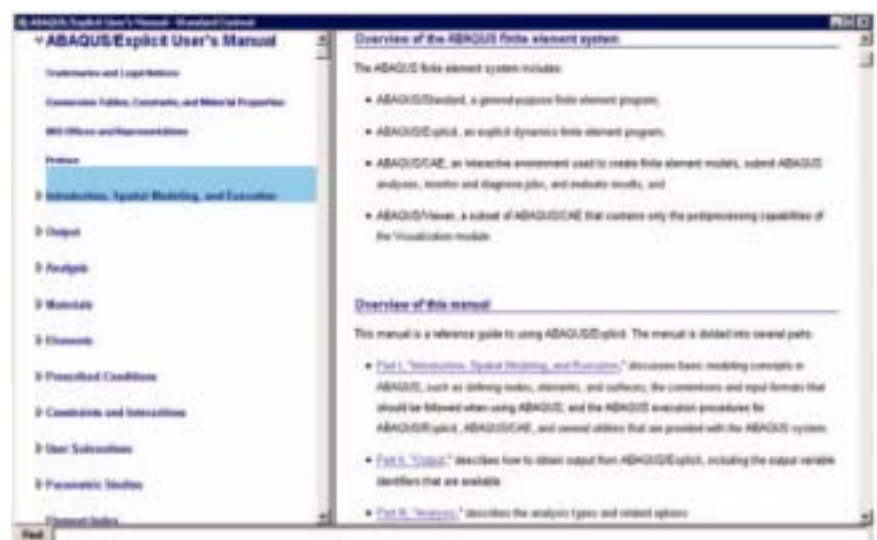
想了解更多的兼容硬件信息或者更详细的支持平台信息，请访问我公司网站：

www.abaqus.com

问题的大小与性能

ABAQUS/Explicit 所运算问题的大小没有内在的限制。算题完全在主存储器中运行。ABAQUS/Explicit 在大量类型的计算机上能有效的运行，对于大型的问题，在矢量/并行结构的计算机上运行尤其有效。ABAQUS 提供了一套在不同的计算机系统下完成的基准计算的时间数据，以此作为这些系统下代码运行性能基本的比较。

ABAQUS 的在线文档允许用户在全文范围内搜索相关的标题。



文 档

用户手册

这册书是 ABAQUS/Explicit 基本的参考文档。有印刷版本和在线两种形式以供使用。它包括对单元、材料模型、步骤、输入指令等的介绍。

关键字手册

这册书包括对 ABAQUS 里所有输入选项的完整介绍。有印刷版本和在线两种形式一供使用。

辅导手册

这本书被设计成为自学的辅导书，它将有助于读者熟悉使用 ABAQUS/Explicit 进行动态和准静态的应力分析；有印刷版本和在线两种形式以供使用。

实例问题手册

这册书包含 75 个以上的详细实例来展示如何进行具体实际意义计算的方法和决策。有印刷版本和在线两种形式以供使用。

基准例题手册

这册书包含用于评估 ABAQUS/Explicit 性能的 200 个以上的基准问题和标准分析；这些测试是使用多种单元对简单的几何体，或对简化了的实际问题进行的验算。又在线的形式以供使用，如需要也可提供印刷版本。

验证手册

只提供在线使用版本，它包括 5000 个以上基本测试例题。通过与精确计算或其它已公布的结果相比较来对每个程序特性进行验证。

理论手册

这册书包括对程序中所有知识点理论方面的详细和明确的讨论。适合具备一定工程背景的用户理解。有在线形式以供使用，如需要也可提供印刷版本。

产 品 支 持

维护与支持

ABAQUS/Standard 的商业用户通常选择完全的维护与支持服务。每当新版本发布时，这些用户就可以收到新版本。以在线的形式列出已知的程序缺陷及其解决方案的状态报告。ABAQUS 遍布各地的办公室和代表处网络给具备年度使用许可或选择付费的不间断支持许可的商业用户提供了广泛的、无限制的支持。这些支持包括对选择合适的单元、材料或步骤的建议，有关 ABAQUS 全面的信息和提供有关使用 ABAQUS 进行特殊模拟的指导。学术上的用户可以以较小的额外费用得到这些支持。

质量检测服务

ABAQUS 满足严格的质量保证标准并且达到了 ISO9001 和美国国家标准协会/美国机械工程师协会 (ANSI/ASME) 的 NQA-1 号规范要求。对于那些需要监督他们的供应商的质量保证行为的用户，ABAQUS 提供了一个质量监督服务。

安装

程序通常由用户来安装。根据要求，ABAQUS 的工程师或当地的代理将在用户的现场进行初始安装。安装服务包括对软件的检查和验证和参加培训研讨班。

培训和用户会议

ABAQUS 在其公司和当地的代表处组织经常和定期的公共培训班，还有在用户地点召开的研讨班。入门性的研讨班系列包括两个补充部分：ABAQUS/CAE 入门以及 ABAQUS/Standard, ABAQUS/Explicit 入门。为期两天的 ABAQUS/CAE 入门研讨班主要集中在使用 ABAQUS/CAE 进行模型前处理，提交和监督分析任务以及对模拟结果的交互式管理。为期三天的 ABAQUS/Standard 和 ABAQUS/Explicit 入门研讨涉及到一些分析的原理，集中与由或无接触的非线性静态的动态模拟。在入门研讨班之后提供了实质性的 ABAQUS 上机训练经验的研讨会。

也组织涉及特定主体的高级研讨会。就用户指定的主题进行现场讲解。有 ABAQUS 或 ABAQUS 当地代表处提供的高级研讨会涉及到这样一些主题，如非弹性本构模拟，大应变弹性，单元的选择和金属成型等。

所有的研讨会的培训材料可向 ABAQUS 公司或代表处联系购买。并给新手提供了一种辅导手册，即 ABAQUS/Explicit 入门指南。

ABAQUS 每年主办世界范围的用户年会。另外，所有世界上的 ABAQUS 用户群体组织一个地区性的用户年会。这些聚会给用户提供了学习和交流经验的论坛，一起讨论 ABAQUS 的能力，性能的提高以及 ABAQUS 及其代表处的相关服务。

产 品 综 述

简 介

ABAQUS/Standard 是一套专门为高级分析而设计的通用产品化有限元程序。它提供的虚拟分析工具广泛地适用于各种各样的问题中。

ABAQUS/Standard 能有效地运行基于 Windows NT 或 UNIX 操作系统的桌面计算机、各级服务器和超级计算机。

分析能力

ABAQUS/Standard 提供了大量的时域和频域分析的程序。这些程序分为两类：一类是通用分析 (General Analysis)，其响应既可以是线性的，也可以是非线性的；另一类是线性摄动分析 (Linear Perturbation)，由在某一特定的基准状态基础上计算结构的响应给予一个通用的可能是非线性的基态计算出线性响应。一次计算分析流程中可以包括多个分析步骤和多种分析类型。

通用分析

- 静应力/位移分析
- 粘弹性/粘弹性响应
- 瞬时动应力/位移分析
- 瞬时或稳态热传导分析
- 瞬态或稳态质量扩散分析
- 稳态传输分析
- 声学分析
- 耦合问题
 - 热力耦合(迭代低或者完全耦合)
 - 热电耦合
 - 多孔介质的流体力学耦合
 - 应力-质量扩散耦合
 - 压电耦合 (线性)
 - 声波-力学耦合 (线性)

线性摄动分析

- 静力/位移分析
 - 线性静应力/位移分析
 - 特征值屈曲载荷瞬态响应
- 动态应力/位移分析
 - 确定固有模态和频率
 - 模态叠加的瞬态响应
 - 简谐载荷的稳态响应
 - 响应谱分析
 - 随机荷载的动态响应

材料库

ABAQUS/Standard 提供的材料本构关系模型有金属、静力学流体、橡胶、塑料、复合材料、可回弹可挤压的泡沫、混凝土、沙子、粘土和连接的岩石，每一种材料表现了高度的非线性特性。提供了包括一般弹性，弹性-塑性，弹性-粘弹性等材料特性。可以模拟各向同性材料和各向异性材料，用户还可以通过用户子程序接口自定义材料。

几何模型

可以模拟结构和连接介质。提供了一维、二维和三维的实体单元以及梁单元、薄膜单元和壳单元。梁单元和壳单元是基于现代离散 Kirchhoff 或者剪切变形弯曲理论所构成的非常有效的单元。壳单元提供了热传导和热应力分析功能，它能够直接分析热荷载作用下的壳体结构。ABAQUS/Standard 是模块化程序，任何单元的组合以及任何适当材料的模型都可以用于同一种分析中。

运动学特性

ABAQUS/Standard 的所有单元（不包括一些特殊用途单元）均能够为任意大小的位移、旋转和应变提供准确的模拟。

预设条件

边界条件包括预先设定的运动约束（单点和多点约束）和预先设定的基础条件。载荷条件包括集中载荷，分布载荷和热载荷。在装配系统中，可以通过一种特殊的加载方法对螺栓或其他紧固荷载直接指定。可以在适当的位置引入伴随力影响，如压力、离心力和 Coriolis 等。提供了多孔介质流体压力场、电势场和其他的标量场的载荷和边界条件。可以给定温度、速度、应力和其他许多场的初始条件。

直接作用

提供了模拟物体之间相互作用的通用功能，包括有或无摩擦的面-面接触。提供了完全耦合的热-力相互作用功能，如热和力可以进行转换，解除表面间的热阻力可能取决于接触面之间的压力或截面间的力学分离。对于动力学和振动分析：提供基于表面的相互作用功能来对结构和声波介质模型进行耦合分析。还提供含多孔介质流体流动-应力耦合和热-电耦合的相互作用。

其他分析方法和模拟技巧

- 对始于 ABAQUS/Explicit 的模型继续模拟
- 将结果传递给 ABAQUS/ Explicit 继续模拟
- 从中间状态重新启动分析
- 子结构
- 子模型
- 材料的减少与增加
- 断裂力学设计评估
- 对称模型的建立及结果的转化
- 循环对称模型的建模
- 惯性平衡
- 过约束的自动求解
- 自动的过约束处理
- 重新加强
- 嵌入单元
- 多坐标系导入
- 局部自由度
- 流体静力学单元
- 熄火
- 超级单元和子结构
- 参数化法和参数研究

附加模块

ABAQUS/Standard 的分析能力在与下列模块联合使用时可以得到提高

ABAQUS/Design

作为 ABAQUS/Standard 功能的扩展，提供了设计灵敏度分析的功能。

ABAQUS/Aqua

应用了 ABAQUS/Standard 进行的海洋工程结构分析功能

界面产品

界面产品的使用使得 ABAQUS/ Standard 显示出没有使用这些模块时更强的分析功能。界面产品可以是单向的也可以是双向的，单向的界面产品允许在其它产品中进行的分析继续在 ABAQUS/ Standard 中继续进行；双向界面产品除了能支持此功能外还允许在 ABAQUS/Standard 中进行的分析在其它产品中继续进行。可应用的界面产品：

ABAQUS/MOLDFLOW
ABAQUS/C-MOLD
ABAQUS/ADAMS

性能

ABAQUS/Standard 用高性能、并行、稀疏、多波前方程求解器的解来解决方程对称和非对称系统，并自动根据问题的物理要求决定是否采用非对称的方法。并行计算可被用于绝大多数的硬件平台，对于特征值问题 ABAQUS/Standard 采用对于大型模型很有效的 Lanczos 特征值求解器。在非线性问题中，一大挑战是如何花费最小的费用得到一个收敛解。这个挑战可以通过时间增量的自动控制功能达到目标。这项功能在所有相关分析程序中都能提供。用户定义“一步”（整个分析历史的一部分，例如在一个加工处理过程中的热传递，或者一个动态事件），然后 ABAQUS/Standard 自动选择这一步所要求的收敛公差和增量。这个方法对于非线性问题是十分有效的，因为在分析过程中模型响应的变化可能是非常剧烈的。自动控制可以使用户对非线性问题不必有大量的经验便能自如地运用。这是 ABAQUS/Standard 许多特色中的一个很好的例子，正是这些特色使 ABAQUS/Standard 成为一种注重效益与产出的分析工具，并与其他有限元程序相区别。

分析功能

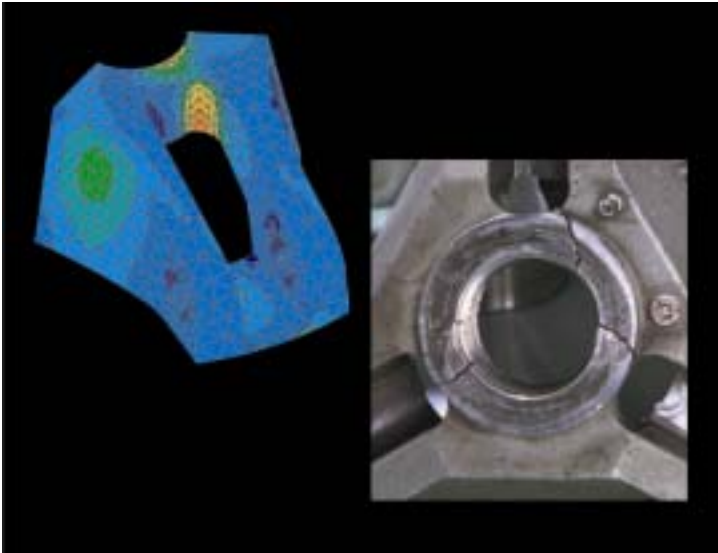
ABAQUS/Standard 的分析程序可以以任意的混合方式，例如在一个一次计算模拟中可以包括一个非线性静态分析，同时跟随一个非线性动态分析，静态分析的最终计算结果是动态响应的初始条件。

为了使用方便，用户可以将载荷力成分若干个步骤加载。对于一个纯线性的分析，每一步在本质上都是一个加载事件。而对于一个非线性分析，每一步都是典型的整个加载历史的一个步骤。在每一步中每一分析类型都有明确的规定。

线性分析可以对非线性基础状态做线性扰动。比如：一个橡胶部件在一个非线性静态分析中产生变形并被预加应力，接着通过一系列线性扰动研究，应用由基础状态导出的刚度和几何性质来获得该部件的自然频率和小振动响应。

对于非线性分析，每一步的初始条件都是上一步结束时模型的状态。这种依赖性为分析复杂的加载历史，比如制造过程，提供了一种便捷的方法，每一步被细分为微小增量，对于每一增量，ABAQUS/Standard 在大多数情况下应用完全牛顿方法使方程迭代至平衡。用户不必考虑这些公差，收敛准则由 ABAQUS/Standard 自动决定。

分析状态可以在 ABAQUS/Standard 和 ABAQUS/Explicit 间传递。这种结果传递允许模拟在两种 ABAQUS 求解器下运行，允许在模拟的每一过程都能用最合适的求解器技术。例如：几个构件能同时用 ABAQUS/Standard 装配来建立初始静态预加载模型，然后可继续在 ABAQUS/Explicit 中建立有预加载的冲击问题模型，同时，也可预先在 ABAQUS/Explicit 中进行成型模拟，然后将模型传递给 ABAQUS/Standard 中来确定考虑拆除工具和切割构件后的回弹量。



在比赛状态，高性能雪橇的离合器的轮毂可能产生很大的离心机械力。发动机功率超过其额定功率时很可能引起轮毂的机械失效。ABAQUS/Standard 用来决定疲劳失效的原因，并检验其重新设计的合理性。

一般非线性分析

这些分析可以考虑模型中任何非线性因素的影响。

• 静应力/位移分析

提供了两种静载荷分析方法。一种针对必须遵循规定的加载历史（比如在热振动中的瞬时温度）的情况，这种方法中ABAQUS有一个选项用于自动控制局部不稳定行为。另一种方法是弧长（修正 Riks）方法，用于分析全场不稳定静态问题，比如完全破坏或后屈曲的情况。

• 粘弹性/粘弹性响应

ABAQUS/Standard 提供了显式和隐式的时间积分方法，并且能保证最大计算效率的条件下它们之间自动转换。

• 动态响应/位移分析

对于完全的非线性问题，ABAQUS/Standard 包括直接的、隐式的时间积分，采用 Hilber-Hughes 算子（可控制值得阻尼的 Newmark 方法）。基于中心差分方法的显示积

分在 ABAQUS/Explicit 中是可用的。两种积分方法中都采用自动时间增量。

对于不明显的非线性问题提供了一种投影方法，应用系统的特征模式，对于非线性解答将其响应发展为整体基本函数。这些特征以模式系统初始构性为基础，并能在求解过程中被周期性更新。这种方法对一些涉及局部非线性响应的重要应用非常有效，例如带有非线性约束的管道系统。

• 热传导分析（瞬态和稳态）

主要涉及传导、辐射和强迫对流，还包括完全空洞辐射功能（在“相互作用”一节还有进一步的介绍）。

• 质量扩散分析（瞬态和稳态）

集中和静水压应力梯度都能造成质量扩散。以此来分析一种物质通过另一种物质的扩散（比如：氢气通过金属的扩散）。

• 稳态传输

物质通过一种固定的参数框架，像物质绕一固定的轴的旋转一样，都可以采用混合拉格朗日

（Lagrangian）欧拉法（Eulerian）来描述。物质的运动可以看作是刚体转动的一种组合，可用空间或欧拉法方式描述。这种方法对于建立轮胎的稳态旋转模型是特别有效的。

• 声学分析

声学分析能力使得对于声学介质中的声音的传播、反射、辐射的建模成为可能。

• 耦合问题：

- 热力耦合

进行连续的热应力分析使可用一个简单的数据选项，通过瞬态热中的自动增量直接把热传导计算结果传递给应力分析。这种能力使热振动分析变得相当便捷。另外，对于包括双重耦合的问题（比如摩擦生热）完全耦合分析可同时求解温度场和位移场。

- 热电耦合

温度场和电势场可同时求解。

- 压电耦合

耦合位移场和电势场的线性解可同时计算。

- 有孔流场的流力耦合

ABAQUS/Standard 的这个功能可以应用于等效应力和孔流场流动耦合问题。可以解决涉及到地下水表压力和毛细作用的半渗透问题的耦合问题。

- 声力耦合

在频域或时域中解决声波-建筑物的完全或者顺序耦合振动分析问题。

- 热/力质量扩散耦合

质量扩散模拟可以从热传导和应力分析的结果导出。

线性摄动分析

ABAQUS/Standard 这些分析提供了分析关于基本状态的扰动引起的线性响应功能，这种扰动可能是结构的起始状态，也可能是由先前的一般非线性分析分析造成的。用 Lanczos 法或空间迭代法可以提取屈曲问题的特征值和求解问题的固有频率。Lanczos 特征值求解器处理较大模型或较多特征值时都很有效。

• 静态应力/位移分析

- 线性静态应力/位移分析

线性静态分析包括荷载情况和边界条件的详细说明。

- 屈曲问题特征值预测

可指定任意的预加载荷和动态荷载，在提取特征值过程中的边界条件可以与预加载过程中的边界条件不相同。

• 动态应力/位移分析

- 固有频率提取

由于程序在分析过程中的每一时刻都可能被调用，所以预加载的影响可能也包括在内。

- 瞬时响应

用结构的特征模态迭加的方法求解线性化系统的瞬时响应。

- 简谐和载荷稳态响应

某些周期荷载在一定的频率范围内通常可以得到结构特征模态的稳态响应。

- 响应的谱分析

由用户提供的响应谱和系统的特征模态可以计算响应变量的峰值。有可供选择的几种模态组合的方法。

- 随机响应分析

基于系统的固有模态，计算模型对随机激励的线性响应。

材料定义

提供了大量的材料模型。多数材料参数依赖于温度场或预定义的场变量，比如在多物质中某一特定项密度。提供一选项，其作用是通过材料属性的输入网格和应力/应变的输出网格确定局部相位。这个选项对于模型复合材料层合系统和其他各向异性材料是很有用的。

弹性分析

• 线弹性

弹性增量可以是各向同性、正交各向异性或各向异性。

• 平面应力正交各向异性失效

提供了与线弹性结合的失效理论。它们可以被用于后处理目标输出文件和典型的复合壳材料的分析。

• 多孔弹性

提供含孔洞的材料模型，其体积的

弹性部分的变化取决于压应力的对数值。这种模型经常用于定义土壤和可挤压泡沫的弹性特性。

• 亚弹性

亚弹性允许模量随应变发生变化。

• 超弹性

ABAQUS/Standard 用这些模型研究橡胶类材料的大应变弹性响应。

软件提供了五种超弹性模型：一般多项式应变能函数（包括 neo-Hookean 和 Mooney-Rivlin），Ogden 模型，仅有第一不变量的缩减多项式模型（包括 Yeoh 模型），Arruda-Boyce 模型和 Vander Waals 模型。上述模型可用于完全不可压缩或接近不可压缩响应。对于完全不可压缩行为可以应用杂交单元（即位移和压力的混合差值）。

Bergstrom-Boyce 模型可以作为任何存在弹性滞后或其跟速度有关的超弹性模型间的媒介。还提供用于描述含大量空洞的，有弹性的泡沫模型。所有的大应变弹性模型的材料常数可以被直接确定或由用户提供数据用 ABAQUS /Standard 计算得出。

• 粘弹性

提供了既有时域又有频域的粘弹性模型。时域模型可以用 Prony 序列表示法对小应变问题进行描述，Prony 序列常数由用户指定的测试数据创建，可以用 ABAQUS/Standard 计算得到。粘弹性材料可以看作简单热流体（简称 TRS）；软件提供了 Williams-Landel-Ferry 关系，其它的 TRS 关系可以由用户程序确定。时域的粘弹性模型既可以和线粘弹性模型也可以和超粘弹性模型组合。

塑性和蠕变

• 金属塑性

金属包括符合 Mises 屈服准则的各向同性塑性模型和遵循 Hill 各向异性屈服准则的各向异性塑性模型。流动准则是相关流动，硬化准则是各项同性，双线性运动的 ORNL 理论。同时，还有用于非弹性的循环荷载引起的非线性各向同性/运动硬化。另外，还提供用于作为空核、应变硬化的基本材料的多孔金属的 Gurson 塑性模型。

• 铸铁

在拉伸时为 Rankine 屈曲准则。在拉伸而不是压缩时流动时允许非弹性膨胀，而单向拉伸和单轴向压缩对应于不同的硬化曲线。

• 蠕变

提供了包括 Singh-Mitchell 模型在内的时间硬化和应变硬化定律的各向同性蠕变的各向异性蠕变功能。其他特殊的蠕变定律可由用户子程序定义。当显示时间步受数值稳定的原因限制时，ABAQUS/Standard 会自动切换到隐式时间步，这为解决长时间蠕变问题提供了一种有效解法。对于 Mises, Duncher-Pager 和 Cap 塑性提供了一种一致集成各向同性蠕变模型。

• 体积蠕变

以一种场变量函数的形式提供了各向同性和各向异性材料随时间的体积变化情况。应用相应表格或用户子程序都可以确定体积膨胀率。

• 双层粘塑性

这种模型的建立是基于 Mises 或 Hill 屈服准则，以及 ABAQUS/Standard 提供的其它能量蠕变模型。它不同

于常规的塑性或蠕变模型，它考虑了粘性和塑性特性的耦合。这种模型在模拟大温度变化范围内交变载荷作用下的结构响应时非常有效。

• 扩展 Drucker-Prager 模型

这种模型提供了各种压力相关的屈服面和应变硬化/软化的表征。应变率，粒状材料如沙子的非相关流，材料如橡胶等拉压特性的不同等都可以在这种模型中考虑。

• Capped Drucker-Prager 模型

这个模型中把临界状态模型和扩展的 Drucker-Prager 模型结合在一起。这种模型适用于地质工程行业，例如隧道挖掘。

• Cam-clay 模型

ABAQUS/Standard 提供了粘土类土壤的临界塑性状态，它定义了由三种应力变量表示的屈曲函数确定的材料非弹性行为，用相关流动假设定义塑性应变速率，通过非弹性体积应变改变屈曲表面尺寸的应变硬化理论。

• Mohr-Coulomb 模型

该模型针对诸如沙子的粒状材料提出，它使用 Mohr-Coulomb 屈曲准则，但是带有光滑 Menetrey-Willam 流动势。这种模型跟 Capped Drucker-Prager 模型很相似，但是有不光滑小屈服表面。

• 可挤压泡沫

这种模型适合于模拟可高度挤压的材料，例如消费品的包装以及车辆安全装置中的一些材料。

• 有接缝的材料

这种模型用来分析类似沉积岩那样有裂缝或有缺陷的材料。其响应包括有沿着接缝开裂口或散装材料失效处摩擦滑动引起的影响。

• 与应变速率相关的塑性

伴随着应变的增加，许多材料的屈服强度也会提高。就像扩展的 Drucker-Prager 模型和可压缩的泡沫塑料模型，所有金属材料塑性的硬化模型可能跟速率无关，也可能是跟速率有关的（粘塑性）。源于实验数据的速率相关硬化数据可以用简单的列表方式定义，这种方式可以自动插入数据。另外，还提供了 Cowper-Symonds 过应力模型。

• 混凝土

这种模型提供了混凝土弹塑性破坏理论，包括利用弹性断裂概念分析拉伸断裂、压缩断裂、混凝土-钢筋交互作用以及裂纹出现后的响应等。

附加材料特性

• 密度

密度对于动态问题或热传导问题是必要的。

• 热膨胀

定义了各向同性和各向异性材料的热膨胀系数，这些系数依赖于温度场或指定场变量。

• 热传导率和导电率

定义了与温度和场变量相关的各向同性、正交各向异性或完全各向异性材料的传导率。

• 比热

定义了与温度相关或与场变量相关的比热。

• 潜热

应用一种内部能量方法来保证与相位变化相关的剧烈潜热影响预测的精度。

• 压电属性

定义了各向同性、正交各向异性或完全各向异性材料的电解质特性。

- **材料阻尼**

对通用分析流程，可以指定刚度或质量比立阻尼。对线性摄动分析，则有更多的阻尼模型可供选择。

- **流体静力学特性**

气体和液体的特性如质量密度、体积模量、温度扩展系数等可以指定为温度和其他场变量的函数

- **质量扩散特性**

材料的溶解性、各项同性、正交各项异性和各项异性质量扩散特性可以定义为浓度、温度和其他场变量的函数。

- **流特性**

可以定义充满液体的多孔材料的各种特性。各项同性、正交各项异性或完全各项异性材料的渗透性可以依赖于空隙率、饱和度和温度等。多孔材料体积膨胀率可以定义为温度及各种吸收和外渗行为的函数。另外，也可以定义多孔介质的实体框架的膨胀特性。

- **声音介质属性**

这些属性是与频率和温度相关的。

- **无拉力模型**

这个模型消除了拉伸主应力。

- **无压力模型**

这个模型消除了压缩主应力。

- **用户材料**

通过用户子程序可以定义任何补充的材料模型。与任意数量的材料常数都可以作为数据被读取一样。ABAQUS 对于任何数量的与解相关的状态变量在每一材料计数点都提供了存储功能，以便在这些子程序中应用。

单元库

单元库为几何建模提供了最大限度的可选范围。单元有如下分类：按基本理论的不同分为连续体单元、壳单元、梁单元、构架单元等；按维数或应力表示法的不同分为一维单元、二维单元、平面应变单元、平面应力单元、轴对称单元、三维单元等；按主要变量的不同分为位移单元、温度单元等；按公式表示法或积分法的不同分为缩减积分单元、杂交单元等。向小位移分析一样，对于大位移或有限应变都有应力单元的列式。

实体单元

- **插值函数的阶次**

采用一次、二次插值的单元。

- **拓扑**

一维问题单元可直接连接；对二维问题和轴对称问题（包括轴对称模型受非对称荷载）对三角形或四边形单元；对三维问题可提供四面体、五面体单元或六面体单元。对于二次插值的六面体单元的接触问题可提供特殊的“中面”结点单元。对于接触问题还可提供特殊二次插值的三角形和四面体单元。任何六面体单元均可被定义为多层固体单元来模拟复合材料固体。

- **数值积分**

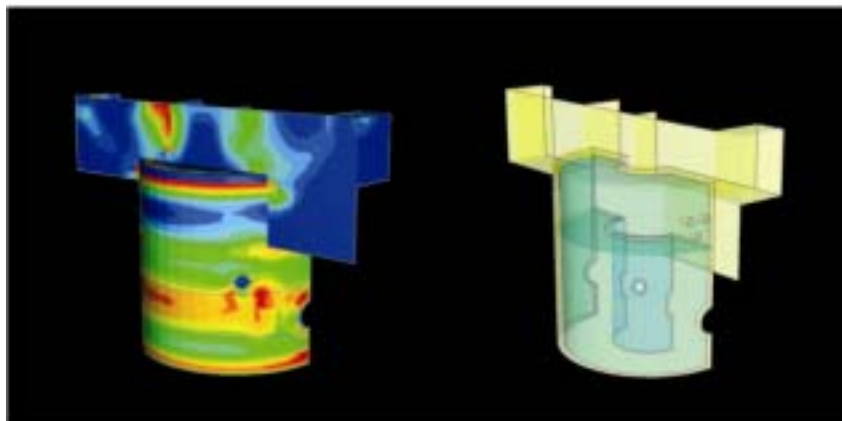
对于三角形和四面体单元采用完全积分。对于没有位移自由度的单元只能采用完全积分方案、选择性的缩减积分方案和沙漏控制的缩减积分方案。对于有明显弯曲的响应和不可压缩情况可分别采用“非协调”单元或杂交单元模型。

- **应用**

- **应力分析**

上述单元适用于以下应力类型的分析：三维问题、平面应力问题、平面应变问题、广义平面应变问题（包括有初始弯曲的问题）、轴对称问题、广义轴对称问题（即运行有限扭转问题）、轴对称结构非对称问题（即允许轴对称结构产生非线性变形问题）。

ABAQUS/Standard 的混凝土模型可以用来进行核反应堆加强混凝土外壳的设计。核反应堆外壳承受内压载荷，通常通过测量拉伸破损变量进行其结构设计。ABAQUS/Standard 混凝土结构破损塑性模型可以验证上述设计的有效性。



- 热传导和质量扩散分析

具有模拟一维、二维和三维问题的单元。对单纯热传导和有强迫对流的热传导问题都有可用热传导单元。

- 声音介质模型

有适用一维、二维、轴对称和三维问题的单元。

- 耦合问题

可以模拟温度-位移耦合，有孔流场-位移耦合，压电耦合，热-电耦合，声波-结构耦合响应。

壳单元

• 插值函数的阶次

采用一次、二次插值的壳单元。

• 拓扑

对于三维问题可提供 3 节点、6 节点的三角形或这 4 节点、8 节点、9 节点的四边形壳单元（包括几何轴对称模型受非对称荷载问题）。所有的壳单元都能模拟复合材料层合结构。由结点位置确定的壳单元参考面可以放置在壳厚度方向任何位置。

• 数值积分

提供采用完全积分的三角形和完全积分或减缩积分的四边形壳单元。壳单元界面的刚度在全部分析过程中可以不断地被重新计算，以便反映非线性的材料性质；对花费小的线性材料响应只需做一次积分即可。无论在何种情况都可以考虑几何非线性的影响。在 ABAQUS 中，壳单元是真正的双曲线壳单元，并且既有考虑剪切变形壳单元（“厚”壳），又有“薄”壳单元。壳的初始厚度在单元或节点处指定，并可重现最终厚度的分布。

• 应用

- 应力分析

- 三维热传导分析

- 完全耦合的温度-位移分析

薄膜单元

• 插值函数分析

采用一次、二次插值的薄膜单元。

• 拓扑

对于三维问题，可以提供 3 节点、6 节点的三角形或者 4 节点、8 节点、9 节点的四边形薄膜单元。另外，还提供 2 节点、3 节点的轴对称和广义轴对称（即允许有限扭转）膜元。

• 数值积分

对三角形膜元采用完全积分，对四边形膜元可采用完全积分、减缩积分。薄膜的初始厚度在单元或结点处指定，并可重现最终厚度。

• 应用

薄膜单元只能用于应力分析。

梁单元、管单元、肘状单元

• 插值函数阶数

采用一次、二次插值单元。当用户想在支持体和连接体间模拟一个单元的情况下，梁单元库提供了描述此类框架结构的两结点立方体单元。

• 拓扑

对于二维和三维问题可提供 2 节点或 3 节点梁单元或管单元，而 2 节点或 3 节点的肘状单元只适用于三维问题。

• 数值积分和截面性质

可以提供 Timoshenko 和 Euler-Bernoulli 弯曲理论。允许开截面梁单元翘曲；允许管单元横截面的均匀膨胀，所以可以模拟内压强的影响，特别是弹塑性弯曲应力响应中环向应力的影响，肘状单元在非线

性问题中可以模拟椭圆形弯曲影响。对于梁单元可以提供截面库，其中包括：矩形截面、梯形截面、管状截面、圆截面、“I”型截面、“L”型截面、六边形截面和任意横截面。用户可以选择截面的数值积分（模拟材料的非线性）或者指定一般的线性或非线性截面响应矩阵。

• 应用

这些单元可以在多种应力分析中应用。梁单元与响应阶次的壳单元和固体单元协调连接，并经常被用于有加强筋情况的壳单元中。杂交（混合）梁单元和管单元常用于细长或刚度过大的情况（几乎不可伸展的梁）。实例包括柔软的海底管道和弹性动力学分析（诸如交通工具的刹车系统）中的升管系统或刚性部分。肘状单元用于椭圆形或翘曲截面对整个系统的刚度影响过大的那些管道问题。

框架单元

• 拓扑

对二、三维问题可提供 2 结点框架单元。

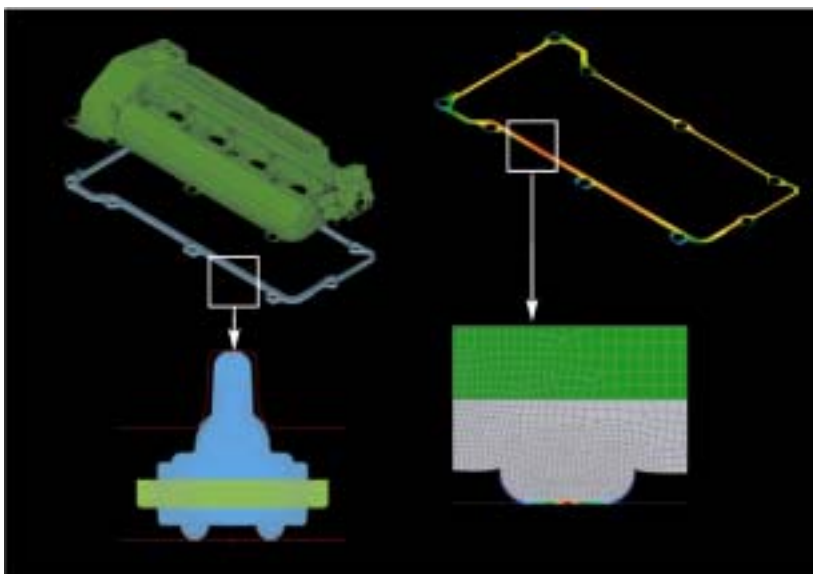
• 框架特性

弹性响应由 Euler-Bernoulli 梁理论导出，对横向位移采用四阶插值。塑性响应集中在单元末端（塑性铰发生处），由包括非线性动态硬化的塑性模型控制。应用 Mrshall 压杆在管道横截面装配来承受载荷时，框架单元可以体现塑性屈曲。

• 应用

框架单元描述细长、初始为直梁的框架类结构的小应变弹性或弹塑性分析。典型的例子是一个简单框架单元可以描述连有两个连结头的整个结构构件。

汽车发动机结构的垫片执行两种功能。其首要的功能就是提供汽车结构整个寿命中发动机工作环境下的密封。另外垫片刚度或其他特性还应该设计成避免结构的过大振动和噪声。ABAQUS/Standard 提供的专用的垫片单元提供了模拟实际垫片结构厚度及三维空间中缝隙和压力分布等特性的工具。



桁架结构

• 插值函数的阶次

提供采用一次、二次插值单元。

• 拓扑

对于二维、三维问题提供了 2、3 节点桁架单元。

• 应用

- 应力分析

单元仅承受轴向荷载。杂交的桁架单元可以用于模拟向对于分析模型其它部分非常刚硬的构件。

- 热传导分析

可以模拟沿单元的热传导。

- 温度-位移完全耦合的分析

- 压电耦合分析

垫片单元

• 插值函数的阶次

提供了采用一次、二次插值单元。

• 拓扑

对二维问题中可以提供三角形或四边形单元，对三维问题中可提供五面体或六面体单元。另外，在二维和三维问题中采用 2 节点单元模拟

结点附近的行为，三维问题中也用线性单元模拟柱型、环型等等构造。

• 垫片结构

单元用于自由度为面内和厚度方向或仅为厚度方向的情况。对于这两种类型的单元，垫圈特性在整个厚度方向可以是弹塑性或非线弹性，包括破坏的影响。这些特性被定义为一系列由试验数据确定的压力封闭曲线。这些测试数据选项在软件中已经建立，也可以是用户自定义的小应变材料模型。带有面内自由度的单元可以反映弹性和横向剪切行为，还可以用来研究垫片的摩擦效应。除此之外，还包括垫圈的热膨胀和蠕变。

• 应用

这些单元用来模拟垫片和其它在厚度方向有复杂的非线性行为的构件。它们允许用测试结果直接定义垫片单元的行为，而不必拟合某些材料模型结果。当应用 ABAQUS 的接触功能时，垫片的网格划分不必跟相连部分的网格相匹配。自由度仅在厚度方向的垫片单元可以对整

体装配的分析十分有效。例如用超级单元模拟头部和滑轮的发动机模型。

惯性、刚性和热容量单元

• 质点和转动惯量

可以指定对角线或非对角线上的质量和转动惯量的项。

• 刚性单元

可提供二维和三维单元模拟刚性体接触的相互作用。刚性单元也可以与可变形体是相连接。

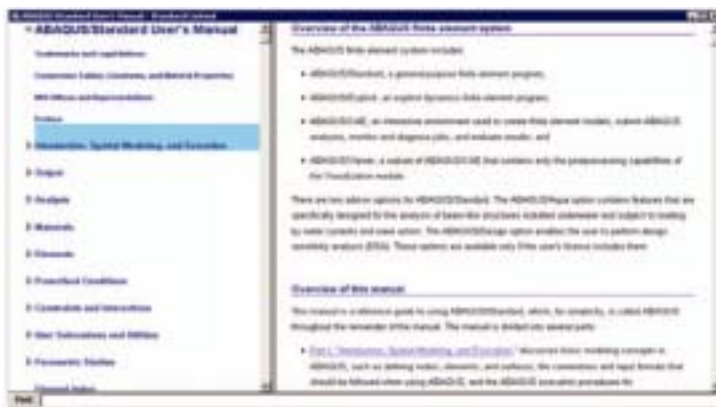
• 容量单元

点的热容量单元允许从一点把集中的热容量引入。

刚性体和等温体

• 刚性体

刚性体常被用于在模型中变形相对于其它部分可以被忽略的地方，比如橡胶封处的硬结构。刚性体可以有几种方法定义：有几何特征；有刚性单元；任意指定能作为刚性结构组合，如：梁单元、连结体单元、垫圈单元、薄膜单元、壳单元、桁



用户可以通过 ABAQUS 在线帮助在手册中自动搜索相关的主题。

架单元。结点组也可被作为刚性体的一部分，同时这种设置也提供了一种定义确定的约束比较简便的方法。刚性体的重心、质量和惯量可以由材料密度和几何离散度直接确定或由 ABAQUS/Standard 自动计算得出。

• 显示体

显示体和刚体类似，但它只用于显示，没有任何节点和单元参与分析，但是在后处理过程中可以显示。显示体的运动由参考点的运动控制。显示体在由连接单元连接的多刚体的机构分析和多体动态分析中非常有用。在这种情况下这部分可以以简单的刚体的形式来显示也可以以复杂的显示体形式来表示。

• 等温体

等温体是指热量相等的刚性体，它可被用于热传导和温度-位移耦合的分析中模拟物体温度均匀但随时间变化的情况。

连接单元

• 连接单元

连接单元用于模拟节点间离散的物理连接，可以在带有任意柔性或刚性部分的情况下使用；实例中包括运动约束（诸如夹槽、卷槽约束等），单一部件非线性材料响应和单向接

触约束。此外，带有部件相对运动的连接单元（即与从运动学角度没有被约束的相对运动自由度）允许激励运动，在这种激励运动的连接处，比如齿轮装置的臂或水压机的活塞等，相对运动部件的位移历史和受力历史是已知的。

• 线性和非线性弹簧、阻尼器和连接点

弹簧和阻尼器可以用来固定方向或放置在结点之间。弹簧和阻尼器的并联可以看作表示有内部刚度和阻尼的连接来描述柔软、有转动的连接点。弹塑性连接单元结合集中弹性响应来模拟结构构件间的连接或结构构件与固定支撑的连接。

• 弹簧/摩擦/阻尼器组合单元

这些单元用于模拟管道和支撑结构间的相互作用（诸如蒸汽式发电机中气流流动引起的振动研究）。

• 静水流体单元

提供二维和三维的静水流体单元用来模拟在充满流体空间中流体温度和压力在每一点都恒保持一致的问题。流体连接单元允许流体在两个流体空间流动。这里所指的流体可以是气体，也可以时刻压缩或不可压缩的液体，还可以通过用户子程序定义其性质。其应用包括水压式发动机装置，空气式减震器装置和

水压式激励器。

• 管道支撑单元

管道支撑单元用于模拟当管道和支撑体的连接发生分离时管道与它临近的支撑体之间的相互作用。

• 分布式耦合单元

分布式耦合单元通过用户定义的加权因子在单元节点与单元节点组之间分配质量和荷载。

特殊要求的单元

• 线弹簧单元

线弹簧单元用弹性或弹塑性材料行为模拟壳中的短裂纹。

• 无限单元

可以提供一次和二次插值的无限单元，在二维和三维问题涉及半无限或足够大空间的问题中与通常的有限单元组合应用。在静态分析中，它们可以模拟域内的弹性响应；在动态分析中，它们能模拟一种不向模型体内部反射压力波的“静”边界。

• 管道-土壤相互作用单元

管道-土壤单元模拟埋入的管道的周围土壤之间的相互作用。

• 用户定义单元

用户自定义的任何类型的线性或非线单元都可以被引入模型中，对于线性单元刚度矩阵和质量矩阵可

以直接确定。同时，用户子程序也可被用来定义这些单元的线性和非线性特性。

几种其它的以单元为基础构成的模型、工具将在随后的“连接作用”部分中讨论。

预设条件

• 幅值曲线

所谓的振幅曲线可以通过离散数据点、Fourier 级数和其它函数描述，这些函数可以在描述任何荷载与边界条件的变化中参考使用。

• 初始条件

初始条件可以由很多场变量定义，数据可以从列表中读入，也可以从其它 ABAQUS 分析中引入，还可以由不同的用户子程序定义。

• 边界条件

边界条件可以用模型中任意有效的自由度上指定，也可以用经过一段时间加载后的当前值确定。

• 荷载

每一种荷载在相应的幅值曲线中都有涉及，诸如在地震分析中的地表加速度或有复杂的压力脉冲历史分析。分布荷载可以直接加在单元或表面。不均匀的分布荷载也可以由用户子程序定义给出。在相应的问题中可以应用下列荷载：均匀体力、不均匀体力、均匀压力、不均匀压力、静水压力、旋转加速度、离心荷载、Coriolis 力、弹性基础，伴随力效应（包括荷载刚度项）。

用户还可以应用集中力和弯矩，包括在任意时间变化内指定的伴随力；温度；场变量和非零位移，转角，速度或加速度。对于热量和其他非结构模型也提供相应的荷载。

• 规定组合荷载

对于有紧固螺栓或连接物的部件的规定的组合荷载。

• 预定义场

这些是温度以外的场，而材料特性也许会依赖于他们。

连接作用

模型的各部件可以有多种方式互相作用。

• 通过接触

• 通过已有的运动约束

• 通过已有的铰接约束

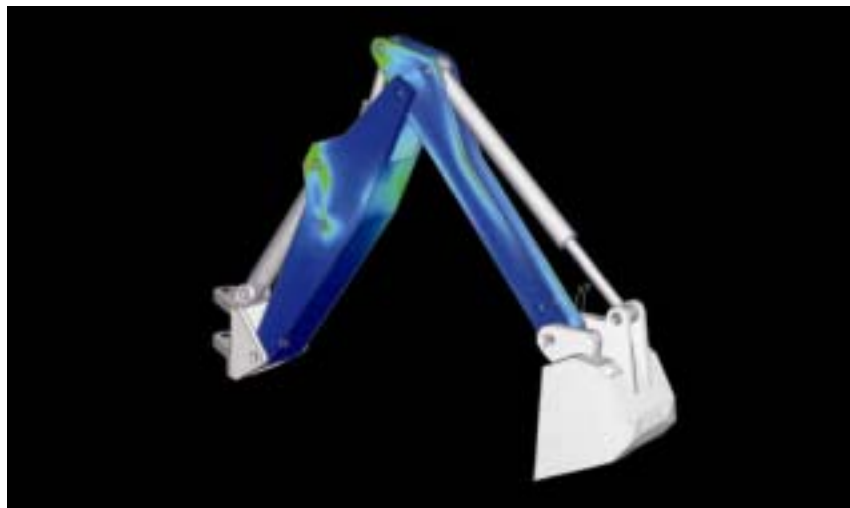
• 通过辐射热的交换

接触交互作用

ABAQUS/Standard 提供了大量可延伸的功能来模拟接触和表面相互作用问题。提供了两种基本方法：基于表面的模型和基于单元的模型。

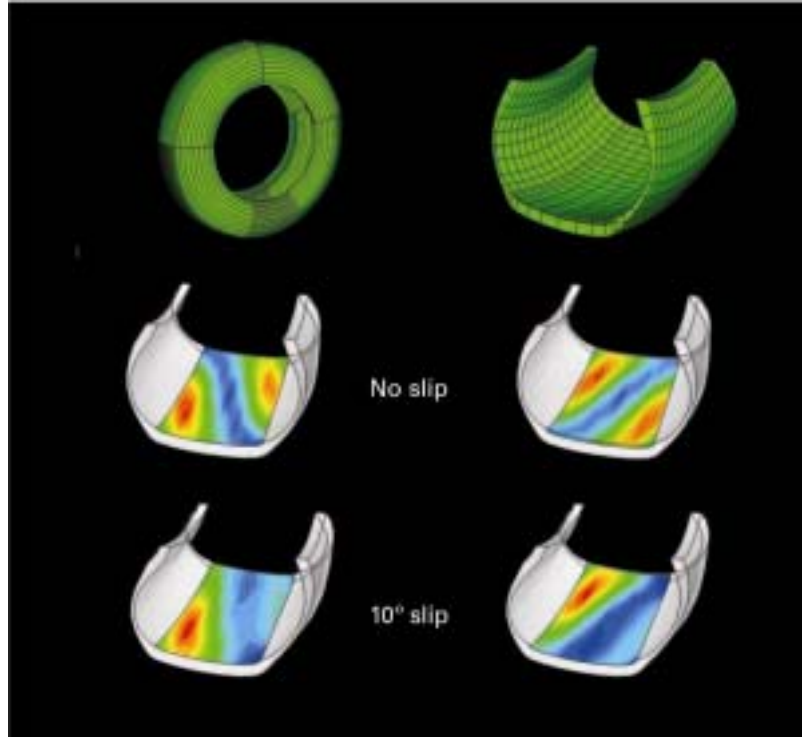
• 基于表面的模型

典型模拟接触问题的方法是确定可能接触的两个表面并给此接触对命名。这对接触既包括两个变形体之间的相互作用，也包括一个变形体和一个刚性体之间的相互作用。刚性体可以通过刚性单元来离散，也可以通过旋转/扩展二维表面来生成三维表面的法解析地生成。二维和三维问题中接触体之间的小滑动和有限滑动也可以被模拟。在二维问题中，用自接触算法处理一个表面和它本身的接触问题。



连接单元、刚体和变形体单元以及显示体等组合起来可以快速和精确地模拟右图所示挖掘机构动力学特性。

轮胎中的应力会随着运动方向轮胎轴的方向之间的夹角（即侧滑角）有显著的变化。ABAQUS/Standard 有几种专门的方法——比如圆柱单元、对称转动、加强筋定义等——可以高效率的模拟轮胎在不同条件下的响应。



• 表面相互作用的属性

多数情况下的接触问题都可以被模拟。

- 力学的接触问题

用静态的或运动的 Coulomb 摩擦模型可以描述剪切相互作用。摩擦系数取决于切向滑动速度，接触压力，平均表面温度和场变量。对于更加复杂的情况相应可以通过用户子程序定义摩擦特性。表面可以被完全绑定在一起或根据一个指定的规则绑定。提供各种有间隙的接触压力模型。默认模型是“硬”接触特性，即随着接触现象及接触压力立即产生。另外，“软”接触模型允许压力和间隙之间是指数关系或在表格中可查关系。最后，对接触压力的与间隙有关的粘性

阻尼关系允许高度不稳定的接触条件来研究。

- **热学接触问题** 可以提供不同的变量（一般压力、接触间隙等）函数描述传导和辐射属性。

- **电接触问题** 可以提供一个或多个变量表示的电传导率函数。

- **有孔压力接触问题** 可以使用有孔压力接触来确保两个接触体之间的有孔流压力的连续性。

- **压强渗透问题** 压强渗透荷载用于模拟沿着接触体表面的流场渗透问题。

• 基于单元模型

在一些特定的情况下接触单元比接触表面能够更好地定义接触体之间的相互作用。

- 离散点的接触问题

用缝隙单元定义会比用接触表面定义更合适。

- 管-管接触单元

用来模拟特殊管道的相互作用，即一个管道位于另一个管道体内，或两个管道不想穿透的情况。

ABAQUS/Standard 的接触算法是非常强大的，也已经运行了很多年，实践证明这些算法能很好地用于大量的实际问题。

声波-结构相互作用

提供基于表面的相互作用功能，用来对声音介质和用壳或连续体单元模拟的结构进行耦合分析。不需要在声音介质和结构表面生成与相匹配的单元网格。可以认为在声音介质的外边界，是形如圆柱体、球体、椭圆体的形状的非反射声波的边界条件。

运动约束

提供了线性和非线性的多点约束 (MPCs)，包括刚性链、刚性梁、壳体-固体连接、循环对称约束和运动耦合。线性约束方程由相关自由度的系数定义，非线性 MPCs 在约束库中没有定义，但用户可以在子程序中定义。

铰连接

可以定义铰连接。这些可选择的连接放松了在梁单元和管单元中力矩和扭矩的传递。

空穴辐射相互作用

ABAQUS 有一项通用空穴辐射性能，包括试图系数设计、阴影和自动计算。辐射表面用跟接触表面类似的方式定义。除了定义跟辐射有关的其他非线性情况外还定义了与温度有关的发射率。可提供带有大量对称选项的二维、三维和轴对称几何体。

- 线反射或平面反射
- 周期对称
- 循环对称

在用辐射模拟瞬时热传导中刚体位移的描述是可能的。变化的视图系数可以被连续更新，这在模拟运动物体的加热与冷却过程中是很有意义的。

其它模型的特征

• 输入

导入 计算结果可以由二进制文件的形式在 ABAQUS/Standard 和 ABAQUS/Explicit 之间传递。这种能力使得 ABAQUS/Explicit 的所有功能可以在 ABAQUS/Standard 的计算结果的基础之上运用，反之亦然。也可以从一个 ABAQUS/Standard 计算的结果中取出某个特定时刻的某个构件，放入另一个包含其他构件的 ABAQUS/Standard 文件中进行分析。

一种典型的导入的应用是 ABAQUS/Standard 进行装配预应力分析后的模型导入到 ABAQUS/Explicit 中进行分析；另一种典型应用：使用 ABAQUS/Explicit 分析成型过程后，模型导入 ABAQUS/Standard 中进行回弹和自振频率的分析。

• 再启动

这项功能是用户在周期的间隔时段保存分析的全部状态，并可以随时从加载历程的任一时刻重新进入分析。

• 子结构

ABAQUS/Standard 具有包含通用的多级子结构分析的能力。子结构被存储在一个用户定义的二进制文件中；一旦生成，它们可以被引入任何分析的模块中。任何子结构的几何都可以在分析模型中重复多次使用，可以进行平移和转动、镜

像。子结构可以用于模型的动态和静态应力/位移分析。这些分析可以是非线性的。这是一种高效率的分析技术，它可以包括弹性体之间的接触，也就是非线性的分析。在几何非线性分析中，子结构的运动可以包括有限转动和平动。子结构也可以预加载，也就是子结构刚度在加载历程中的应力状态可以被引入。

• 子模型

这种技术提供了用户研究更精细网格划分的局部模型的方法，对局部模型的分析是基于整体模型的研究。子模型的分析是独立的，它与整体模型的联系是子模型在某时刻边界上节点位置是基于整体模型相应时刻的节点位移。子结构边界上的节点不必与整体模型节点一一对应。

ABAQUS/Standard 的子模型功能是一个通用功能。子模型的单元和材料特性可以与主模型的对应区域不同。子模型和主模型都可以是非线性的，并可以应用到不同的分析流程。

• 材料的去除与添加

ABAQUS/Standard 允许单元和接触对在分析过程中被去除（也可以在后续的分析步骤中被重新引入）。这种特征可以应用到地质结构如水渠和水闸构造分析，焊接分析，以及回弹计算过程中的夹具去除等。

- **几何体的自动扰动**

从屈曲特征值中迭加模态的贡献，为后屈曲计算提供了初始、不完全的几何体。相似的，每一分析的位移结果都可以用于定义单独分析的初始几何体。

- **加强**

一般钢筋的定义可以包含于连续体单元、梁单元、壳单元和薄膜单元中用来模拟复合材料，例如：钢筋混凝土或轮胎类强化的橡胶材料等。

- **循环对称模型**

具有循环对称性的问题可以通过模拟最小扇面来分析 360 度的结构。这种周期对称的功能使用与承受循环对称荷载作用的循环对称结构的一般非线性分析。在提取特征值分析中既可以计算对称的特征模态，也可以计算非对称的特征模态，不需要扇形的对称表面的网格相匹配。

- **嵌入单元**

是在一组材料中嵌入另一可定义特性的材料。例如：可以将构架单元和加强筋隔膜单元嵌入三维的固体单元中，或将一种固体单元嵌入另一种固体单元中。被嵌入固体单元的节点和嵌入固体的节点可以是不一致的。

- **多重坐标系统输入**

对于每一个初始点都可以采用笛卡尔坐标、柱坐标或球坐标系统。

- **多重坐标系统输入**

对于每一个初始点都可以采用笛卡尔坐标、柱坐标或球坐标系统。

- **断裂分析**

可以计算断裂力学参数如 C_t, J , 应力强度因子(K_I, K_{II}, K_{III})和 T 应力等。求解这些参数的方法是区域积分方法。裂纹方向可以通过定义裂纹扩展方向或指定裂纹面的法向来实现。如果法向被指定了，那么裂纹方向可以通过裂纹尖端的法向和切向自动决定。可以计算裂纹扩展方向以决定已存在裂纹延伸的角

度。二阶均质单元可以应用一致性节点和四节点技术来模拟裂纹尖端的奇异性。具有若干个裂纹扩展准则来判断和定义裂纹扩展过程中材料分离。

- **惯性平衡**

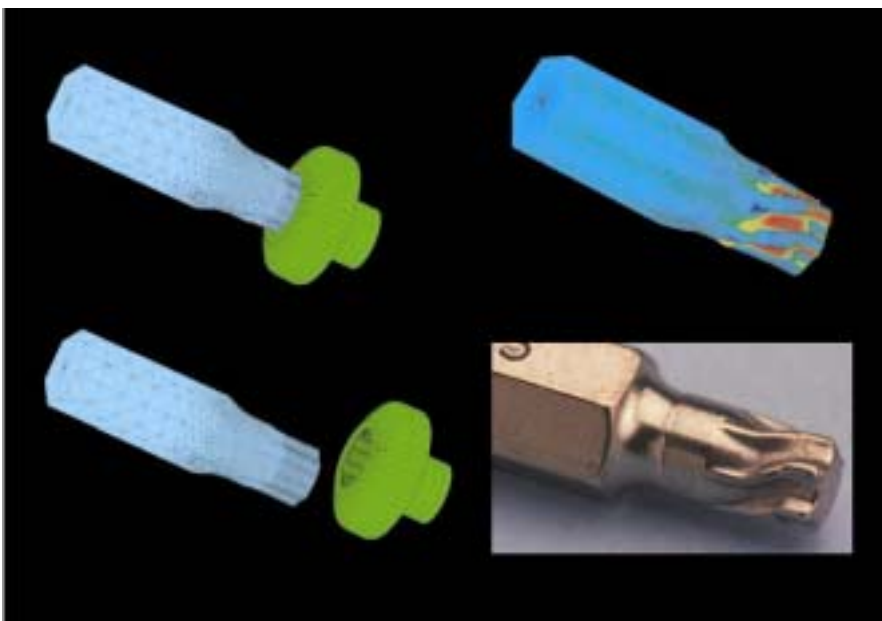
自动的惯性平衡功能可以用来自由或部分约束结构的准静态响应。惯性平衡可以应用到几何线性和非线性分析，静力和瞬态响应分析等。一个应用惯性平衡的实例是火箭在均匀推进力作用下的应力状态分析。

- **数据参数化和参数化研究**

参数化研究为用户提供了一种产生、执行和收集多个分析作业结果的工具，这些作业只是在部分输入参数上有所不同。

- **计算结果传送**

在轴对称模型中得到的结果会自动传递到后续将要进行一般三维分析的三维模型中。相似的，存在对称平面的部分的三维问题的分析结果也可以传递到完全三维问题的分析中。



TORX PLUS 传动系统的显著优点是它可以传递很大的扭矩载荷而不使接合件锁死或滑脱。在这个例子中，在传动器顶端施加 50NM 的扭转载荷，尽管传动器顶端产生了很大的永久变形，接合件保持足够的强度而没有失效。

- **过度约束的自动求解问题**

ABAQUS/Standard 采用了一种算法来解决在复杂模型中出现的普遍的过度约束问题。

- **局部坐标**

任意节点的自由度可以被转换到其他直角坐标系、圆柱坐标系或球坐标系。

- **液态流体腔**

ABAQUS 可以模拟二维或三维的流体填充的空腔。基于流体静力学公式，可以得到任意时刻流体的压力。流体部分可以在分析过程中加入或者删除。ABAQUS 有一维连接单元模拟流体在空腔中的流动。实际应用包括：水力发动机安装，空气冲击吸收，液压传动装置等。

- **退火**

材料融化和重新凝固的高温变形过程可以模拟。如果温度超过退火温度相应的硬化的尺度将被重新设定。如果材料温度降低，低压退火温度，材料可以重新硬化。

- **用户子程序**

ABAQUS/ Standard 允许运行用户通过子程序来扩展主程序的功能，用户可以自定义材料模型、单元、MPCs（多点约束）、摩擦类型和最一般加载条件。

求解技术

- **稀疏求解**

在默认状态下，ABAQUS/Standard 无论对于对称还是非对称的矩阵应用多波前、分块消去技术。对于稀疏问题的这种求解器高度优化，对减少 CPU 运行时间和磁盘空间方面是很好的。它可以在高性能计算机的完全利用并计算。

- **Lanczos 特征值解法**

ABAQUS/Standard 对于对称或非对称的矩阵应用 Lanczos 特征求解器。在大模型中它可以有效地处理特征模态数量很多的问题，它跟相应的线性静态问题要求相通的核心内存。

- **几何非线性**

ABAQUS/ Standard 对于有限应变的计算应用完全的、一致的运动学规律。拉格朗日公式和修正的拉格朗日公式分别用于求解有限应变的弹性和和弹塑性问题。ABAQUS/Standard 一般用完全的牛顿方法求解非线性方程。这种方法特别适用于有本程序建立的一般高度非线性问题，也提供了修正的牛顿法。

- **本构积分**

对于用比率形式描述的材料模型（如弹塑性模型），ABAQUS/Standard 对于最大的可能应变应用隐式的完全积分确保解的稳定性。这种方法，联合调和的雅可比方法一起保证包括复杂材料行为的大应变问题的求解应变。

输入输出文件

输入文件

ABAQUS/Standard 的输入文件通常是由 ABAQUS/CAE 程序或其它前处理程序产生的文本文件。执行分析前要进行大量的输入数据的检查。

• 关键字

输入文件由直观的 关键词和相关的 数据组成。关键词表明了所选的选项，数据为自由输入各式。

• 集的概念

可以把结点和单元 组合成“集”，每个集由用户指定一个名称。集可以嵌套的。这种集的概念给材料、载荷、约束的定义、输出的编辑等提供了一种简单易懂的引用方法。这个概念尤其对大型复杂的模型更有价值，它在分析模型的开发过程中简化了数据的处理。

• 简单网格生成选项

输入文件允许单元沿直线或曲线方向的增量填充，区域的填充以及对结点块的参考映射。

• 多重坐标系

具备笛卡尔坐标系、圆柱坐标系和球坐标系。对于结点位置、自由度方向以及材料方位可以指定独立的坐标系。

• 部件及装配

ABAQUS 提供把有限元模型定义成各个零散部件的选项，随后在将这些部件装配在一起。这个方案允许多次使用同一部件的定义来生产大的模型。也允许在模型力相互分离的部件中重复使用结点和单元的编号。

• NASTRAN 数据块

ABAQUS 带有一个可将 NASTRAN 的

数据块翻译成 ABAQUS 的输入文件对其进行分析或输入 ABAQUS/ CAE 中进行建模和其它附加操作。ABAQUS/CAE 中进行建模和其它附加操作。

输出文件

• 交互式图象的后处理

ABAQUS /Viewer (包含在 ABAQUS/Explicit 的使用许可中) 提供了网格图、结果的等值线图、变形后的网格图、动画、时程变化图、矢量图、X-Y 图。还提供“点击”查询结果的功能。

• 打印输出

对于大范围变量包括应力、应变、位移和反作用采用列表式打印输出。用户定义每一个表中每一列的变量，在需要时以便输出。

• 外部文件输出

分析结果可以选择性的写入输出数据库和结果文件中。存储在输出数据库中的数据可以被 ABAQUS/Viewer 读取，以此进行后处理。结果文件是和标准的第三方后处理包进行交流的基础。

• 重新启动输出

重新启动输出可以将所处理的问题分成方便的几个部分进行输出，以防止意想不到的程序终止。它的用途广泛，使用起来非常容易方便。

• 错误信息

ABAQUS/Standard 对出错的信息进行了描述包括对出错的解释和建议。并且提供了一个含有时间积分细节的特殊诊断文件。

硬 件 与 性 能

硬件兼容性

ABAQUS/Standard 是使用 FORTRAN、C 及 C++ 语言编写的，保持着多个版本，并被大多数的工程计算机所支持。其代码是用双精度还是单精度类型由计算机决定。ABAQUS/Viewer 支持标准图形和绘图设备。

ABAQUS/Standard 及其界面产品在下列计算机平台上均可使用：

- Compaq Alpha
- HP
- IBM
- SGI
- Intel Pentium
 - Windows NT/2000/XP
 - LINUX
- Intel Itanium
 - HP-UX
 - LINUX
- Sun

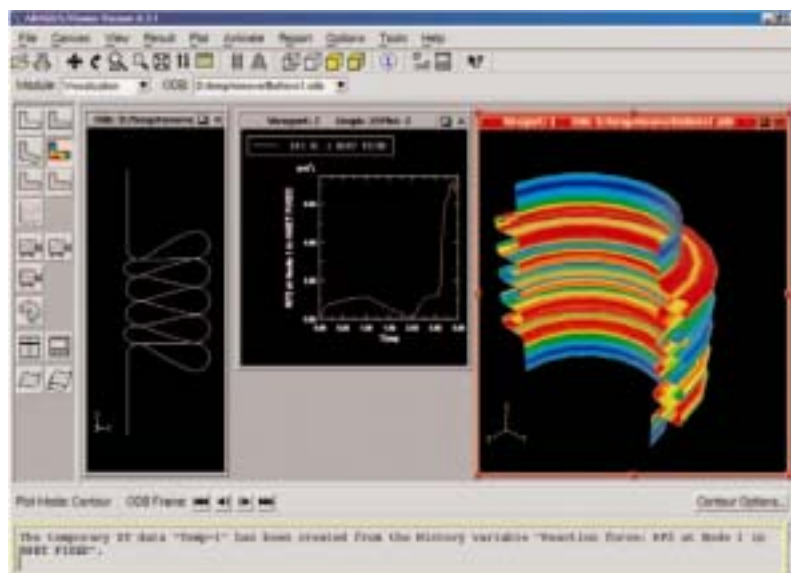
想了解更多的兼容硬件信息或者更详细的支持平台信息，请访问我公司网站：

www.abaqus.com

问题的大小与性能

ABAQUS/Standard 在问题大小上没有内置的局限，小问题完全可以在主内存中运行，在稍大的问题中会自动应用第二缓存。ABAQUS/Standard 在大型计算机上执行效率很高，特别能有效地在高级计算机体系中运行大型问题。ABAQUS 提供了一套在不同的计算机系统下完成的基准计算的时间数据，以此作为这些系统下代码运行性能基本的比较。

ABAQUS/Standard 的分析结果可以用
ABAQUS/Viewer 作互动后处理



文 档

ABAQUS/Standard 提供了一种最彻底的有限元系统，可以参照下面的手册：

用户手册

对于应用 ABAQUS/Standard,这是基本的参考文档，有印刷版本和在线两种形式以供使用。

关键字手册

这本手册提供了在 ABAQUS/ Standard 中用到的所有的输入选项的详细描述，有印刷版本和在线两种以供使用。

辅导手册

按自己的学习节奏设计，这本书将帮助读者成为应用 ABAQUS/Standard 进行静态或动态应力模式分析的行家里手，有印刷版本和在线两种形式以供使用。

实例问题手册

这本手册含有超过 75 个详细的实例，这些例子用来解释执行有意义的线性和非线性分析需要用到的方法和结论，它也可以从出版物或在线得到。典型的实例由弹塑性管撞击刚性墙壁产生的大变形，薄壁肘状物的非弹性屈曲失效，弹性、粘塑性细圆环体的突然加载，基体凝固，有孔复合壳的屈曲和金属薄片的拉伸。

基准例题手册

该手册含有 200 多个用于评估 ABAQUS 性能的基准问题和标准分析，测试是简单几何体或简化后的实际问题的多重单元测试，它可以在线查找，如果需要，可以查阅相关出版资料。

验证手册

在线的手册含有 5000 多个基本测试实例，提供了依靠精确计算或已公布的结果的各程序特点的验证。

理论手册

这一再线手册详细包含了所有程序理论方面的精确讨论，其难易程度是所有具有工程师背景的用户均能理解的。

界面用户手册

为所有的如 ABAQUS/ADAMS 等的界面产品单独设计的手册，这一手册有印刷和在线版本可供选择。

产 品 支 持

维护与支持

ABAQUS/Standard 的商业用户通常选择完全的维护与支持服务。每当新版本发布时，这些用户就可以收到新版本。以在线的形式列出已知的程序缺陷及其解决方案的状态报告。ABAQUS 遍布各地的办公室和代表处网络给具备年度使用许可或选择付费的不间断支持许可的商业用户提供了广泛的、无限制的支持。这些支持包括对选择合适的单元、材料或步骤的建议，有关 ABAQUS 全面的信息和提供有关使用 ABAQUS 进行特殊模拟的指导。学术上的用户可以以较小的额外费用得到这些支持。

质量检测服务

ABAQUS 满足严格的质量保证标准并且达到了 ISO9001 和美国国家标准协会/美国机械工程师协会（ANSI/ ASME）的 NQA-1 号规范要求。对于那些需要监督他们的供应商的质量保证行为的用户，ABAQUS 提供了一个质量监督服务。

安装

程序通常由用户来安装。根据要求，ABAQUS 的工程师或当地的代理将在用户的现场进行初始安装。安装服务包括对软件的检查和验证和参加培训研讨班。

培训和用户会议

ABAQUS 在其公司和当地的代表处组织经常和定期的公共培训班，还有在用户地点召开的研讨班。入门性的研讨班系列包括两个补充部分：ABAQUS/CAE 入门以及 ABAQUS/Standard, ABAQUS/Explicit 入门。为期两天的 ABAQUS/CAE 入门研讨班主要集中在使用 ABAQUS/CAE 进行模型前处理，提交和监督分析任务以及对模拟结果的交互式管理。为期三天的 ABAQUS/Standard 和 ABAQUS/Explicit 入门研讨涉及到一些分析的原理，集中与由或无接触的非线性静态的动态模拟。在入门研讨班之后提供了实质性的 ABAQUS 上机训练经验的研讨会。

也组织涉及特定主体的高级研讨会。就用户指定的主题进行现场讲解。有 ABAQUS 或 ABAQUS 当地代表处提供的高级研讨会涉及到这样一些主题，如非弹性本构模拟，大应变弹性，单元的选择和金属成型等。

所有的研讨会的培训材料可向 ABAQUS 公司或代表处联系购买。并给新手提供了一种辅导手册，即 ABAQUS/Explicit 入门指南。

ABAQUS 每年主办世界范围的用户年会。另外，所有世界上的 ABAQUS 用户群体组织一个地区性的用户年会。这些聚会给用户提供了学习和交流经验的论坛，一起讨论 ABAQUS 的能力，性能的提高以及 ABAQUS 及其代表处的相关服务。

ABAQUS/Standard 的优势

ABAQUS/Standard 是一个真正的通用程序，它提供了大量的各种各样的线性和非线性的分析功能。ABAQUS/Standard 的广度和深度为培训一个人掌握一种分析包提供了最小的费用。

完全的支持和维护服务确保用户能得到软件的有效利用和高级分析的专门技术指导。

它满足 ISO9001 和美国国家标准协会/美国机械工程师协会（ANSI/ASME）的 NQA-1 号规范的质量保证要求。ABAQUS/Standard 是 ABAQUS 一套程序中的一部分，这套程序包括 ABAQUS/Explicit，用于高度非线性，瞬态响应分析；ABAQUS/CAE，用于数据准备，分析管理及结果评价。另外，ABAQUS/Standard 和大多数工业标准的前处理和后处理器兼容。

它提供了独立的材料库和单元库，任何单元可以用于任何的材料模型中，而且在一个模型中不同的材料或单元的数量是有限制的。

在所有分析程序中自动的时间增量和自动的收敛标准的选择确保了解的可靠性，甚至在最困难的非线性应用中。

ABAQUS 方程的求解方案效率是很高的，而且能在大量不同的计算机上发挥它们最优化的性能。在单一的模拟计算种可以采用几种不同的分析类型。

对于效率和应力精度，ABAQUS 中包括已被证明的、流行的单元库，所有的单元对于线性和非线性分析都是适用的。

多用途的重启动和恢复功能能确保应付意外的分析终止。

用户子程序功能是高级应用成为可能。

ABAQUS 拥有大量的全世界范围的用户基础，普遍在各种类型的应用中的到使用。大量的使用证明了程序的高效性，也有助于保证程序的可靠性。

ABAQUS 及其相关的支持服务使复杂的线性的和非线性分析就像已有的数值方法一样简单和可靠。

Abaqus 使用问答

Q: abaqus 的图形如何 copy?

A: file>print>file 格式为 png, 可以用 Acdsee 打开。

Q: 用 Abaqus 能否计算[Dep]不对称的问题?

A: 可以, 并且在 step 里面的 edit step 对话框 other 里面的 matrix solver 有个选项。

Q: 弹塑性矩阵【D】与 ddsdde 有何联系?

A: stress=D*stran; d(stress)=ddsdde*d(stran)。

Q: 在 abaqus 中, 如果采用 umat, 利用自己的本构, 如何让 abaqus 明白这种材料的弹塑性应变, 也就是说, 如何让程序返回弹性应变与塑性应变, 好在 output 中输出, 我曾想用最笨地方法, 在 uvarm 中定义输出, 利用 getvrm 获取材料点的值, 但无法获取增量应力, 材料常数等, 研究了帮助中的例子, umatmst3.inp, umatmst3.for, 他采用 mises J2 流动理论, 我在 output history 显示他已进入塑性状态, 但他的 PE 仍然为 0!! ?

A: 用 uvar() 勉强成功。

Q: 本人在用 umat 作本构模型时,

***static,**

1,500,0.000001,0.1 此时要求的增量步很多, 即每次增量要很小,

***static**

1,500 时, 在弹性向塑性过度时, 出现错误, 增量过大, 出现尖点.?

A: YOU CAN TRY AS FOLLOWS:

***STEP, EXTRAPOLATION=NO, INC=2000000**

***STATIC**

0.001, 500.0, 0.00001, 0.1。

Q: 模型中存在两个物体的接触, 计算过程中报错, 怎么回事?

A: 接触问题不收敛有两个方面不妨试试:

一、在*CONTACT PAIR 里调试 ADJUST 参数;

二、调一些模型参数, 比如 FRICTION 等。

Q: 在边界条件和加载时, 总是有 initial 这个步, 然后是我们自己定义的加载步, 请问这个 initial 步, 主要作用是什么? 能不能去掉?

A: 不能去掉, 所有的分析都有, 是默认的步。

Q: A solid extrusion base feature 这句话是什么意思?

extrusion、revolution 等是什么意思?

A: 这两的是三维建模时候, 在画完二维图形, 如何来生成三维图形,

extrusion 意思是你给定一个厚度, 然后二维图形第三个方向上面伸展这么多形成三维图形

revolution 意思是你给定一个旋转轴, 二维图形绕其旋转后形成三维轴对称图形。

Q: 偶在 umat 中调用求主应力函数

CALL SPRINC(STRESS,PS,LSTR,NDI,NSHR)

后，存储主应力得数组 PS 中

各个主应力排列顺序是什么？

PS1>PS2>PS3 ?

PS1<PS2<PS3 ?

PS1>PS3>PS2 ?

A: 第二个 。

Q: 在*USER MATERIAL 的定义中， $\Delta \sigma$ 对 $\Delta \epsilon$ 的偏倒数，即

DDSDDE 被称为：

"material stiffness matrix";

而在 UMAT 中，DDSDDE 被称为：

"material's Jacobian matrix"。

请问 DDSDDE 和材料的切线刚度矩阵的关系是什么？二者是一个概念么？

A: 一般说可以这样理解：

$$\sigma = ddsdde * \Delta \epsilon$$

有点像我们常说的弹塑性矩阵：Dep。

Q: 请问 field output 和 history output 什么区别？

关键字*node output 和*node print 有什么区别？ ?

A: field output 和 history output 在 viewer 模块中很明显。

field output 是场量输出，history output 为历史数据输出，会记录场量随时间的曲线

至于*node output 与*node print 的区别在于他们写入不同的后缀文件，比如*.odb, *.dat 等，在 help 中有详细介绍 *node output 是给 CAR 或 VIEWER 做后处理用的，是二进制文件，而*node print 则是写到 DAT 文件中，你可以自己看的文本文件。

field output 用来输出模型中较大部分 (a large portion of the model) 的那些输出频率较小的变量，如模型的等值线，变形图等；

而 history oupput 用来输出模型中较小部分的那些输出频率较大的变量，如荷载作用点处的荷载——位移图等。

所以，应力，应变，位移，反力等既可以作为 field output 也可以作为 history oupput 输出。 。

Q: 我在学习 ABAQUS 时，遇到以下专有名词想请教各位。

1、orphan mesh instance,

2、self-contact,

3、elastic foundation,

4、convective interaction,

5、amplitude,

6、solution-dependent state variable,

7、datum,

8、thermal film condition ?

A:

- 1、独立网格实体;
- 2、自接触;
- 3、弹性基础, 如弹性地基梁;
- 4、对流相互作用;
- 5、幅度, 数值大小, 如定义随时间变化的荷载;
- 6、依赖于解的状态变量, 在 UMAT 中经常用到, 它的大小取决于某一增量步收敛解;
- 7、辅助数据, 在 CAE 中经常用于定义数据点、刚体参考点、辅助平面等;
- 8、不知道:)

Q: (1),请问如何得到 M,C,K 矩阵?用什么命令

(2) ABAQUS 中能实现这样的东西吗?就是我需要平滑 ABAQUS 产生的位移场, 还是这个平滑只能在其他环境中完成 ?

A: (1) 试一试: *element matrix output

(2) 试试这个输出选项:

*El print,Position=average at Nodes.

Q: solution-dependent variable 和 time-dependent variable 这两种变量有什么差别?

A: solution-dependent variable

从字面上理解, 即为“与解答有关的变量”, 它的值与每一增量结束时的变量有关, 常用于 UMAT 中, 即 SDV, 可以由*DEPDV 来定义其个数。

time-dependent variable

从字面上理解, 即为“与时间有关的变量”, 常用于定义随时间变化的量如地震荷载等, 可以由*AMPLITUDE 来定义。。

Q: S4R 单元可以输出 sth(就是 section thickness 单元厚度变化), 但 C3D8R 却不能输出 sth 该怎么看单元层厚度方向的变化 ?

A: 个人觉得

定义了局部坐标方向, 特别是对于各向异性问题, 有限元在材料方向上计算应力, 应变, 输出也就在材料方向, 假如第三方向为厚度方向, 那第三方向的塑性应变就是他的厚度变化。。

Q: ABAQUS 在运行过程中, 对于一些比较大的问题, 经常会出现以下的信息:

ABAQUS Info: License Timeout set to 70(可能是不同的值) minutes. ?

A: 个人感觉是没有问题的, 你放心吧:)

Q: 在计算固结过程中, msg 文件总是有一下信息 ***ERROR: TOO MANY ATTEMPTS MADE FOR THIS INCREMENT: ANALYSIS TERMINATED

改变其最小时间变量也不行, 太郁闷了, 是不能收敛吗? 各位大侠救命。请指教可能是什么原因?

A: 很多原因

比如边界条件不对 ; 约束不够 ; 接触定义不对; 单元划分畸变等等。

Q: ?

A: 个人觉得:

umat 实现自己的本构没有固定的方法,对于不同的本构有可能必须采用不同的方法。这要靠自己不断地摸索。有可能一种方法对于简单加载问题还行,但有可能对于复杂问题并不收敛。最重要一点,就是 umat 中采用的算法必须 consistent.再就是 ddsdde 必须正确,(如果采用 back_Euler 方法等一些算法,ddsdde 错误有时不影响结果(对于简单加载问题没有影响,能收敛,)),但对于复杂问题不收敛。

uptonow,你这个算法对于 Mises, hill, J2, J2d 等一类的屈服函数是正确的,但具体的本构还要灵活运用,这我也正学习,正在摸索。

有时,umat 需要很强的有限元基础,并且对采用的本构要很熟悉,不要在一颗树上吊死才好。首先要确认自己的 umat 没有错误,如果没有,但就是不收敛(在不断减小加载步长的情况下,当然最好对步长不敏感,特别是对于粘弹性,粘塑性,内变量一类的材料,有的本构取决于背应力的计算)。那就应该考虑换一种算法。

一点体会,请大家探讨。

Q: 第一次安装 abaqus6.2.1,装完 exceed6.2&3D 后,开始装 6.2.1 的 Product installation for network licensing,结果每到进度为 75%时,弹出界面:

An error occurred during the move data process: -115

Component:Complete Insallation

File Group: fg_common

File:c:\abaqus\6.2-1\cae\External\ebt\adi3xcol.dll

就停止安装了,重新安装依然如此,现在感到头都大了,哪位好心人帮帮我,不深感激 ?

A: 没有关闭防火墙!

Q: WARNING: THE SYSTEM MATRIX HAS 1 NEGATIVE EIGENVALUES.

一般在什么情况下会发生系统矩阵出现负特征值?

A: 很多情况

比如边界条件定义不对;接触定义不对。

Q: 就是手册的 umatmst3.for

1) Mises 各向同性的子程序中,调用硬化曲线函数中的 Table (2, nvalue) 这个二维数值保存是应力应变曲线的数据,可是 ABAQUS 并没有告诉 UMAT 中 Table 数值这些应力应变的数值啊,UMAT 里面 Table 怎么知道的呢?

2) $RHS = SMISESS-EG3*DEQPL-SYIELD$ 这个式子是什么意思?尤其是 $3G*DEQPL$ 是什么意思?

A: 就是 Constant=8 中的从第三个开始的数值,数组名传递。

Q: 我在计算时 MSG 文件出现如下错误,是不是由于节点数太多啦?该如何处理这个问题?

ERROR: SPECIFIED STANDARD_MEMORY VALUE OF 8000000 IS TOO SMALL TO RUN THE NALYSIS. STANDARD_MEMORY MUST BE INCREASED.

MINIMUM POSSIBLE VALUE IS 23477555. LOOK AT MEMORY ESTIMATES SECTION OF .dat FILE FOR FURTHER INFORMATION ?

A: 对 abaqus_v6. env 文件中的 STANDARD_MEMORY 的值进行修改。

修改 Site 文件夹下的 abaqus_v6. env 中的配置，如下：

```
#
#      System-Wide ABAQUS Environment File
#      -----
pre_memory = 33554432
standard_memory = 33554432  #####修改这里#####
#
# NT specific settings .
```

**Q: WARNING: THE SYSTEM MATRIX HAS 148 NEGATIVE EIGENVALUES
1 ABAQUS VERSION 6.3-1 DATE 27-NOV-2002 TIME 22:08:00 PAGE..
For use by None user license from HKS Inc. ..
STEP 1 INCREMENT 1 STEP TIME 0.00
STEP 1 STEADY STATE S..
AUTOMATIC TIME CONTROL WITH -
A SUGGESTED INITIAL TIME INCREMENT OF 0.300?**

A: 将你的 INITIAL TIME INCREMENT 改小些试试看，不过，一般出现此类问题，多半是你的模型有问题，欠约束或者其它什么的。

Q: ZERO PIVOT 是什么意思 ?

A: zero pivot 可以理解为刚度矩阵出了问题，例如奇异。

可能有不同的原因，如： 你所模拟的是软化性质材料，该点因破坏等原因而软化至不能吃劲； 模型有问题，如约束不够，或者是单元拓扑出错等；或者是你的 UMAT 中写的 [ddsdde] 有错；。

Q: abaqus-uamt 的老问题，缺少 'ABA_PARAM.INC' 文件 ?

A: 在 cvf6.5 调试时，显示 缺少 'ABA_PARAM. INC' 文件！

这个没有任何关系的，这个错误将在 ABAQUS 调用 UMAT 的时候自动会找到，仅仅有这个错误将没有任何影响的。也就是说，ABAQUS 中调用的时候，实际并不存在这个错误。FT，忘了说一句了，你把 ABA_PARAM. INC. dp 或 ABA_PARAM. INC. sp 拷到你的程序工作空间后，应该将把 ABA_PARAM. INC. dp 或 ABA_PARAM. INC. sp 的后缀. sp 或. dp 去掉，即将 ABA_PARAM. IN C. dp 或 ABA_PARAM. INC. sp 改名为 ABA_PARAM. INC。

呵呵，他的意思是在 Visual Fortran 中调试其子程序，我觉得这是一个好办法，我当时也是这么办的，毕竟在 ABAQUS 中调试是非常麻烦的，只有当你的 UMAT 没有语法或者明显的逻辑错误，你在 ABAQUS 中调试才能事半功倍。

CONTENTS

Lecture 1

Introduction

| | |
|---|-------|
| Introduction | L1.2 |
| Classical and Modern Design Approaches. | L1.3 |
| Some Cases for Numerical (Finite Element) Analysis. | L1.8 |
| Experimental Testing and Numerical Analysis | L1.11 |
| Requirements for Realistic Constitutive Theories | L1.13 |

Lecture 2

Physical Testing

| | |
|---|-------|
| Physical Testing | L2.2 |
| Basic Experimental Observations | L2.4 |
| Testing Requirements and Calibration of Constitutive Models . . | L2.11 |

Lecture 3

Constitutive Models

| | |
|---|-------|
| Stress Invariants and Spaces. | L3.2 |
| Overview of Constitutive Models | L3.10 |
| Elasticity. | L3.12 |
| Mohr-Coulomb Model | L3.15 |
| Description | L3.17 |
| Usage and Calibration | L3.24 |
| Modified Drucker-Prager Models | L3.28 |
| Linear Drucker-Prager Model | L3.31 |
| Hyperbolic Model | L3.35 |
| Exponent Model | L3.38 |

| | |
|---|--------|
| Flow in the Hyperbolic and Exponent Models | L3.40 |
| Usage | L3.43 |
| Matching Experimental Data | L3.45 |
| Linear Drucker-Prager Model | L3.50 |
| Hyperbolic Model | L3.52 |
| Exponent Model | L3.53 |
| Matching Mohr-Coulomb Parameters | L3.55 |
| Matching Plane Strain Response | L3.59 |
| Matching Triaxial Test Response | L3.62 |
| Coupled Creep and Drucker-Prager Plasticity | L3.64 |
| Basic Assumptions | L3.64 |
| Creep Laws | L3.67 |
| Time Hardening Creep Law | L3.67 |
| Strain Hardening Creep Law | L3.67 |
| Singh-Mitchell Creep Law | L3.68 |
| Creep Flow Potential | L3.68 |
| Usage | L3.69 |
| Modified Cam-Clay Model | L3.71 |
| Description | L3.75 |
| Usage and Calibration | L3.84 |
| Example | L3.89 |
| Modified Cap Model | L3.95 |
| Description | L3.97 |
| Usage and Calibration | L3.106 |
| Example | L3.111 |
| Coupled Creep and Cap Plasticity | L3.117 |
| Basic Assumptions | L3.117 |
| Cohesion Creep | L3.119 |
| Consolidation Creep | L3.121 |
| Creep Laws | L3.121 |
| Creep Flow Potentials | L3.122 |
| Usage | L3.124 |
| Jointed Material Model | L3.126 |

| | |
|-------------------------------|--------|
| Description | L3.130 |
| Usage and Calibration | L3.137 |
| Example | L3.142 |
| Numerical Implementation..... | L3.148 |

Lecture 4

Analysis of Porous Media

| | |
|--|-------|
| Basic Assumptions and Effective Stress | L4.3 |
| Stress Equilibrium and Flow Continuity | L4.8 |
| Types of Analyses and Usage | L4.17 |
| Examples | L4.29 |
| Fully Saturated Example | L4.29 |
| Partially Saturated Example | L4.40 |

Lecture 5

Modeling Aspects

| | |
|---------------------------------------|-------|
| Element Technology..... | L5.2 |
| Infinite Domains..... | L5.4 |
| Pore Fluid Surface Interactions | L5.26 |
| Geostatic States of Stress | L5.28 |
| Element Addition and Removal..... | L5.34 |

Lecture 6

Example Problems

| | |
|---|-------|
| Dry Problems | L6.3 |
| Limit Analysis of Foundation | L6.3 |
| Slope Stability Problem | L6.20 |
| A Dynamic Analysis | L6.33 |
| Saturated Problems..... | L6.44 |
| Consolidation Problem (Transient) | L6.44 |

| | |
|---|--------|
| Dam Problem (Steady-State) | L6.53 |
| Partially Saturated Problems | L6.77 |
| Demand Wettability Problem (Uncoupled) | L6.77 |
| Desaturation of Soil Column (Transient) | L6.98 |
| Phreatic Surface Calculation (Steady-State) | L6.114 |
| Excavation and Building Analysis | L6.127 |
| Tunneling Problem | L6.128 |

Appendix A

Stress Equilibrium and Fluid Continuity Equations

| | |
|--|------|
| Fully Saturated Fluid Flow | A.2 |
| Special Cases | A.5 |
| Partially Saturated Fluid Flow | A.11 |
| Special Cases | A.15 |

Appendix B

Bibliography of Geotechnical Example Problems

Analysis of Geotechnical Problems with ABAQUS

ABAQUS, INC.



The information in this document is subject to change without notice and should not be construed as a commitment by ABAQUS, Inc.

ABAQUS, Inc., assumes no responsibility for any errors that may appear in this document.

The software described in this document is furnished under license and may be used or copied only in accordance with the terms of such license.

No part of this document may be reproduced in any form or distributed in any way without prior written agreement with ABAQUS, Inc.

Copyright © ABAQUS, Inc., 2003.

Printed in U.S.A.
All Rights Reserved.

ABAQUS is a registered trademark of ABAQUS, Inc.

The following are trademarks of ABAQUS, Inc.:
ABAQUS/ADAMS; ABAQUS/Aqua; ABAQUS/CAE; ABAQUS/C-MOLD;
ABAQUS/Design; ABAQUS/Explicit; ABAQUS/MOLDFLOW; ABAQUS/Standard;
ABAQUS/Viewer; and the ABAQUS, Inc., logo.

All other brand or product names are trademarks or registered trademarks of their respective companies or organizations.

Revision Status

| | | |
|------------|------|---------------|
| Lecture 1 | 2/03 | Minor Changes |
| Lecture 2 | 2/03 | Minor Changes |
| Lecture 3 | 2/03 | Minor Changes |
| Lecture 4 | 2/03 | Minor Changes |
| Lecture 5 | 2/03 | Minor Changes |
| Lecture 6 | 2/03 | Minor Changes |
| Appendix A | 2/03 | Minor Changes |
| Appendix B | 2/03 | Minor Changes |

Course Schedule

Analysis of Geotechnical Problems with ABAQUS

Day 1

- Lecture 1: Introduction
- Lecture 2: Physical Testing
- Lecture 3: Constitutive Models
- Lecture 4: Analysis of Porous Media

Day 2

- Lecture 5: Modeling Aspects
- Lecture 6: Example Problems
- Appendix A: Stress Equilibrium and Fluid Continuity Equations
- Appendix B: Bibliography of Geotechnical Example Problems

Lecture 1

Introduction

Overview

- Introduction
- Classical and Modern Design Approaches
- Some Cases for Numerical (Finite Element) Analysis
- Experimental Testing and Numerical Analysis
- Requirements for Realistic Constitutive Theories

Introduction

In this lecture we discuss the philosophy on which the usage of numerical (finite element) analysis for geotechnical problems is based.

Lecture 2 deals with experimental testing and how it relates to the calibration of constitutive models for geotechnical materials.

The different ABAQUS constitutive models applicable to geotechnical materials are presented in Lecture 3. Their usage, calibration, implementation, and limitations are discussed.

In Lecture 4 we outline the treatment of porous media in ABAQUS and discuss the coupling between fluid flow and stress/deformation.

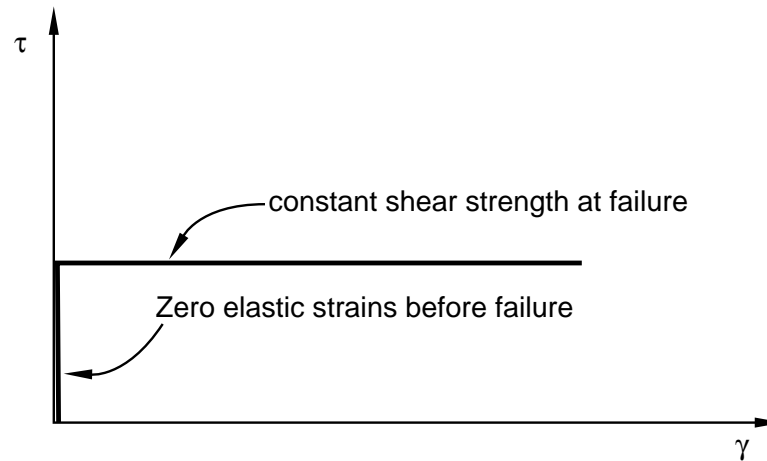
Several modeling issues relating to geotechnical situations are discussed in Lecture 5.

In Lecture 6 typical problems are used as illustrative examples.

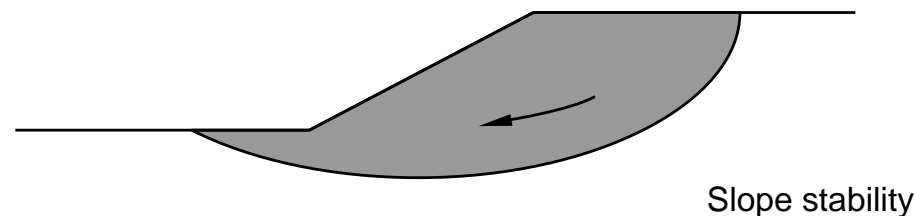
Classical and Modern Design Approaches

In the classical approach two basic types of calculations are done: failure estimates and deformation estimates.

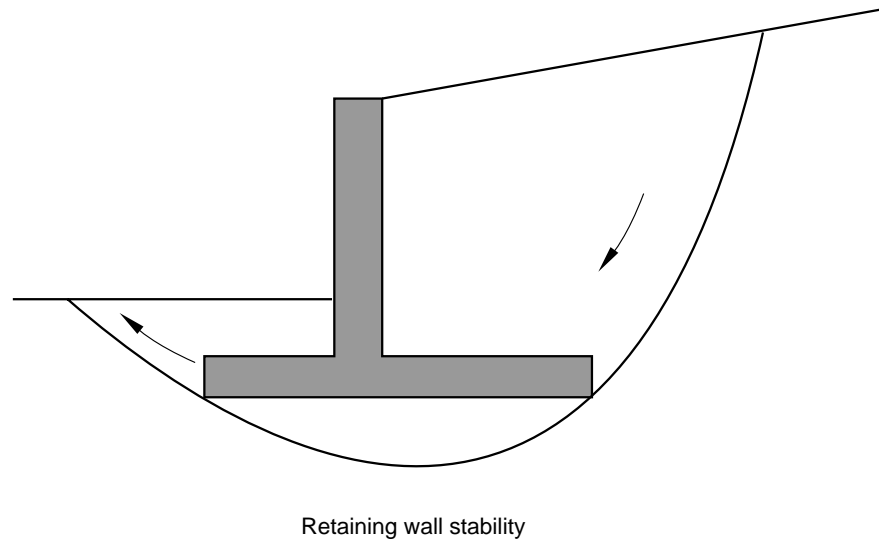
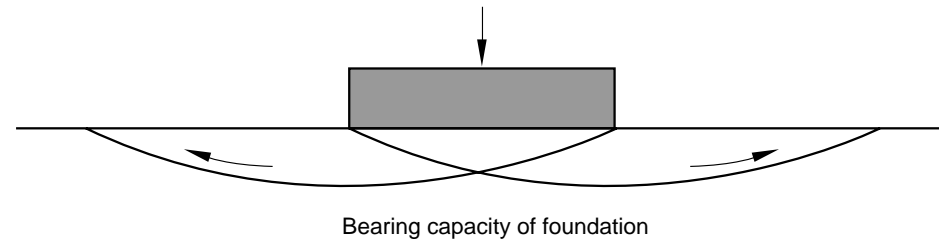
Failure estimates are based on rigid perfectly plastic stress-strain assumptions:



Examples:

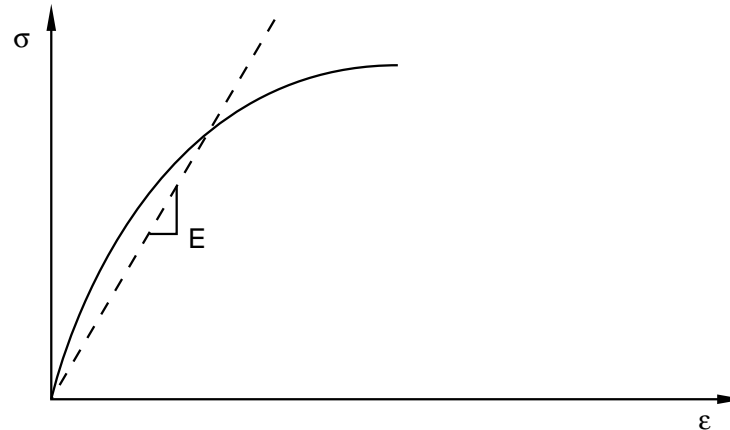


Examples (*cont.*):



The result is a factor of safety, which is evaluated based on experience (design code).

Deformation estimates assume linear elastic behavior with average elastic properties:



Foundation settlement example:

$$\text{settlement, } w = p \ b \left(\frac{1 - \nu^2}{E} \right) f ,$$

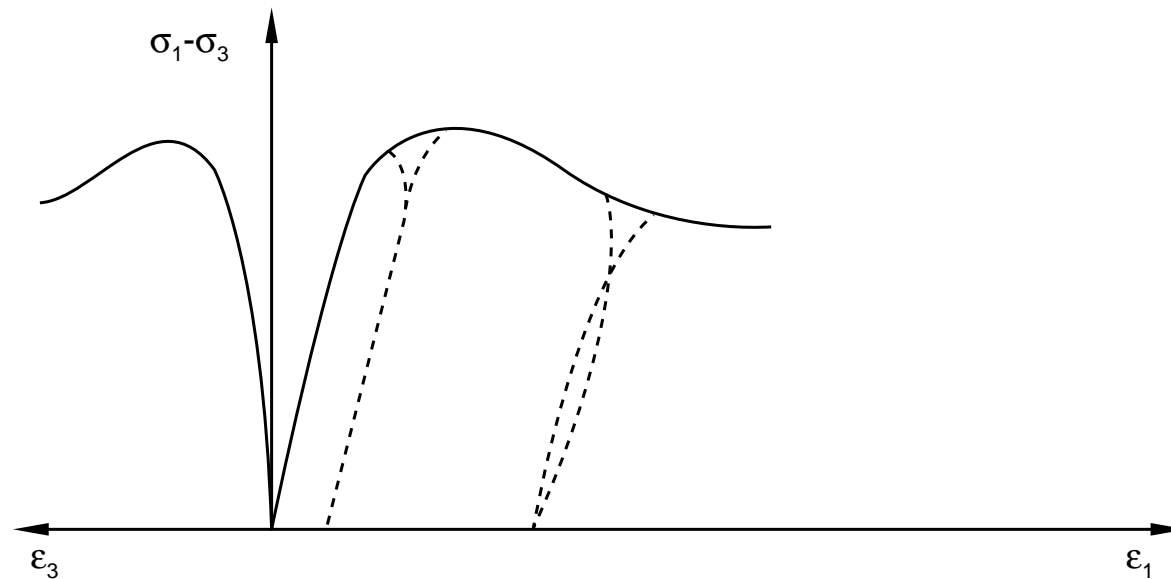
p is bearing pressure

b is width of foundation

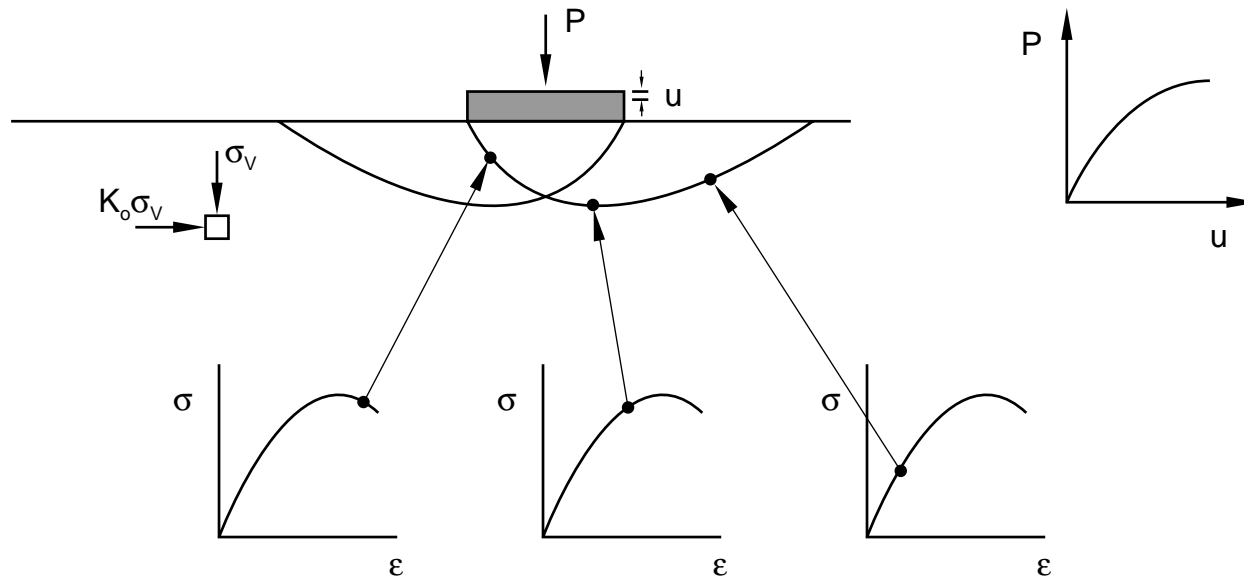
E , ν are average elastic properties

f is shape factor (based on small scale tests)

In the modern approach, failure and deformation characteristics are obtained from the same analysis. The analysis requires a complete constitutive model



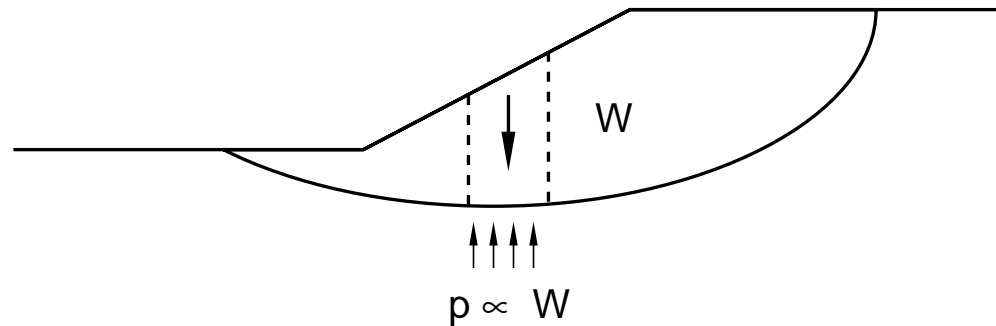
and the numerical solution of a boundary value problem.



Numerical (finite element) analysis can handle arbitrary geometries.

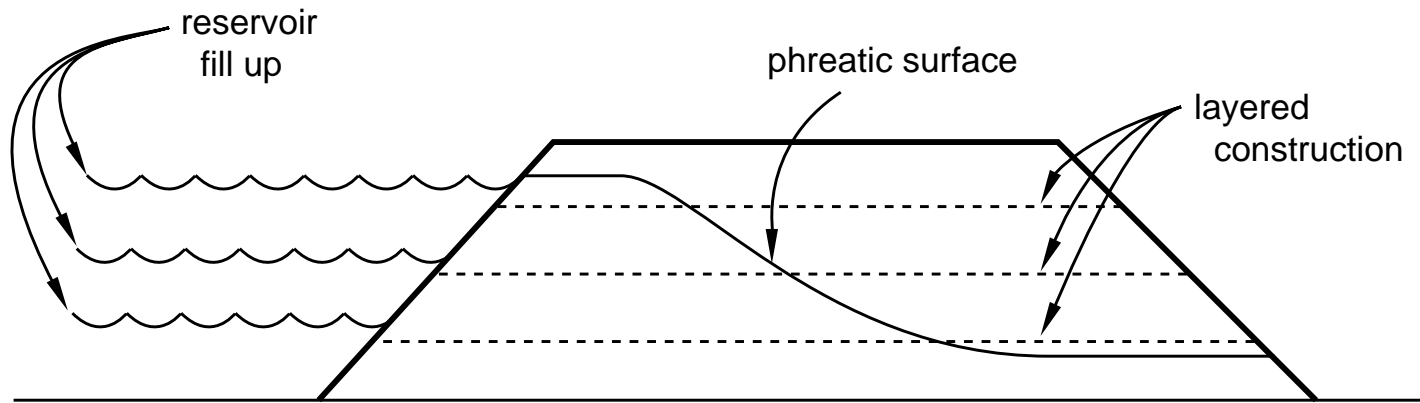
Some Cases for Numerical (Finite Element) Analysis

Cases when self weight of soil plays an important role, such as slope stability:



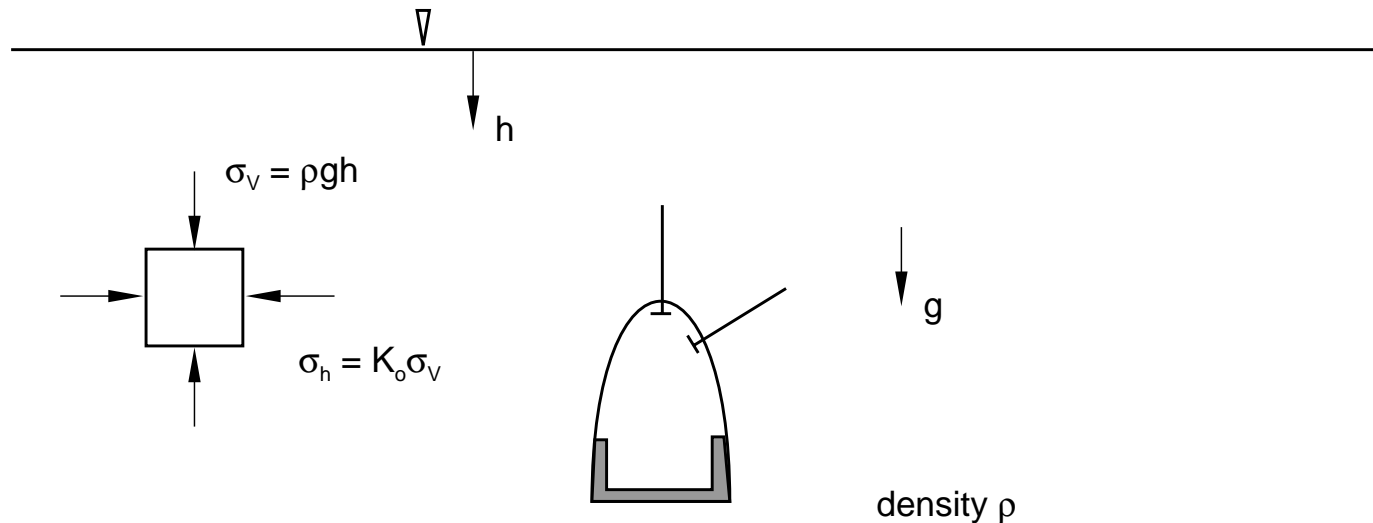
Classical limit failure calculations can predict ultimate stability of a slope accurately because collapse stresses on the failure plane are proportional to the weight of the soil and independent of the detailed soil behavior. Modern numerical analysis is necessary for calculation of deformations.

Cases when detailed soil behavior plays an important role, such as building of earth dam and subsequent filling of reservoir:



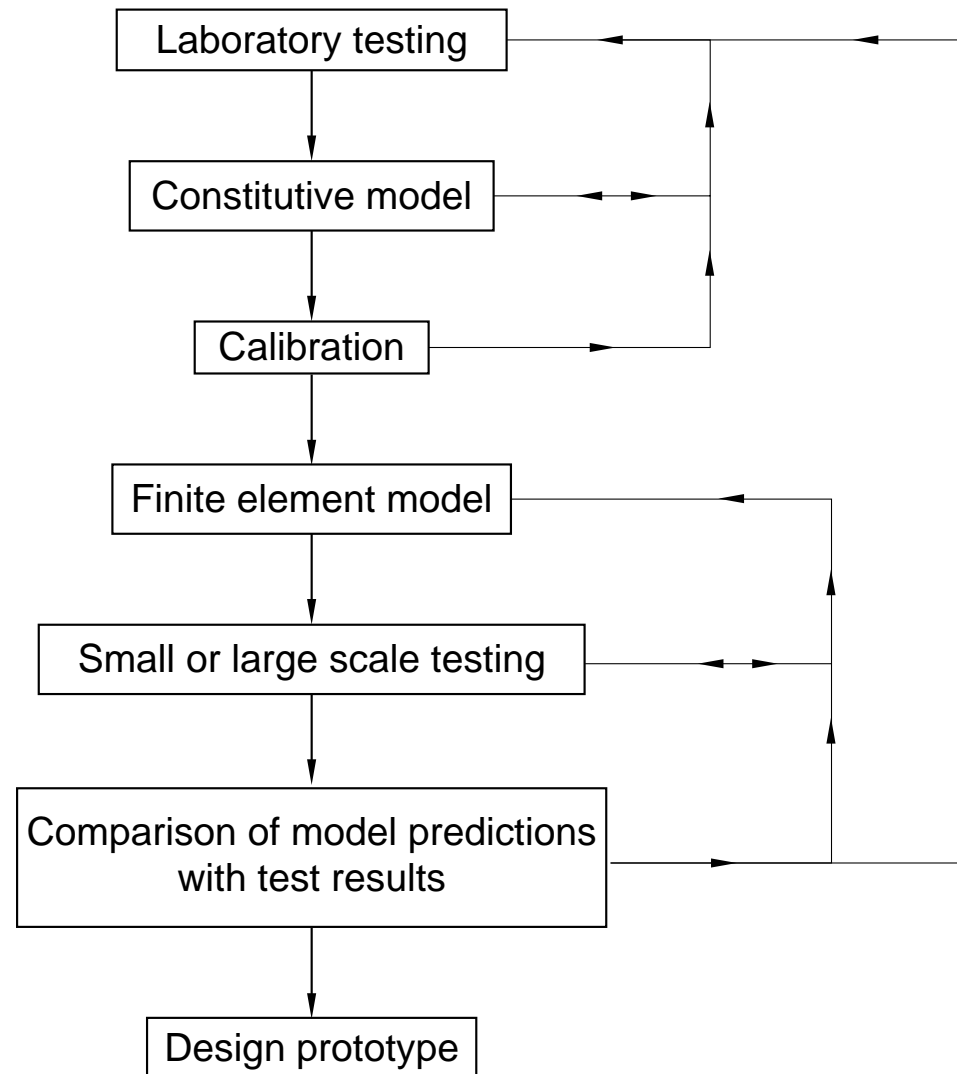
Local soil failure (stress or wetting driven) may trigger overall collapse or hamper functionality of structure. The sequence of events (construction, filling of reservoir, and long term consolidation) must be considered using numerical analysis.

Cases when the initial state of stress of the soil or rock mass is important, for example, tunneling:



The virgin state of stress caused by the weight of the soil and tectonic effects must be taken into account at the start of the analysis. The stability of the excavation depends on the virgin stress state as well as the sequence of the excavation process. It is possible to control the stability of the excavation by designing the excavation sequence (and perhaps using aids such as liners and rock bolts).

Experimental Testing and Numerical Analysis



The measurements required in the simple laboratory tests depend on the proposed constitutive model. The constitutive model must be proposed based on simple experimental observations. Laboratory testing and constitutive model development are closely tied.

The constitutive model must first be chosen qualitatively: it is important to capture the major features of material behavior while minor features may be ignored in the model. Calibration (or quantitative choice) of the model parameters follows. Calibration should not be attempted beyond available (and repeatable) experimental results.

The finite element model must capture important features of the physical situation, without irrelevant detail. Use of an adequate constitutive model is critical although simplifications are often justifiable.

Small or large scale testing usually requires some knowledge of the physical behavior being modeled. Details of the physical tests and finite element models must be compatible for meaningful comparisons.

Ultimately, design requires engineering judgment and a good deal of experience. Testing and numerical simulation are only useful tools to aid the design.

Requirements for Realistic Constitutive Theories

Realistic constitutive models should help us to better understand the mechanical behavior of the material. Their development must be based on the understanding of the micromechanical behavior of the material, translated to a macro model simple enough to use in numerical calculations, thus creating a tool for rational design.

Realistic constitutive models must be general, in that they must be capable of representing material behavior in any relevant spatial situation (one-dimensional, plane strain, axial symmetry, and full three-dimensional analyses).

Realistic models must be based on experimental data that are relatively easy to obtain. They must then be able to extrapolate to conditions that cannot be reproduced with laboratory testing equipment.

Lecture 2

Physical Testing

Overview

- Physical Testing
- Basic Experimental Observations
- Testing Requirements and Calibration of Constitutive Models

Physical Testing

Geotechnical materials are generally voided and, thus, sensitive to volume changes. These volume changes are closely tied to the magnitude of the hydrostatic pressure stress, so it is important to test the materials over the range of hydrostatic pressure of interest.

Most laboratory testing facilities are capable of performing standard tests:

- Hydrostatic (or isotropic) compression tests
- Oedometer (or uniaxial strain) tests
- Triaxial compression and extension tests
- Uniaxial compression tests (a special case of triaxial compression)
- Shear tests

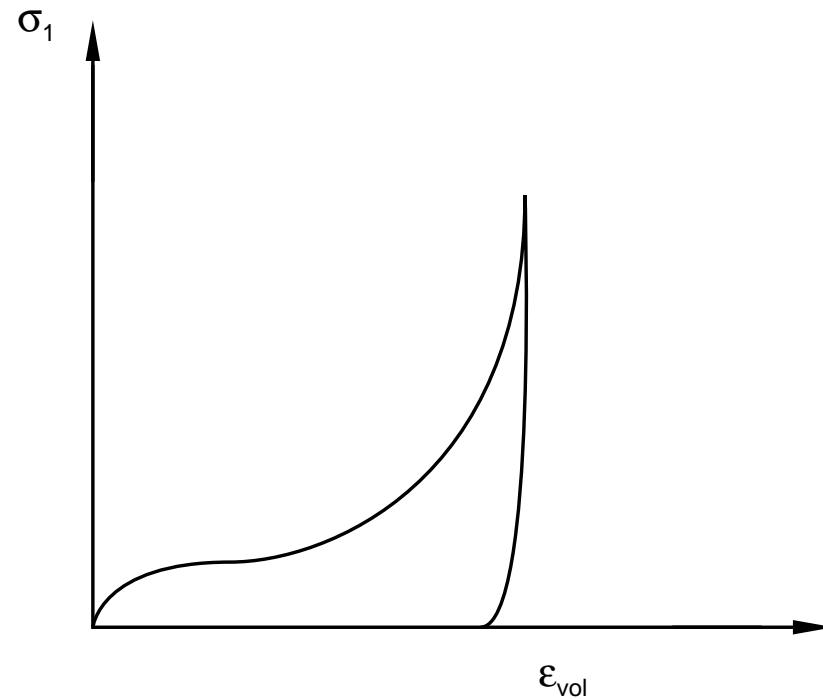
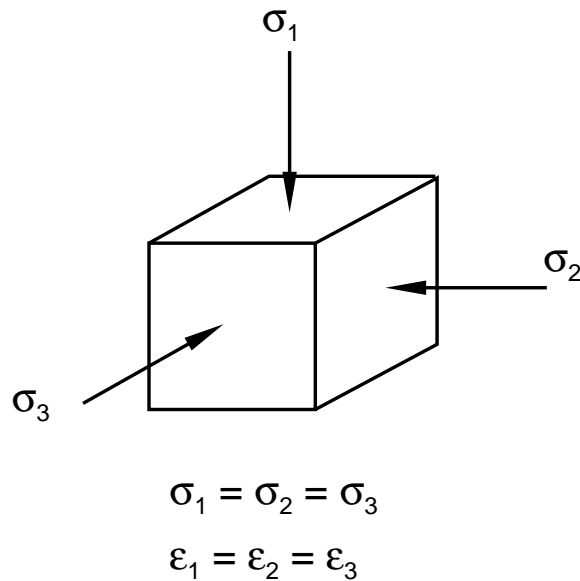
A practical constitutive model should require for calibration only information generated by these standard tests.

More sophisticated laboratory tests can be performed only at a very limited number of testing facilities. Truly triaxial tests require cubical devices that are very expensive and not easy to operate. Any kind of direct tensile test is difficult to perform since it requires a very “stiff” machine (the same applies to compression tests in brittle materials that soften significantly in compression). In most practical constitutive models, assumptions are made regarding the tensile as well as the true triaxial behavior of the material because the tests required for calibration are generally not available.

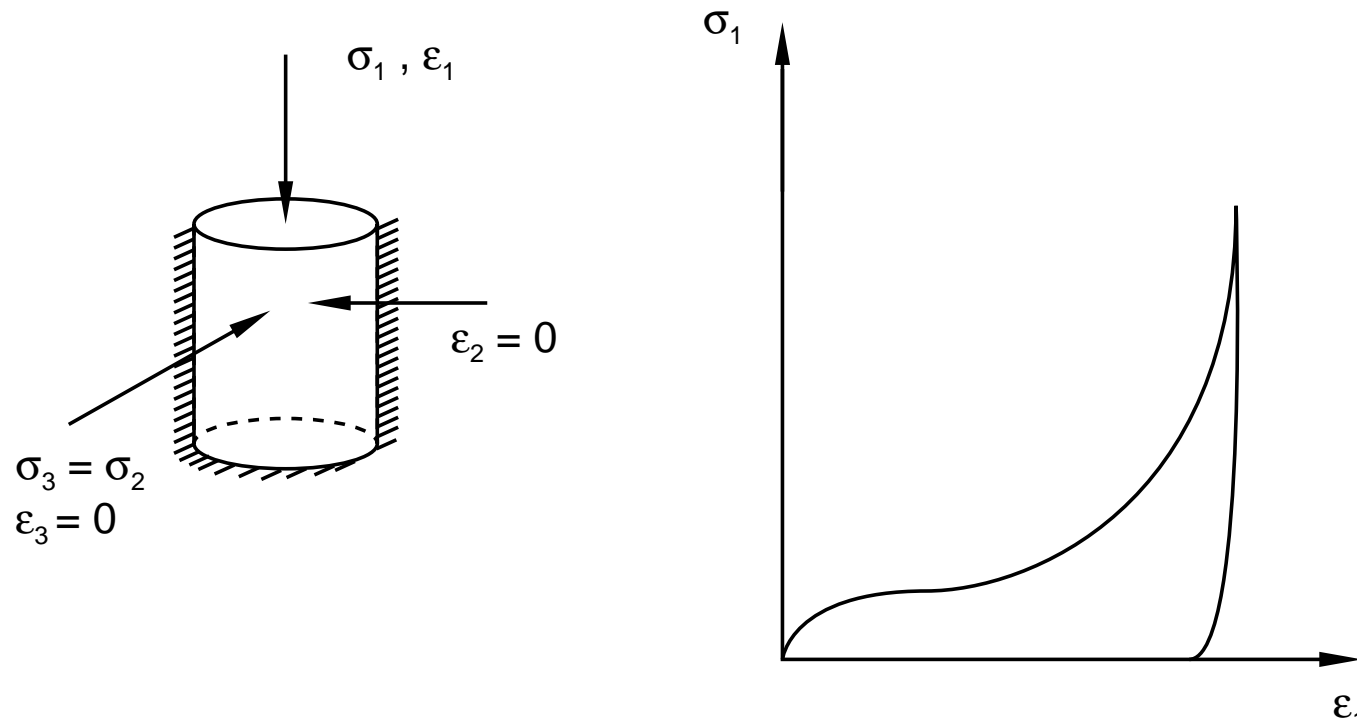
The diversity of geotechnical materials means that a wide range of behaviors is possible. What follows are some very general observations for frictional materials.

Basic Experimental Observations

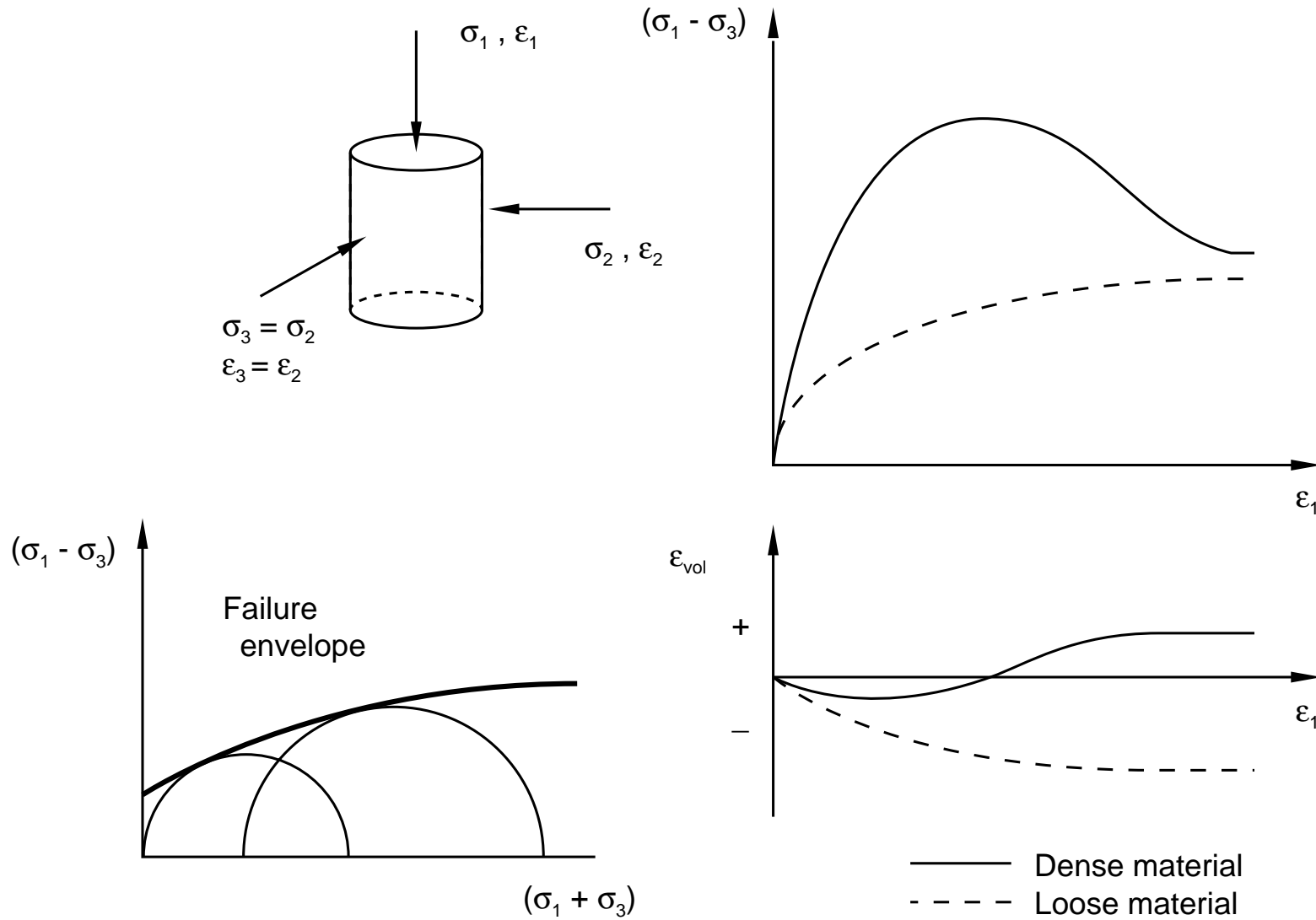
Isotropic compression test:



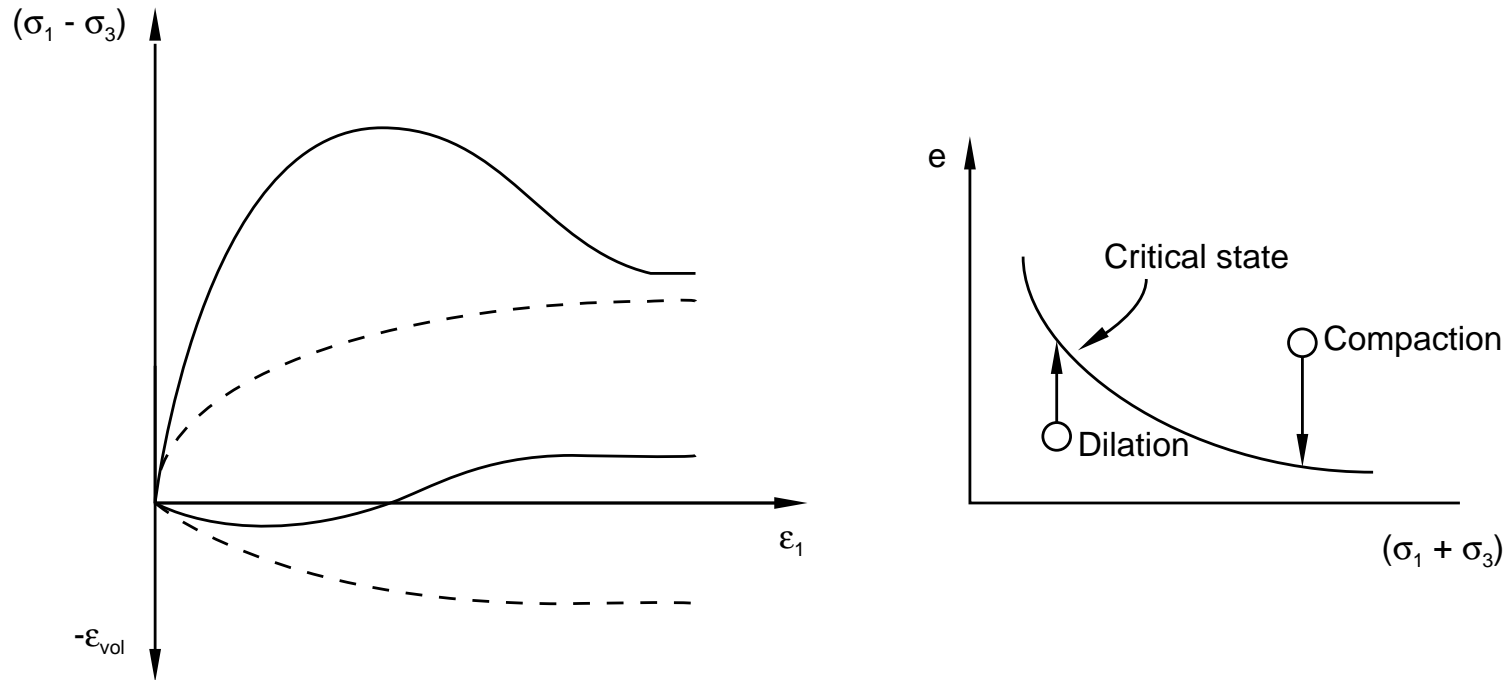
Oedometer (uniaxial strain) test:



Triaxial compression tests:



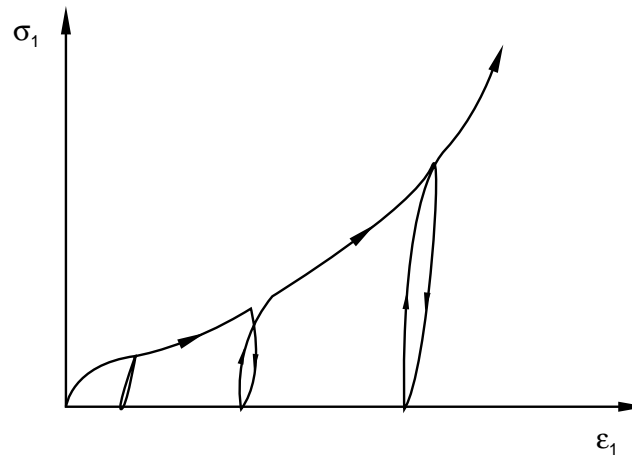
The “critical state” concept:



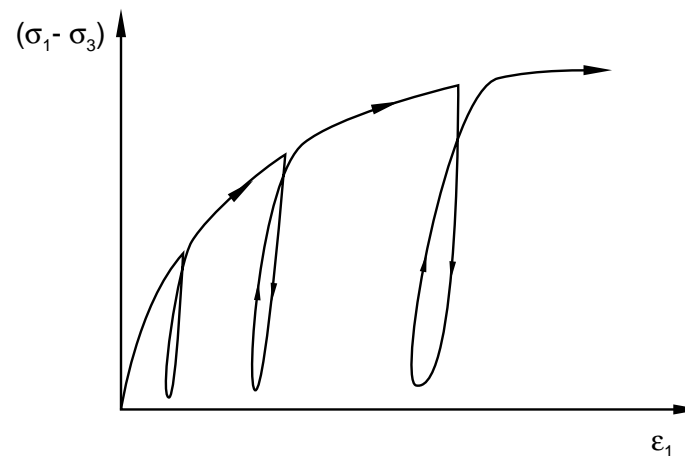
Casagrande defined “critical state” as the state (for monotonic loading) at which continued shear deformation can occur without further change in effective stress and volume (void ratio) of the material.

Cyclic tests:

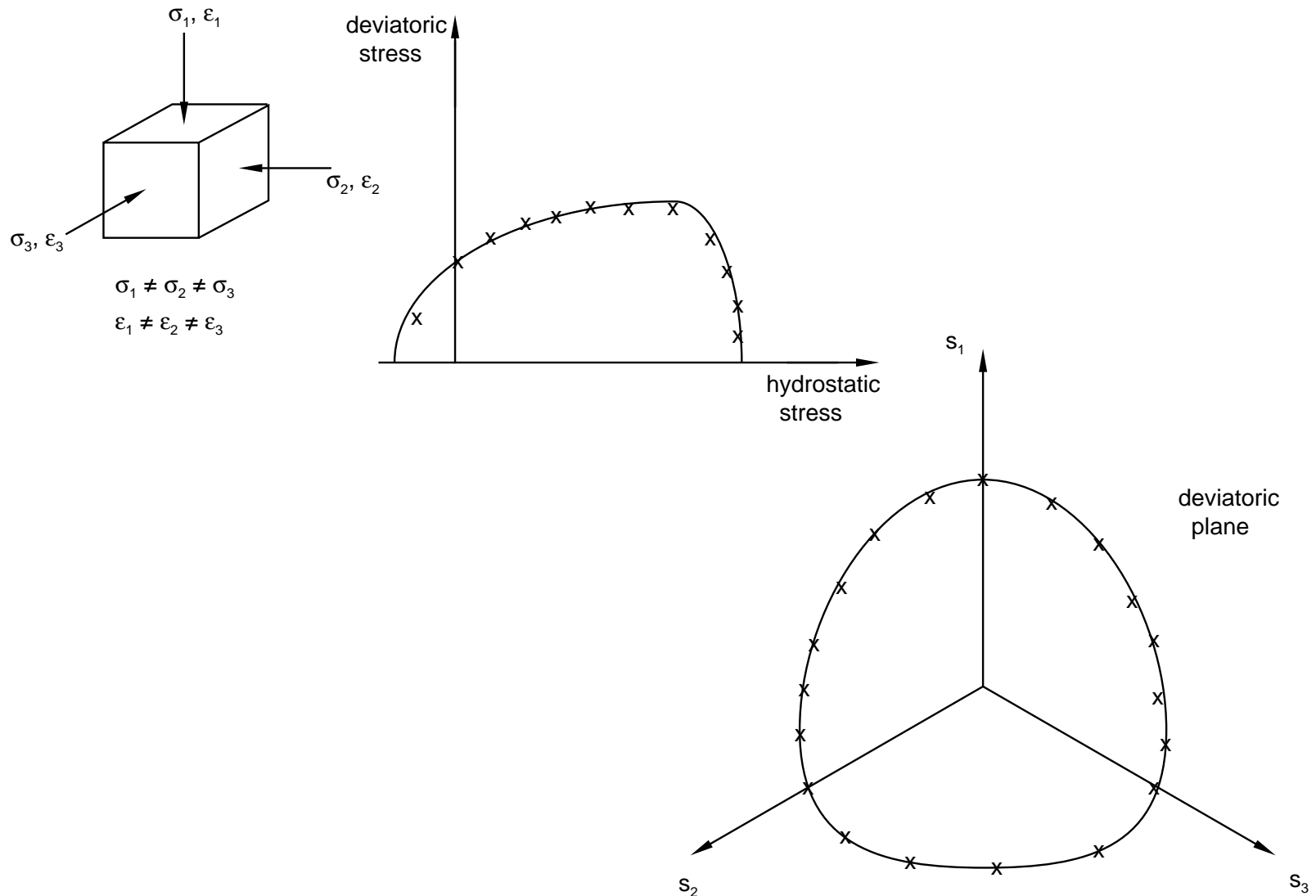
- Isotropic compression or oedometer tests



- Triaxial or uniaxial compression tests



Truly triaxial (cubical) tests:



Essential aspects of behavior of voided frictional materials:

- + Nonlinear stress-strain behavior
 - + Irreversible deformations
 - + Influence of hydrostatic pressure stress on “strength”
 - + Influence of hydrostatic pressure on stress-strain behavior
 - + Influence of intermediate principal stress on “strength”
 - + Shear stressing-dilatancy coupling
 - + Influence of hydrostatic pressure stress on volume changes
 - + Hardening/softening related to volume changes
 - + Stress path dependency
 - + Effects of small stress reversals
 - Effects of large stress reversals (hysteresis)
 - Degradation of elastic stiffness after large stress reversals
-
- + Included in most constitutive models
 - Not included in most models

Testing Requirements and Calibration of Constitutive Models

Basic requirements for laboratory testing of geotechnical materials:

- Specimens must be tested under the assumption that they represent an average material behavior (in the ground there will be some variation within the same soil or rock mass and the spatial scale of such variations may be large compared to laboratory test specimens).
- Tests must simulate the in situ conditions as closely as possible: range of stresses, drainage conditions and density of the material (for deep mining cases this may be difficult).
- All stresses and strains must be measured throughout the stress-strain response to allow complete characterization of the constitutive behavior.

Laboratory testing should be guided by a previously proposed constitutive model. Understanding of this model is necessary for correct interpretation of laboratory tests. Model parameters should be physical and measurable in practicable experiments.

The following is a list of laboratory tests and the corresponding components of the constitutive model that they help calibrate:

- Isotropic compression test or oedometer test. One test is required to calibrate hydrostatic behavior. One unloading is necessary to calibrate the elastic part of this behavior.
- Triaxial compression tests. Two (preferably more) tests are required to calibrate the shear behavior and its hydrostatic pressure dependence. One unloading (in each test) is necessary to calibrate the elastic part of this behavior.
- Triaxial extension tests. Two (preferably more) tests are required to calibrate the intermediate principal stress dependence of the shear behavior.
- Direct tension test. One test is required to calibrate tension behavior of cohesive materials (rocks or soils with cohesion).

- Truly triaxial (cubical) tests. Many tests are required to calibrate the behavior of the material when subjected to different stresses in all directions.
- Shear box tests and indirect tension (Brazilian) tests. These may be useful to calibrate the cohesive properties of the material.
- Multiple unloading-reloading cycles in any of above tests. This is necessary to calibrate effects of large stress reversals such as hysteresis and elastic degradation.

Lecture 3

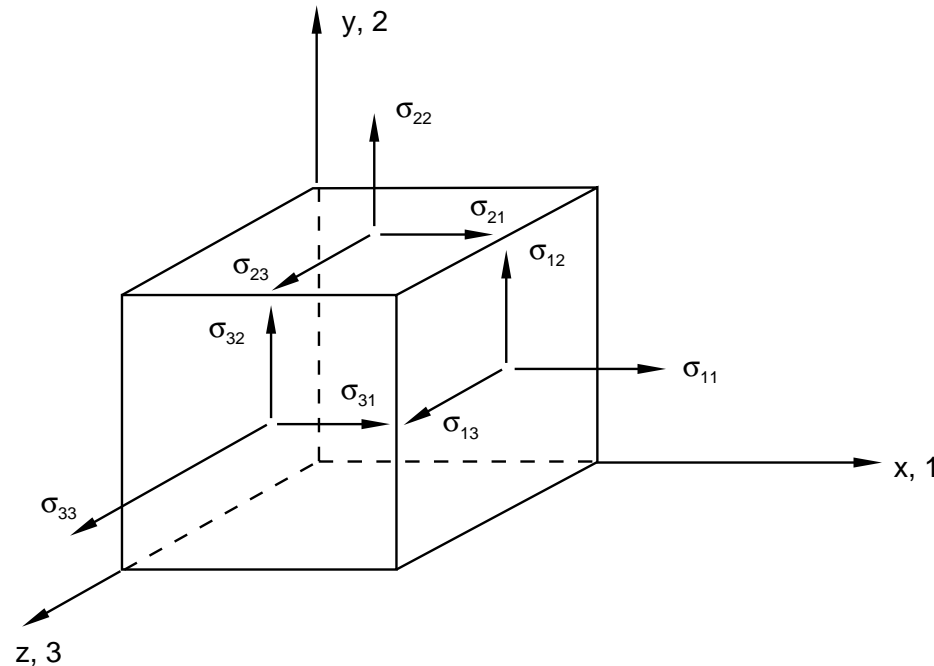
Constitutive Models

Overview

- Stress Invariants and Spaces
- Overview of Constitutive Models
- Elasticity
- Mohr-Coulomb Model
- Modified Drucker-Prager Models
- Coupled Creep and Drucker-Prager Plasticity
- Modified Cam-Clay Model
- Modified Cap Model
- Coupled Creep and Cap Plasticity
- Jointed Material Model
- Numerical Implementation

Stress Invariants and Spaces

Stress in three dimensions: three direct and three shear components.

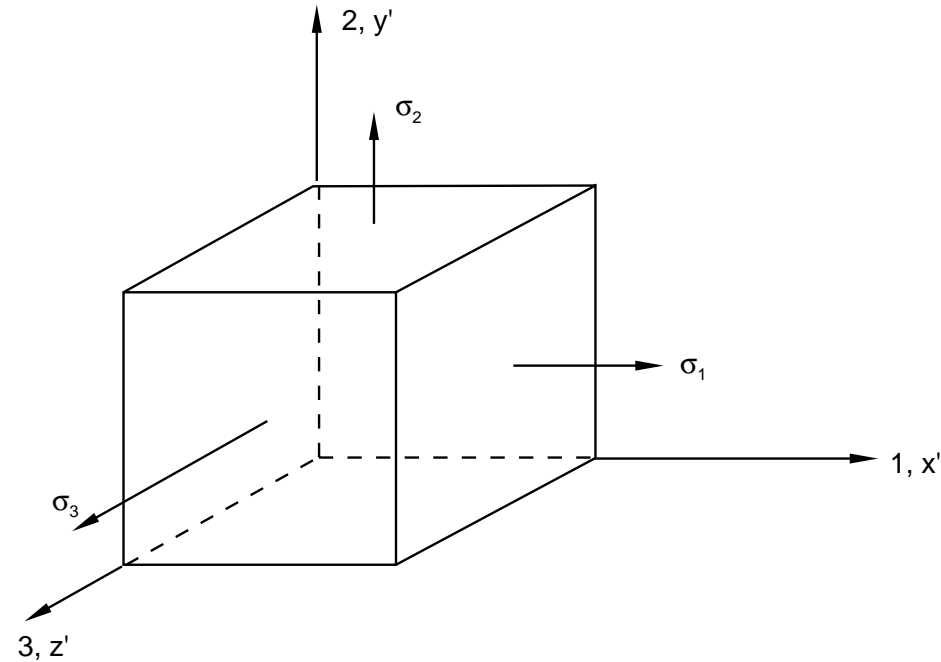


Symmetry of stress tensor:

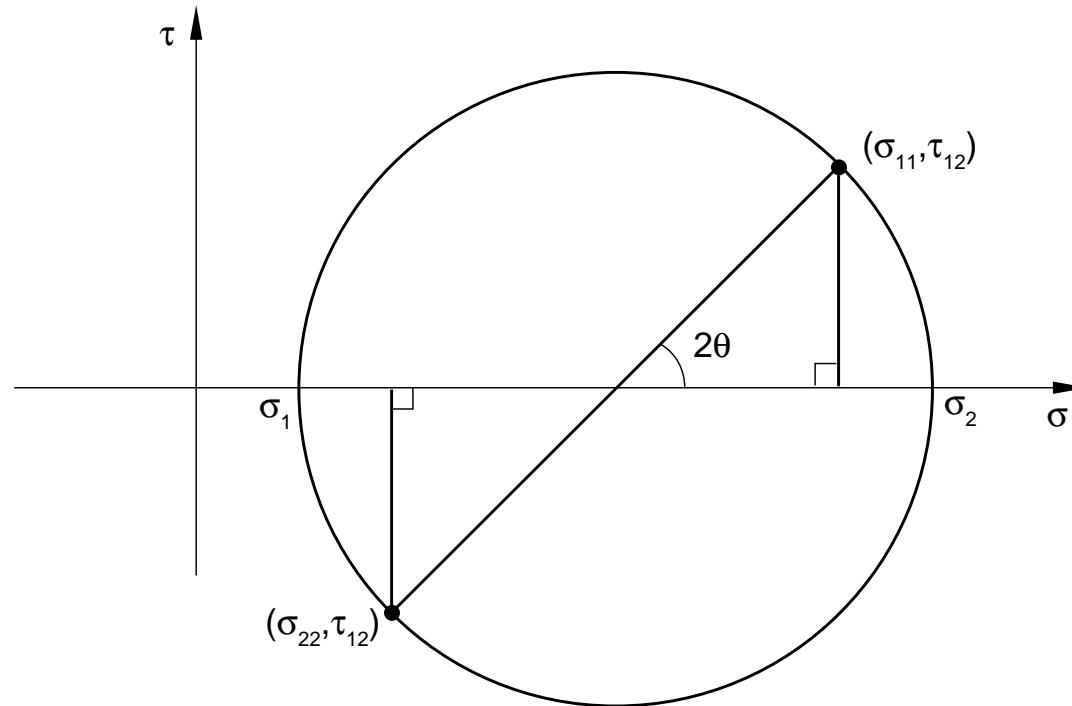
$$\sigma_{12} = \sigma_{21}, \sigma_{13} = \sigma_{31}, \sigma_{23} = \sigma_{32}.$$

ABAQUS convention: tensile stress is positive.

Principal stresses: stresses normal to planes in which shear stresses are zero.



In two dimensions (Mohr's circle):



$$\sigma_{1,2} = \frac{\sigma_{11} + \sigma_{22}}{2} \pm \sqrt{\left(\frac{\sigma_{11} - \sigma_{22}}{2}\right)^2 + \tau_{12}^2}$$

$$\tan 2\theta = \frac{2\tau_{12}}{\sigma_{11} - \sigma_{22}}$$

Stress decomposition: deviatoric plus hydrostatic:

$$\boldsymbol{\sigma} = \boldsymbol{S} - p\boldsymbol{I}.$$

ABAQUS invariants:

$$\text{pressure stress, } p = -\frac{1}{3} \text{trace}(\boldsymbol{\sigma}),$$

$$\text{Mises equivalent stress, } q = \sqrt{\frac{3}{2}(\boldsymbol{S} : \boldsymbol{S})},$$

$$\text{third invariant, } r = \left(\frac{9}{2} \boldsymbol{S} \cdot \boldsymbol{S} : \boldsymbol{S}\right)^{\frac{1}{3}}.$$

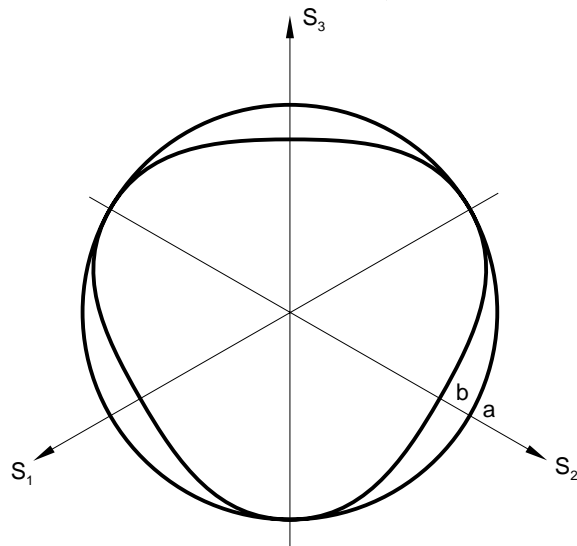
For all models except Mohr-Coulomb, also define deviatoric stress measure:

$$t = \frac{q}{2} \left[1 + \frac{1}{K} - \left(1 - \frac{1}{K} \right) \left(\frac{r}{q} \right)^3 \right],$$

so that $t = q/K$ in triaxial tension ($r = q$) and $t = q$ in triaxial compression ($r = -q$). If $K = 1$, $t = q$.

K is typically between 0.8 and 1.0.

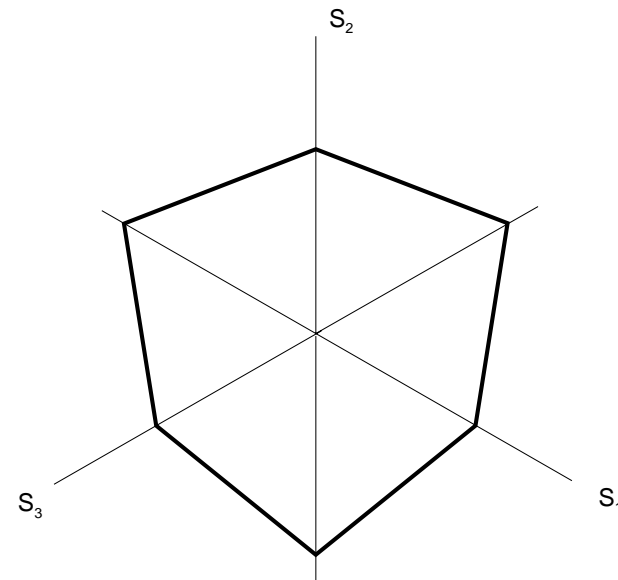
($t = \text{constant}$ is a “rounded” surface in the deviatoric plane—not close to Coulomb behavior.)



Linear Drucker-Prager

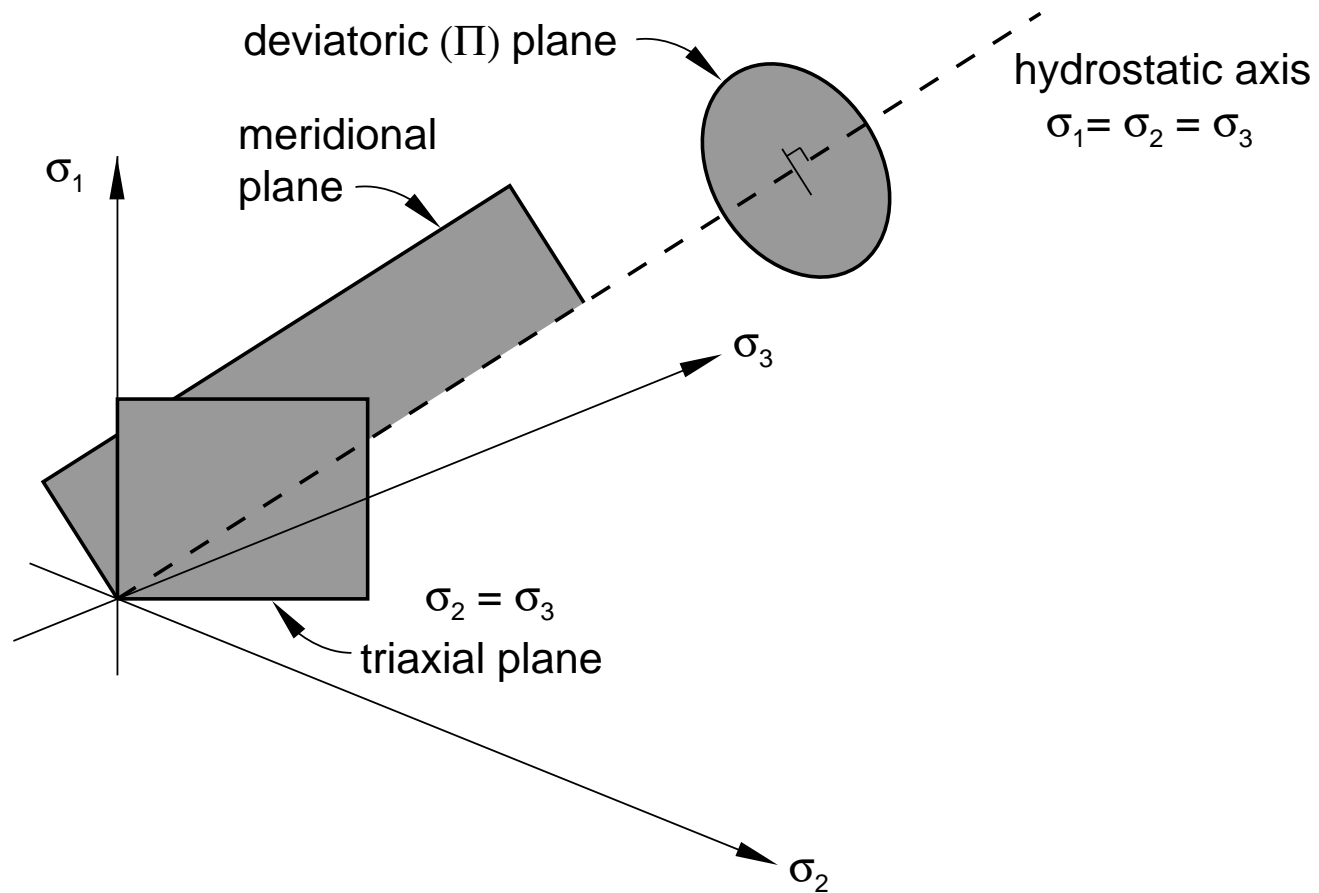
$$t = \frac{1}{2} q \left[1 + \frac{1}{K} - \left(1 - \frac{1}{K} \right) \left(\frac{r}{q} \right)^3 \right]$$

| Curve | K |
|-------|-----|
| a | 1.0 |
| b | 0.8 |



Mohr-Coulomb

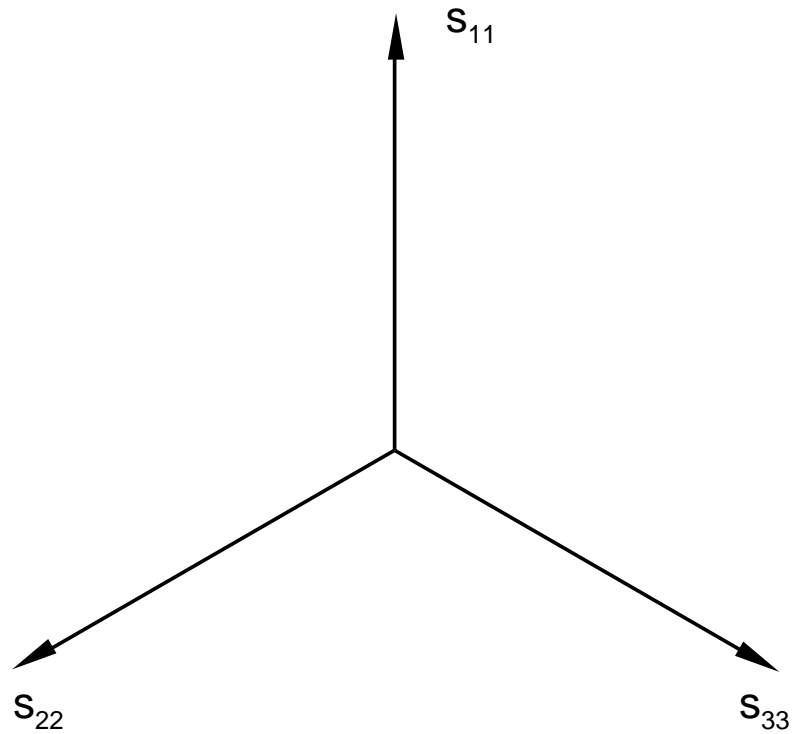
Useful planes:



Meridional plane:



Deviatoric (or Π) plane:



Overview of Constitutive Models

Elasticity models:

- Linear, isotropic
- Porous, isotropic (nonlinear)
- Damaged, orthotropic (nonlinear; used in concrete, jointed material)

Plasticity models:

- Open surface, pressure independent (Mises)
- Open surface, pressure dependent (Drucker-Prager, Mohr-Coulomb)
- Closed surface (Cam-clay, Drucker-Prager with Cap)
- Multisurface (jointed material)
- Nested surfaces (bounding surface †)

Other inelastic models:

- Continuum damage theories †
- Endochronic theories †

None of the available models (with the possible exception of the jointed material model) is capable of accurately handling large stress reversals such as those occurring during cyclic loading or severe dynamic events.

†Not available in ABAQUS for geotechnical materials

Elasticity

Either linear elasticity or nonlinear, porous elasticity can be used with the plasticity models described in the following sections.

Classical linear isotropic elasticity is defined by Young's modulus and Poisson's ratio.

Porous elasticity is a nonlinear, isotropic, elasticity model in which the pressure stress varies as an exponential function of volumetric strain:

$$p = -p_t^{el} + (p_0 + p_t^{el}) \exp \left[\frac{1 + e_0}{\kappa} (1 - \exp(\epsilon_{vol}^{el})) \right]$$

or

$$\frac{\kappa}{(1 + e_0)} \ln \left(\frac{p_0 + p_t^{el}}{p + p_t^{el}} \right) = J^{el} - 1,$$

where $J^{el} - 1$ is the nominal volumetric strain.

Throughout these notes $J = dV/dV^0$ is the ratio of current volume to reference volume, so $\epsilon_{vol} = \ln(J)$ and $J = \exp(\epsilon_{vol})$, where ϵ_{vol} is the logarithmic measure of volumetric strain.

This model allows a zero or nonzero elastic tensile stress limit, p_t^{el} .

The deviatoric behavior is defined either by choosing a constant shear modulus,

$$\mathbf{S} = 2G\mathbf{e}^{el},$$

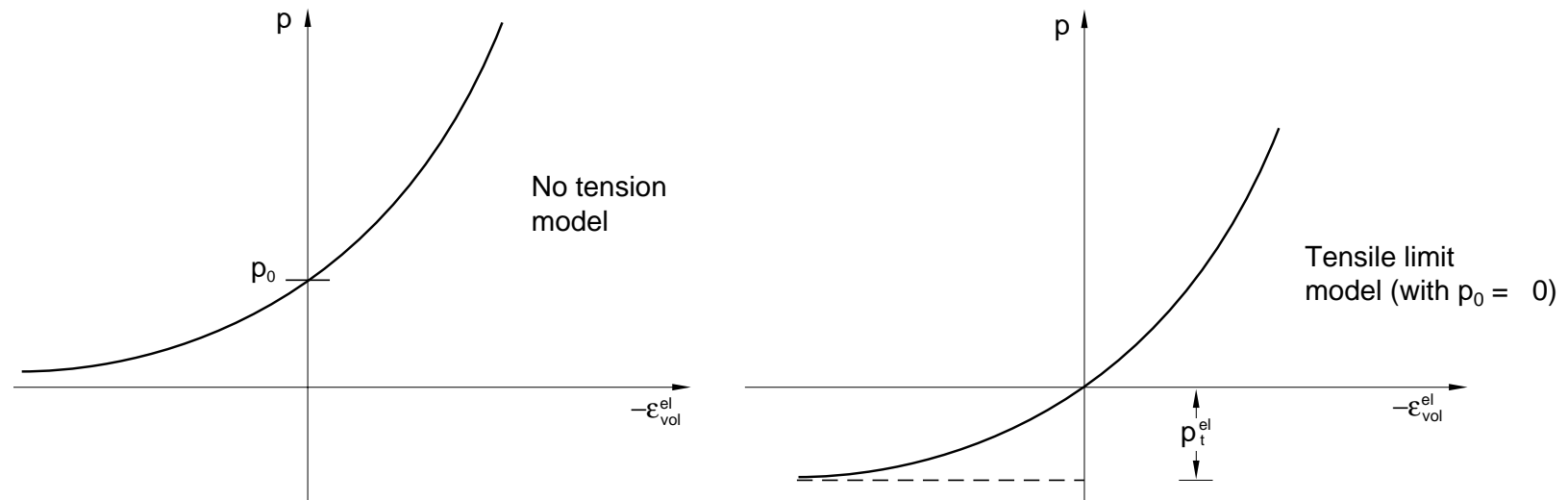
thus making the deviatoric elastic stiffness independent of pressure stress, or choosing a constant Poisson's ratio that makes the deviatoric stiffness dependent on the pressure stress,

$$d\mathbf{S} = 2\hat{G} d\mathbf{e}^{el},$$

where the instantaneous shear modulus, \hat{G} , is

$$\hat{G} = \frac{3(1-2\nu)(1+e_0)}{2(1+\nu)\kappa} (p + p_t^{el}) \exp(\epsilon_{vol}^{el}).$$

κ , p_t^{el} , G , ν are material parameters; p_0 is the initial value of hydrostatic pressure stress, and e_0 is the initial voids ratio.



Porous Elasticity

ϵ_{vol}^{el} has an arbitrary origin, defined so that $p = p_0$ at $\epsilon_{vol}^{el} = 0$.

Mohr-Coulomb Model

The Mohr-Coulomb plasticity model is intended for modeling granular materials such as soils under monotonic loading conditions and does not consider rate dependence.

The ABAQUS Mohr-Coulomb plasticity model has the following characteristics:

- There is a regime of purely linear elastic response, after which some of the material deformation is not recoverable and can, thus, be idealized as being plastic.
- The material is initially isotropic.
- The yield behavior depends on the hydrostatic pressure. One of the consequences of this is that the material becomes stronger as the confining pressure increases.
- The yield behavior may be influenced by the magnitude of the intermediate principal stress.

- The material may harden or soften isotropically.
- The inelastic behavior will generally be accompanied by some volume change: the flow rule may include inelastic dilation as well as inelastic shearing.
- The plastic flow potential is smooth and nonassociated.
- Temperature may affect the material properties.
- It does not consider rate-dependent material behavior.

Description

Linear isotropic elasticity must be used with the Mohr-Coulomb model.

The Mohr-Coulomb yield function is written as

$$F = R_{mc}q - p \tan \phi - c = 0,$$

where

$R_{mc}(\Theta, \phi)$ is a measure of the shape of the yield surface in the deviatoric plane,

$$R_{mc} = \frac{1}{\sqrt{3} \cos \phi} \sin\left(\Theta + \frac{\pi}{3}\right) + \frac{1}{3} \cos\left(\Theta + \frac{\pi}{3}\right) \tan \phi,$$

ϕ is the slope of the Mohr-Coulomb yield surface in the $R_{mc}q-p$ stress plane, which is commonly referred to as the friction angle of the material, $0 \leq \phi < 90$;

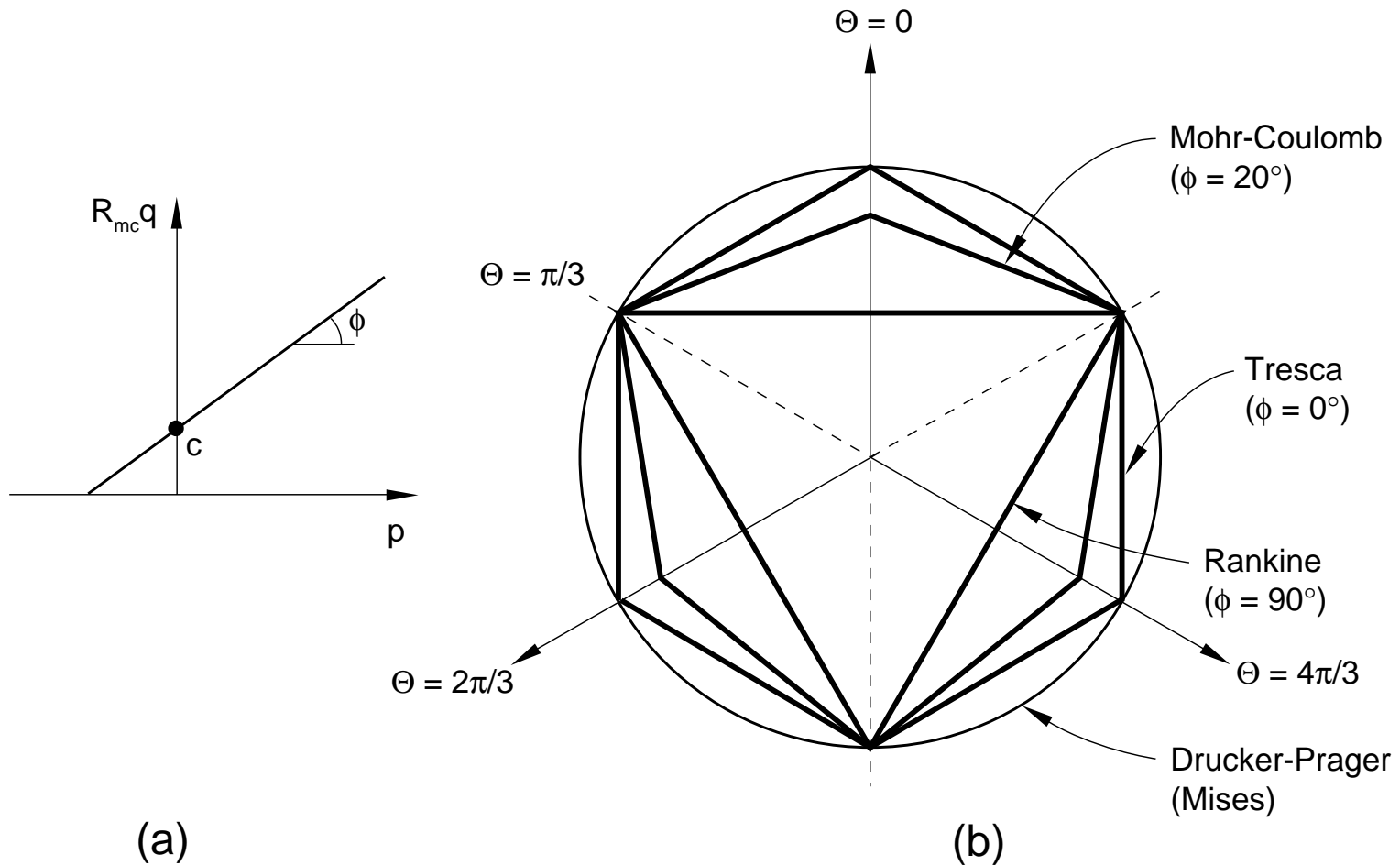
c is the cohesion of the material; and

Θ is the deviatoric polar angle defined as

$$\cos(3\Theta) = \frac{r^3}{q^3}.$$

The Mohr-Coulomb model assumes that the hardening is defined in terms of the material's cohesion, c . The cohesion can be defined as a function of plastic strain, temperature, or field variables.

The hardening is isotropic.



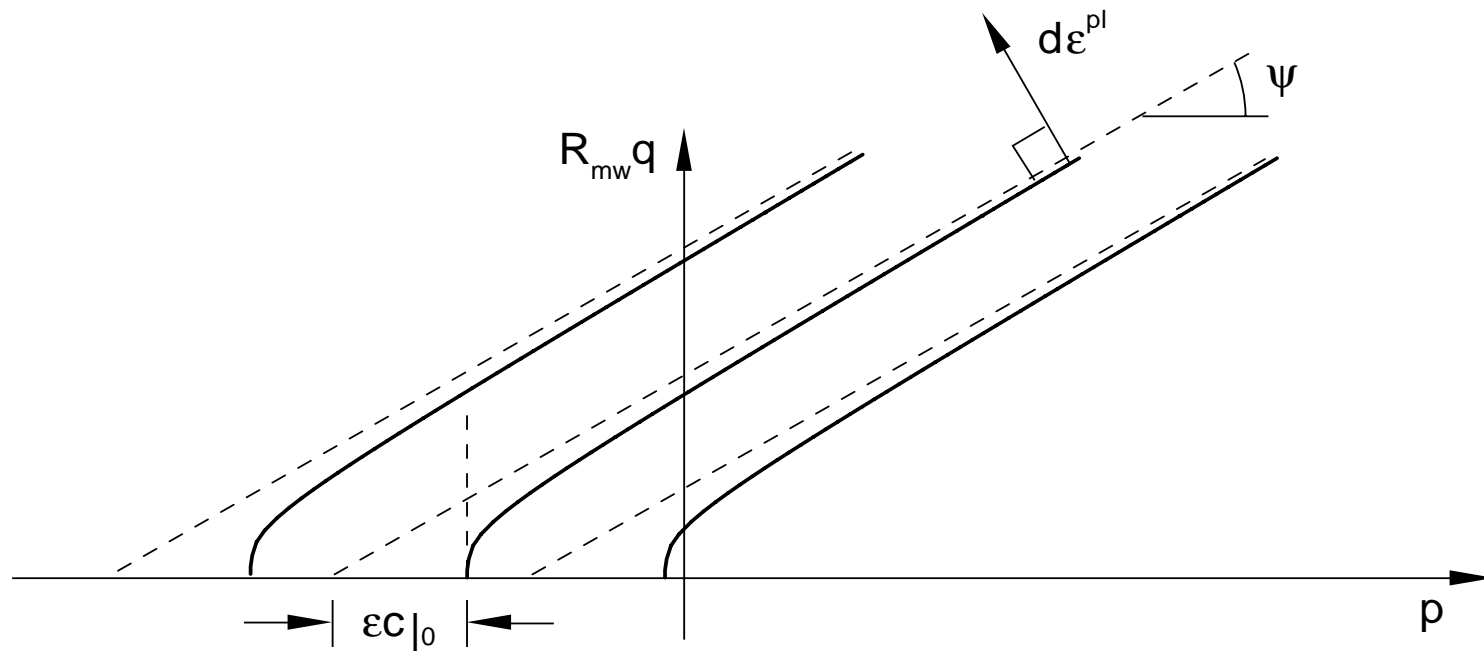
Yield Surface in the Meridional Plane (a) and the Deviatoric Plane (b)

The flow potential, G , is chosen as a hyperbolic function in the meridional stress plane and the smooth elliptic function proposed by Menétrey and Willam (1995) in the deviatoric stress plane:

$$G = \sqrt{(\varepsilon c|_0 \tan \psi)^2 + (R_{mw} q)^2} - p \tan \psi.$$

The initial cohesion of the material, $c|_0 = c(\bar{\varepsilon}^{pl} = 0.0)$; the dilation angle, ψ ; and the meridional eccentricity, ε , control the shape of G in the meridional plane.

ε defines the rate at which G approaches the asymptote (the flow potential tends to a straight line in the meridional stress plane as the meridional eccentricity tends to zero).



Mohr-Coulomb Flow Potential in the Meridional Plane

$R_{mw}(\Theta, e, \phi)$ controls the shape of G in the deviatoric plane:

.

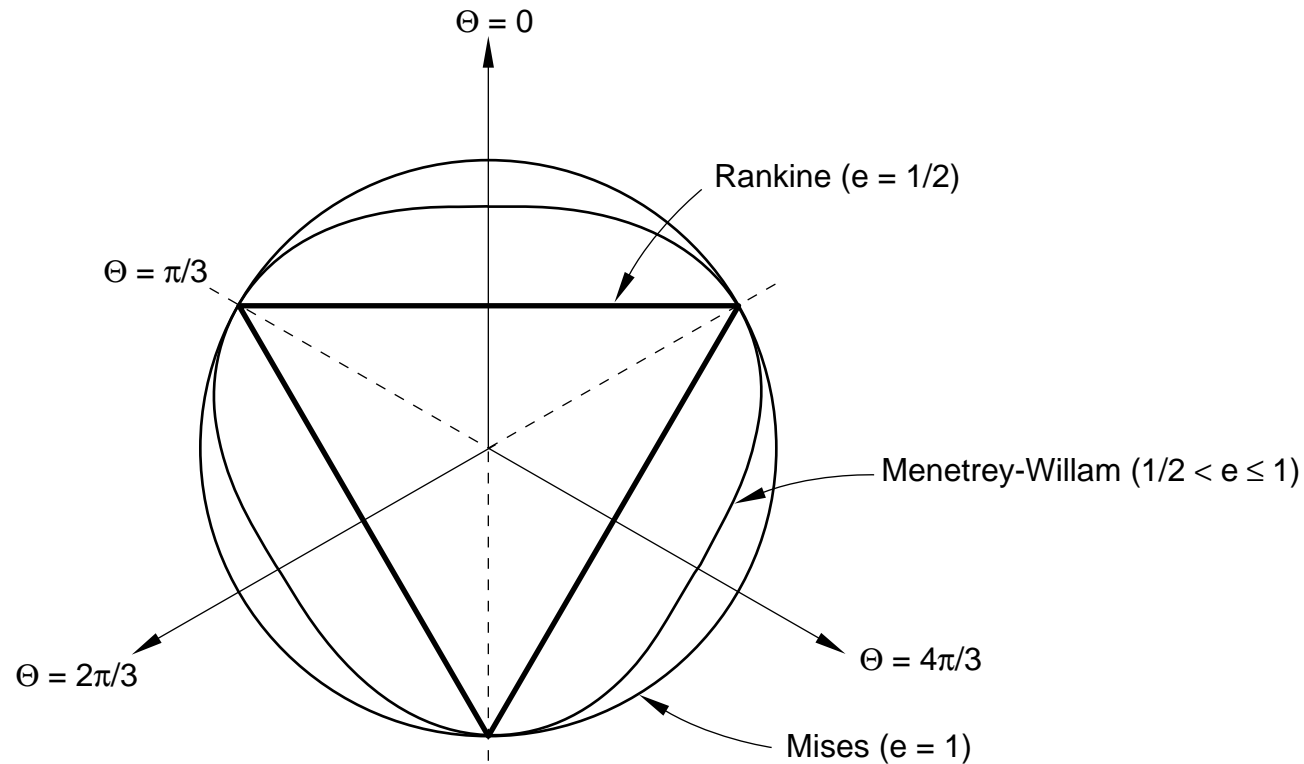
$$R_{mw} = \frac{4(1 - e^2)(\cos \Theta)^2 + (2e - 1)^2}{2(1 - e^2)\cos \Theta + (2e - 1)\sqrt{4(1 - e^2)(\cos \Theta)^2 + 5e^2 - 4e}} R_{mc}\left(\frac{\pi}{3}, \phi\right)$$

The deviatoric eccentricity, e , describes the “out-of-roundedness” of the deviatoric section in terms of the ratio between the shear stress along the extension meridian ($\Theta = 0$) and the shear stress along the compression meridian ($\Theta = \pi/3$).

The default value of the deviatoric eccentricity is calculated by

$$e = \frac{3 - \sin \phi}{3 + \sin \phi} \text{ and allows the ABAQUS Mohr-Coulomb model to match}$$

the behavior of the classical Mohr-Coulomb model in triaxial compression and tension.



The deviatoric eccentricity may have the following range: $\frac{1}{2} < e \leq 1.0$.

If the user defines e directly, ABAQUS matches the classical Mohr-Coulomb model only in triaxial compression.

Plastic flow in the deviatoric plane is always nonassociated.

Usage and Calibration

The *ELASTIC, TYPE=ISOTROPIC option (linear, isotropic elasticity) must be used.

The *MOHR COULOMB option is used to define ψ , ϕ , e , and ε .

- The ECCENTRICITY parameter is used to define ε . The default value is 0.1.
- The DEVIATORIC ECCENTRICITY parameter can be used to define e . The deviatoric eccentricity may have the following range:
$$\frac{1}{2} < e \leq 1.0.$$
- If the user defines e directly, ABAQUS matches the classical Mohr-Coulomb model only in triaxial compression.

The friction angle, ϕ , and the dilation angle, ψ , can be functions of temperature and field variables.

The `*MOHR-COULOMB` option must always be accompanied by the `*MOHR-COULOMB HARDENING` material option, where the evolution of the cohesion, c , of the material is defined. This can be given as a function of temperature and predefined field variables.

`*EXPANSION` can be used to introduce thermal volume change effects.

Plastic flow in the deviatoric plane is always nonassociated; therefore, the unsymmetric solver (`*STEP, UNSYMM=YES`) should be used when a material has Mohr-Coulomb plastic deformation.

Typically the Mohr-Coulomb model is calibrated using the critical stress states from several different triaxial tests. These critical stress states are plotted in the meridional plane to provide an estimate of the friction angle, ϕ , and the cohesion, c , of the material.

- The dilation angle, ψ , is chosen so that the volume change during the plastic deformation matches that seen experimentally.
- If the material is going to harden under plastic deformation, one of the triaxial tests should be used to provide the hardening data.

Because the ABAQUS Mohr-Coulomb model uses a smooth plastic flow potential, it does not always provide the same plastic behavior as a classical (associated) Mohr-Coulomb model, which has a faceted flow potential.

- With the default value of deviatoric eccentricity, e , ABAQUS does match classical Mohr-Coulomb behavior under triaxial extension or compression.
- Benchmark Problem 1.14.5, *Finite deformation of an elastic-plastic granular material*, shows how to match the ABAQUS Mohr-Coulomb model to the classical Mohr-Coulomb model for plane strain deformation.

Modified Drucker-Prager Models

This set of models is intended to simulate material response under essentially monotonic loading, such as the limit load analysis of a soil foundation.

These models are the simplest available for simulating frictional materials.

The basic characteristics of this set of models are:

- There is a regime of purely elastic response, after which some of the material deformation is not recoverable and can, thus, be idealized as being plastic.
- The material is initially isotropic.
- The yield behavior depends on the hydrostatic pressure. One of the consequences of this is that the material becomes stronger as the confining pressure increases. The material may harden or soften isotropically. The models differ in the manner in which the hydrostatic pressure dependence is introduced.

- The inelastic behavior will generally be accompanied by some volume change: the flow rule may include inelastic dilation as well as inelastic shearing. Two different flow rules are offered.
- The yield behavior may be influenced by the magnitude of the intermediate principal stress.
- The material may be sensitive to the rate of straining.
- Temperature may affect the material properties.

Either linear elasticity or nonlinear porous elasticity, as described in **Elasticity** (p. L3.12), can be used with these models.

A choice of three different yield criteria is provided. The differences are based on the shape of the yield surface in the meridional plane: a linear form, a hyperbolic form, or a general exponent form.

The hyperbolic and exponent models are available only in ABAQUS/Standard.

In ABAQUS/Explicit only the linear model is available.

The choice of model to be used depends largely on the kind of material, on the experimental data available for calibration of the model parameters, and on the range of pressure stress values that the material is likely to see. Calibration is discussed later.

Linear Drucker-Prager Model

The yield surface of the linear model is written as

$$F = t - p \tan \beta - d = 0.$$

The cohesion, d , is related to the hardening input data as

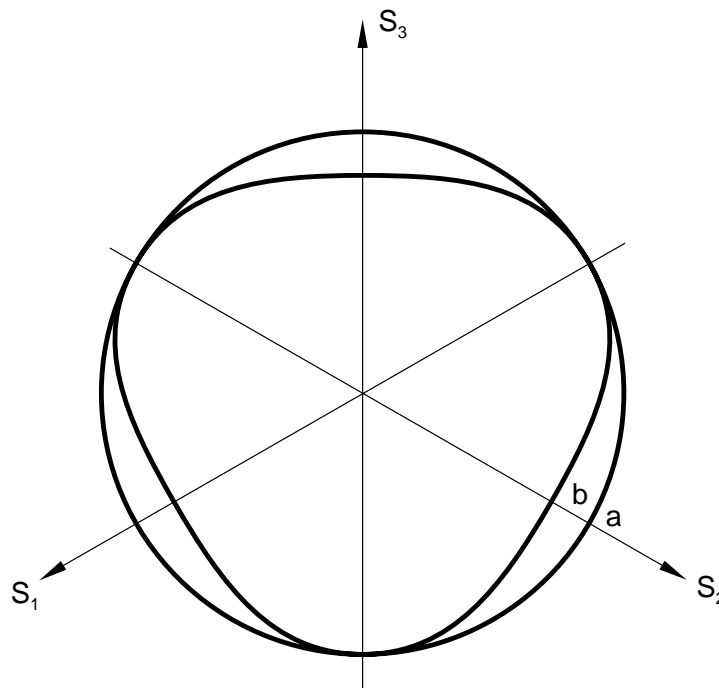
$$d = (1 - \frac{1}{3} \tan \beta) \sigma_c \quad \text{if hardening is defined by uniaxial compression, } \sigma_c ;$$

$$d = \left(\frac{1}{K} + \frac{1}{3} \tan \beta \right) \sigma_t \quad \text{if hardening is defined by uniaxial tension, } \sigma_t ; \text{ and}$$

$$d = d \quad \text{if hardening is defined by shear (cohesion), } d.$$

β (the friction angle) and K are material parameters. d , σ_c , or σ_t is used as the (isotropic) hardening parameter, which is assumed to depend on the equivalent plastic strain.

The measure of deviatoric stress, t , allows matching of different stress values in tension and compression in the deviatoric plane, thus providing flexibility in fitting experimental results. However, as mentioned previously, the surface is too smooth to be a close approximation to the Mohr-Coulomb surface.



$$t = \frac{1}{2} q \left[1 + \frac{1}{K} - \left(1 - \frac{1}{K} \right) \left(\frac{r}{q} \right)^3 \right]$$

| Curve | K |
|-------|-----|
| a | 1.0 |
| b | 0.8 |

We assume a (possibly) nonassociated flow rule, where the direction of the inelastic deformation vector is normal to a linear plastic potential, G :

$$d\epsilon^{pl} = \frac{d\bar{\epsilon}^{pl}}{c} \frac{\partial G}{\partial \sigma},$$

where $G = t - p \tan \psi$, c is a constant that depends on the type of hardening data,

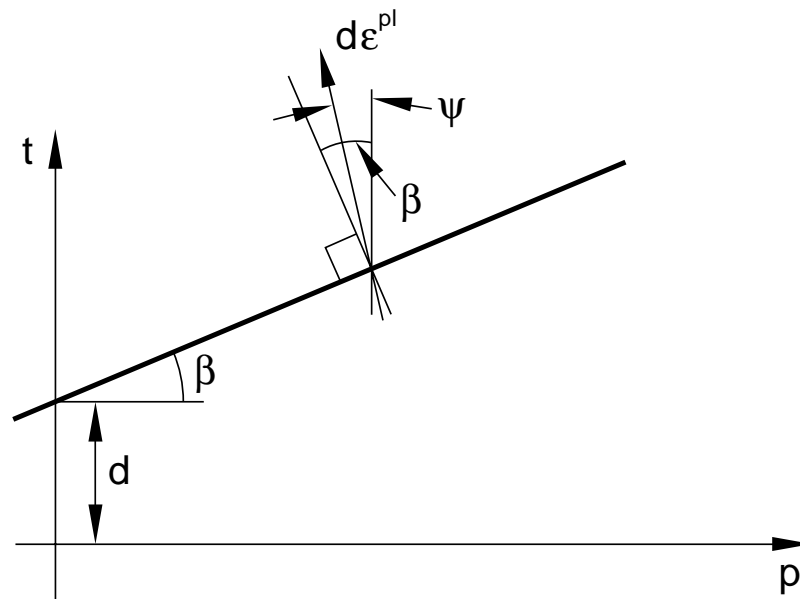
$$d\bar{\epsilon}^{pl} = |d\epsilon_{11}^{pl}| \text{ in uniaxial compression,}$$

$$d\bar{\epsilon}^{pl} = d\epsilon_{11}^{pl} \text{ in uniaxial tension, and}$$

$$d\bar{\epsilon}^{pl} = \frac{d\gamma^{pl}}{\sqrt{3}} \text{ in pure shear.}$$

ψ is the dilation angle in the p - t plane. This flow rule definition precludes dilation angles $\psi > 71.5^\circ$ ($\tan \psi > 3$), which is not likely to be a limitation for real materials.

Flow is associated in the deviatoric plane but nonassociated in the p - t plane if $\psi \neq \beta$. For $\psi = 0$, the material is nondilatational; and if $\psi = \beta$, the model is fully associated.



Hyperbolic Model

The hyperbolic yield criterion is a continuous combination of the maximum tensile stress condition of Rankine (tensile cut-off) and the linear Drucker-Prager condition at high confining stress. It is written as

$$F = \sqrt{l_0^2 + q^2} - p \tan \beta - d' = 0 ,$$

where d' is the hardening parameter that is related to the hardening input data as

$$d' = \sqrt{l_0^2 + \sigma_c^2} - \frac{\sigma_c}{3} \tan \beta \quad \text{if hardening is defined by uniaxial compression, } \sigma_c;$$

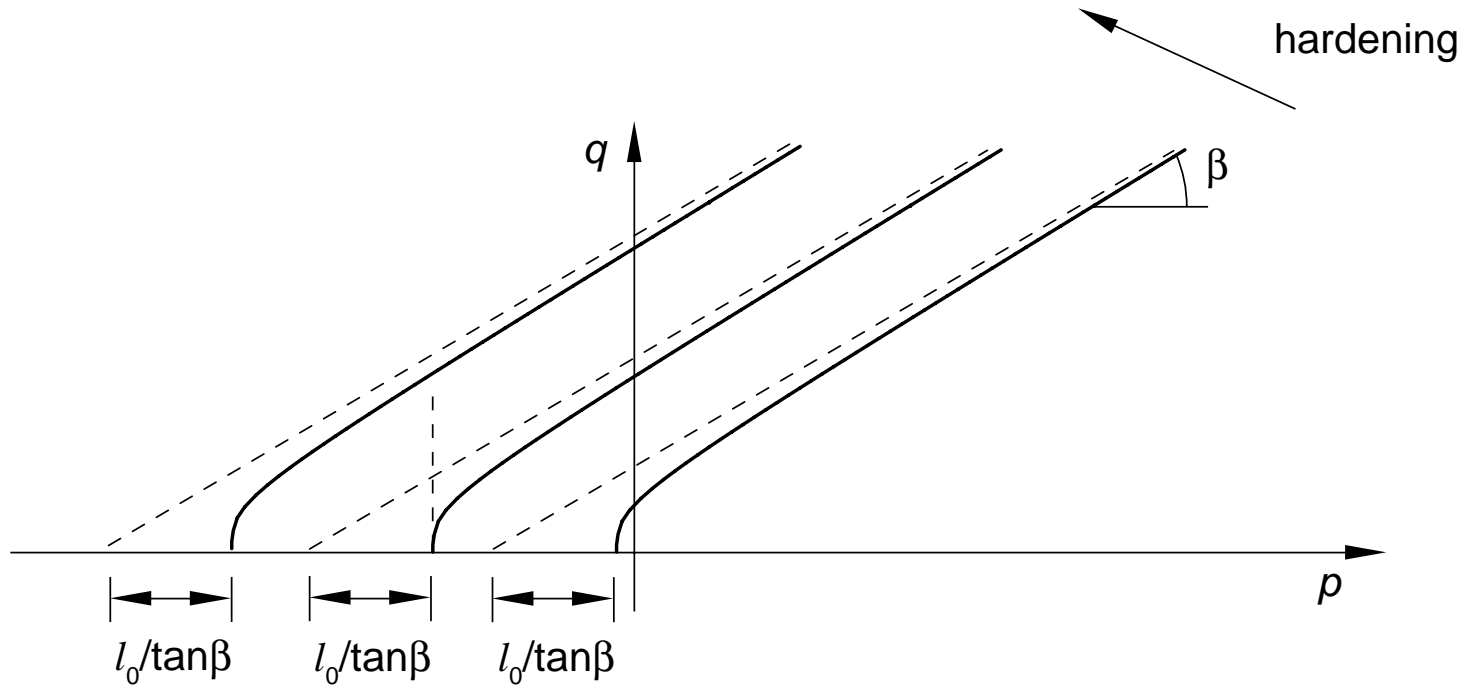
$$d' = \sqrt{l_0^2 + \sigma_t^2} + \frac{\sigma_t}{3} \tan \beta \quad \text{if hardening is defined by uniaxial tension, } \sigma_t;$$

$$d' = \sqrt{l_0^2 + d^2} \quad \text{if hardening is defined by shear (cohesion), } d.$$

$l_0 = d'|_0 - p_t|_0 \tan \beta$ determines how quickly the hyperbola approaches its asymptote (see sketch).

$p_t|_0$ is the initial hydrostatic tension strength of the material, $d'|_0$ is the initial value of d' , and β is the friction angle measured at high confining pressure.

The model treats β and l_0 as constants during hardening.



The yield surface is a von Mises circle in the deviatoric stress plane. (The K parameter is not available for this model.)

Exponent Model

The general exponent form provides the most general yield criterion available in this class of models. The yield function is written as

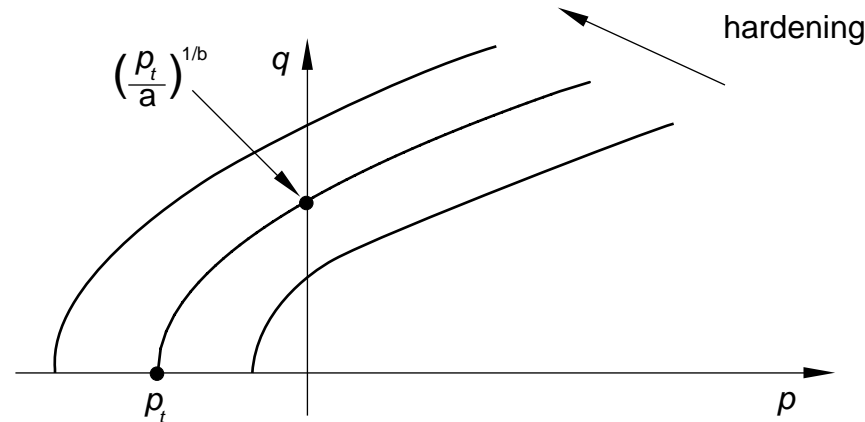
$$F = aq^b - p - p_t = 0,$$

where a and b are material parameters independent of plastic deformation and p_t is the hardening parameter that represents the hydrostatic tension strength of the material and is related to the input data as

$$p_t = a\sigma_c^b - \frac{\sigma_c}{3} \text{ if hardening is defined by uniaxial compression, } \sigma_c;$$

$$p_t = a\sigma_t^b + \frac{\sigma_t}{3} \text{ if hardening is defined by uniaxial tension, } \sigma_t; \text{ and}$$

$$p_t = ad^b \text{ if hardening is defined by shear (cohesion), } d.$$



The yield surface is a von Mises circle in the deviatoric stress plane. (The K parameter is not available for this model.)

The material parameters a , b , and p_t can be given directly; or, if triaxial test data at different levels of confining pressure are available, ABAQUS will determine the material parameters from the triaxial test data using a least squares fit.

Flow in the Hyperbolic and Exponent Models

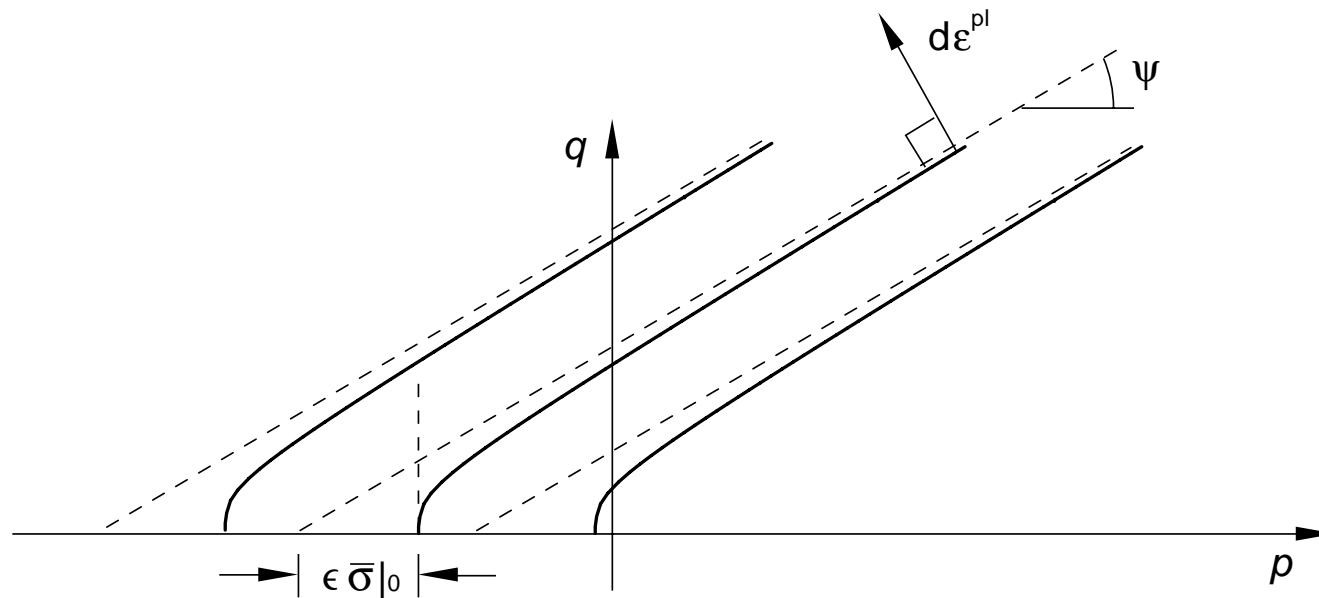
Plastic flow in the hyperbolic and general exponent models is governed by the hyperbolic flow potential

$$G = \sqrt{(\varepsilon \bar{\sigma}|_0 \tan \psi)^2 + q^2} - p \tan \psi ,$$

where ψ is the dilation angle in the meridional plane at high confining pressure; $\bar{\sigma}|_0$ is the initial yield stress; and ε is a parameter (referred to as the eccentricity) that defines the rate at which the function approaches its asymptote (the flow potential tends to a straight line as the eccentricity tends to zero).

This flow potential, which is continuous and smooth, ensures that the flow direction is always defined uniquely.

The function approaches the linear Drucker-Prager flow potential asymptotically at high confining pressure stress and intersects the hydrostatic pressure axis at 90° . It is, therefore, preferred as a flow potential for the Drucker-Prager models over the straight line potential, which has a vertex on the hydrostatic pressure axis.



The potential is the von Mises circle in the deviatoric stress plane.

Associated flow is obtained in the hyperbolic model if $\beta = \psi$ and

$$\varepsilon = \frac{l_0}{\bar{\sigma}|_0 \tan \psi}.$$

In the general exponent model flow is always nonassociated in the meridional plane. The default flow potential eccentricity is $\varepsilon = 0.1$, which implies that the material has almost the same dilation angle over a wide range of confining pressure stress values.

Increasing the value of the eccentricity provides more curvature to the flow potential, implying that the dilation angle increases more rapidly as the confining pressure decreases. Values of the eccentricity less than the default value may lead to convergence problems if the material is subjected to low confining pressures because of the very tight curvature of the flow potential near its intersection with the p -axis.

Usage

The modified Drucker-Prager plasticity models in ABAQUS are invoked with the `*DRUCKER PRAGER` material option. The `SHEAR CRITERION` parameter is set to `LINEAR`, `HYPERBOLIC`, or `EXPONENT` to define the yield surface shape.

The `*DRUCKER PRAGER` option must always be accompanied by the `*DRUCKER PRAGER HARDENING` option. This option defines the evolution of the yield stress in uniaxial compression (`TYPE=COMPRESSION`), in uniaxial tension (`TYPE=TENSION`), or in pure shear (`TYPE=SHEAR`).

It is possible to make the yield function rate dependent by using the `*RATE DEPENDENT` option or by specifying the yield stress as a function of the plastic strain rate. A rate dependency is rarely used for geotechnical materials, but these same yield models are sometimes used for other materials such as polymers where it is important. The manner of introducing rate dependence is described in the User's Manual.

The elasticity is defined with the *ELASTIC material option in the case of linear elasticity or with the *POROUS ELASTIC option if porous elasticity is chosen.

All of the material parameters can be entered as functions of temperature and field variables.

*EXPANSION can be used to introduce thermal volume change effects.

*INITIAL CONDITIONS, TYPE=RATIO is required to define the initial voids ratio (porosity) of the material if porous elasticity is used.

Analyses using a nonassociated flow version of the model may require the use of the UNSYMM=YES parameter on the *STEP option because of the resulting unsymmetric plasticity equations. If UNSYMM=YES is not used when the flow is nonassociated, ABAQUS may not find a converged solution.

Matching Experimental Data

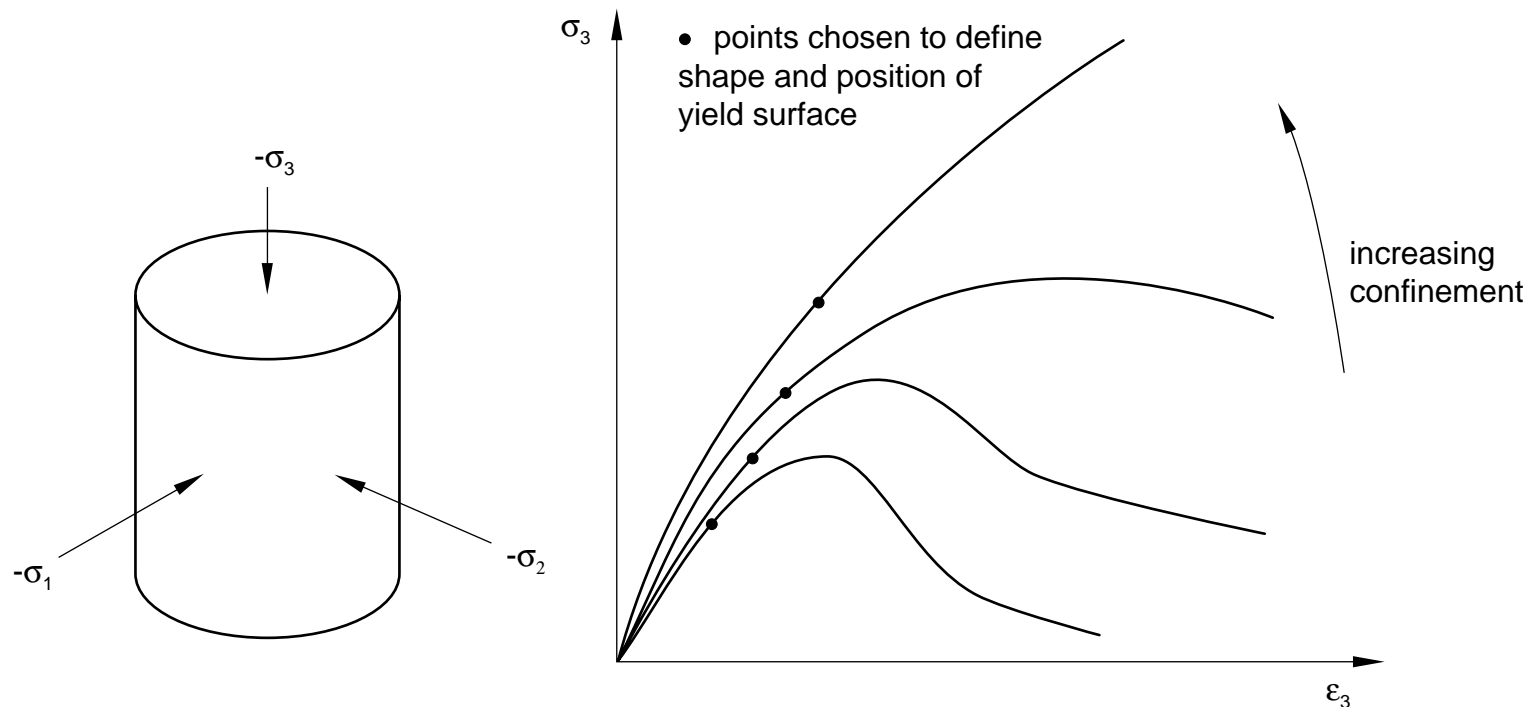
At least two experiments are required to calibrate the simplest version of the Drucker-Prager plasticity model (linear model, rate independent, temperature independent, and yielding independent of the third stress invariant).

For geotechnical materials the most common experiments performed for this purpose are uniaxial compression (for cohesive materials) and triaxial compression or tension tests. However, other experiments can be used as alternatives: for example, shear tests for cohesive materials.

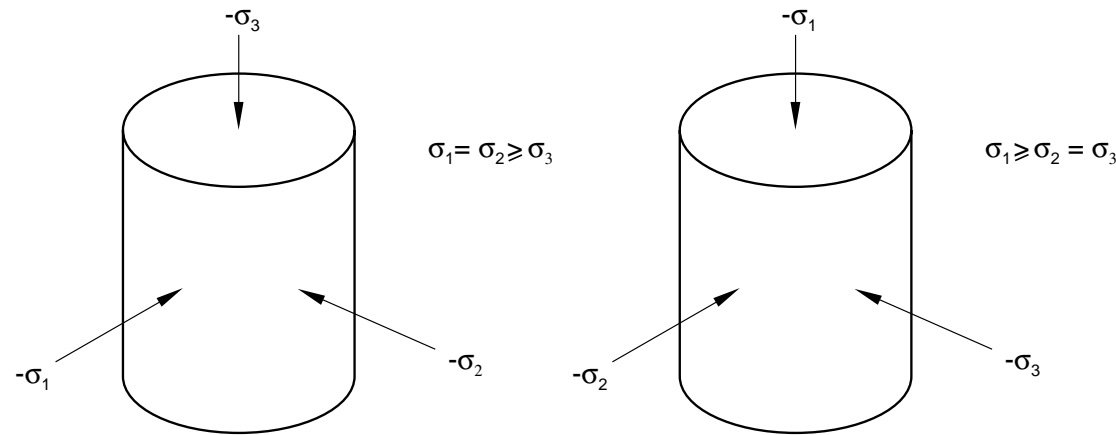
The uniaxial compression test involves compressing the sample between two rigid platens. The load and displacement in the direction of loading are recorded. The lateral displacements should also be recorded so that the correct volume changes can be calibrated.

Triaxial test data are required for a more accurate calibration.

Triaxial compression/tension experiments are performed using a standard triaxial machine where a fixed confining pressure is maintained while the differential stress is applied. Several tests covering the range of confining pressures of interest are usually performed. Again, the stress and strain in the direction of loading are recorded, together with the lateral strain, so that the correct volume changes can be calibrated.



In a triaxial compression test the specimen is confined by pressure and an additional compression stress is superposed in one direction. Thus, the principal stresses are all negative, with $0 \geq \sigma_1 = \sigma_2 \geq \sigma_3$.



Triaxial Compression and Tension Tests

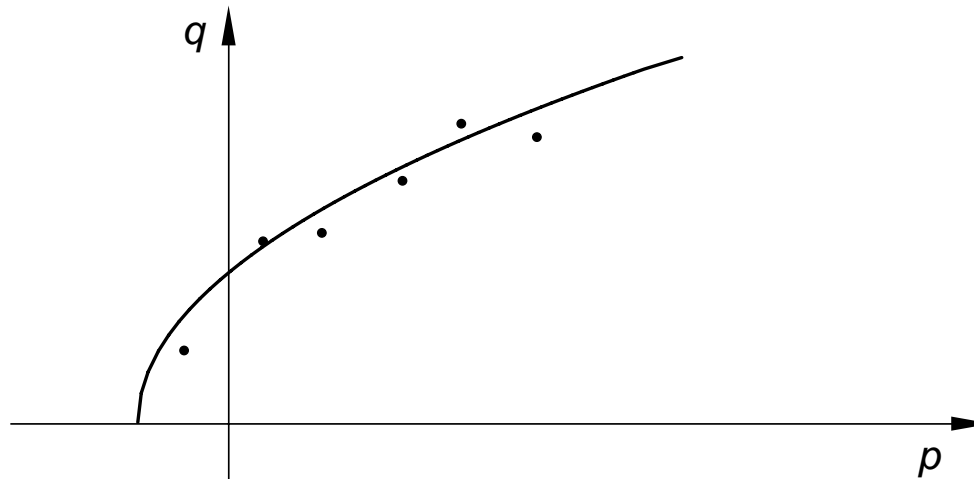
The stress invariant values in triaxial compression are

$$p = -\frac{1}{3}(2\sigma_1 + \sigma_3), \quad q = \sigma_1 - \sigma_3, \quad r = -q, \quad t = q.$$

The triaxial results can, thus, be plotted in the q - p plane.

The stress state corresponding to some user-chosen critical level (the stress at onset of inelastic behavior or the ultimate yield stress) provides one data point for calibrating the yield surface material parameters.

Additional data points are obtained from triaxial tests at different levels of confinement. These data points define the shape and position of the yield surface in the meridional plane.



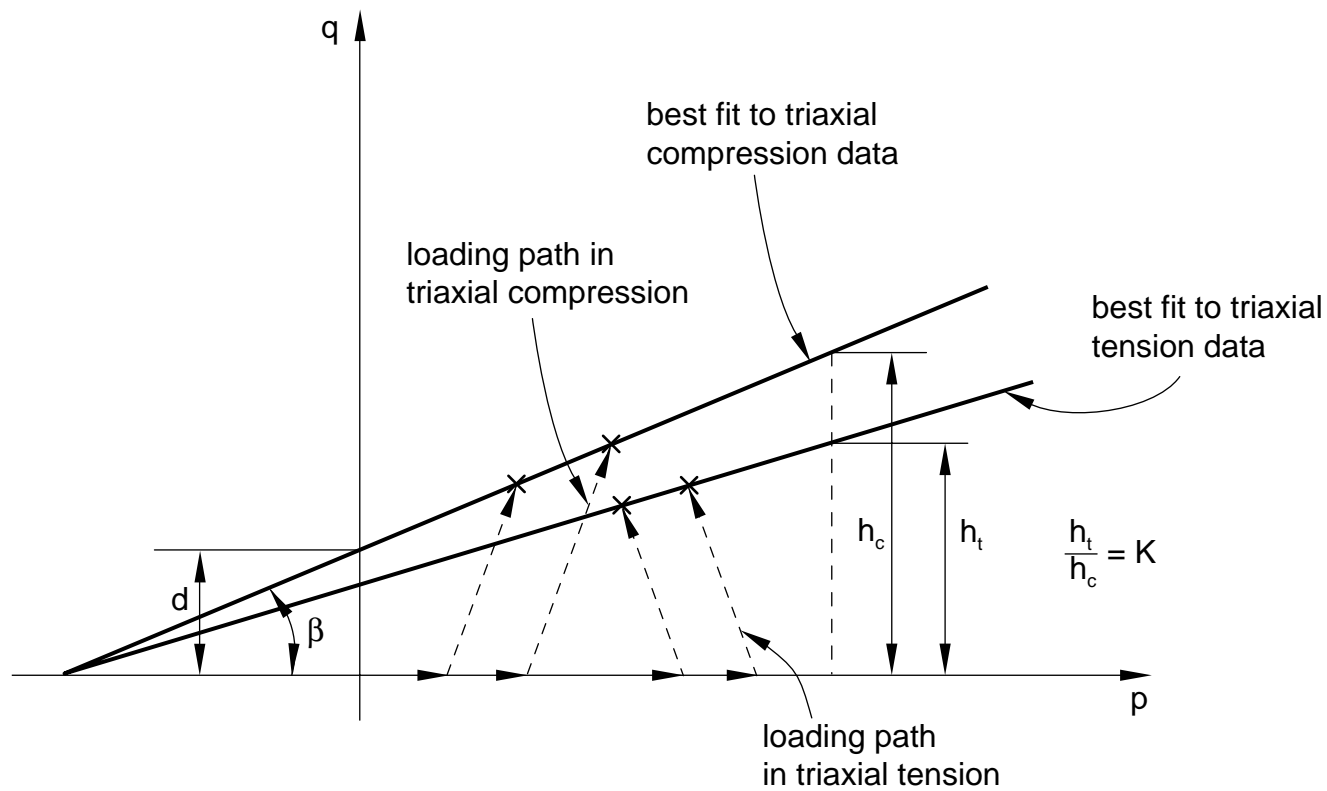
Defining the shape and position of the yield surface is adequate to define the model if it is to be used as a failure surface.

To incorporate isotropic hardening, one of the stress-strains curves from the triaxial tests can be used to define the hardening behavior. The curve that represents hardening most accurately over a wide range of loading conditions should be selected.

Unloading measurements in these tests are useful to calibrate the elasticity, particularly in cases where the initial elastic region is not well defined.

Linear Drucker-Prager Model

Fitting the best straight line through the results provides the friction angle β .



Triaxial tension test data are also needed to define K . Under triaxial tension the specimen is again confined by pressure, then the pressure in one direction is reduced. In this case the principal stresses are $0 \geq \sigma_1 \geq \sigma_2 = \sigma_3$. The stress invariants are now

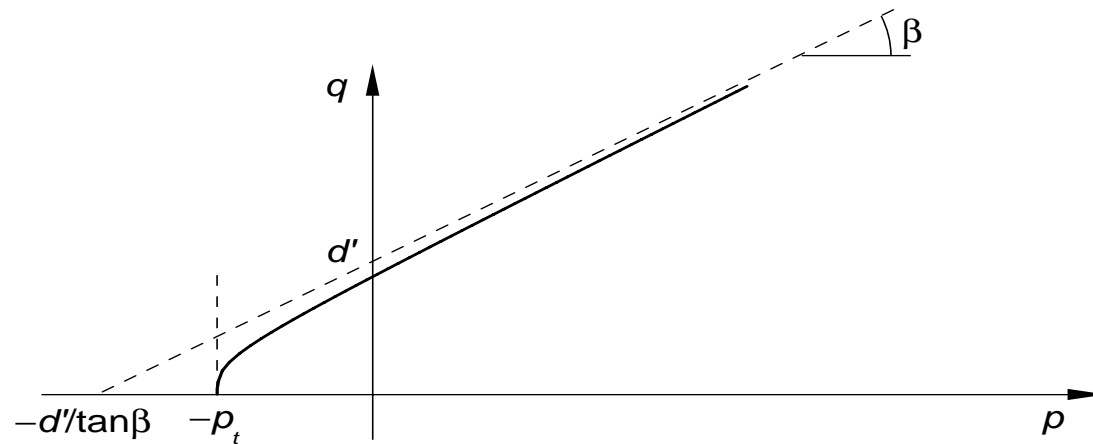
$$p = -\frac{1}{3}(\sigma_1 + 2\sigma_3), \quad q = \sigma_1 - \sigma_3, \quad r = q, \quad t = \frac{q}{K}.$$

K can, thus, be found by plotting these test results as q versus p and again fitting the best straight line. The ratio of values of q for triaxial tension and compression at the same value of p then gives K .

The dilation angle ψ must be chosen such that a reasonable match of the volume changes during yielding is obtained. Generally, $0 \leq \psi \leq \beta$.

Hyperbolic Model

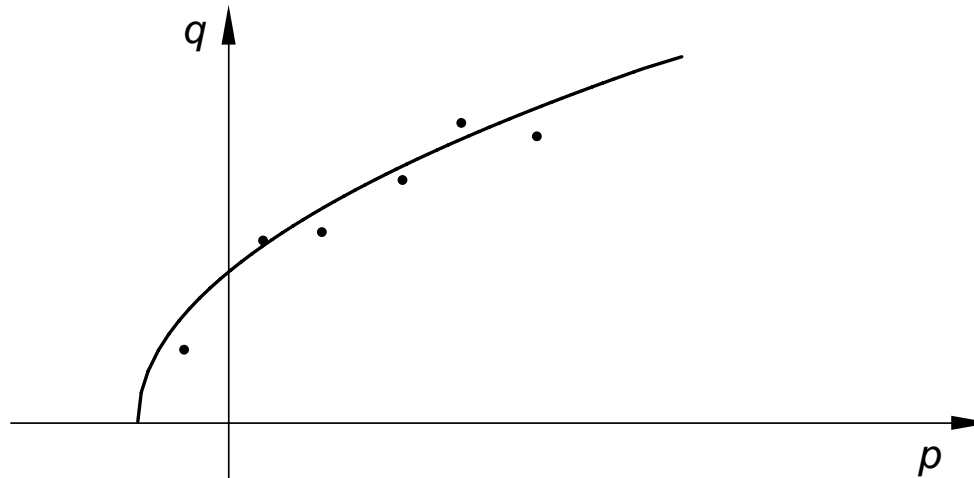
Fitting the best straight line through the triaxial compression results at high confining pressures provides β and d' for the hyperbolic model. In addition, hydrostatic tension data, p_t , are required to complete the calibration.



b) Hyperbolic:
$$F = \sqrt{(d'|_0 - p_t|_0 \tan \beta)^2 + q^2} - p \tan \beta - d' = 0$$

Exponent Model

ABAQUS provides a capability to determine the material parameters a , b , and p_t required for the exponent model from triaxial data, which is done on the basis of a “best fit” of the triaxial test data at different levels of confining stress.



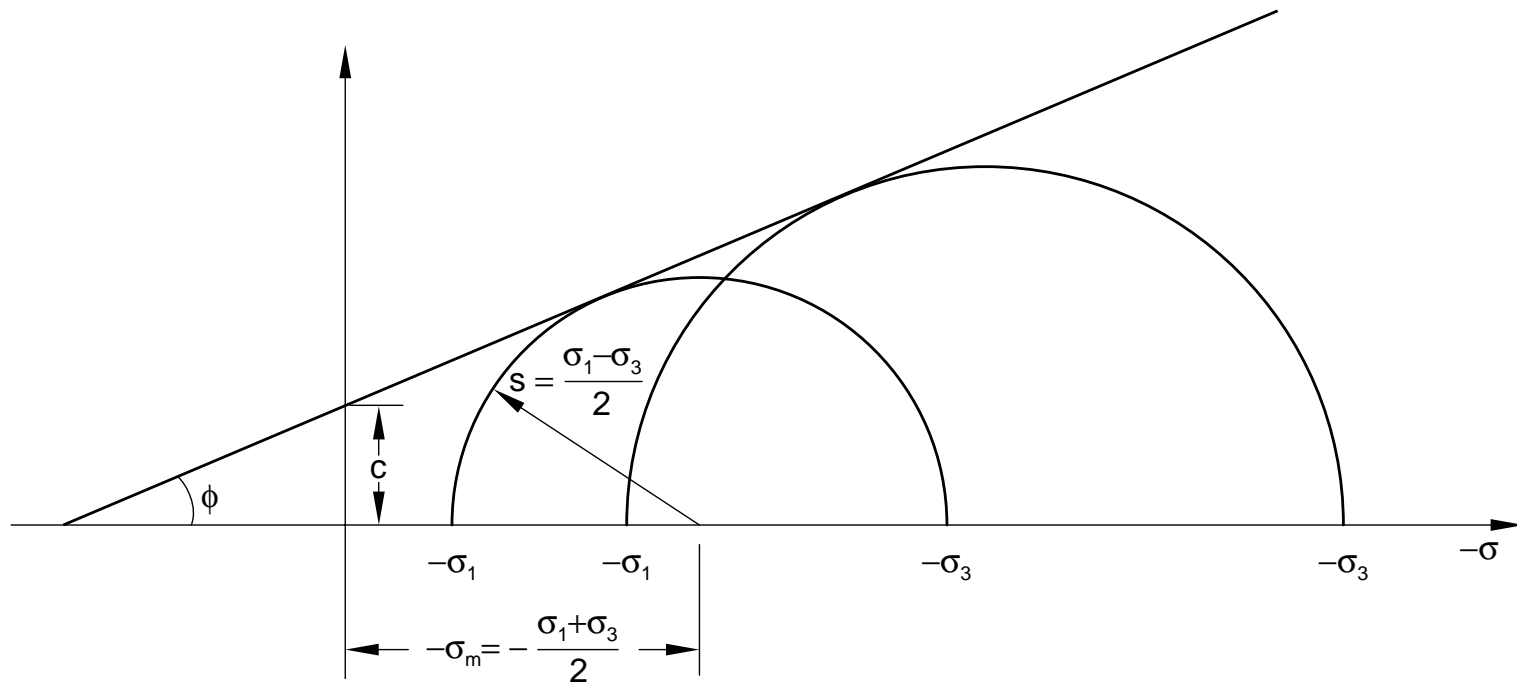
The data points obtained from triaxial tests are specified using the `*TRIAXIAL TEST DATA` option. The `TEST DATA` parameter is required on the `*DRUCKER PRAGER` option to use this feature. The `*TRIAXIAL TEST DATA` option must be used with the `*DRUCKER PRAGER` option.

The capability allows all three parameters to be calibrated, or, if some of the parameters are known, to calibrate only the unknown parameters.

Matching Mohr-Coulomb Parameters

Sometimes only the friction angle and cohesion values for the Mohr-Coulomb model are provided. We need to calculate values for the parameters of the linear Drucker-Prager model to provide a reasonable match to the Mohr-Coulomb parameters.

The Mohr-Coulomb model is based on plotting Mohr's circle for stresses at failure in the plane of the maximum and minimum principal stresses. The failure line is the best straight line that touches these Mohr's circles.



The Mohr-Coulomb model is, thus,

$$s + \sigma_m \sin \phi - c \cos \phi = 0,$$

where

$$s = \frac{1}{2}(\sigma_1 - \sigma_3)$$

is half of the difference between the maximum and minimum principal stresses (and is, therefore, the maximum shear stress) and

$$\sigma_m = \frac{1}{2}(\sigma_1 + \sigma_3)$$

is the average of the maximum and minimum principal stresses.

The Coulomb friction angle, ϕ , is different from the angle β used in the (p, q) plane in the linear Drucker-Prager model.

We see that the Mohr-Coulomb model assumes that failure is independent of the value of the intermediate principal stress. The Drucker-Prager model does not. The failure of typical granular geotechnical materials generally includes only small dependence on the intermediate principal stress, so the Mohr-Coulomb model is generally more realistic than the Drucker-Prager model.

Matching Plane Strain Response

Plane strain problems are often encountered in geotechnical analysis. Therefore, the constitutive model parameters are often matched to provide the same flow and failure response as a Mohr-Coulomb model in plane strain.

Since we wish to match only the behavior in one plane, we can assume $K = 1$. Using the plane strain constraint, we can derive the relationships

$$\sin \phi = \frac{\tan \beta \sqrt{3(9 - \tan^2 \psi)}}{9 - \tan \beta \tan \psi},$$

$$c \cos \phi = \frac{\sqrt{3(9 - \tan^2 \psi)}}{9 - \tan \beta \tan \psi} d.$$

For associated flow $\psi = \beta$, which gives

$$\tan \beta = \frac{\sqrt{3} \sin \phi}{\sqrt{1 + \frac{1}{3} \sin^2 \phi}} \quad \text{and} \quad \frac{d}{c} = \frac{\sqrt{3} \cos \phi}{\sqrt{1 + \frac{1}{3} \sin^2 \phi}} .$$

For nondilatant flow $\psi = 0$, which gives

$$\tan \beta = \sqrt{3} \sin \phi \quad \text{and} \quad \frac{d}{c} = \sqrt{3} \cos \phi .$$

The difference between assuming associated or nondilatant flow increases with the friction angle, but for typical friction angles the results are not very different, as shown below:

| Mohr-Coulomb friction angle, ϕ | Associated | | Nondilatant | |
|--|--------------------------------|-------|--------------------------------|-------|
| | D-P friction angle, β | d/c | D-P friction angle, β | d/c |
| 10° | 16.7° | 1.70 | 16.7° | 1.70 |
| 20° | 30.2° | 1.60 | 30.6° | 1.63 |
| 30° | 39.8° | 1.44 | 40.9° | 1.50 |
| 40° | 46.2° | 1.24 | 48.1° | 1.33 |
| 50° | 50.5° | 1.02 | 53.0° | 1.11 |

The results obtained for a foundation problem using the different Drucker-Prager matches described here are given in **Dry Problems** (p. L6.3) of these notes.

Matching Triaxial Test Response

An alternative approach to matching Mohr-Coulomb and linear Drucker-Prager model parameters is to make the two models provide the same failure definition in triaxial compression and tension. This approach yields the following Drucker-Prager parameters:

$$\tan\beta = \frac{6\sin\phi}{3 - \sin\phi},$$

$$K = \frac{3 - \sin\phi}{3 + \sin\phi},$$

$$\sigma_c^0 = 2c \frac{\cos\phi}{1 - \sin\phi}.$$

The value of K in the Drucker-Prager model is restricted to $K \geq 0.778$ for the yield surface to remain convex. Rewriting the second equation as

$$\sin \phi = 3 \left(\frac{1 - K}{1 + K} \right)$$

shows that this implies $\phi \leq 22^\circ$.

Many real materials have a larger Mohr-Coulomb friction angle than this value. In such cases one approach is to choose $K = 0.778$ and then to use the first equation to define β and the third equation to define σ_c^0 .

This matches the models for triaxial compression only, while providing the closest approximation that the model can provide to failure being independent of the intermediate principal stress. If ϕ is significantly larger than 22° , this approach may provide a poor Drucker-Prager match of the Mohr-Coulomb parameters.

Coupled Creep and Drucker-Prager Plasticity

Geomaterials may creep under certain conditions. When the loading rate is of the same order of magnitude as the creep time scale, the plasticity and creep equations must be solved using a coupled solution procedure.

ABAQUS has a creep model that can be used to augment the Drucker-Prager plasticity for such problems.

Basic Assumptions

ABAQUS always uses the coupled solution procedure when both Drucker-Prager plasticity and creep are active.

Using the Drucker-Prager creep model implies that the Drucker-Prager plasticity model uses isotropic linear elasticity, a hyperbolic plastic flow potential, and the linear Drucker-Prager yield surface with a circular yield surface in the deviatoric plane ($K = 1$).

The creep laws for the Drucker-Prager creep models are written in terms of an equivalent creep stress, $\bar{\sigma}^{cr}$, which is a measure of the creep “intensity” of the state of stress at a material point.

The definition of $\bar{\sigma}^{cr}$ depends upon the type of hardening (compression, tension, or shear) used with the linear Drucker-Prager plasticity model, but in all cases $\bar{\sigma}^{cr} = \bar{\sigma}^{cr}(q, p, \beta)$:

$$\begin{aligned}\bar{\sigma}^{cr} &= \frac{(q - p \tan \beta)}{(1 - (1/3) \tan \beta)} \quad (\text{compression}) \\ &= \frac{(q - p \tan \beta)}{(1 + (1/3) \tan \beta)} \quad (\text{tension}) \\ &= (q - p \tan \beta) \quad (\text{shear})\end{aligned}$$

The equivalent creep stress defines surfaces that are parallel to the yield surface in the meridional plane.

Points on the same surface have the same creep “intensity.”

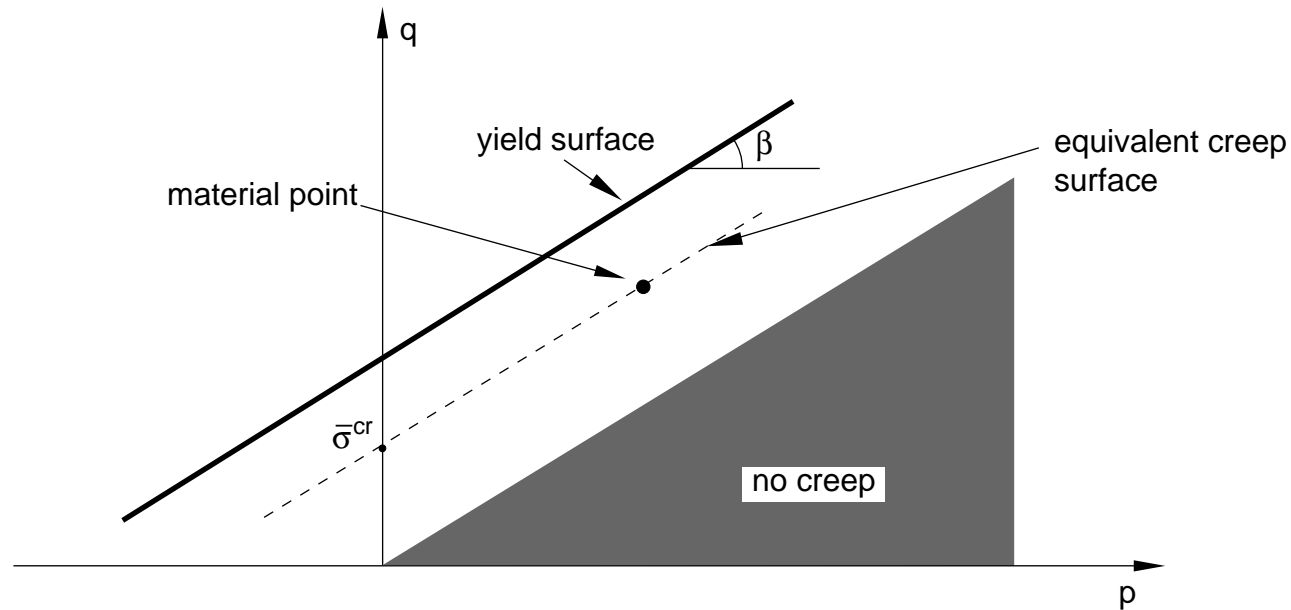


Figure 3–1. Equivalent Creep Surface in the Meridional Plane

There is a cone in the meridional plane in which no creep deformation will occur.

Creep Laws

The default creep laws provided are simple and are intended to model the secondary creep of the material.

Time Hardening Creep Law

Use this creep law when the stress in the material remains essentially constant:

$$\dot{\bar{\epsilon}}^{cr} = A(\bar{\sigma}^{cr})^n t^m.$$

Strain Hardening Creep Law

Use this creep law when the stress in the material varies during the analysis:

$$\dot{\bar{\epsilon}}^{cr} = (A(\bar{\sigma}^{cr})^n [(m+1)\bar{\epsilon}^{cr}]^m)^{\frac{1}{m+1}}.$$

Singh-Mitchell Creep Law

Use this creep law when an exponential relationship between stress and creep strain rate is needed:

$$\dot{\bar{\epsilon}}^{cr} = A e^{(\alpha \bar{\sigma}^{cr})} (t_1/t)^m.$$

Creep Flow Potential

The Drucker-Prager creep model uses a hyperbolic creep flow potential that ensures the creep (deformation) flow direction is always defined uniquely:

$$G^{cr} = \sqrt{(\epsilon \bar{\sigma}|_0 \tan \psi)^2 + q^2} - p \tan \psi.$$

The initial yield stress, $\bar{\sigma}|_0$, is defined on the *DRUCKER PRAGER HARDENING option.

Usage

The *DRUCKER PRAGER CREEP option must be used in conjunction with the *DRUCKER PRAGER and *DRUCKER PRAGER HARDENING options.

The *DRUCKER PRAGER CREEP option must be used with the linear Drucker-Prager model with a von Mises (circular) section in the deviatoric stress plane ($K = 1$; i.e., no third stress invariant effects are taken into account) and can be combined only with linear elasticity.

The material parameters in the default creep laws— A , n , m , t_1 , and α —can be defined as functions of temperature and/or field variables on the *DRUCKER PRAGER CREEP option.

- To avoid numerical problems with round-off, the values of A should be larger than 10^{-27} .

The time in these creep laws is the total analysis time, so the duration of steps where creep is not considered (such as *STATIC steps) should be relatively short.

More complex creep laws are defined with user subroutine **CREEP**.

The eccentricity of the creep potential, ε , is by default 0.1. Use the **ECCENTRICITY** parameter on the *DRUCKER PRAGER option to specify a different value.

- Using values much smaller than 0.1 can create convergence problems.

The creep flow potential uses the same dilation angle, ψ , as the Drucker-Prager plasticity model.

- Therefore, it is possible for the creep equations to be unsymmetric when $\beta \neq \psi$. In this case the *STEP, UNSYMM=YES option should be used.

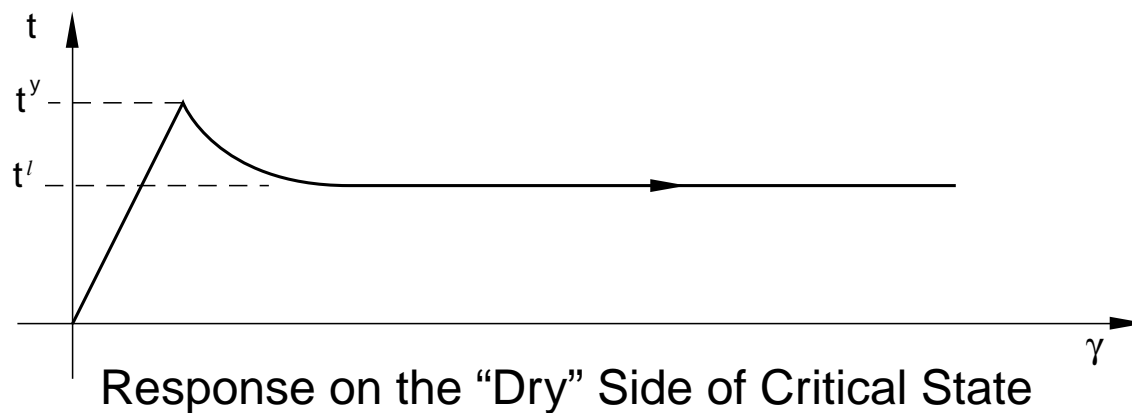
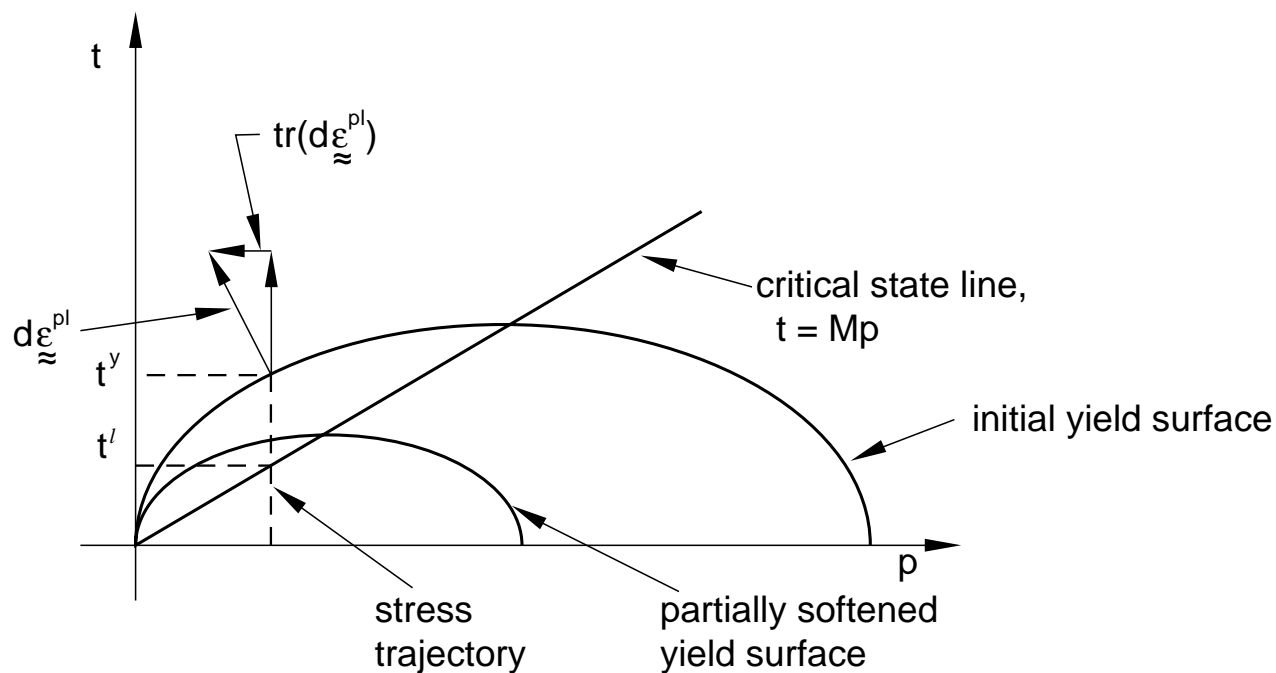
Modified Cam-Clay Model

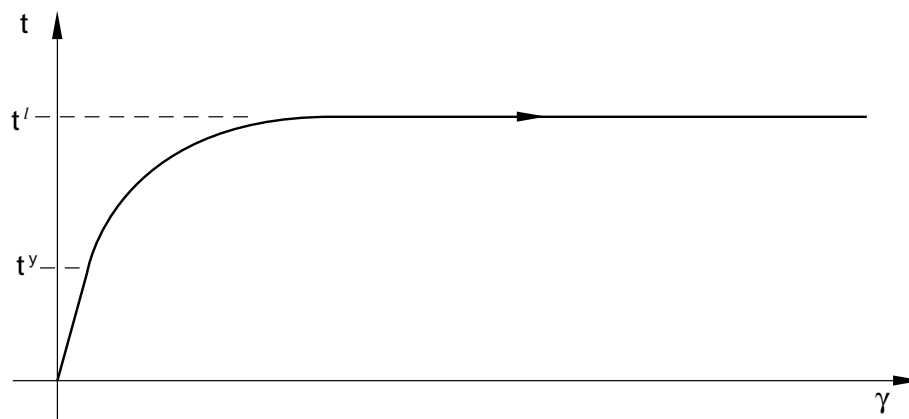
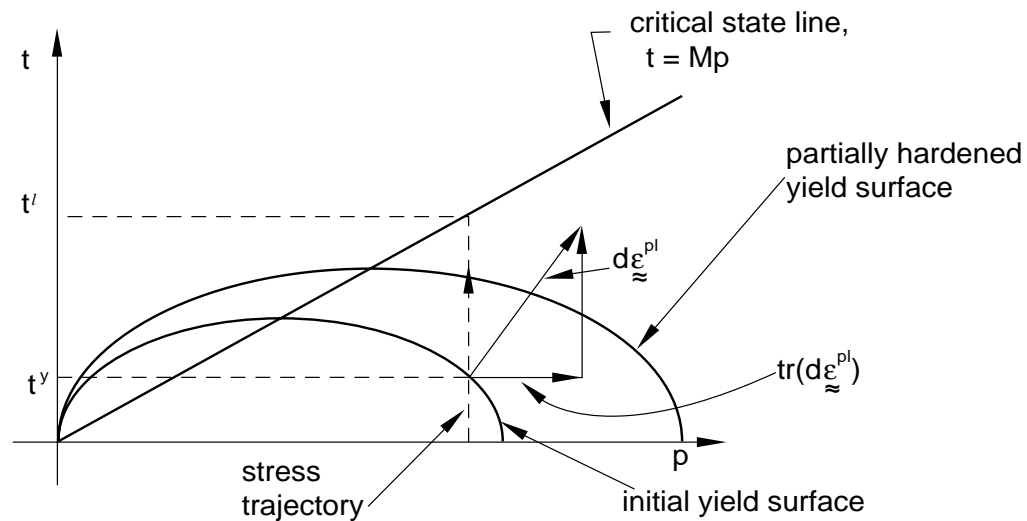
This model is intended to simulate the constitutive behavior of cohesionless materials. It is an extended version of the classical critical state theories originally developed at Cambridge from 1960–1970.

The basic characteristics of the model are:

- There is a regime of nonlinear elastic response, after which some of the material deformation is not recoverable and can, thus, be idealized as being plastic.
- The material is initially isotropic.
- The yield behavior depends on the hydrostatic pressure. The critical state line separates two distinct regions of behavior: on the “dry” side of critical state the material softens, while on the “wet” side it hardens (and also stiffens). The hardening/softening behavior is a function of the volumetric plastic strain.

- The inelastic behavior is generally accompanied by volume changes: on the “dry” side the material dilates, while on the “wet” side it compacts. On the critical state line the material can yield indefinitely at constant shear stress without changing volume.
- The yield behavior may be influenced by the magnitude of the intermediate principal stress.
- The model assumes the material is cohesionless.
- Under large stress reversals the model provides a reasonable material response on the “wet” (cap) side of critical state; however, on the “dry” side the model is acceptable only for essentially monotonic loading.
- Temperature may affect the material properties.





Response on the "Wet" Side of Critical State

Description

Either linear elasticity or nonlinear porous elasticity—see **Elasticity** (p. L3.12)—can be used with the Cam-clay model.

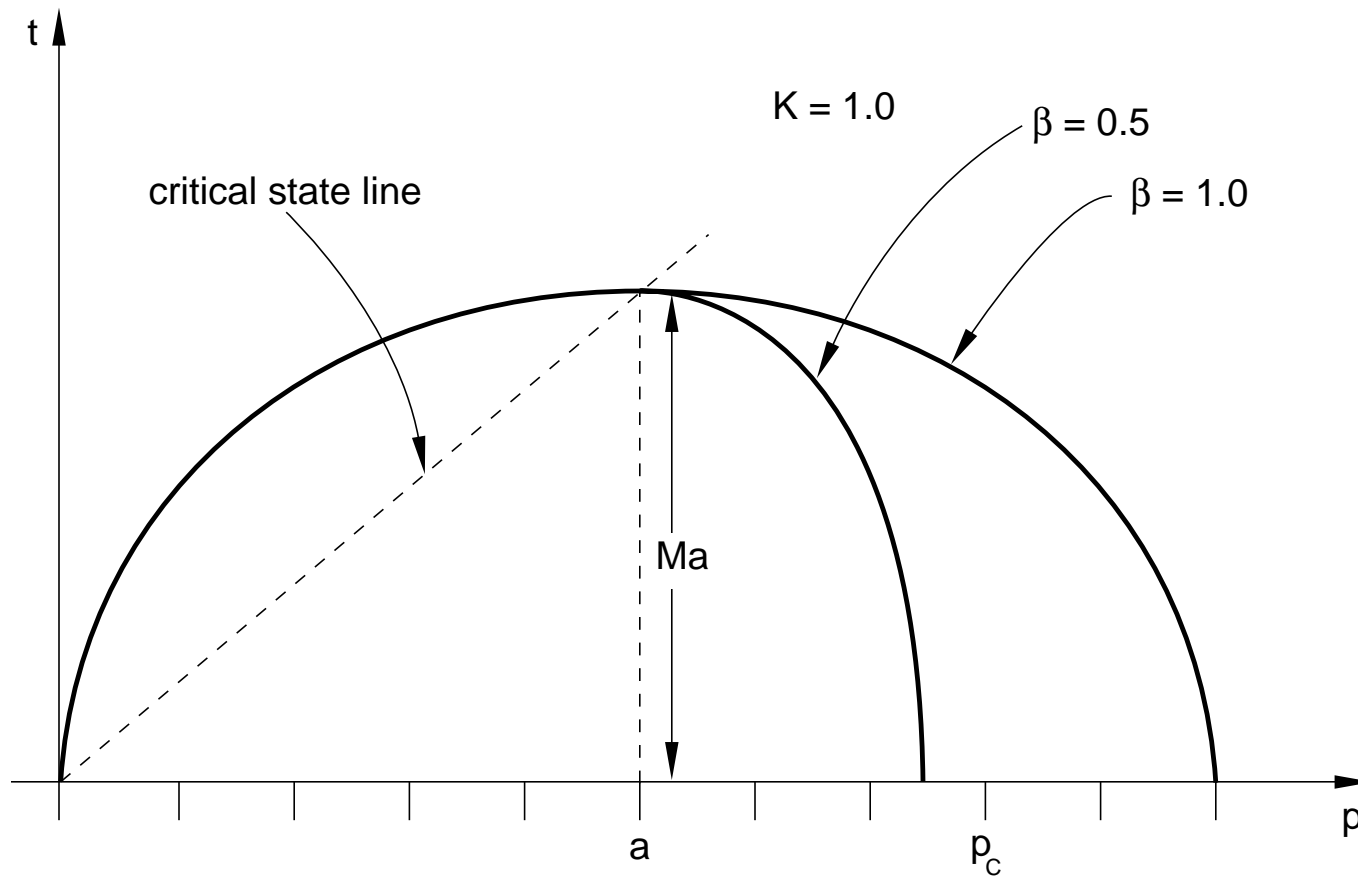
The modified Cam-clay yield surface is elliptical in the meridional plane and also includes a dependence on the third stress invariant:

for $p > a$ (the “wet” side of critical state),

$$f(p, q, r) = \frac{1}{\beta^2} \left(\frac{p}{a} - 1 \right)^2 + \left(\frac{t}{Ma} \right)^2 - 1 = 0 ;$$

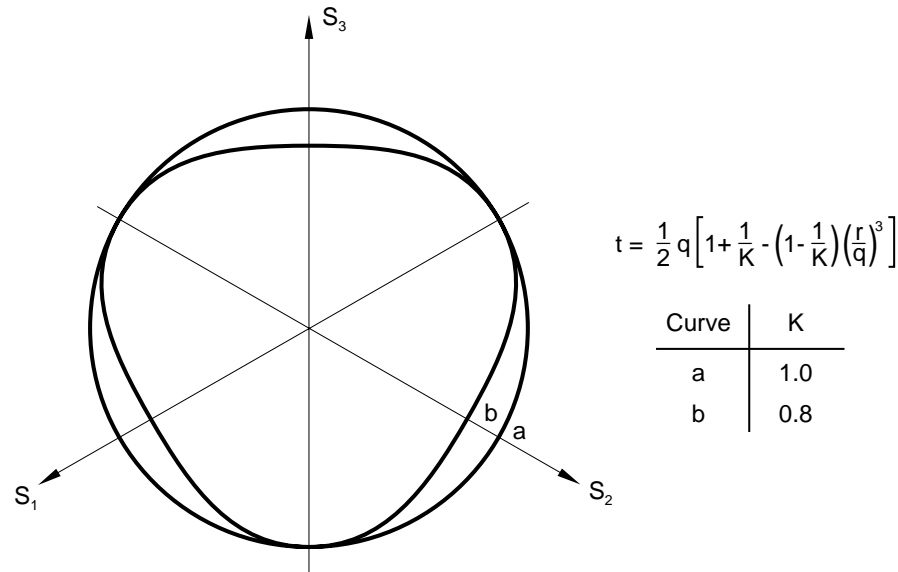
for $p \leq a$ (the “dry” side of critical state),

$$f(p, q, r) = \left(\frac{p}{a} - 1 \right)^2 + \left(\frac{t}{Ma} \right)^2 - 1 = 0 .$$

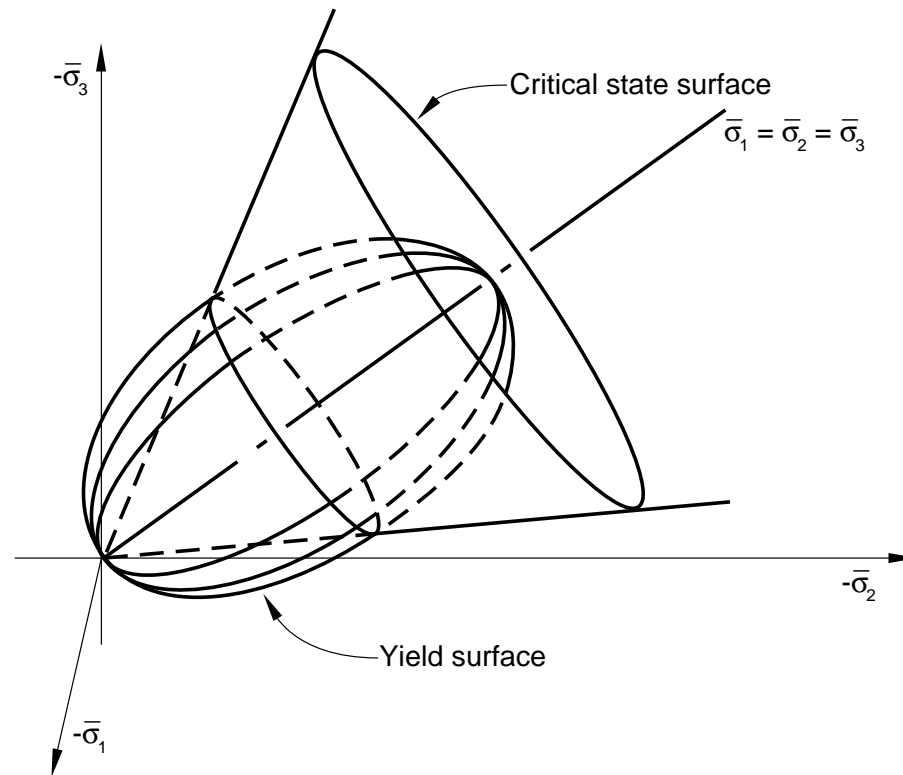


β is a constant used to modify the shape of the yield surface on the “wet” side of critical state so that the elliptic arc on the “wet” side of critical state has a different curvature from the elliptic arc used on the “dry” side: $\beta = 1$ on the “dry” side of critical state, while $\beta < 1$ in most cases on the “wet” side.

The measure of deviatoric stress, t , allows matching of different stress values in tension and compression in the deviatoric plane, as discussed previously in the context of the Drucker-Prager models—see **Linear Drucker-Prager Model** (p. L3.31).



M is the slope of the critical state line in the $p-t$ plane (the ratio of t to p at critical state).



Cam-Clay Yield and Critical State Surfaces in Principal Stress Space

Associated flow is used with the modified Cam-clay model. The size of the yield surface is defined by a . The evolution of this variable, therefore, characterizes the hardening or softening of the material.

ABAQUS provides two approaches to defining the evolution $a(\epsilon_{vol}^{pl})$. For some materials, over the range of confining pressures of interest it is observed experimentally that, during plastic deformation,

$$de = -\lambda d(\ln p),$$

where λ is a constant and e is the voids ratio. Integrating this equation:

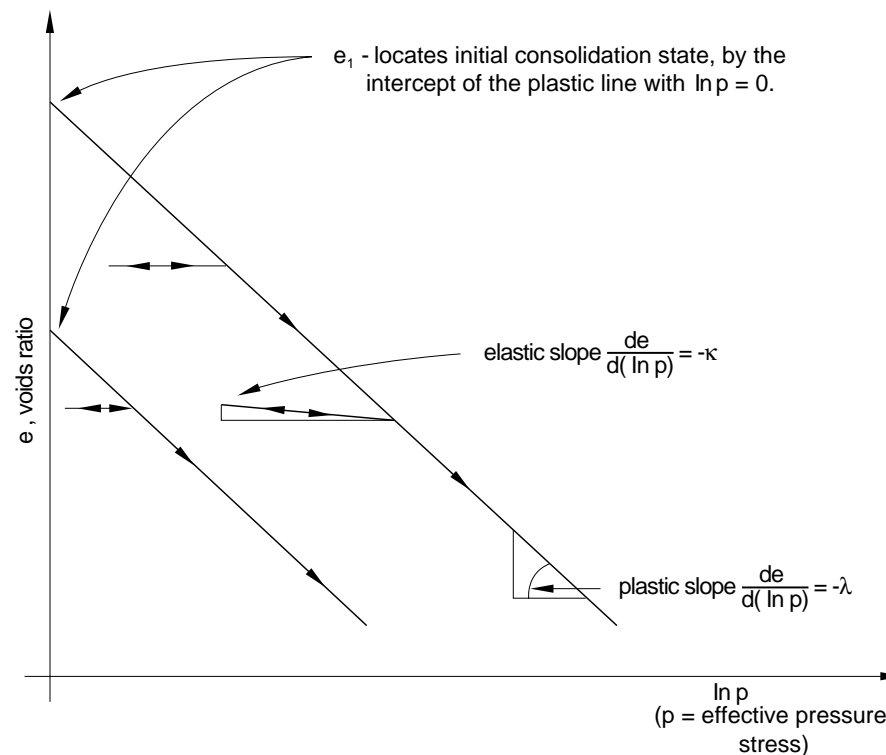
$$a = a_0 \exp \left[(1 + e_0) \frac{1 - J^{pl}}{\lambda - \kappa J^{pl}} \right],$$

where e_0 is the initial voids ratio, κ is the porous elasticity volumetric constant (the logarithmic bulk modulus), and a_0 defines the position of a at the start of the analysis—the initial overconsolidation of the material.

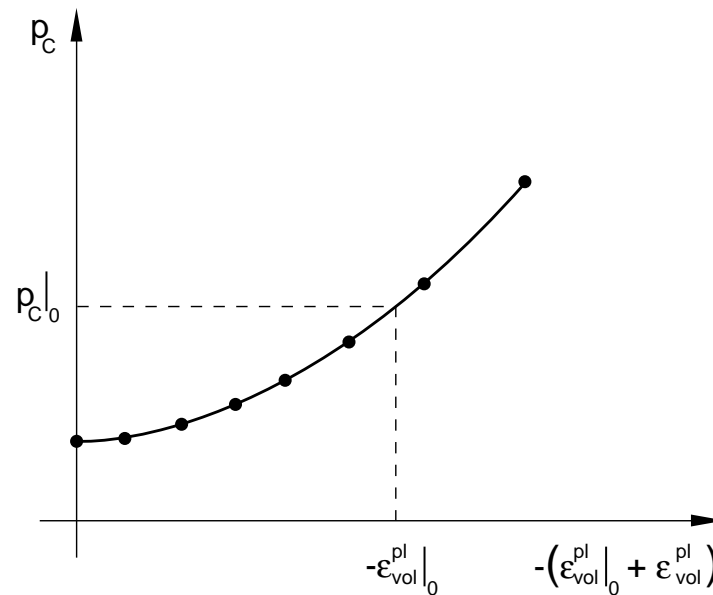
The value of a_0 can be given directly or may be computed as

$$a_0 = \frac{1}{2} \exp \left(\frac{e_1 - e_0 - \kappa \ln p_0}{\lambda - \kappa} \right),$$

where p_0 is the initial value of the pressure stress and e_1 is the intercept of the virgin consolidation line with the voids ratio axis in a plot of voids ratio versus pressure stress.



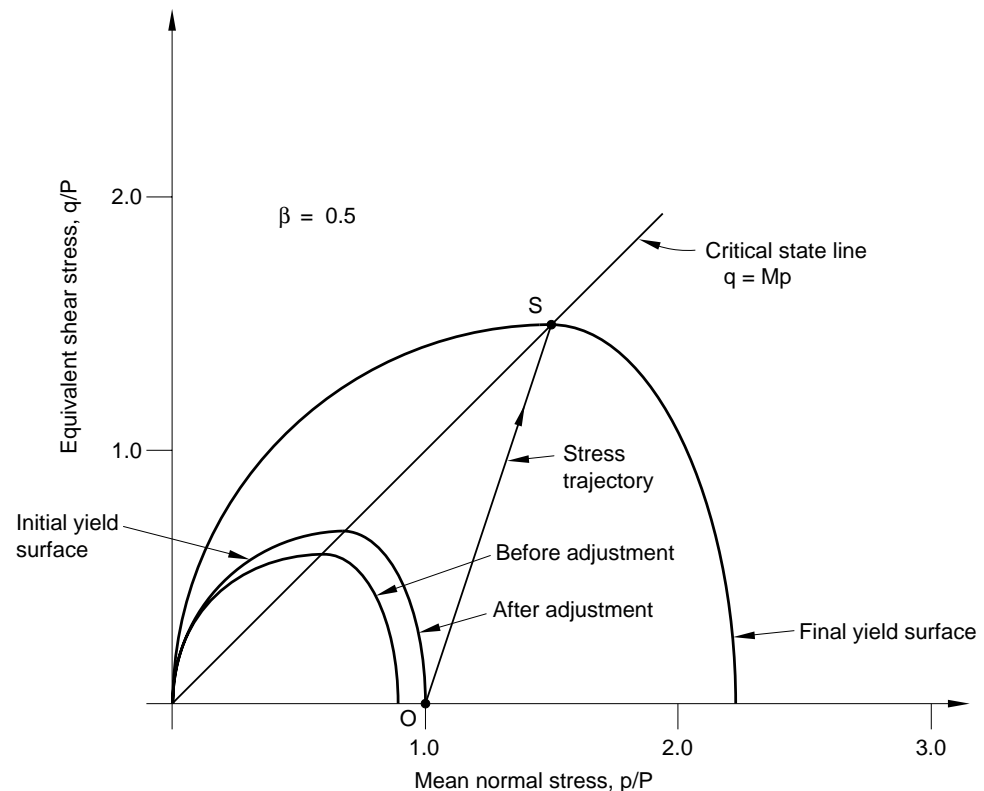
Alternatively, the evolution of the yield surface can be defined as a piecewise linear function relating yield stress in hydrostatic compression, p_c , and volumetric plastic strain, ϵ_{vol}^{pl} : $p_c = p_c(\epsilon_{vol}^{pl})$.



The evolution parameter is then given by $a = \frac{p_c}{(1 + \beta)}$.

The volumetric plastic strain axis has an arbitrary origin: $\epsilon_{\text{vol}}^{pl} \big|_0$ is the position on this axis corresponding to the initial state of the material, thus defining the initial hydrostatic pressure, $p_c \big|_0$, and, hence, the initial yield surface size, a_0 . Data must be provided over a wide enough range of values of p_c to cover all situations that will arise in the application.

ABAQUS checks that the yield surface is not violated by the user-specified material constants and the initial effective stress conditions defined at each point in the material. At any material point where the yield function is violated and a warning message is issued, a_0 is adjusted so that the yield function is satisfied exactly (and, hence, the initial stress state lies on the yield surface).



Usage and Calibration

The modified Cam-clay model in ABAQUS is invoked with the `*CLAY PLASTICITY` option. This option defines the yield. It also defines the hardening if logarithmic hardening is chosen. The `*CLAY HARDENING` option can be used to define piecewise linear hardening. These parameters can be entered as functions of temperature and predefined field variables.

The elasticity is defined with the `*ELASTIC` or `*POROUS ELASTIC` option. If logarithmic hardening is used, the `*POROUS ELASTIC` option must be used (in this case the logarithmic elastic bulk modulus, κ , must be specified together with either a constant shear modulus, G , or a constant Poisson's ratio, ν).

In the porous elasticity case, the version with zero tensile strength ($p_t^{el} = 0$) is normally used since the material is assumed to be cohesionless. The elasticity parameters can be entered as functions of temperature and predefined field variables.

- *EXPANSION can be used to introduce thermal volume change effects.
- *INITIAL CONDITIONS, TYPE=RATIO is required to define the initial voids ratio (porosity) of the material. User subroutine **VOIDRI** can be used to specify complex initial voids ratio distributions.
- *INITIAL CONDITIONS, TYPE=STRESS is required to define the initial effective stress state in the material. User subroutine **SIGINI** can be used to specify complex initial stress distributions.

At least two experiments are required to calibrate the simplest version of the Cam-clay model: a hydrostatic compression test (an oedometer test is also acceptable), and a triaxial compression test (more than one triaxial test is useful for a more accurate calibration).

The hydrostatic compression test is performed by pressurizing the sample equally in all directions. The applied pressure and the volume change are recorded.

Triaxial compression experiments are performed using a standard triaxial machine where a fixed confining pressure is maintained while the differential stress is applied. Several tests covering the range of confining pressures of interest are usually performed. Again, the stress and strain in the direction of loading are recorded together with the lateral strain so that the correct volume changes can be calibrated.

Unloading measurements in these tests are useful to calibrate the elasticity, particularly in cases where the initial elastic region is not well defined. From these we can identify whether a constant shear modulus or a constant Poisson's ratio should be used and what its value is.

The onset of yielding in the hydrostatic compression test immediately provides the initial position of the yield surface, a_0 . The logarithmic bulk moduli, κ and λ , are determined from the hydrostatic compression experimental data by plotting the logarithm of pressure versus voids ratio. The voids ratio, e , is related to the measured volume change as

$$J = \exp(\epsilon_{vol}) = \frac{(1 + e)}{(1 + e_0)} .$$

The slope of the line obtained for the elastic regime is $-\kappa$, and the slope in the inelastic range is $-\lambda$. For a valid model $\lambda > \kappa$.

The triaxial compression tests allow the calibration of the yield parameters M and β . M is the ratio of the shear stress, q , to the pressure stress, p , at critical state and can be obtained from the stress values when the material has become perfectly plastic (critical state). β represents the curvature of the cap part of the yield surface and can be calibrated from a number of triaxial tests at high confining pressures (on the “wet” side of critical state). β must be between 0 and 1.

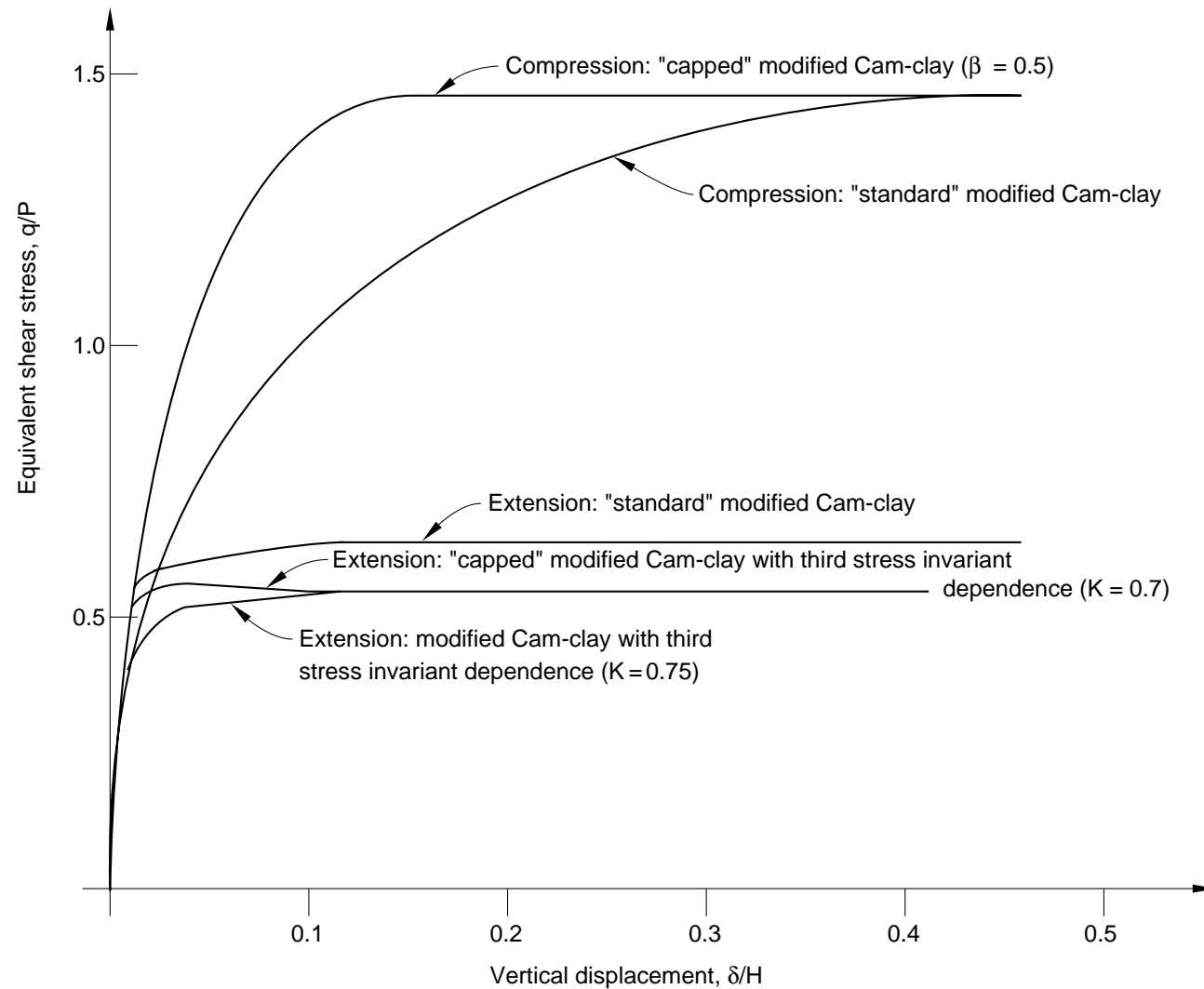
To calibrate the parameter K , which controls the yield dependence on the third stress invariant, experimental results obtained from a true triaxial (cubical) test are necessary. These results are generally not available, and the user may have to guess (the value of K is generally between 0.8 and 1.0) or ignore this effect.

Example

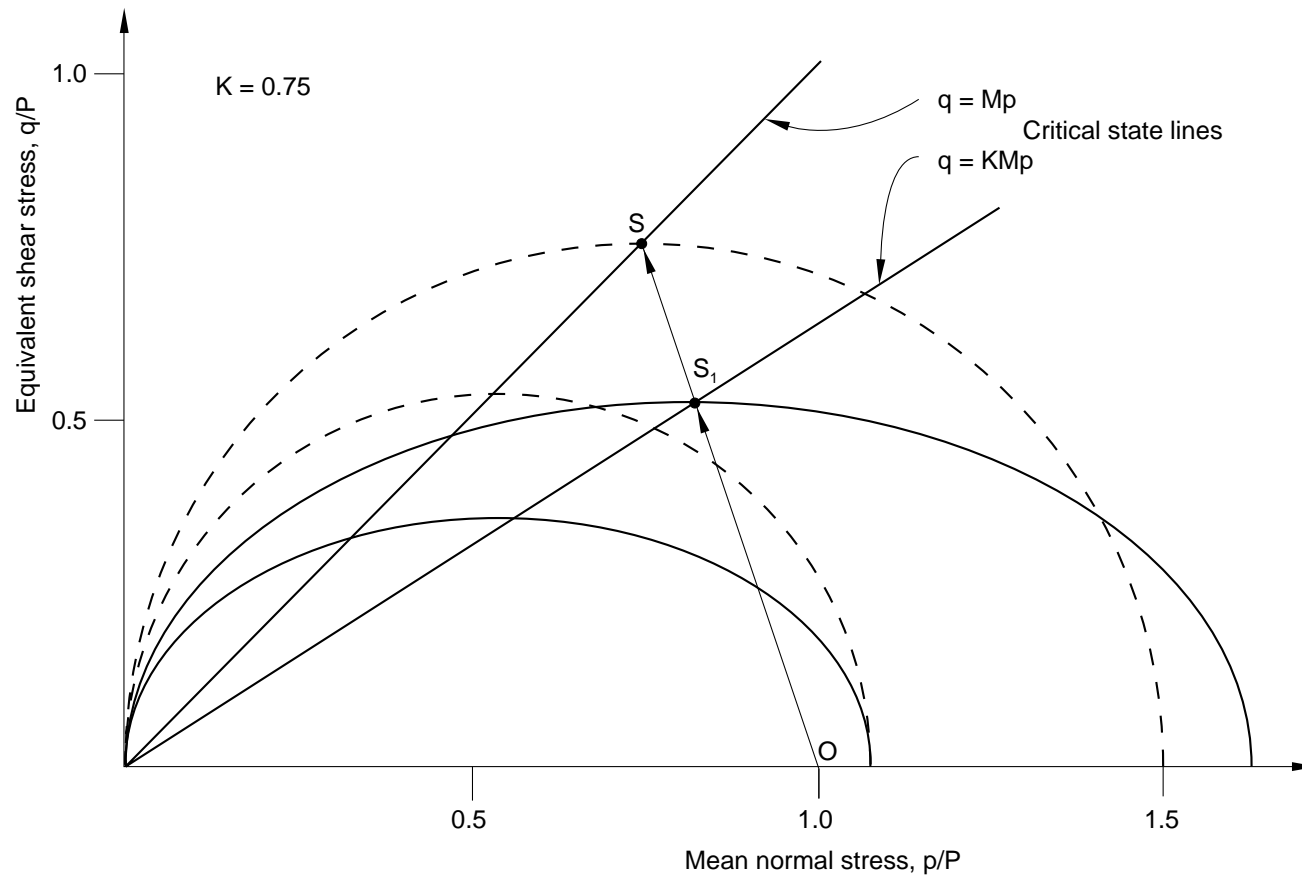
We consider the homogeneous deformation of a single element as a demonstration of the modified Cam-clay plasticity model (Benchmark Problem 3.2.4 *Triaxial tests on a saturated clay*). Our modified Cam-clay model provides two extensions of the original Cam-clay model: “capping” of the yield ellipse on the wet side of critical state and consideration of the third stress invariant in the yield function. Both of these extensions are included in this example. The specimen is initially stressed hydrostatically. Subsequently it is subjected to triaxial compression or triaxial extension. The material parameters used in this example are:

| | |
|--|------------------------|
| Logarithmic elastic bulk modulus, κ : | 0.026 |
| Poisson's ratio, ν : | 0.3 |
| Logarithmic hardening modulus, λ : | 0.174 |
| Critical state ratio, M : | 1.0 |
| Wet cap parameter, β : | 0.5 |
| Third stress invariant parameter, K : | 0.75 |
| Initial overconsolidation parameter, a_0 : | 58.3 kN/m ² |

Material response:



Yield surface evolution for triaxial extension:





Input Listing:

```
*HEADING
  CAM CLAY EXAMPLE - DRAINED TRIAXIAL TESTS
*NODE
1
3,1.
23,1.,1.
21,,1.
*NGEN,NSET=BOTTOM
1,3
*NGEN,NSET=TOP
21,23
*NGEN
1,21,10
3,23,10
*NSET,NSET=SOIL,GENERATE
1,23
*NSET,NSET=LHS
1,11,21
*ELEMENT,TYPE=CAX8R,ELSET=SOIL
1,1,3,23,21,2,13,22,11
```



```
*SOLID SECTION,MATERIAL=SAMPLE,ELSET=SOIL
*MATERIAL,NAME=SAMPLE
*POROUS ELASTIC
.026,.3
*CLAY PLASTICITY
.174,1.,58.3
*INITIAL CONDITIONS,TYPE=RATIO
SOIL,1.08,0.,1.08,1.
*INITIAL CONDITIONS,TYPE=STRESS,GEOSTATIC
SOIL,-100.,0.,-100.,10.,1.
*STEP
    GEOSTATIC INITIAL STRESS STATE
*GEOSTATIC
*DLOAD
1,P2,100.
*EL PRINT
S
SINV
E
PE
EE
```

```
*NODE PRINT
U
RF
*EL FILE
SINV
*NODE FILE,NSET=TOP
U
*BOUNDARY
TOP,2
BOTTOM,2
LHS,1
*END STEP
*STEP,INC=20
    TRIAXIAL COMPRESSION
*STATIC,DIRECT
1.,20.
*BOUNDARY
TOP,2,2,-.5
*END STEP
```

Modified Cap Model

This model is intended to simulate the constitutive response of cohesive geological materials. It adds a “cap” yield surface to the linear Drucker-Prager model, which serves two main purposes: it bounds the model in hydrostatic compression, and it helps control volume dilatancy when the material yields in shear.

The basic characteristics of this model are:

- There is a regime of purely elastic response, after which some of the material deformation is not recoverable and can, thus, be idealized as being plastic.
- The yield behavior depends on the hydrostatic pressure. There are two distinct regions of behavior: on the failure surface the material is perfectly plastic, while on the cap yield surface it hardens (and also stiffens). The hardening/softening behavior is a function of the volumetric plastic strain.

- The inelastic behavior is generally accompanied by volume changes: on the failure surface the material dilates, while on the cap surface it compacts. At the intersection of the surfaces, the material can yield indefinitely at constant shear stress without changing volume.
- The yield behavior may be influenced by the magnitude of the intermediate principal stress.
- Under large stress reversals the model provides reasonable material response on the cap region; however, on the failure surface region the model is acceptable only for essentially monotonic loading.
- The material is initially isotropic.
- Temperature may affect the material properties.

Description

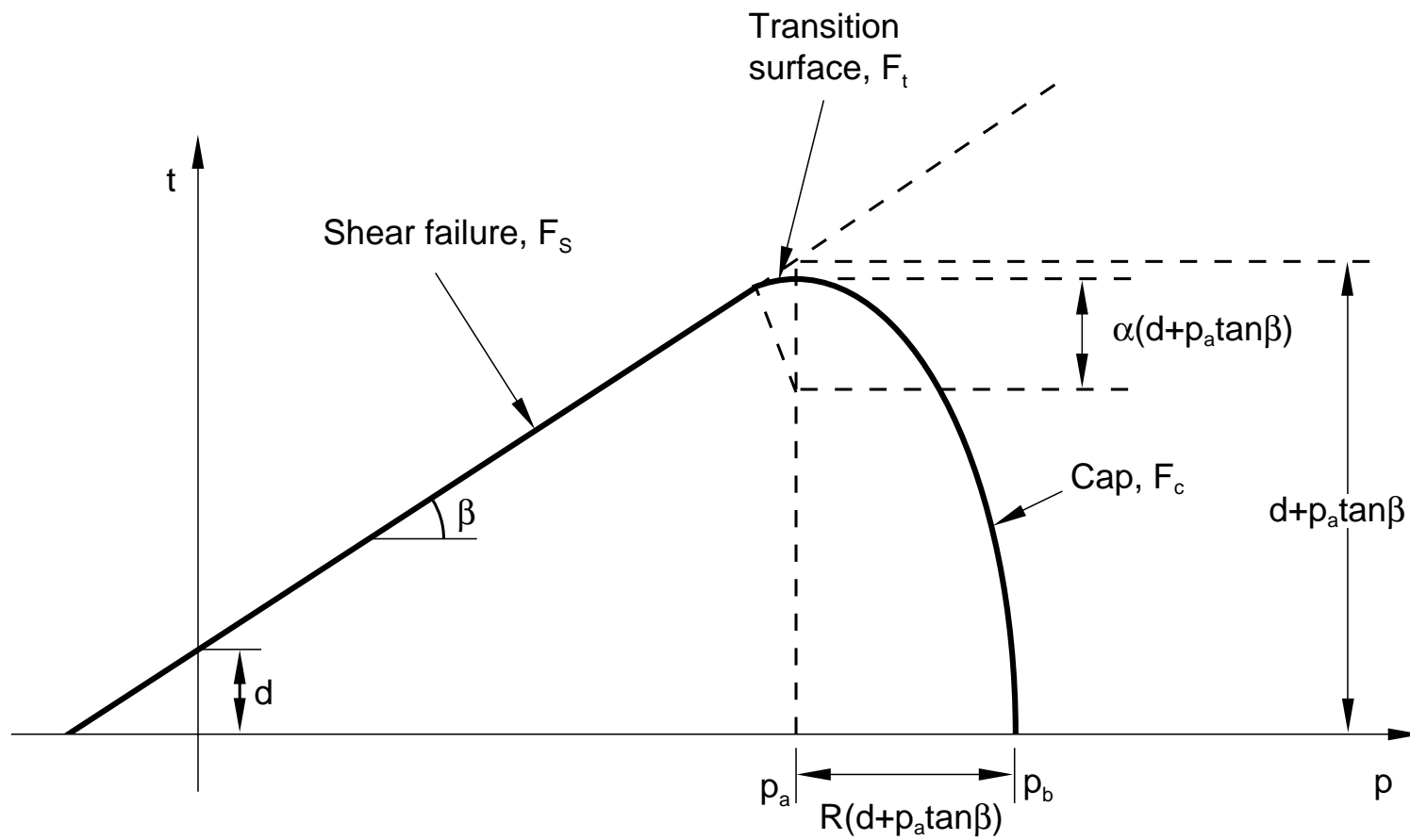
Linear elasticity or nonlinear porous elasticity—see **Elasticity** (p. L3.12)—can be used with this model.

The model uses two main yield surface segments: a linearly pressure-dependent Drucker-Prager shear failure surface and a compression cap yield surface. The Drucker-Prager failure surface itself is perfectly plastic (no hardening), but plastic flow on this surface produces inelastic volume increase, which causes the cap to soften. The Drucker-Prager failure surface is

$$F_s = t - p \tan \beta - d = 0.$$

β is the angle of friction, and d is the cohesion of the material.

The measure of deviatoric stress, t , allows matching of different stress values in tension and compression in the deviatoric plane, as discussed previously in the context of the Drucker-Prager models.



The cap yield surface has an elliptical shape with constant eccentricity in the meridional ($p-t$) plane and also includes dependence on the third stress invariant in the deviatoric plane. The cap surface hardens or softens as a function of the volumetric plastic strain: volumetric plastic compaction (when yielding on the cap) causes hardening, while volumetric plastic dilation (when yielding on the shear failure surface) causes softening.

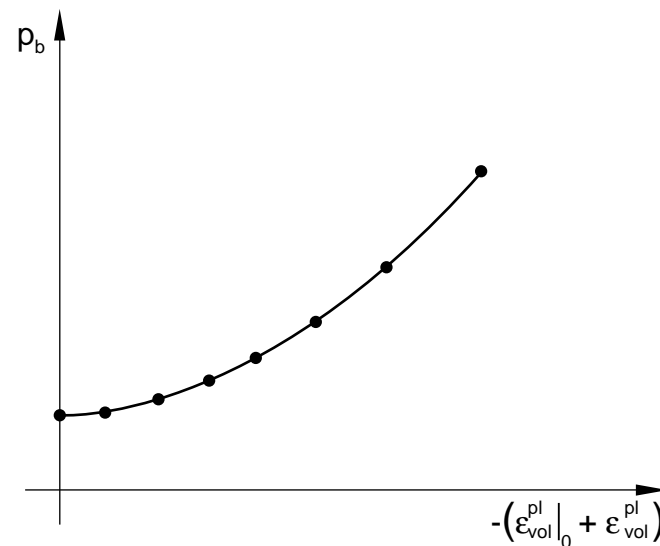
The cap yield surface is

$$F_c = \sqrt{(p - p_a)^2 + \left[\frac{Rt}{(1 + \alpha - \alpha/\cos\beta)} \right]^2} - R(d + p_a \tan\beta) = 0 ,$$

where R is a material parameter that controls the shape of the cap, α is a small number, and $p_a(\epsilon_{vol}^{pl})$ is an evolution parameter that represents the volumetric plastic strain driven hardening/softening.

The hardening/softening law is a user-defined piecewise linear function relating the hydrostatic compression yield stress, p_b , and the corresponding volumetric plastic strain,

$$p_b = p_b(\epsilon_{\text{vol}}^{\text{pl}}|_0 + \epsilon_{\text{vol}}^{\text{pl}}) .$$



This relationship is defined in the *CAP HARDENING option. The range of values for which p_b is defined should be sufficient to include all values of effective pressure stress that the material will be subjected to during the analysis.

The volumetric plastic strain axis in the hardening curve has an arbitrary origin: $\varepsilon_{\text{vol}}^{pl}|_0$ is the position on this axis corresponding to the initial state of the material when the analysis begins, thus defining the position of the cap (p_b) at the start of the analysis.

The evolution parameter p_a is then given as

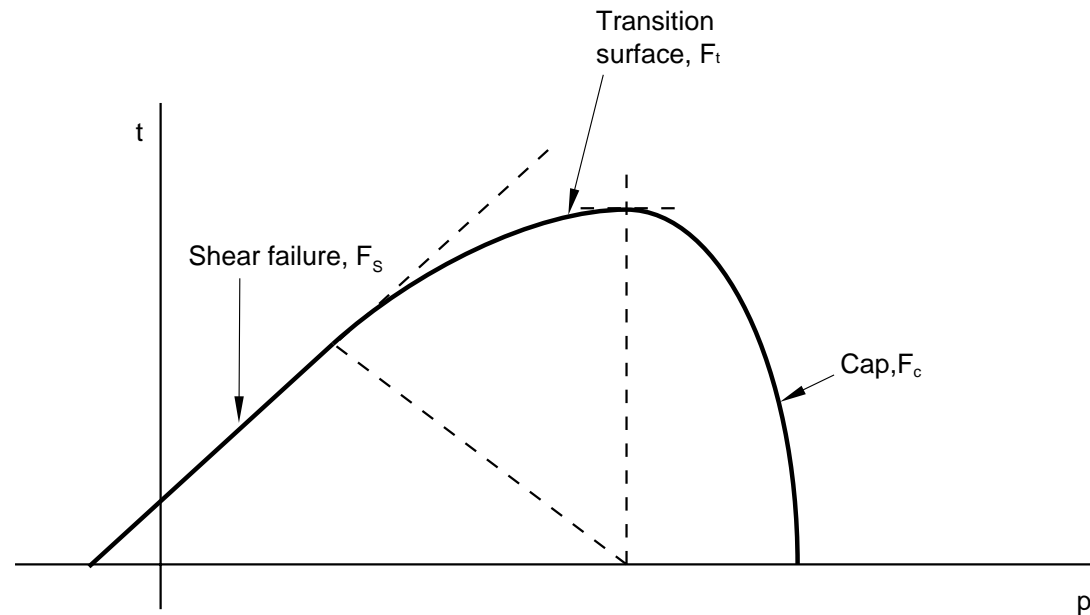
$$p_a = \frac{p_b - Rd}{(1 + R \tan \beta)}.$$

The parameter α is a small number (typically 0.01 to 0.05) used to define a transition yield surface,

$$F_t = \sqrt{(p - p_a)^2 + \left[t - \left(1 - \frac{\alpha}{\cos \beta} \right) (d + p_a \tan \beta) \right]^2} - \alpha (d + p_a \tan \beta) = 0,$$

so that the model provides a smooth intersection between the cap and failure surfaces.

A larger value of α can be used to construct more complex (curved) failure surfaces:



This approach has practical value, in that the curved surface provides a better fit of experimentally observed shear failure and also provides a softening surface that is consistent with observed shear failure.

The value of α can be set to zero, in which case there is no transition surface and no true softening behavior (i.e., softening while yielding on the same surface) in the model.

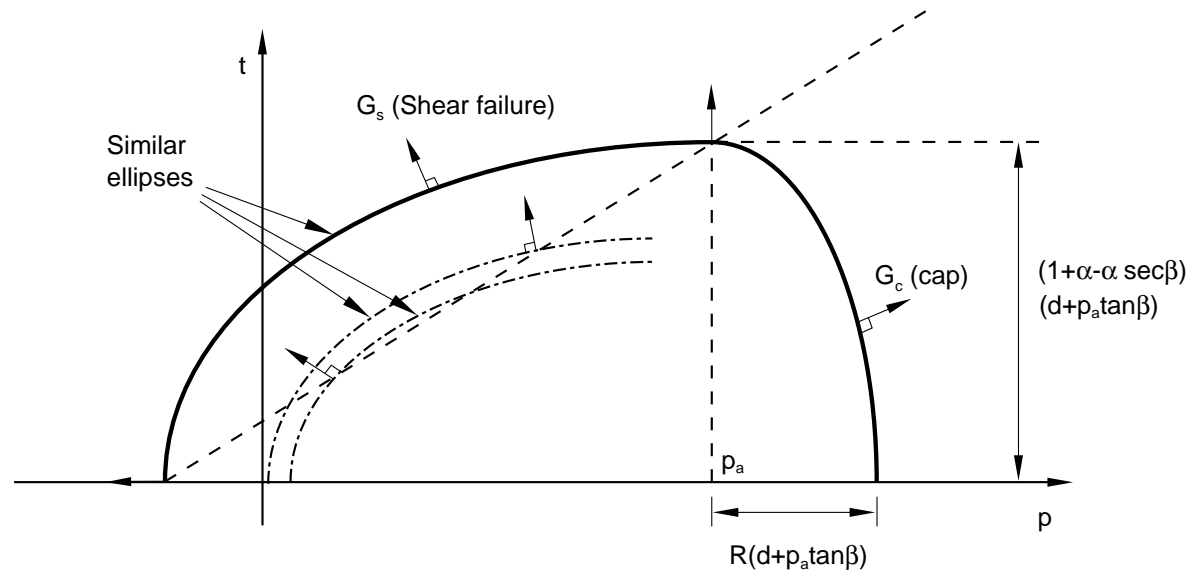
Plastic flow is defined by a flow potential that is associated in the deviatoric plane, associated in the cap region in the meridional plane, and nonassociated in the failure surface and transition regions in the meridional plane. The flow potential surface we use in the meridional plane is made up of an elliptical portion in the cap region that is identical to the cap yield surface,

$$G_c = \sqrt{(p - p_a)^2 + \left[\frac{Rt}{(1 + \alpha - \alpha/\cos\beta)} \right]^2},$$

and another elliptical portion in the failure and transition regions that provides the nonassociated flow component in the model,

$$G_s = \sqrt{[(p_a - p)\tan\beta]^2 + \left[\frac{t}{(1 + \alpha - \alpha/\cos\beta)} \right]^2}.$$

The two elliptical portions form a continuous and smooth potential surface.



On the failure and transition regions the volumetric plastic strain rate is proportional to $(p_a - p)\tan\beta$ and the deviatoric plastic strain rate is proportional to t . Thus, the flow is purely volumetric at the apex of the Drucker-Prager cone, while the flow is purely deviatoric at the intersection of the Drucker-Prager cone with the cap (i.e., the critical state condition). Moving along the Drucker-Prager failure surface between these two extremes, the ratio between the volumetric and deviatoric plastic strain rates varies linearly.

If the initial stress is given such that the stress point lies outside the initially defined cap or transition yield surfaces, ABAQUS will try to adjust the initial position of the cap to make the stress point lie on the yield surface and a warning will be issued.

If the stress point lies outside the Drucker-Prager failure surface, an error message will be issued and the analysis will be terminated.

Usage and Calibration

The modified Cap plasticity model in ABAQUS is invoked with the `*CAP PLASTICITY` material option. This option allows the yield and flow rule parameters to be made dependent on temperature and predefined field variables.

The `*CAP PLASTICITY` option must always be accompanied by the `*CAP HARDENING` material option, where the evolution of the yield stress in hydrostatic compression is defined. The yield stress can be given as a function of temperature and predefined field variables.

The elasticity is defined with the `*ELASTIC` material option in the case of linear elasticity or with the `*POROUS ELASTIC` option if nonlinear elasticity is chosen. The elasticity parameters can be entered as functions of temperature and predefined field variables.

`*EXPANSION` can be used to introduce thermal volume change effects.

*INITIAL CONDITIONS, TYPE=RATIO is required to define the initial voids ratio (porosity) of the material if nonlinear elasticity is used. User subroutine **VOIDRI** can be used to specify complex initial voids ratio distributions.

The nonassociated flow present in the failure surface of the model produces an unsymmetric material stiffness matrix. The **UNSYMM=YES** parameter on the *STEP option should be used if there is a significant plastic flow due to shearing. When ABAQUS uses a symmetric solver with unsymmetric equations, the rate of convergence may be slow. If the region of the model in which nonassociated flow occurs is confined, it may be possible to omit **UNSYMM=YES** and still get an acceptable rate of convergence.

At least three experiments are required to calibrate the simplest version of the Cap model: a hydrostatic compression test (an oedometer test is also acceptable) and two uniaxial and/or triaxial compression tests (more than two tests is useful for a more accurate calibration).

The hydrostatic compression test is performed by pressurizing the sample equally in all directions. The applied pressure and the volume change are recorded.

The uniaxial compression test involves compressing the sample between two rigid platens. The load and displacement in the direction of loading are recorded. The lateral displacements should also be recorded so that the correct volume changes can be calibrated.

Triaxial compression experiments are performed using a standard triaxial machine where a fixed confining pressure is maintained while the differential stress is applied. Several tests covering the range of confining pressures of interest are usually performed. Again, the stress and strain in the direction of loading are recorded, together with the lateral strain, so that the correct volume changes can be calibrated.

Unloading measurements in these tests are useful to calibrate the elasticity, particularly in cases where the initial elastic region is not well defined.

The hydrostatic compression test stress-strain curve gives the evolution of the hydrostatic compression yield stress, $p_b(\epsilon_{vol}^{pl})$, required in the *CAP HARDENING option.

The friction angle, β , and cohesion, d , which define the shear failure dependence on hydrostatic pressure, are calculated by plotting the failure stresses of any two uniaxial and/or triaxial compression experiments in the pressure stress (p) versus shear stress (q) space: the slope of the straight line passing through the two points gives the angle β , and the intersection with the q -axis gives d . See the discussion in **Linear Drucker-Prager Model** (p. L3.31).

R represents the curvature of the cap part of the yield surface and can be calibrated from a number of triaxial tests at high confining pressures (in the cap region). R must be between 0 and 1.

To calibrate the parameter K , which controls the yield dependence on the third stress invariant, experimental results obtained from a true triaxial (cubical) test are necessary. These results are generally not available, and the user may have to guess (the value of K is generally between 0.8 and 1.0) or ignore this effect. See the discussion in **Linear Drucker-Prager Model** (p. L3.31).

Example

We simulate the behavior of a sample of McCormack Ranch sand under uniaxial strain conditions. The response is compared to the experimental result given by DiMaggio and Sandler (1976).

The specimen has the following Cap model properties:

$$E = 100 \text{ Ksi}$$

$$\nu = 0.25$$

$$\beta = 14.56^\circ$$

$$d = 0.1732 \text{ Ksi}$$

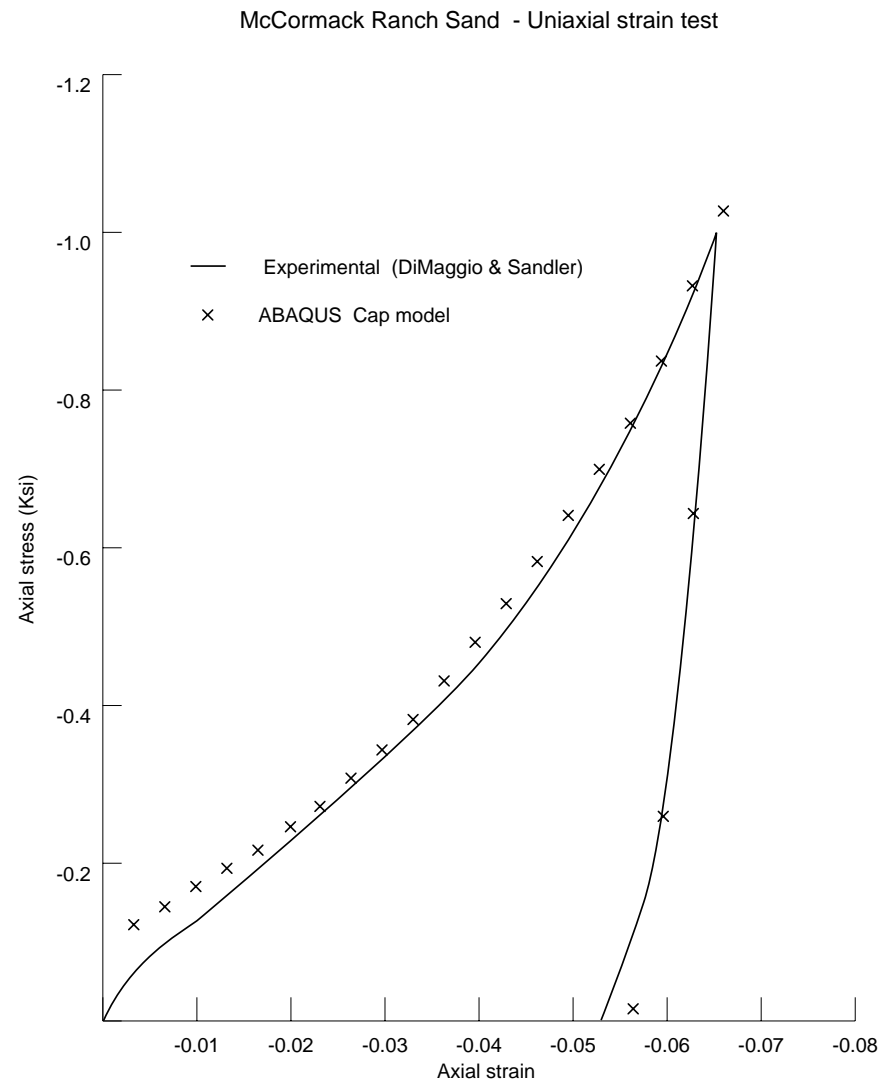
$$R = 0.1$$

$$\varepsilon_{\text{vol}}^{pl} \Big|_0 = 0.001$$

$$K = 1.0$$

Hardening as shown in the *CAP HARDENING option in the input listing

Material response:





Input listing:

```
*HEADING
CAP PLASTICITY,McCORMACK RANCH SAND,UNIAXIAL STRAIN, C3D8
*** KSI UNITS
*NODE, NSET=BOT
1,0.,0.,0.
2,1.,0.,0.
3,1.,1.,0.
4,0.,1.,0.
*NODE, NSET=TOP
5,0.,0.,1.
6,1.,0.,1.
7,1.,1.,1.
8,0.,1.,1.
*NSET, NSET=ALLN
BOT, TOP
*NSET, NSET=BACK
1,4,5,8
*NSET, NSET=FRONT
2,3,6,7
```




```
*NSET, NSET=LHS
1,2,5,6
*NSET, NSET=RHS
3,4,7,8
*ELEMENT, TYPE=C3D8, ELSET=EL1
1,1,2,3,4,5,6,7,8
*SOLID SECTION, ELSET=EL1, MATERIAL=CAPL
*MATERIAL,NAME=CAPL
*ELASTIC
100.,.25
*CAP PLASTICITY
**COHESN, BETA, BIGR, EVOLPI, ALPHA, BIGK
    .1732, 14.56, 0.1, 0.001, , 1.0
*CAP HARDENING
** PB, EVOLP
    .02 ,.0
    .025,.005
    .063,.01
    .13 ,.02
    .24 ,.03
    .4  ,.04
    .6  ,.05
```



```
1.      ,.06
5.      ,.1
*BOUNDARY
BACK,1
LHS,2
BOT,3
RHS,2
TOP,3
*STEP, INC=20,UNSYMM=YES
*STATIC, DIRECT
1., 20.
*BOUNDARY
FRONT,1,, -.066
*EL PRINT
S
SINV
E
PE
PEQC
*NODE PRINT
U,RF
*END STEP
```



```
*STEP, INC=5, UNSYMM=YES  
*STATIC, DIRECT  
1., 5.  
*BOUNDARY  
FRONT, 1, , - .05  
*END STEP
```

Coupled Creep and Cap Plasticity

Geomaterials can creep under certain conditions. When the loading rate is of the same order of magnitude as the creep time scale, the plasticity and creep equations must be solved using a coupled solution procedure.

ABAQUS has a creep model that can be used to augment the Cap plasticity for such problems.

Basic Assumptions

Cap plasticity with creep always uses the coupled solution procedure.

The Cap creep model can be used if the Cap plasticity model uses isotropic linear elasticity, a circular yield surface in the deviatoric plane ($K=1$), and no transition zone between the shear failure region and the cap region ($\alpha = 0$).

The creep model has two creep mechanisms:

- Cohesive creep, which is active in both the shear failure region and the cap region.
- Consolidation creep, which is active only in cap region.

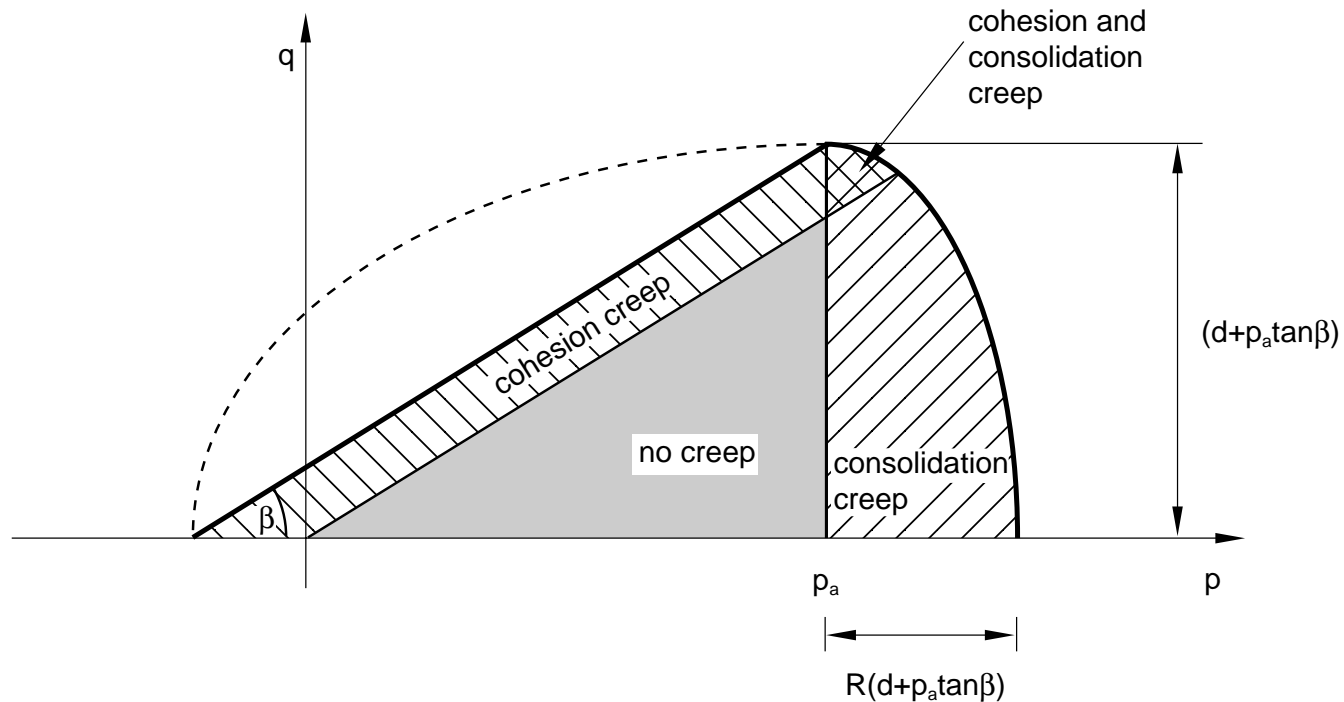


Figure 3–2. Equivalent Creep Surface for the Cap Creep Model

Cohesion Creep

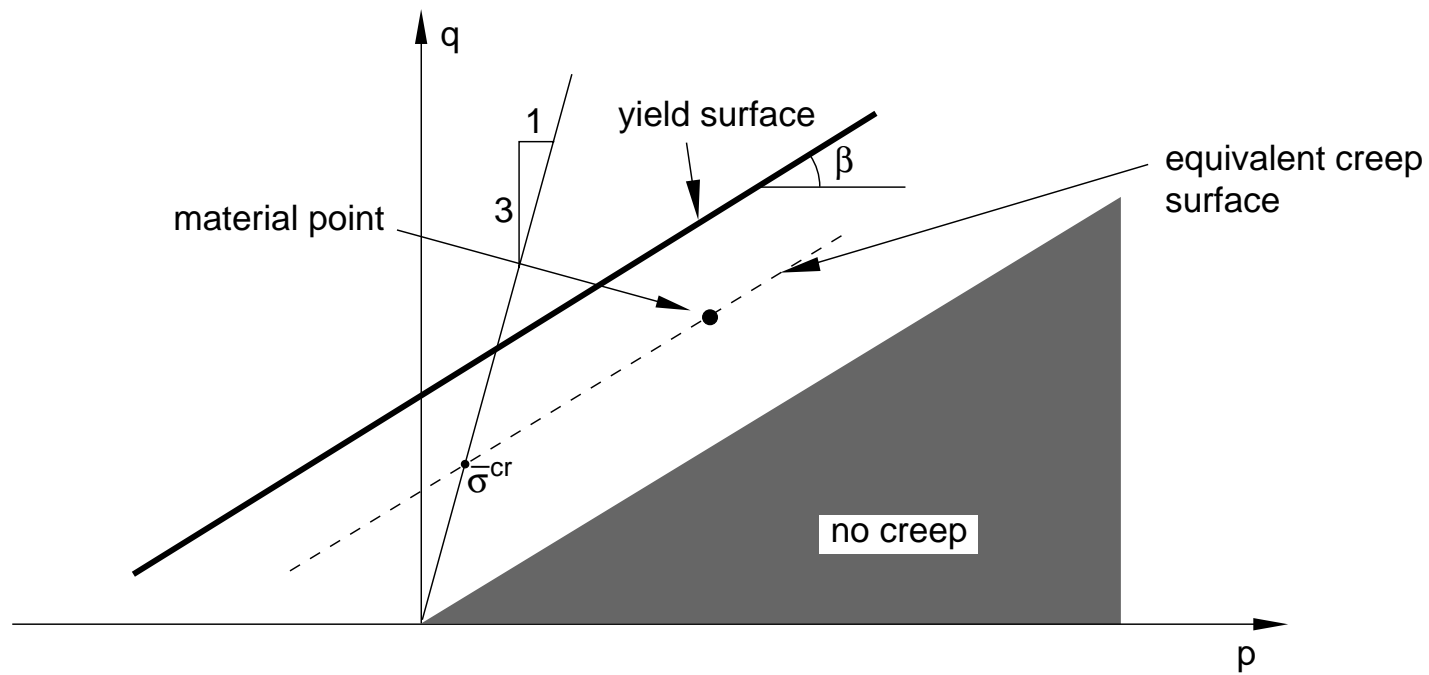
The cohesion creep mechanism is written in terms of an equivalent creep stress, $\bar{\sigma}^{cr}$, which is a measure of the creep “intensity” of the state of stress at a material point.

The cohesive creep properties must be measured in uniaxial compression. The format of $\bar{\sigma}^{cr}$ is

$$\bar{\sigma}^{cr} = \frac{(q - p \tan \beta)}{\left(1 - \frac{1}{3} \tan \beta\right)}.$$

The equivalent creep stress defines surfaces that are parallel to the shear failure surface in the meridional plane (see Figure 3–2).

There is a cone in the meridional plane where no creep deformation occurs. ABAQUS also requires that $\bar{\sigma}^{cr}$ be positive.



Consolidation Creep

The consolidation creep mechanism is dependent on the hydrostatic pressure above a threshold value of p_a , with a smooth transition to the areas in which the mechanism is not active.

Therefore, equivalent creep surfaces are constant hydrostatic pressure surfaces (vertical lines in the $p - q$ plane).

The consolidation creep laws are expressed in terms of an equivalent consolidation creep pressure stress, $\bar{p}^{cr} = p - p_a$.

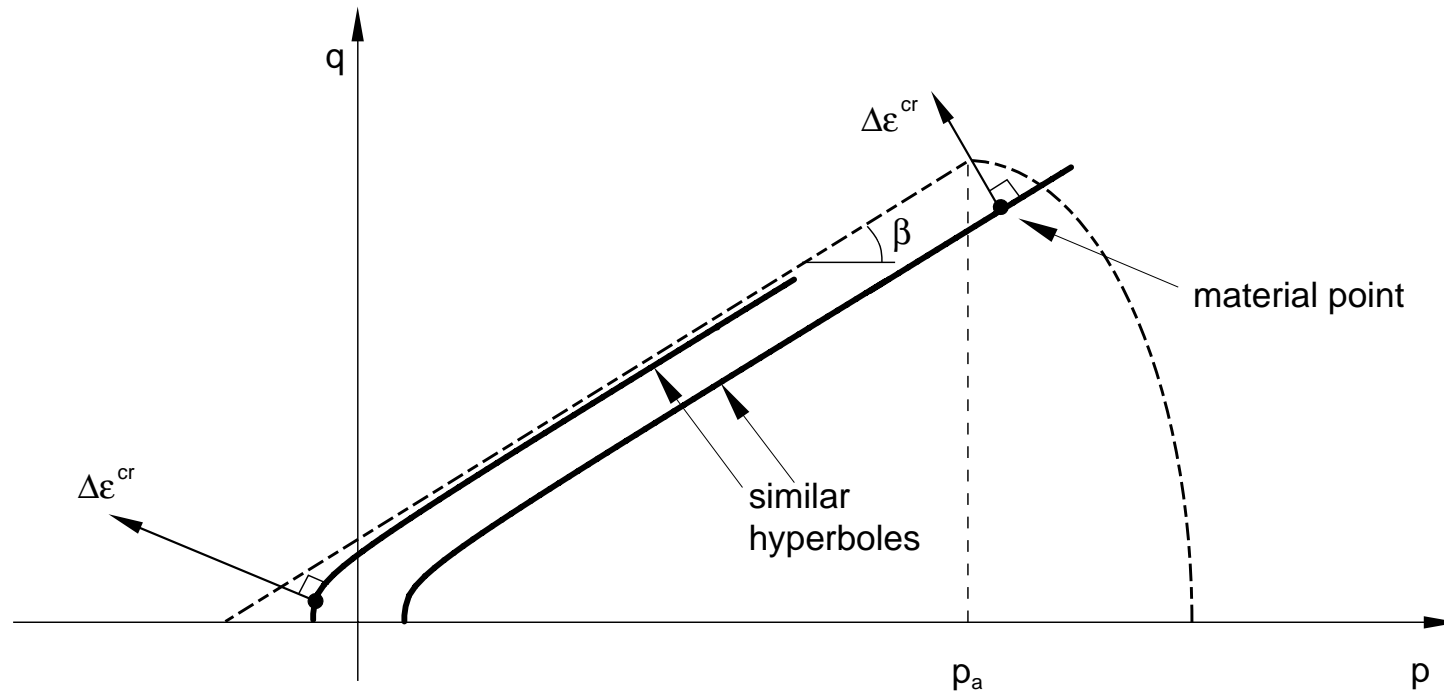
Creep Laws

The default creep laws available for the Cap creep models are the same as those available for the Drucker-Prager creep model: time and strain hardening laws and a Singh-Mitchell creep law.

- See **Coupled Creep and Drucker-Prager Plasticity** (p. L3.64) for details.

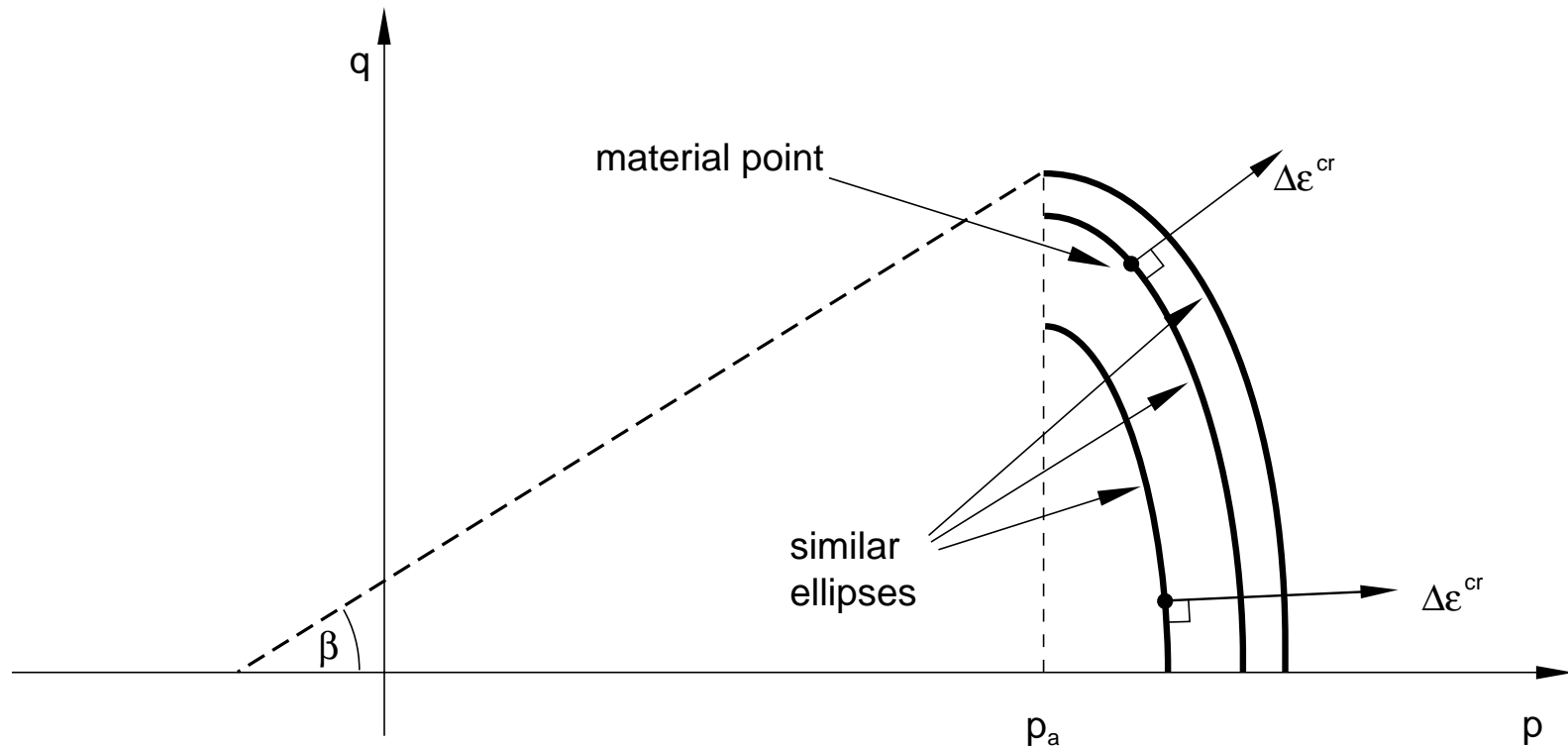
Creep Flow Potentials

The cohesion creep mechanism uses a hyperbolic creep potential in the meridional plane.



This creep flow potential, which is continuous and smooth, ensures that the flow direction is always defined uniquely. The cohesion creep potential is the von Mises circle in the deviatoric stress plane.

The consolidation mechanism uses an elliptical flow potential that is similar to the Cap plasticity flow potential in the $p - q$ plane. The consolidation creep potential is the von Mises circle in the deviatoric stress plane.



Usage

The *CAP CREEP option must be used in conjunction with the *CAP PLASTICITY and *CAP HARDENING options.

The *CAP CREEP option must be used with a cap plasticity model that has no third stress invariant effects ($K = 1$) and has no transition surface ($\alpha = 0$). In addition, it can be combined only with linear elasticity.

The material parameters in the default creep laws— A , n , m , t_1 , and α —can be defined as functions of temperature and/or field variables on the *CAP CREEP option.

- To avoid numerical problems with round-off, the values of A should be larger than 10^{-27} .

Use the **MECHANISM** parameter on the ***CAP CREEP** option to specify which behavior, **CONSOLIDATION** or **COHESION**, is being defined.

ABAQUS requires that cohesion creep properties be measured in a uniaxial compression test.

The time in these creep laws is the total analysis time, so the duration of steps where creep is not considered (such as ***STATIC** steps) should be relatively short.

More complex creep laws are defined with user subroutine **CREEP**.

The use of a creep potential for the cohesion mechanism different from the equivalent creep surface implies that the material stiffness matrix is not symmetric and the unsymmetric matrix storage and solution scheme (**UNSYMM=YES**) should be used.

Jointed Material Model

This model is intended to provide a simple, continuum model for materials containing a high density of parallel joint surfaces in different orientations.

The spacing of the joints of a particular orientation is assumed to be sufficiently close compared to characteristic dimensions in the domain of the model that the joints can be smeared into a continuum of slip systems.

An obvious application is the modeling of geotechnical problems where the medium of interest is composed of significantly faulted rock.

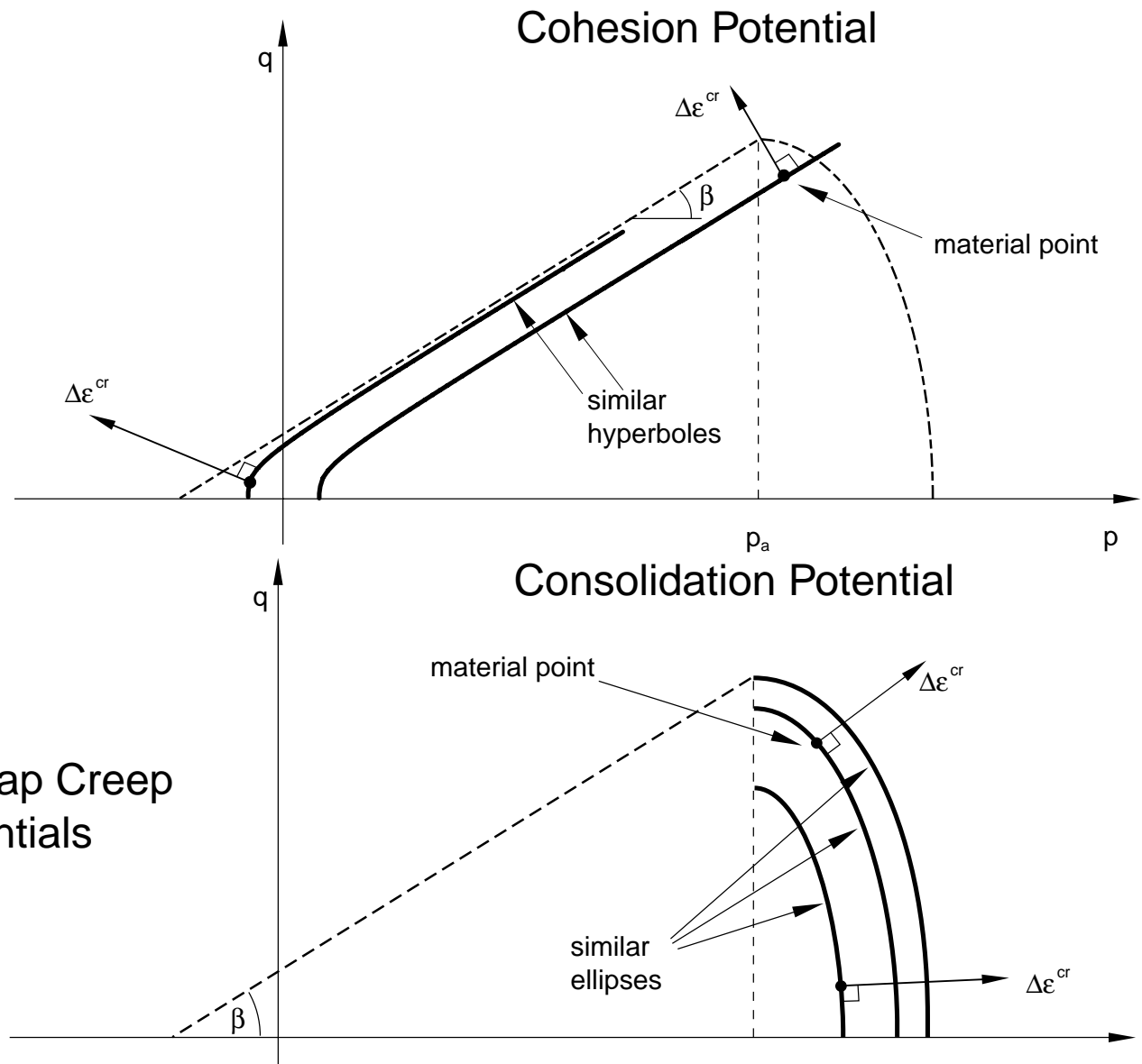
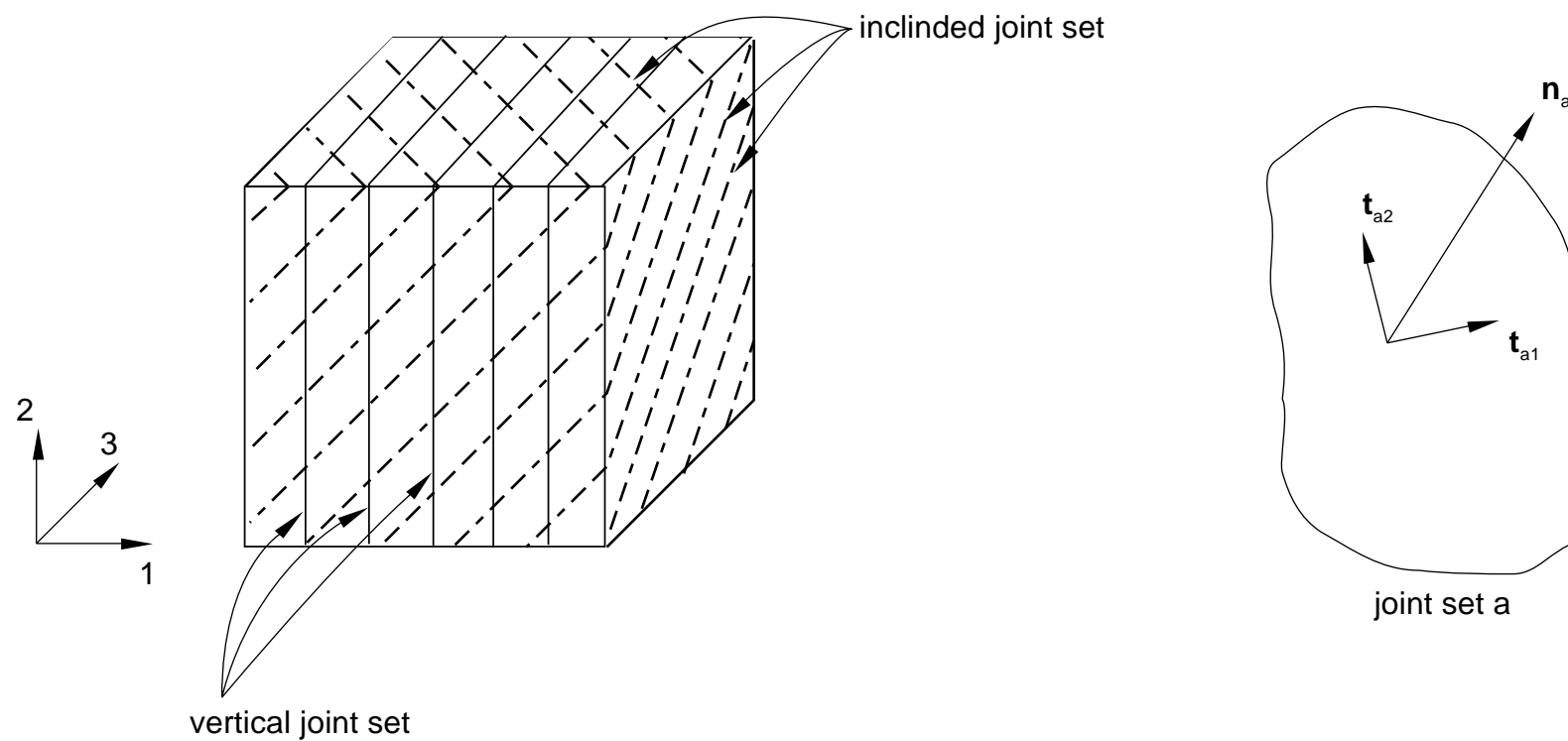


Figure 3–3. Cap Creep Flow Potentials

The basic characteristics of the model are:

- There is a regime of purely elastic response, after which some of the material deformation is not recoverable and can, thus, be idealized as being plastic.
- The model provides for up to three joint systems that may exhibit frictional sliding and may also open and close. Whenever any joint system is open, the material response becomes orthotropic.
- The model also includes a bulk failure mechanism based on a Drucker-Prager model.
- The inelastic sliding mechanisms on the joints and bulk material may be purely frictional or include dilation.
- The model provides a reasonable material response under large stress reversals (including joint opening/closing and cyclic shear).
- Temperature may affect the material properties.



Jointed element and joint orientation

Description

Consider joint a oriented by the normal to the joint surface \mathbf{n}_a .

$\mathbf{t}_{a\alpha}$, $\alpha = 1, 2$, are two unit, orthogonal vectors in the joint surface. The local stresses are the pressure stress and the shear stresses across the joint

$$p_a = -\mathbf{n}_a \cdot \boldsymbol{\sigma} \cdot \mathbf{n}_a,$$

$$\tau_{a\alpha} = \mathbf{n}_a \cdot \boldsymbol{\sigma} \cdot \mathbf{t}_{a\alpha}.$$

We define the shear stress magnitude as

$$\tau_a = \sqrt{\tau_{a\alpha} \tau_{a\alpha}}.$$

The local strains are the normal strain across the joint

$$\varepsilon_{an} = \mathbf{n}_a \cdot \boldsymbol{\varepsilon} \cdot \mathbf{n}_a$$

and the engineering shear strain in the α -direction in the joint surface

$$\gamma_{a\alpha} = \mathbf{n}_a \cdot \boldsymbol{\varepsilon} \cdot \mathbf{t}_{a\alpha} + \mathbf{t}_{a\alpha} \cdot \boldsymbol{\varepsilon} \cdot \mathbf{n}_a.$$

We use a linear strain rate decomposition:

$$d\epsilon = d\epsilon^{el} + d\epsilon^{pl}.$$

If several systems are active (we designate an active system by i , where $i = b$ indicates the bulk material system and $i = a$ is a joint system a):

$$d\epsilon^{pl} = \sum_i d\epsilon_i^{pl}.$$

When all joints at a point are closed, the elastic behavior of the material is isotropic and linear. We use a stress-based joint opening criterion, whereas joint closing is monitored based on strain. Joint system a opens when the estimated pressure stress across the joint (normal to the joint surface) is no longer positive:

$$p_a \leq 0.$$

In this case the material has no elastic stiffness with respect to direct strain across the joint system and may or may not have stiffness with respect to shearing associated with this direction. Thus, open joints create anisotropic elastic response at a point. The joint system remains open so long as

$$\epsilon_{an(ps)}^{el} \leq \epsilon_{an}^{el} ,$$

where ϵ_{an}^{el} is the component of direct elastic strain across the joint and $\epsilon_{an(ps)}^{el}$ is the component of direct elastic strain across the joint calculated in plane stress as

$$\epsilon_{an(ps)}^{el} = -\frac{\nu}{E}(\sigma_{a1} + \sigma_{a2}),$$

where E is the Young's modulus of the material, ν is the Poisson's ratio and

$$\sigma_{a\alpha} = \mathbf{t}_{a\alpha} \cdot \boldsymbol{\sigma} \cdot \mathbf{t}_{a\alpha}$$

are the direct stresses in the plane of the joint.

The failure surface for sliding on joint a is

$$f_a = \tau_a - p_a \tan \beta_a - d_a = 0,$$

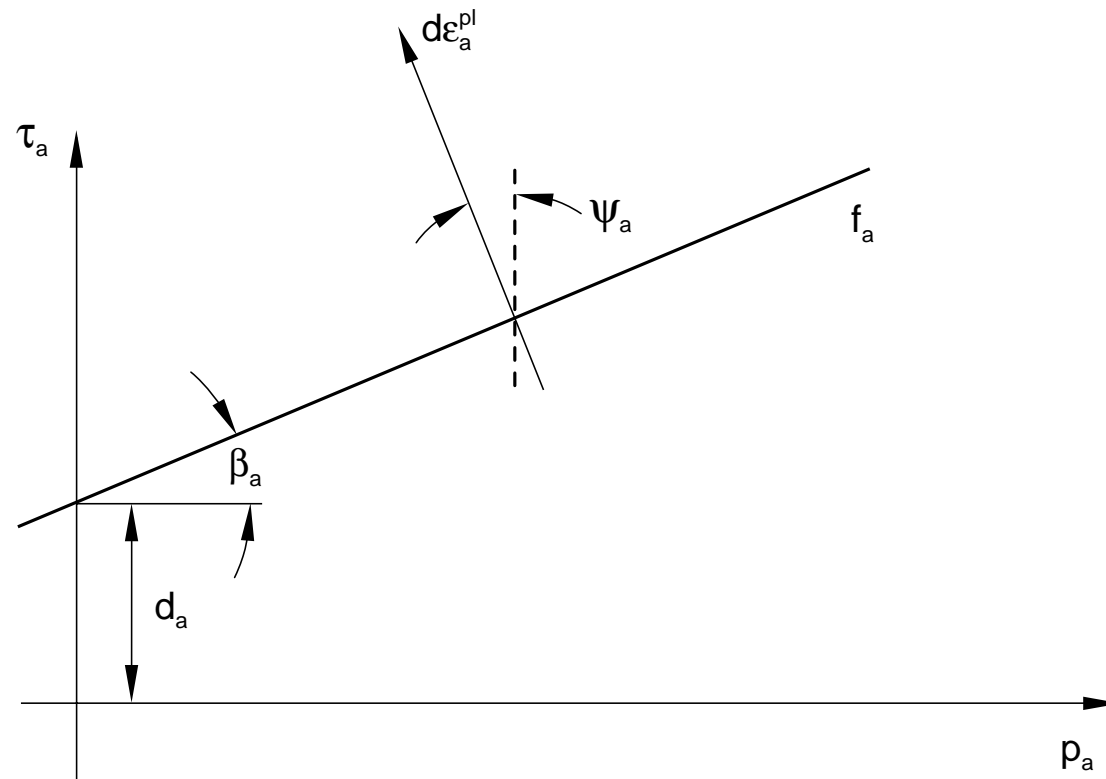
where β is the friction angle and d_a is the cohesion for system a . So long as $f_a < 0$, joint a does not slip. When $f_a = 0$, joint a slips. The inelastic strain on the system is

$$d\epsilon_a^{pl} = \bar{d}\epsilon_a^{pl} \left(\sin \psi_a \mathbf{n}_a \mathbf{n}_a + \frac{\tau_{a\alpha}}{\tau_a} \cos \psi_a (\mathbf{n}_a \mathbf{t}_{a\alpha} + \mathbf{t}_{a\alpha} \mathbf{n}_a) \right),$$

where $\bar{d}\epsilon_a^{pl}$ is the magnitude of the inelastic strain rate and ψ_a is the dilation angle for this joint system (choosing $\psi_a = 0$ provides pure shear flow on the joint, while $\psi_a > 0$ causes dilation of the joint as it slips).

The sliding of the different joint systems at a point is independent, in the sense that sliding on one system does not change the failure criterion or the dilation angle for any other joint system at the same point.

Joint system model:



In addition to the joint systems, the model includes a bulk material failure mechanism based on the linear Drucker-Prager failure criterion

$$q - p \tan \beta_b - d_b = 0,$$

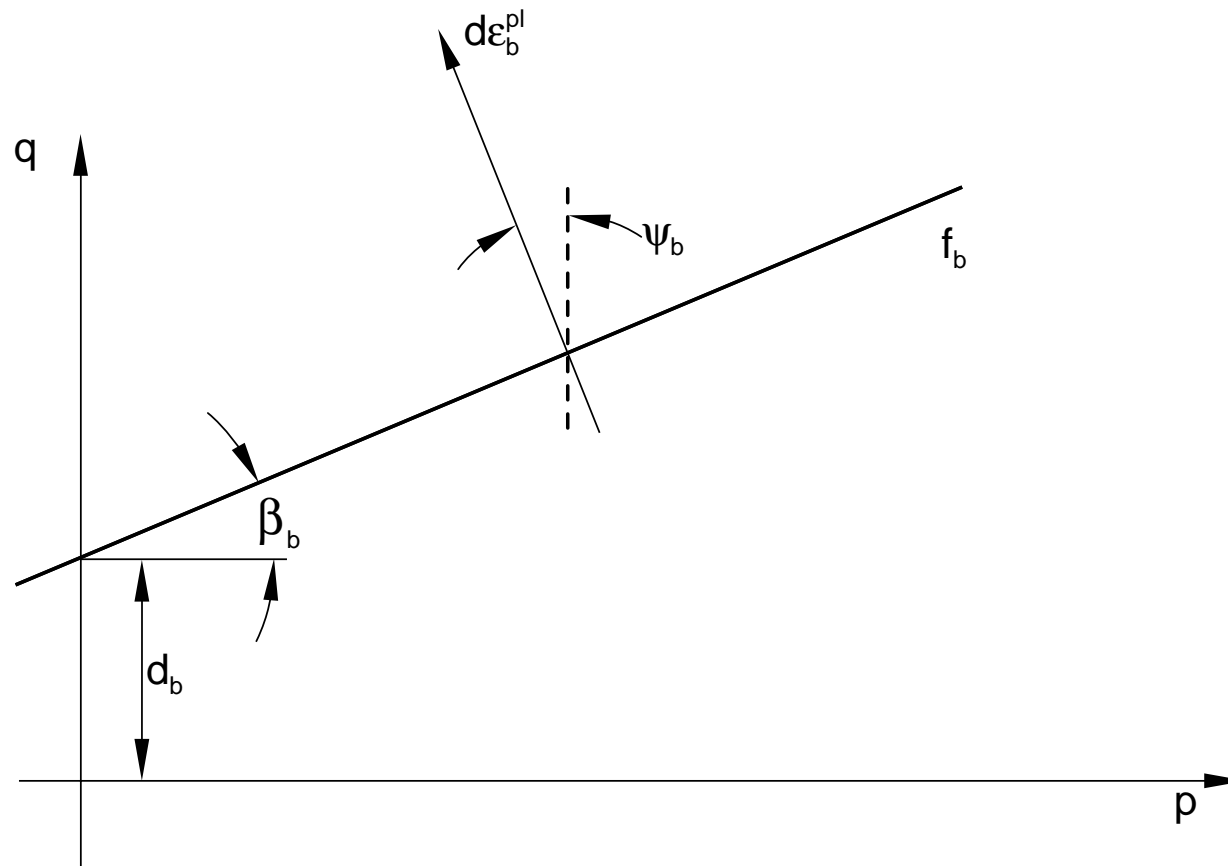
where β_b is the friction angle for the bulk material and d_b is the cohesion for the bulk material. If this failure criterion is reached, the bulk inelastic flow is defined by

$$d\epsilon_b^{pl} = d\bar{\epsilon}_b^{pl} \frac{1}{1 - \frac{1}{3} \tan \psi_b} \frac{\partial g_b}{\partial \sigma}$$

$$g_b = q - p \tan \psi_b,$$

where ψ_b is the dilation angle for the bulk material. This bulk failure model is a simplified version of the modified Drucker-Prager model described earlier in this lecture. As with the joint systems, this bulk failure system is independent of the joint systems in that bulk inelastic flow does not change the behavior of any joint system.

Bulk material model:



Usage and Calibration

The jointed material model in ABAQUS is invoked with the ***JOINTED MATERIAL** material option. This option allows the yield and flow rule parameters to be made dependent on temperature and predefined field variables. This option must be repeated for each existing system (bulk material and up to three joints); it may appear four times.

When defining a joint system, the **JOINT DIRECTION** parameter must be used to refer to the orientation definition corresponding to the joint. The ***ORIENTATION** option must then be used to define the joint orientation in the original configuration. Stress and strain components will still be output in global directions unless the ***ORIENTATION** option is also used on the section definition option associated with the material definition.

When defining the bulk material, the **JOINT DIRECTION** parameter must be omitted.

The ***JOINTED MATERIAL** option may appear a fifth time with the **SHEAR RETENTION** parameter to define a nonzero shear modulus for open joints.

The elasticity must be defined with the `*ELASTIC, TYPE=ISOTROPIC` material option since we assume that the material is linear elastic and isotropic when all joints are closed. The material cannot be elastically incompressible (Poisson's ratio must be less than 0.5).

`*EXPANSION` can be used to introduce thermal volume change effects.

Analyses using a nonassociated flow version of the model may require the use of the `UNSYMM=YES` parameter on the `*STEP` option because of the resulting nonsymmetry of the plasticity equations.

At least two experiments are required to calibrate the behavior of each of the existing inelastic mechanisms.

For the bulk material the experiments commonly performed for this purpose are uniaxial compression (for cohesive materials) and triaxial compression tests.

The uniaxial compression test involves compressing the sample between two rigid platens. The load and displacement in the direction of loading are recorded. The lateral displacements should also be recorded so that the correct volume changes can be calibrated.

Triaxial compression experiments are performed using a standard triaxial machine where a fixed confining pressure is maintained while the differential stress is applied. Several tests covering the range of confining pressures of interest are usually performed. Again, the stress and strain in the direction of loading are recorded, together with the lateral strain, so that the correct volume changes can be calibrated.

For the joint systems the most common experiments are shear tests. In these tests a normal pressure is applied across the joint and then the joint is sheared. Several tests covering the range of pressures of interest are usually performed. Again, the stresses and strains in the normal and shear directions must be recorded.

Unloading measurements in all of the above tests are useful to calibrate the elasticity, particularly in cases where the initial elastic region is not well-defined.

The angle of friction, β , and the cohesion, d , defining the failure stress dependence on pressure are calculated by plotting the failure stresses of any two experiments in the pressure stress versus shear stress space: the slope of the straight line passing through the two points gives β , and the intersection with the shear stress axis gives d .

If more than two experiments are available, a best fit straight line over the range of interest of pressure stress must be used to calculate the slope of the failure surface.

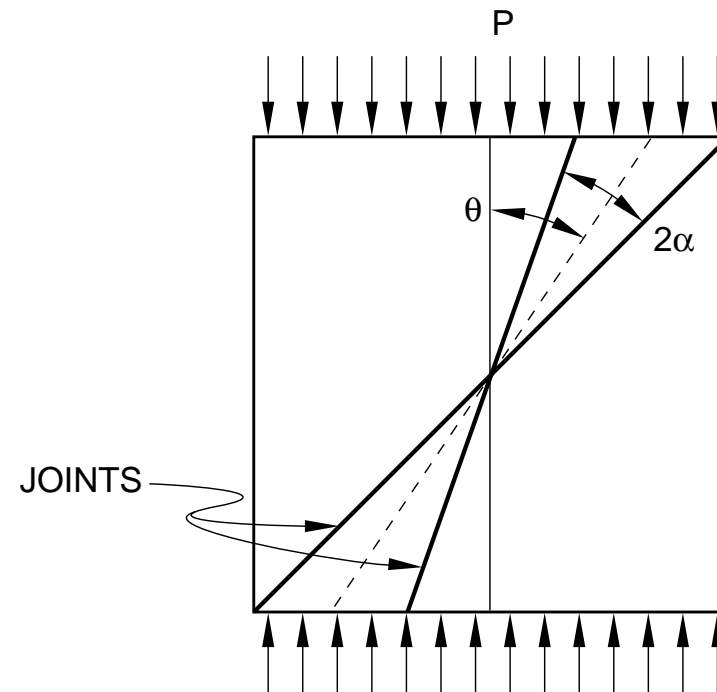
Refer also to the calibration discussion in **Linear Drucker-Prager Model** (p. L3.31).

The dilation angle, ψ , must be chosen such that a reasonable match of the volume changes during yielding is obtained. The volume changes are calculated from the strains in all directions.

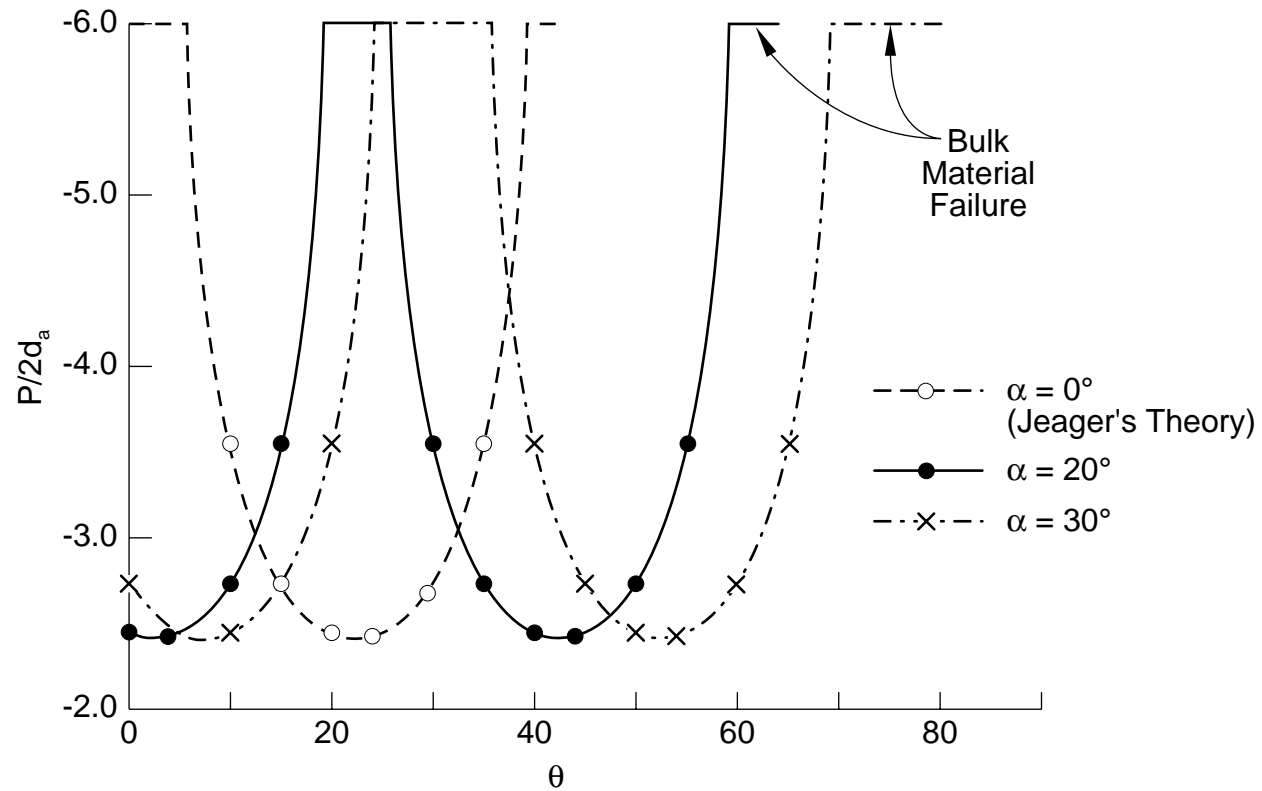
The calibration of the temperature-dependent model requires repetition of the experiments at different temperatures over the range of interest.

Example

We consider a sample of material subjected to uniaxial compression/tension. The material has two sets of planes of weakness having an included angle of 2α . We construct the failure envelope of the material as the orientation (θ) of the planes of weakness is varied. The joints have cohesion $d_a = 1000$ and friction angle $\beta_a = 45^\circ$. The bulk material has cohesion $d_b = 8000$ and friction angle $\beta_b = 45^\circ$. Plastic flow in the joints and bulk material is associated. When all joints are closed, the material is isotropic linear elastic with $E = 3 \times 10^5$ and $\nu = 0.3$. When a joint opens, the material is assumed to have no elastic stiffness. We show the variation of the compressive failure stress $P/2d_a$ with θ for $\alpha = 0^\circ, 20^\circ, 30^\circ$. For certain ranges of orientation of the joints, failure along the joints becomes increasingly improbable and failure of the bulk material takes place first. In tension the material cannot carry any stress since the joints open readily.



Problem Geometry (Benchmark Problem 3.2.5)



Uniaxial Compression Failure Envelopes



Input Listing:

```
*HEADING
UNIAXIAL COMPRESSION TEST,2 JOINTS,ALFA=20 THETA=0
*WAVEFRONT MINIMIZATION,SUPPRESS
*NODE,NSET=ALLN
1,0.,0.,0.
2,1.,0.,0.
3,1.,1.,0.
4,0.,1.,0.
5,0.,0.,1.
6,1.,0.,1.
7,1.,1.,1.
8,0.,1.,1.
*ELEMENT,TYPE=C3D8,ELSET=ALLE
1,1,2,3,4,5,6,7,8
*SOLID SECTION,ELSET=ALLE,MATERIAL=ALLE
*MATERIAL,NAME=ALLE
*ELASTIC
300.E3,.3
*JOINTED MATERIAL
45.,45.,8000.
```




```
*JOINTED MATERIAL,JOINT DIRECTION=JOINT1
45.,45.,1000.
*JOINTED MATERIAL,JOINT DIRECTION=JOINT2
45.,45.,1000.
*ORIENTATION,NAME=JOINT1
-.9397,.342,0.,-.342,-.9397,0.
*ORIENTATION,NAME=JOINT2
.9397,.342,0.,-.342,.9397,0.
*BOUNDARY
1,PINNED
2,2
5,2
6,2
4,1
5,1
8,1
2,3
3,3
4,3
*STEP,INC=20
*STATIC,DIRECT
1.,20.
```



```
*BOUNDARY
7,2,,-.2
3,2,,-.2
4,2,,-.2
8,2,,-.2
*EL PRINT
S
SINV
E
PE
PEQC
EE
*NODE PRINT
U,RF
*EL FILE,FREQUENCY=2
S,E,PE
*END STEP
```

Numerical Implementation

For all the material models presented in this set of notes, the constitutive behavior is given in rate form—the inelastic strain is defined only as a strain rate.

This must be integrated over each finite time increment. We use backward Euler integration:

$$\Delta \epsilon^{pl} = \left. \frac{d\epsilon^{pl}}{dt} \right|_{t+\Delta t} \Delta t,$$

where Δt is the time increment and t is the time at the beginning of the increment.

The backward Euler method (more traditionally called “radial return” because of its simple geometric interpretation for the basic case of a Mises yield and associated flow model) is chosen because it is unconditionally stable. In addition, it provides acceptable accuracy, especially when the strain increment is large compared to the strain to cause yield.

In some simple cases, such as a perfectly plastic Drucker-Prager model, the backward difference equations can be solved in closed form. However, in most cases, Newton's method is used for the numerical solution of the integrated plasticity equations.

In models that involve opening/closing conditions (such as in the jointed material model) and in models that involve more than one yield surface (such as the capped Drucker-Prager model), additional logic is used to handle all the possible combinations of behavior available within the model.

Occasionally ABAQUS fails to find a solution to the integrated constitutive equations. It then gives a warning message: "PLASTICITY ALGORITHM FAILS TO CONVERGE AT n INTEGRATION POINTS." If automatic time incrementation has been chosen (which is always recommended), the program then tries again with a smaller time increment and the problem is, thereby, resolved. If necessary, detailed information about where the algorithms are failing can be obtained by setting *PRINT, PLASTICITY=YES.

ABAQUS provides consistent material Jacobians (tangent stiffnesses) for the global equilibrium iterations so that quadratic convergence can be achieved.

Lecture 4

Analysis of Porous Media

Overview

- Basic Assumptions and Effective Stress
- Stress Equilibrium and Flow Continuity
- Types of Analyses and Usage
- Examples

ABAQUS has capabilities for the treatment of single phase flow through porous media, including fully saturated flow (encountered in many geotechnical applications), partially saturated flow (encountered in irrigation problems and hydrology problems), or a combination of the two (calculation of phreatic surfaces).

Fluid gravity effects may be considered. It is possible to perform analyses in terms of total pore fluid pressure or excess pore fluid pressure.

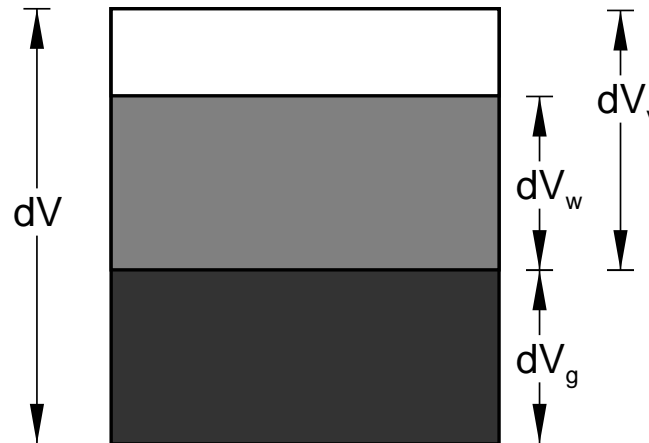
Total pore pressure analysis (including fluid weight) is required when the loading provided by fluid gravity is large, or when “wicking” (transient capillary suction of liquid into a dry body) is of interest.

Two other effects, “gel” swelling and moisture swelling, may be included in partially saturated cases. These are usually associated with modeling of moisture absorption into polymeric systems (such as paper towels) rather than with geotechnical systems and are not discussed in these notes.

Basic Assumptions and Effective Stress

We model a deforming porous medium using the conventional approach that considers the medium as a multi-phase material and adopts an effective stress principle to describe its behavior.

An elementary volume, dV , is made up of a volume of grains of solid material, dV_g , and a volume of voids, dV_v , which is either fully or partly saturated with a volume of wetting fluid, dV_w .



The porosity of the medium, n , is defined as the ratio of the volume of voids to the total volume:

$$n = \frac{dV_v}{dV}.$$

ABAQUS generally uses voids ratio, $e = (dV_v/dV_g)$, instead of porosity. Conversion relationships are:

$$e = \frac{n}{1 - n}, \quad n = \frac{e}{1 + e}, \quad 1 - n = \frac{1}{1 + e}.$$

Saturation, s , is defined as the ratio of wetting fluid volume to void volume:

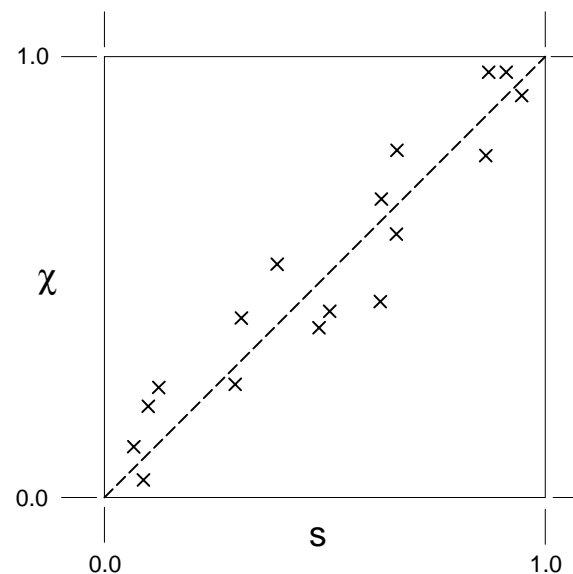
$$s = \frac{dV_w}{dV_v}$$

For a fully saturated medium $s = 1$, while for a completely dry medium $s = 0$.

The total stress acting at a point, σ , is assumed to be made up of an average pressure stress in the wetting fluid, u_w , called the “pore pressure” times a factor, χ , and an “effective stress” in the material skeleton, $\bar{\sigma}$:

$$\bar{\sigma} = \sigma + \chi u_w \mathbf{I}.$$

In general, $\chi = \chi(s)$ can be measured experimentally. Typical experimental data are shown below:



Since such data are difficult to obtain, ABAQUS assumes $\chi = s$.

The effective stress principle is the assumption that the constitutive response of the porous medium consists of simple bulk elasticity relationships for the fluid and for the solid grains, together with a constitutive theory for the material skeleton whereby $\bar{\sigma}$ is defined as a function of the strain history and temperature of the material:

$$\bar{\sigma} = \bar{\sigma}(\text{strain history, temperature, state variables}).$$

Any of the constitutive models in ABAQUS can be used to model the material skeleton of voided materials. Models suitable for soils and rocks were discussed in the previous lectures.

The strain rate decomposition is then

$$d\boldsymbol{\varepsilon} = (d\boldsymbol{\varepsilon}_g^{vol} + d\boldsymbol{\varepsilon}_w^{vol})\mathbf{I} + d\boldsymbol{\varepsilon}^{el} + d\boldsymbol{\varepsilon}^{pl}$$

where $d\boldsymbol{\varepsilon}_g^{vol}$, $d\boldsymbol{\varepsilon}_w^{vol}$ are the volume strain rates in the solid grains and fluid, and $d\boldsymbol{\varepsilon}^{el}$, $d\boldsymbol{\varepsilon}^{pl}$ are the elastic and plastic strain rates in the material skeleton.

Stress Equilibrium and Flow Continuity

Stress equilibrium for the solid phase of the material is expressed by writing the principle of virtual work for the volume under consideration in its current configuration at time t :

$$\int_V (\bar{\boldsymbol{\sigma}} - \chi u_w \mathbf{I}) : \delta \boldsymbol{\varepsilon} dV = \int_S \mathbf{t} \cdot \delta \mathbf{v} dS + \int_V \mathbf{f} \cdot \delta \mathbf{v} dV + \int_V \rho_w \mathbf{g} \cdot \delta \mathbf{v} dV,$$

where $\delta \boldsymbol{\varepsilon} \stackrel{\text{def}}{=} \text{sym}(\partial \delta \mathbf{v} / \partial \mathbf{x})$ is the virtual rate of deformation, $\bar{\boldsymbol{\sigma}}$ is the true (Cauchy) effective stress, $\delta \mathbf{v}$ is a virtual velocity field, \mathbf{t} are surface tractions per unit area, \mathbf{f} are body forces (excluding fluid weight) per unit volume, ρ_w is the density of the fluid, and \mathbf{g} is the gravitational acceleration (assumed constant and in a fixed direction).

This equation is then discretized using a Lagrangian formulation for the solid phase, with displacements as the nodal variables.

The porous medium is thus modeled by attaching the finite element mesh to the solid phase. Fluid may flow through this mesh.

A continuity equation is therefore required for the fluid, equating the rate of increase in fluid volume stored at a point to the rate of volume of fluid flowing into the point within the time increment:

$$\frac{d}{dt} \left(\int_V \frac{\rho_w}{\rho_w^0} sn \, dV \right) = - \int_S \frac{\rho_w}{\rho_w^0} sn \, \mathbf{n} \cdot \mathbf{v}_w \, dS$$

where \mathbf{v}_w is the average velocity of the fluid relative to the solid phase (the seepage velocity) and \mathbf{n} is the outward normal to S . This equation has been normalized by ρ_w^0 , the reference density of the fluid.

The continuity equation is integrated in time using the backward Euler approximation and discretized with finite elements using pore pressure as the variable.

The pore fluid flow behavior is assumed to be governed either by Darcy's law or by Forchheimer's law. Darcy's law is generally applicable to low fluid flow velocities, whereas Forchheimer's law is used for higher flow velocities. Darcy's law may be thought of as a linearized version of Forchheimer's law.

Forchheimer's law describes pore fluid flow as:

$$\mathbf{v}_w = - \frac{1}{sng\rho_w(1 + \beta\sqrt{\mathbf{v}_w \cdot \mathbf{v}_w})} \hat{\mathbf{k}} \cdot \left(\frac{\partial u_w}{\partial \mathbf{x}} - \rho_w \mathbf{g} \right),$$

where g is the magnitude of the gravitational acceleration, $\hat{\mathbf{k}}(s, e)$ is the permeability of the medium (possibly anisotropic) with units of length/time, and $\beta(e)$ is a “velocity coefficient”. [Some texts use a different definition of permeability. This is discussed later.]

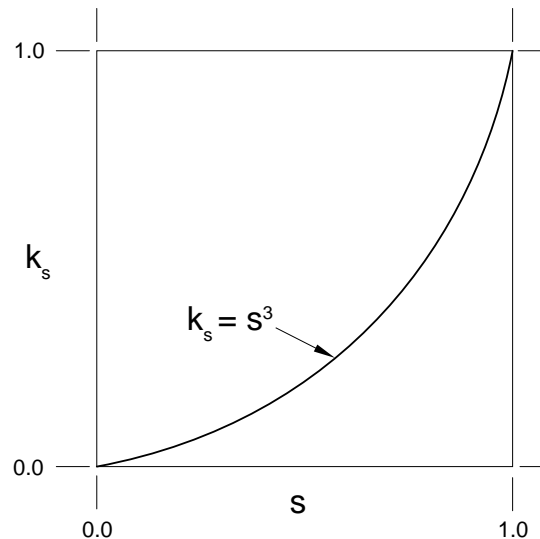
Darcy's law is obtained by setting $\beta = 0$. We see that, as the fluid velocity tends to zero, Forchheimer's law approaches Darcy's law.

The permeability depends on the saturation of the fluid and on the porosity of the medium. We assume these dependencies are separable, so that

$$\hat{\mathbf{k}} = k_s \mathbf{k}$$

where $k_s(s)$ gives the saturation dependency, with $k_s(1) = 1.0$, and $\mathbf{k}(e)$ is the fully saturated permeability. For isotropic materials $\mathbf{k} = k\mathbf{I}$.

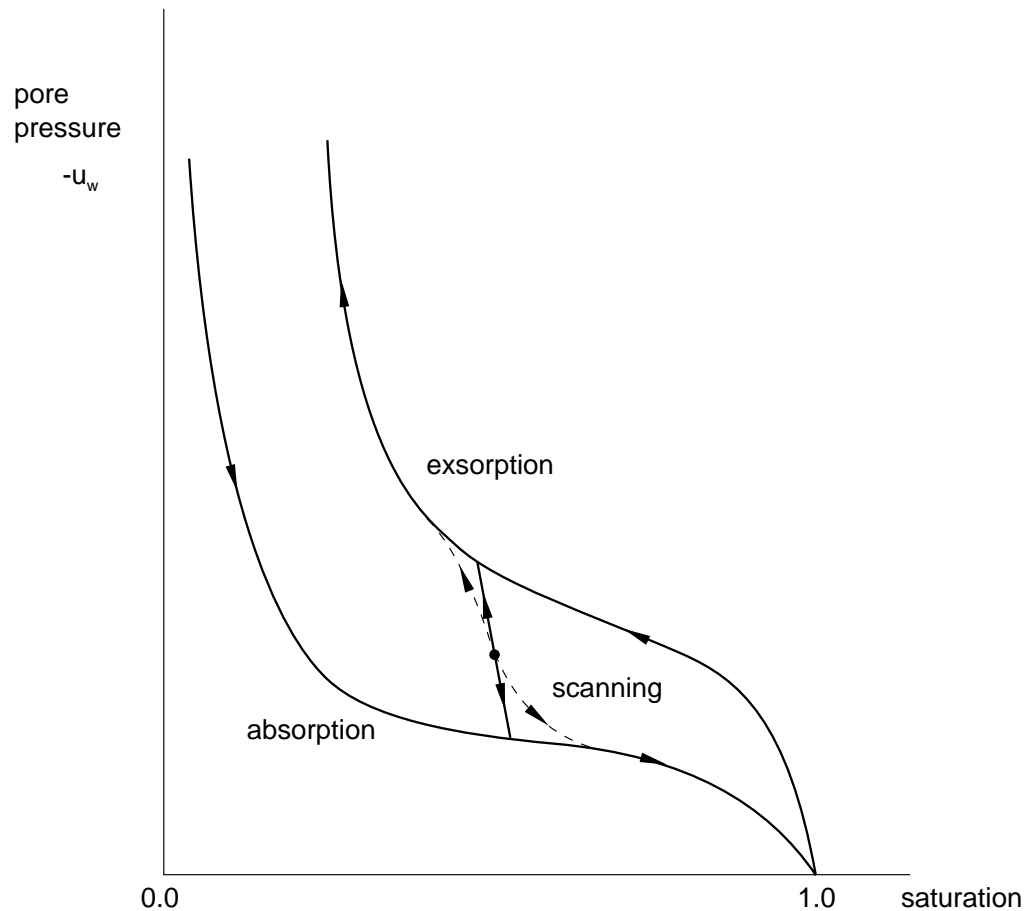
Experimental observation often suggests that, in steady flow through a partially saturated medium, the permeability varies with s^3 .



We, therefore, take $k_s = s^3$ by default. Different forms of behavior for $k_s(s)$ can be defined by using the *PERMEABILITY option.

Because u_w measures pressure in the wetting fluid, the medium is fully saturated for $u_w > 0$. Negative values of u_w represent capillary effects in the medium.

For $u_w < 0$ it is known that, at a given value of capillary pressure, $-u_w$, the saturation lies within certain limits. These limits are defined by using the *SORPTION option. Typical forms are shown below.



We write these limits as $s^a \leq s \leq s^e$, where $s^a(u_w)$ is the limit at which absorption will occur (so that $\dot{s} > 0$) and $s^e(u_w)$ is the limit at which exsorption will occur; thus, $\dot{s} < 0$. We assume that these relationships are uniquely invertible and can also be written as $u_w^a(s)$ during absorption and $u_w^e(s)$ during exsorption. We also assume that some wetting fluid will always be present in the medium: $s > 0$.

The transition between absorption and exsorption, and vice-versa, takes place along “scanning” lines, which are approximated by a single value of du_w/ds at all saturation levels.

Saturation is treated as a state variable that may have to change if the wetting liquid pressure is outside the range for which its value is admissible according to the actual data.

Note on permeability units:

In ABAQUS we define permeability in the flow constitutive equation

$$\mathbf{v}_w = - \frac{1}{sng\rho_w(1 + \beta\sqrt{\mathbf{v}_w \cdot \mathbf{v}_w})} \hat{\mathbf{k}} \cdot \left(\frac{\partial u_w}{\partial \mathbf{x}} - \rho_w \mathbf{g} \right)$$

as $\hat{\mathbf{k}}$, with units of length/time. In this equation ρ_w is the mass density of the fluid, s is the saturation, n is the porosity, β is the velocity coefficient and g is the gravitational acceleration. It is then clear that both sides of the equation have units of length/time.

However, one other definition of permeability (\mathbf{K}) is often used:

$$\mathbf{K} = \frac{\mu}{g\rho_w} \hat{\mathbf{k}}$$

where μ is the fluid viscosity in *poise* units (mass/time-length). In this context, permeability \mathbf{K} has length squared units (or *Darcy*) and what we refer to in ABAQUS as permeability, $\hat{\mathbf{k}}$, is called the *hydraulic conductivity*.

In the coupled problem, the stress equilibrium and fluid continuity equations must be solved simultaneously. In the general nonlinear case, we use a Newton scheme to solve the equations. The Newton equations for various cases of the formulation (transient or steady-state flow, etc.) are described in Appendix A.

Types of Analyses and Usage

The analysis of flow through porous media in ABAQUS is available for plane strain, axisymmetric, and three-dimensional problems. Special coupled displacement/pore pressure elements must be used: these elements have a linear distribution of pore pressure and either a first-order or a second-order distribution of displacement.

The coupled stress/flow problems are solved using the *SOILS procedure. By default, ABAQUS will solve the steady-state problem (*SOILS, STEADY STATE) while the transient problem is invoked with *SOILS, CONSOLIDATION.

The steady-state problem assumes that the time scale is so long that there is no transient effect in the pore fluid diffusion part of the problem. The time scale chosen is then only relevant to any possible rate effects in the constitutive model used for the material skeleton.

Mechanical loads and boundary conditions can be changed gradually over a step, to accommodate nonlinearities in the response.

Uncoupled (purely diffusion) pore pressure elements are not available. These are useful in cases when only the pore fluid flow part of the problem is of interest. In such problems we have used coupled elements and constrained all the displacement degrees of freedom to be computationally inefficient. Coupled deformation/pore pressure infinite elements are not available.

Dynamic coupled stress/fluid flow analysis cannot be performed, since we assume no inertia in the existing coupled analysis capability. This is important in cases such as the behavior of a dam subjected to earthquake loading. Again, liquefaction effects may be important.

Three-way coupled stress/fluid flow/temperature analysis cannot be performed. This is important in applications such as those encountered in nuclear waste disposal and oil reservoir simulation.

The capability for fluid flow through porous media assumes single-phase fluid flow; multi-phase fluid flow is important in cases such as oil reservoir simulation.

The vapor phase is ignored in the partially saturated flow formulation; there are situations for which this assumption is not adequate.

The transient problem includes the time integration of the diffusion effects; therefore, the choice of time increment is important. The integration procedure used in ABAQUS introduces a relationship between the minimum usable time increment and the element size. This minimum is a requirement only for second-order elements, but it is recommended for all diffusion elements.

A simple guideline that can be used for fully saturated flow is

$$\Delta t > \frac{\rho_w g}{6Ek} \left(1 - \frac{E}{K_g}\right)^2 (\Delta l)^2,$$

where Δt is the time increment, E is the Young's modulus of the material skeleton, k is the permeability of the saturated medium (in units of length/time), K_g is the bulk modulus of the solid grains, and Δl is a typical element dimension.

A simple guideline that can be used for partially saturated flow is

$$\Delta t > \frac{\rho_w g n^0}{6 k_s k} \frac{ds}{du_w} (\Delta l)^2,$$

where n^0 is the initial porosity of the material, k_s is the permeability-saturation relationship, and ds/du_w is the rate of change of saturation with respect to pore pressure as defined in the *SORPTION material option.

If time increments smaller than this value are used, spurious oscillations may appear in the solution. If the problem requires analysis with smaller time increments than the above relationship allows, a finer mesh is required.

Generally there is no upper limit on the time increment size, except accuracy, since the integration procedure is unconditionally stable, unless nonlinearities cause numerical problems.

The accuracy of the time integration is controlled by the tolerance UTOL (maximum allowable change in pore pressure during the increment), which is also used to drive the automatic incrementation procedure for *SOILS, CONSOLIDATION analysis.

Transient analysis may be terminated by completing a specified time period, or it may be continued until steady-state conditions are reached, steady state being defined by all fluid pressures changing at less than a user-defined rate.

The porous medium coupled analysis capability can provide solutions either in terms of total or of “excess” pore fluid pressure.

The difference between total and excess pressure is relevant only for cases in which gravitational loading is important.

Total pressure solutions are provided when the GRAV distributed load type is used to define the gravity load on the model. Excess pressure solutions are provided in all other cases (for example, when gravity loading is defined with distributed load types BX, BY, or BZ).

In total pore pressure problems, the *DENSITY material option must be used to specify the density of the dry material only.

The gravity contribution from the pore fluid is defined through the SPECIFIC (weight) parameter on the *PERMEABILITY option, together with the direction of the gravity vector specified in the *DLOAD option with load type GRAV.

The *PERMEABILITY option is used to specify the permeability of the saturated medium, which can be isotropic or anisotropic and a function of void ratio.

The *PERMEABILITY option can be repeated with TYPE=VELOCITY to invoke Forchheimer's flow law instead of the default Darcy's law.

In partially saturated cases, the *PERMEABILITY option can also be repeated with TYPE=SATURATION to specify the dependence of permeability on saturation, $k_s(s)$. By default, $k_s = s^3$.

In partially saturated cases the *SORPTION option is used to specify the dependence of negative (partially saturated) pore pressure on saturation. When used with TYPE=ABSORPTION (default), it defines the absorption curve. When used with TYPE=EXSORPTION, it defines the exsorption curve (by default, the exsorption curve is the same as absorption). Analytical (logarithmic) or tabular input data are permitted.

In partially saturated cases the *SORPTION, TYPE=SCANNING option is used to define the scanning slope between absorption and exsorption. ABAQUS will generate this slope automatically if the user does not specify it.

The *POROUS BULK MODULI material option can be used to specify the bulk modulus of the solid grains and fluid if the user wants to include the compressibility of these components of the porous medium.

*EXPANSION can be used to introduce thermal volume change effects for the solid grains and the pore fluid.

*INITIAL CONDITIONS, TYPE=RATIO is required to define the initial voids ratio (porosity) of the medium. User subroutine **VOIDRI** can be used to specify complex initial void ratio distributions.

*INITIAL CONDITIONS, TYPE=STRESS can be used to define the initial effective stress state in the material. User subroutine **SIGINI** can be used to specify complex initial effective stress distributions.

*INITIAL CONDITIONS, TYPE=PORE PRESSURE can be used to define the initial pore fluid pressure in the medium. The initial pore pressures can be defined as a linear function of elevation in the model or as a constant value. ABAQUS assumes that the vertical (elevation) direction is the 3-direction in three-dimensional models and is the 2-direction in two-dimensional (or axisymmetric) models.

User subroutine **UPOREP** is also available for complicated cases. To use this subroutine, the **USER** parameter must be included on the *INITIAL CONDITIONS, TYPE=PORE PRESSURE option. The user will be given the coordinates of each node in the user subroutine.

The specification of initial conditions in coupled stress partially saturated flow problems with gravity is not always trivial (see **Element Technology** (page L5.2) for more information).

The *DFLOW option allows the outward normal flow velocity, v_n , to be prescribed across a surface. Complex dependencies of v_n on time and position can be coded in user subroutine **DFLOW**.

The *FLOW option defines the outward flow velocity as

$$v_n = k_s(u_w - u_w^\infty),$$

where k_s and u_w^∞ are known values. Again, complex conditions can be coded in user subroutine **FLOW**.

If large-deformation analysis is required because of the presence of large strains, the NLGEOM parameter can be included on the *STEP option.

The UNSYMM=YES parameter on the *STEP option is used automatically if the user requests steady-state analysis or any kind of partially saturated flow analysis. ABAQUS automatically uses UNSYMM=YES when fluid gravity effects are included in a step. For other unsymmetric simulations—such as using NLGEOM, nonlinear permeability, or nonassociated plastic flow—using UNSYMM=YES may improve the rate of convergence.

[Two other saturation-dependent effects can be included in partially saturated flow analysis:

The *MOISTURE SWELLING material option can be used to define saturation driven volumetric swelling (or shrinkage as negative swelling) of the solid skeleton. In this option, the reversible swelling strain is defined as a function of saturation. Anisotropic swelling can be specified by using the *RATIOS option:

$$\epsilon_{ii}^{ms} = r_{ii} \frac{1}{3} \left(\epsilon^{ms}(s) - \epsilon^{ms}(s^I) \right).$$

The *GEL material option can be used to define the growth of gel particles that swell and trap fluid. The growth of the gel particles depends on the saturation of the wetting fluid, the size of the gel particles, and their number per unit of volume of porous material.

An example of the use of these options is given in **Dry Problems** (page L6.3) of these notes.]

Examples

Fully Saturated Example

We consider the one-dimensional Terzaghi consolidation problem. The problem is treated with and without finite-strain effects for illustration.

A body of soil is confined by impermeable, smooth, rigid walls on all but the top surface where perfect drainage is possible, and a load is applied suddenly. Gravity is neglected.

We wish to predict the response of the soil as a function of time, following the load application.

The properties of the soil are described in Benchmark Problem 1.14.1.

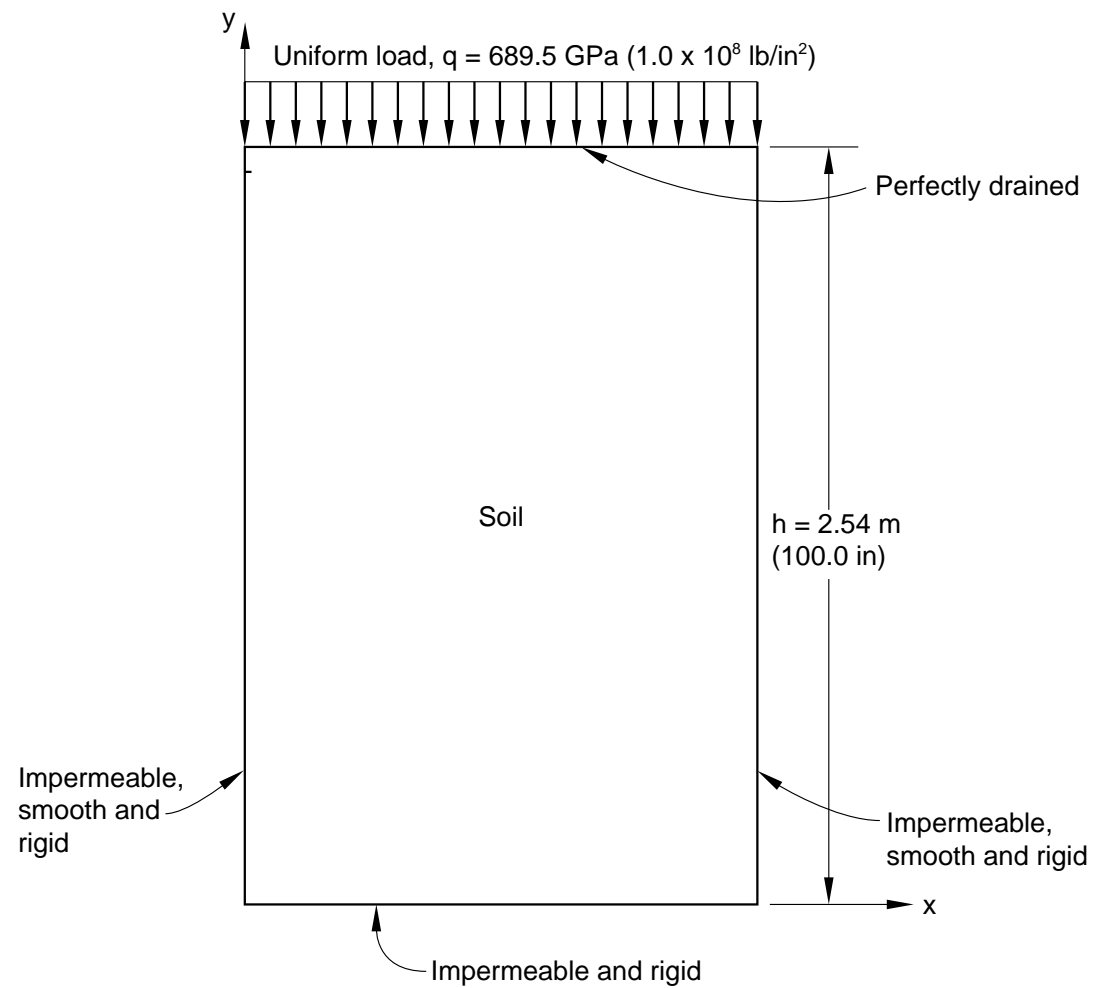
The problem is run in two steps. The first step is a *SOILS, CONSOLIDATION analysis with an arbitrary time period, with no drainage allowed across the top surface (natural boundary condition).

This establishes the initial solution: uniform pore pressure equal to the load throughout the body, with no effective stress carried by the soil skeleton.

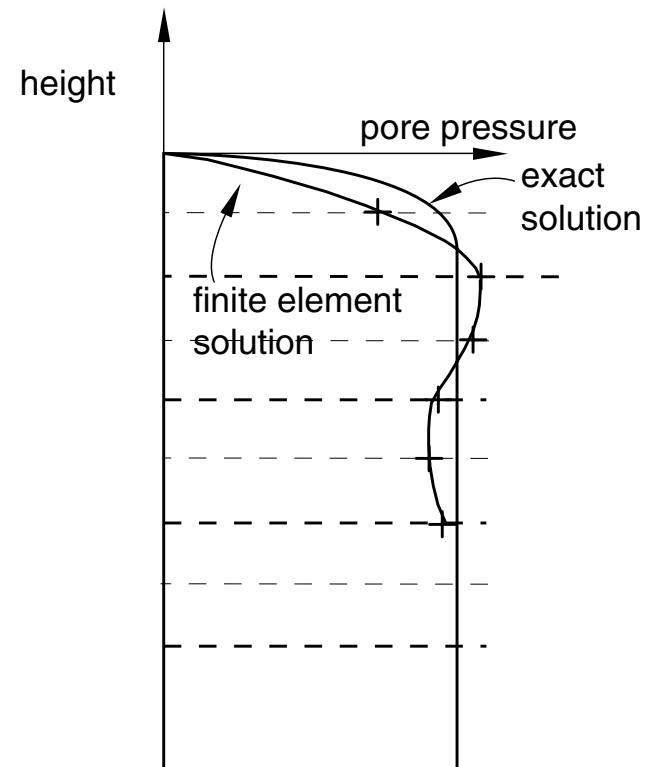
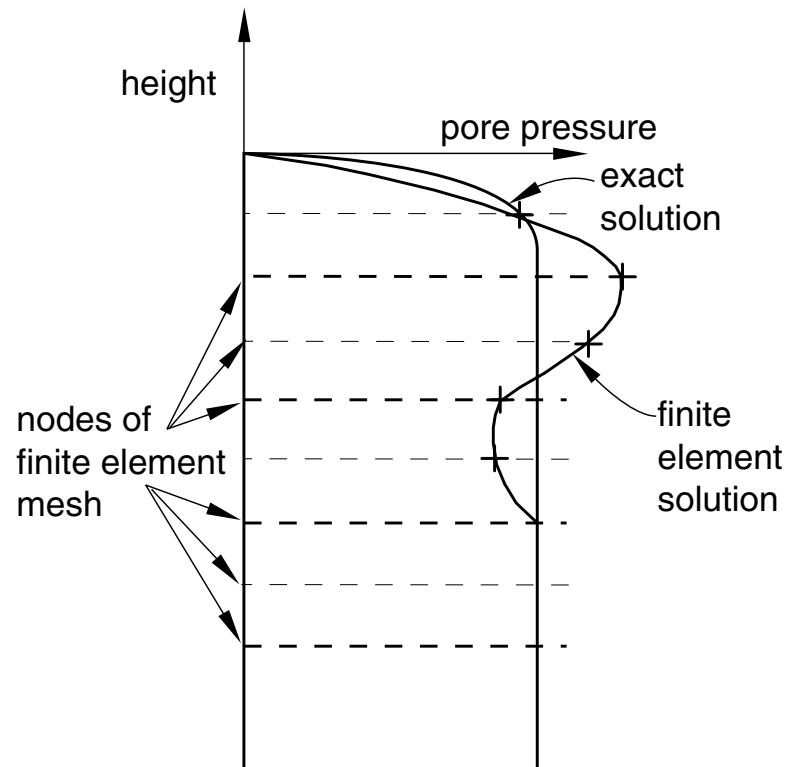
The consolidation is now done with a second *SOILS, CONSOLIDATION step, using automatic time incrementation. The accuracy of the time integration for the second step is controlled by the parameter UTOL.

The spatial element size and the time increment size are related, to the extent that time increments smaller than a certain size give no useful information. This coupling of the spatial and temporal approximations is most obvious at the start of diffusion problems, immediately after prescribed changes in the boundary values.

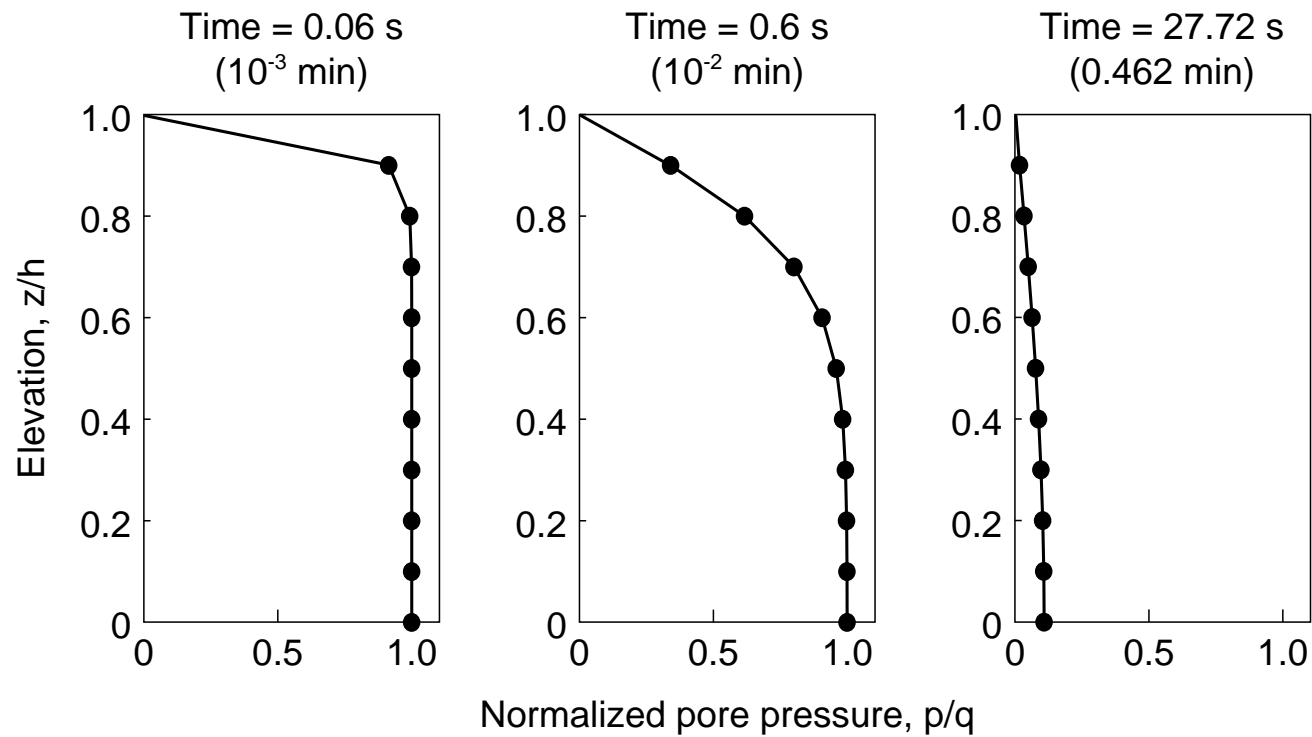
Using the time-space criterion described earlier, an initial time increment of .06 sec (0.001 min) is chosen. This gives an initial solution with no “overshoot.”



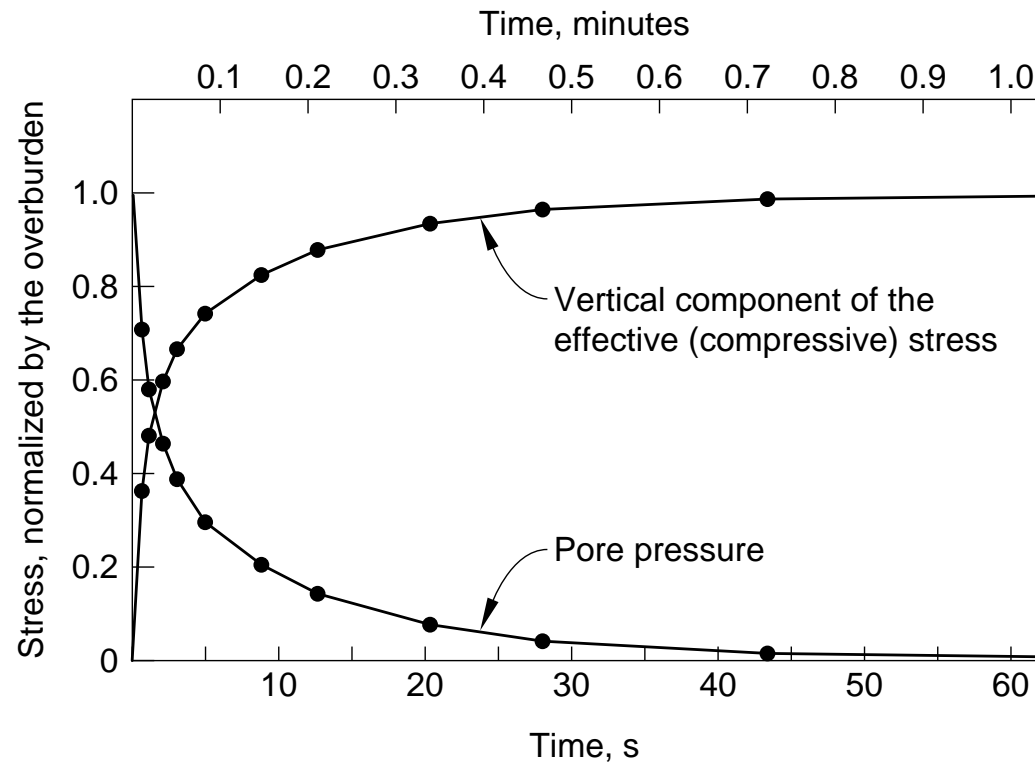
Terzaghi Problem



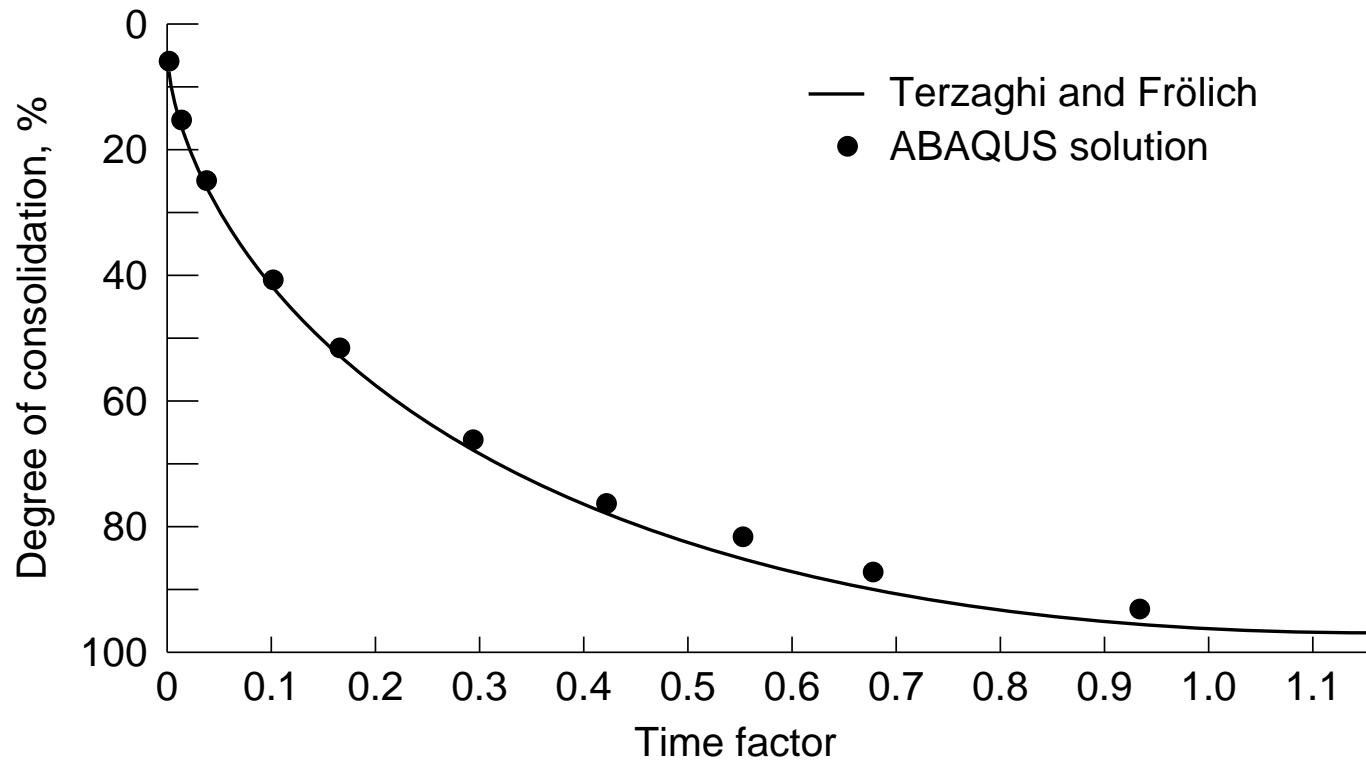
“Overshooting”



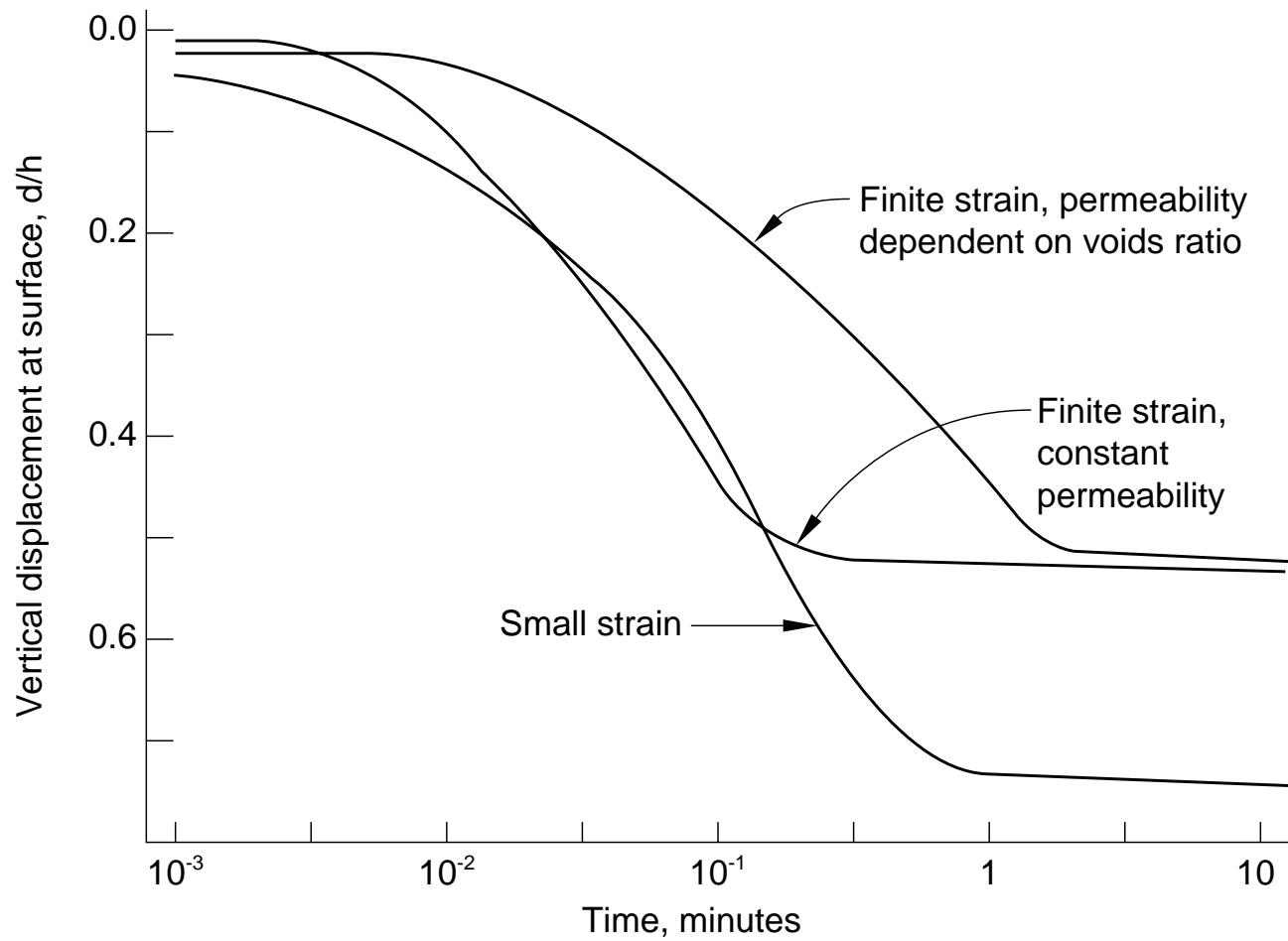
Pore Pressure History



Effective Stress History



Consolidation History



Consolidation History



Input Listing:

```
*HEADING
  TERZAGHI  CONSOLIDATION
*ELEMENT,TYPE=CPE8P,ELSET=ONE
1,1,3,23,21,2,13,22,11
*ELGEN,ELSET=ALL
1,10,20
*ELSET,ELSET=P1
6,7,8
*NODE
1,
2,25.
3,50.
201,,100.
202,25.,100.
203,50.,100.
*NGEN,NSET=NALL
1,201,10
2,202,20
3,203,10
```



```
*NSET,NSET=FILE
141,
*NSET,NSET=TOP
201,202,203
*NSET,NSET=BASE
1,2,3
*SOLID SECTION,MATERIAL=A1,ELSET=ALL
*MATERIAL,NAME=A1
*ELASTIC
1.E8,.3
*PERMEABILITY
.0002
*INITIAL CONDITIONS,TYPE=RATIO
NALL,1.1,0.,1.1,1.
*BOUNDARY
BASE,1,2
NALL,1
*RESTART,WRITE,FREQUENCY=999
*STEP
    SUDDENLY APPLIED LOAD
*SOILS,CONSOLIDATION
1.E-7,1.E-7
```



```
*DLOAD
10,P3,1.E8
*PRINT,RESIDUAL=NO
*EL PRINT,FREQUENCY=999
COORD
S
*EL PRINT,ELSET=P1,FREQUENCY=10
S
*NODE PRINT,FREQUENCY=5
U,POR,RVT
*END STEP
*STEP,INC=100
  CONSOLIDATE
*SOILS,CONSOLIDATION,UTOL=5.E7,END=SS
.001,100.,.001,100.,100.
*BOUNDARY
TOP,8
*NODE FILE,NSET=FILE
U,POR
*EL FILE,ELSET=ONE
S
*END STEP
```

Partially Saturated Example

We consider a one-dimensional “wicking” test where the absorption of fluid takes place against the gravity load caused by the weight of the fluid.

In such a test fluid is made available to the material at the bottom of a column and the material absorbs as much fluid as the weight of the rising fluid permits.

The material properties and initial conditions are described in Section 1.8.3 of the ABAQUS Benchmarks Manual.

The weight is applied by GRAV loading.

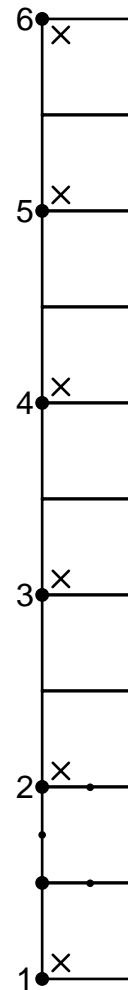
An initial step of *GEOSTATIC analysis is performed to establish the initial equilibrium state; the initial conditions in the column exactly balance the weight of the fluid and dry material so that no deformation or fluid flow takes place.

The bottom of the column is then exposed to fluid by prescribing zero pore pressure (corresponding to full saturation) at those nodes during a transient *SOILS, CONSOLIDATION step.

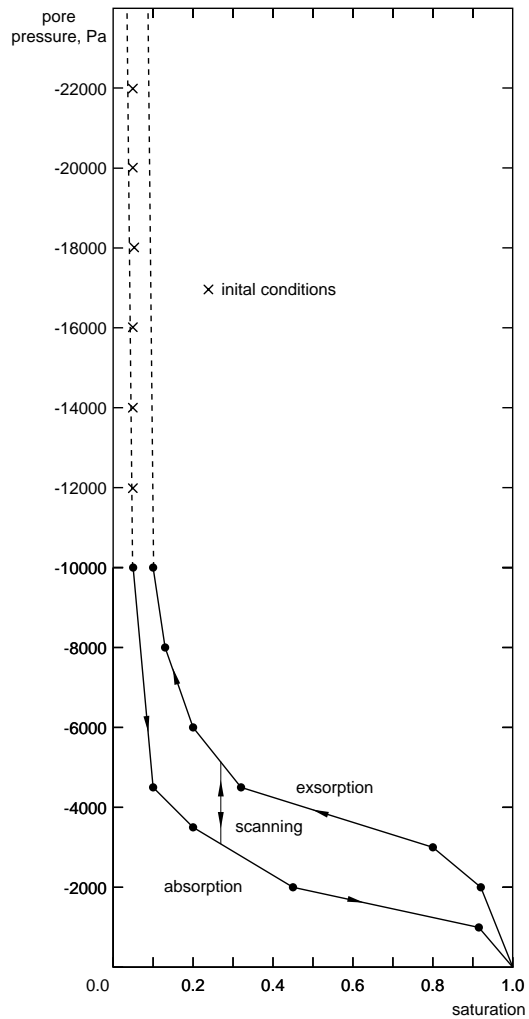
The fluid will seep up the column until the pore pressure gradient is equal to the weight of the fluid, at which time equilibrium is established.

At steady state the pore pressure gradient must equal the weight of the fluid so that pore pressure varies linearly with height and saturation varies in the same way (according to the absorption behavior) with respect to pressure or height.

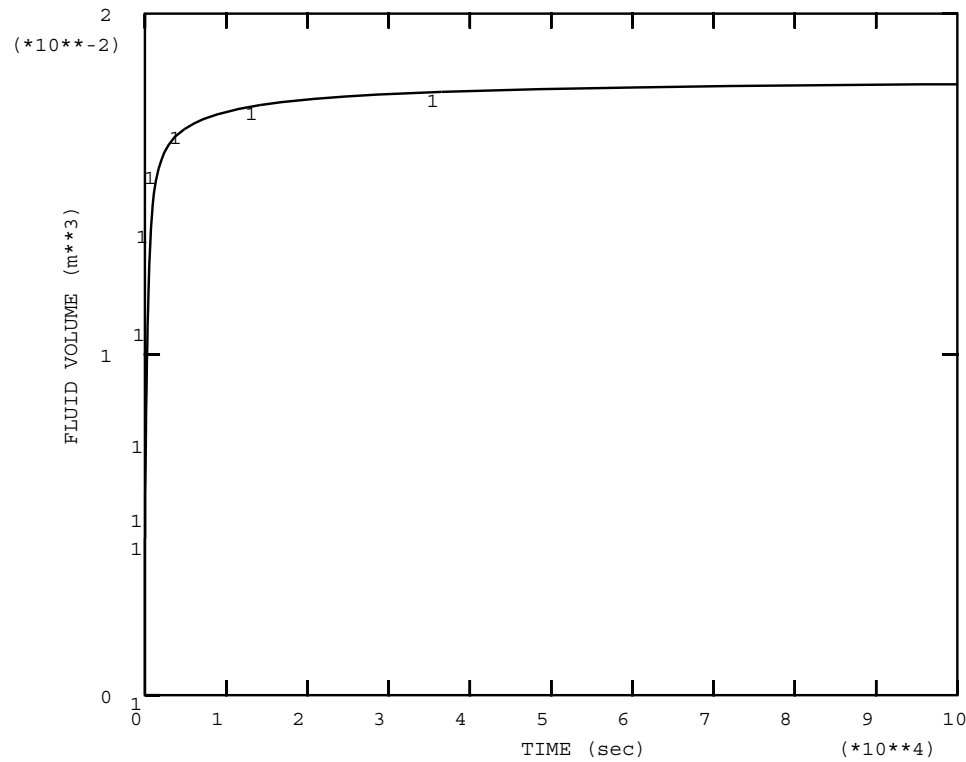
Thus, points close to the bottom of the column are fully saturated, while those at the top are still at 5% saturation. This is illustrated in the last figure, which is nothing more than the absorption curve.



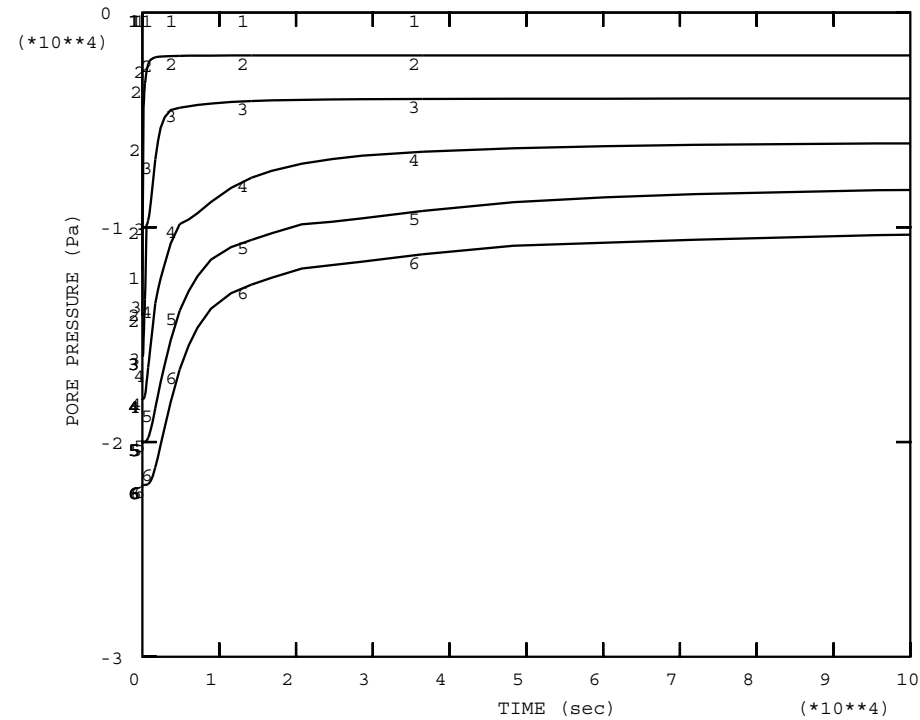
Wicking Model



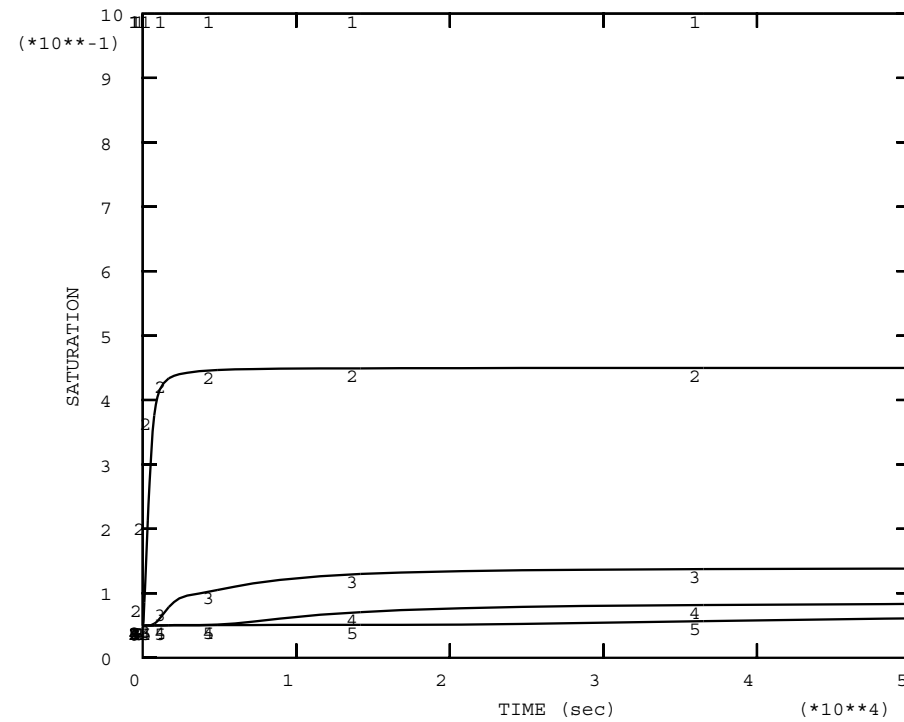
Initial Conditions



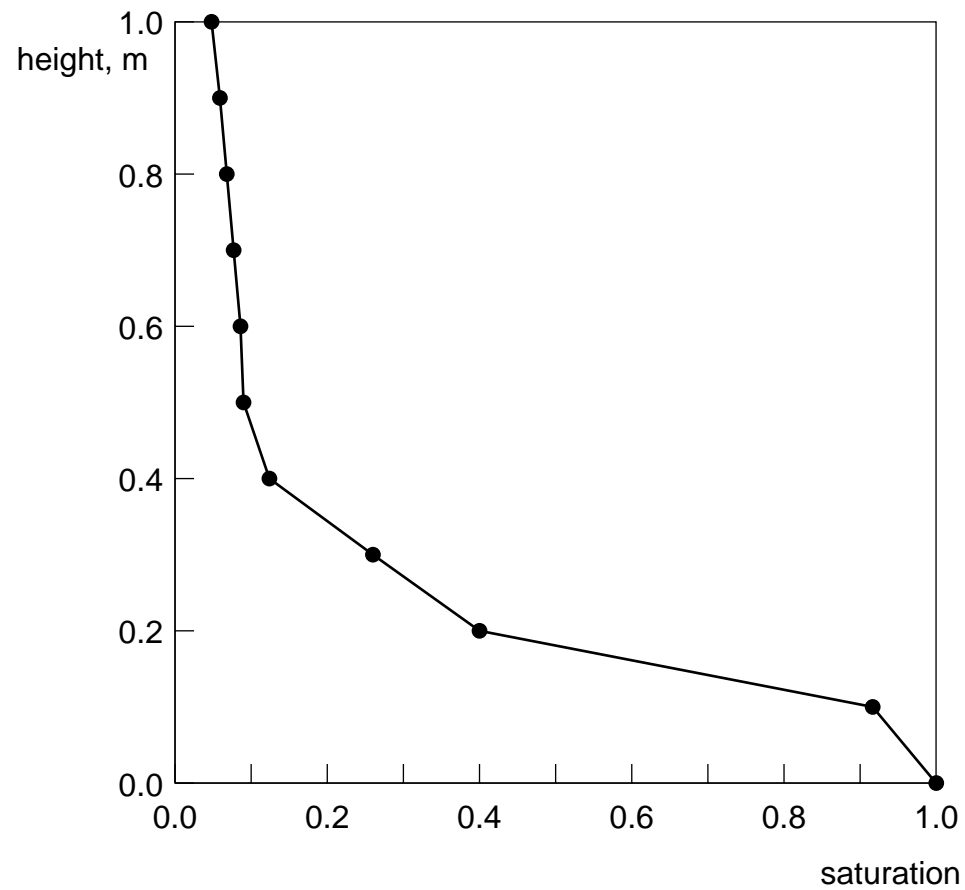
Fluid Volume Absorbed



Pore Pressures



Saturation Histories



Steady-State Profile

Input Listing:

```
*HEADING
ONE DIMENSIONAL WICKING PROBLEM, COUPLED
*** UNITS: M, TON, SEC, KN
*NODE,NSET=ALLN
1,0.,0.
3,.1,0.
101,0.,1.
103,.1,1.
*NGEN,NSET=BOT
1,3,1
*NGEN,NSET=TOP
101,103,1
*NFILL,NSET=ALLN
BOT,TOP,20,5
*NSET,NSET=LHS,GENERATE
1,101,5
*NSET,NSET=RHS,GENERATE
3,103,5
*NSET,NSET=POREP,GENERATE
1, 101, 10
```



```
3, 103, 10
*ELEMENT,TYPE=CPE8RP,ELSET=BLOCK
1,1,3,13,11,2,8,12,6
*ELGEN,ELSET=BLOCK
1,10,10,1
*ELSET,ELSET=OUTE
1,3,5,7,9
*SOLID SECTION,ELSET=BLOCK,MATERIAL=CORE
*MATERIAL,NAME=CORE
*ELASTIC
50.,0.
*DENSITY
.1
*POROUS BULK MODULI
,2.E6
*PERMEABILITY,SPECIFIC=10.
3.7E-4
*SORPTION
-100.,.04
-10.,.05
-4.5,.1
-3.5,.18
```



```
-2.,.45
-1.,.91
0.,1.
*SORPTION,TYPE=EXSORPTION
-100.,.09
-10.,.1
-8.,.11
-6.,.18
-4.5,.33
-3.,.79
-2.,.91
0.,1.
*INITIAL CONDITIONS,TYPE=SATURATION
ALLN,.05
*INITIAL CONDITIONS,TYPE=PORE PRESSURE
POREP, -22.0, 1.0, -12.0, 0.0
*INITIAL CONDITIONS,TYPE=RATIO
ALLN,5.
*INITIAL CONDITIONS,TYPE=STRESS,GEOSTATIC
BLOCK,-1.1,1.,-2.016666667,0.,0.,0.
*EQUATION
2
```



```
3,8,1.,1,8,-1.
*BOUNDARY
ALLN,1
BOT,2
*RESTART,WRITE,FREQUENCY=10
*STEP,INC=1
*GEOSTATIC
1.E-6,1.E-6
*BOUNDARY
1,8,, -12.
*DLOAD
BLOCK, GRAV, 10., 0., -1., 0.
*NODE PRINT, FREQUENCY=5, NSET=LHS
U, RF, POR, RVT
*EL PRINT, FREQUENCY=5, POSITION=AVERAGED AT NODES
S, E
SAT, POR, VOIDR
*NODE FILE, FREQUENCY=10, NSET=LHS
U, RF, POR, RVT
*EL FILE, FREQUENCY=10, ELSET=OUTE
S, E
SAT, POR, VOIDR
```



```
*END STEP
*STEP, INC=100
*SOILS, CONSOLIDATION, UTOL=20.
1., 1000000.
*BOUNDARY
1, 8, , 0.
*CONTROLS, ANALYSIS=DISCONTINUOUS
*CONTROLS, PARAMETERS=FIELD, FIELD=DISPLACEMENT
, 1.,
*CONTROLS, PARAMETERS=FIELD, FIELD=PORE FLUID PRESSURE
, 1.,
*END STEP
```


Lecture 5

Modeling Aspects

Overview

- Element Technology
- Infinite Domains
- Pore Fluid Surface Interactions
- Element Addition and Removal

Modeling issues related to geotechnical problems are considered in this lecture.

Element Technology

The geotechnical constitutive models can be used in plane strain, generalized plane strain, axisymmetry, and three dimensions. All Drucker-Prager models are also available in plane stress, except for the linear Drucker-Prager model with creep.

Cylindrical (CCL) elements are available for modeling structures that are initially circular but are subjected to general, nonaxisymmetric loading. An example is the analysis of a pile foundation where the pile is subjected to axial, horizontal and moment loading.

These elements permit a coarse yet accurate discretization of a structure.

They can be used in contact calculations using the standard surface-based contact modeling approach.

They provide an attractive alternative to axisymmetric-asymmetric (CAXAxxN) family of elements.



The analysis of flow through porous media in ABAQUS is available for plane strain, axisymmetric, axisymmetric-asymmetric, and three-dimensional problems. Special coupled displacement/pore pressure elements must be used: these elements have a linear distribution of pore pressure and either a first-order or a second-order distribution of displacement.

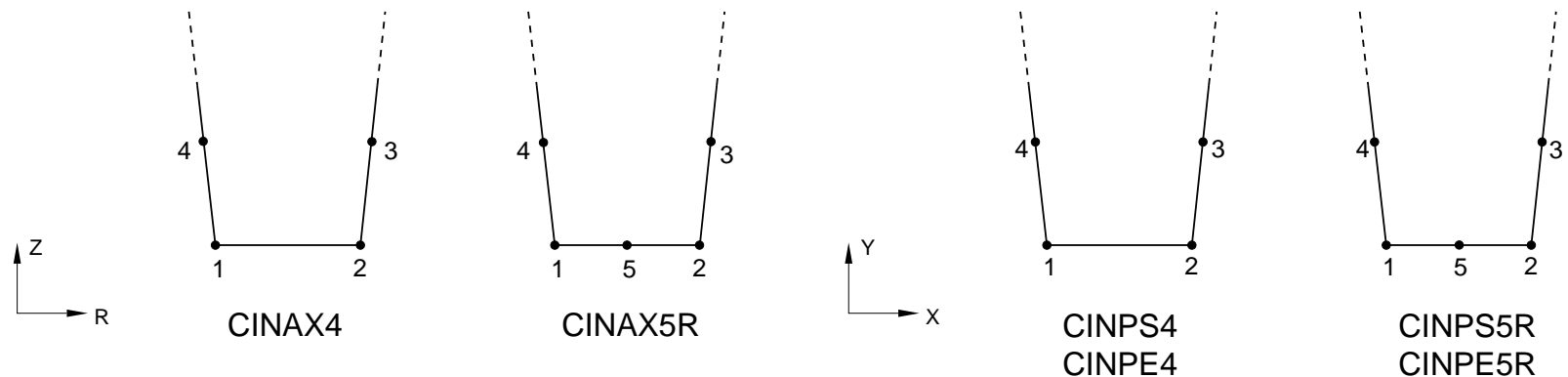
The modified tetrahedral element C3D10MP(H) is particularly well suited for meshing general, complex structures in three dimensions. The element works well in contact interactions.

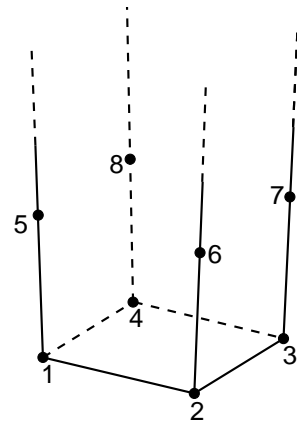
The geotechnical material models can be used in time integration dynamic analysis. Eigenfrequencies of undamped models can also be extracted before or after static deformation.

Infinite Domains

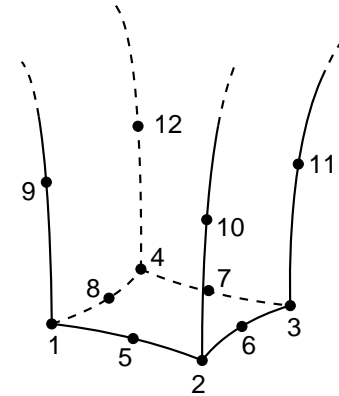
Infinite elements for stress analysis are available in ABAQUS; these are used in conjunction with the standard elements in problems involving infinite or very large domains.

A family of first- and second-order axisymmetric, planar, and three-dimensional infinite elements is available.

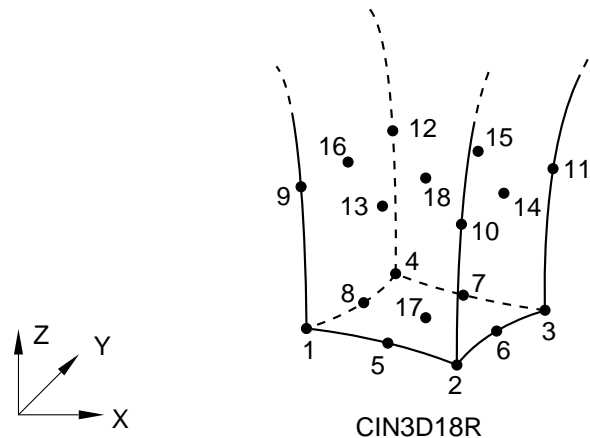




CIN3D8



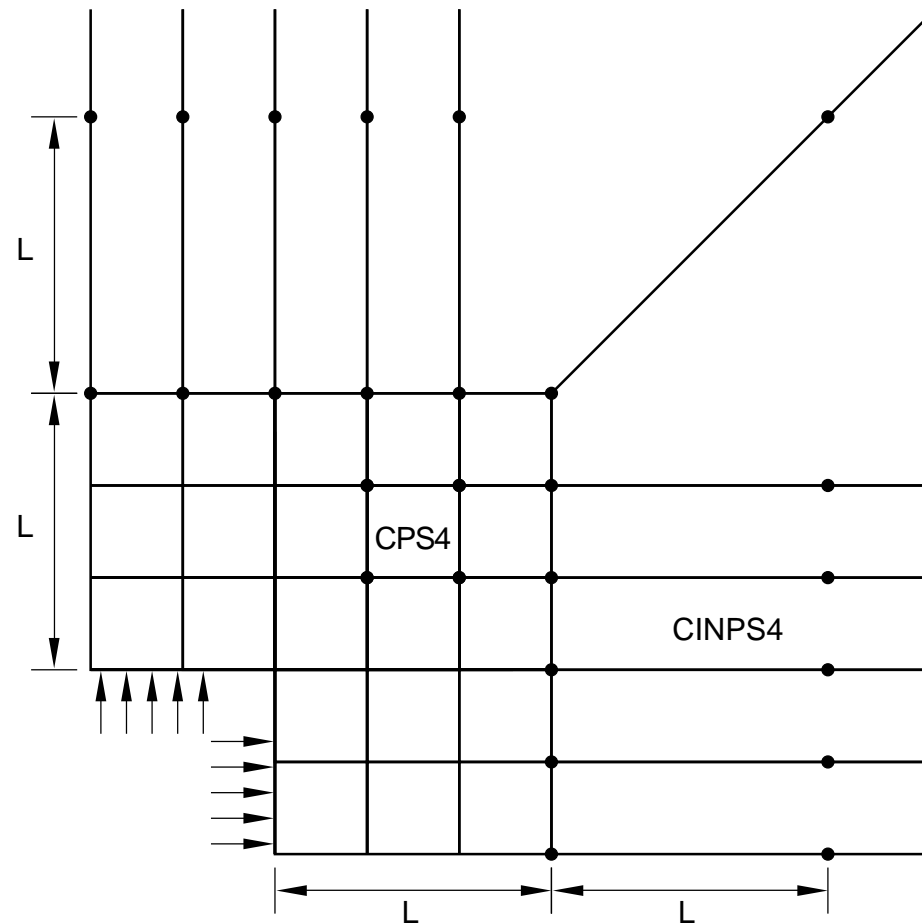
CIN3D12R

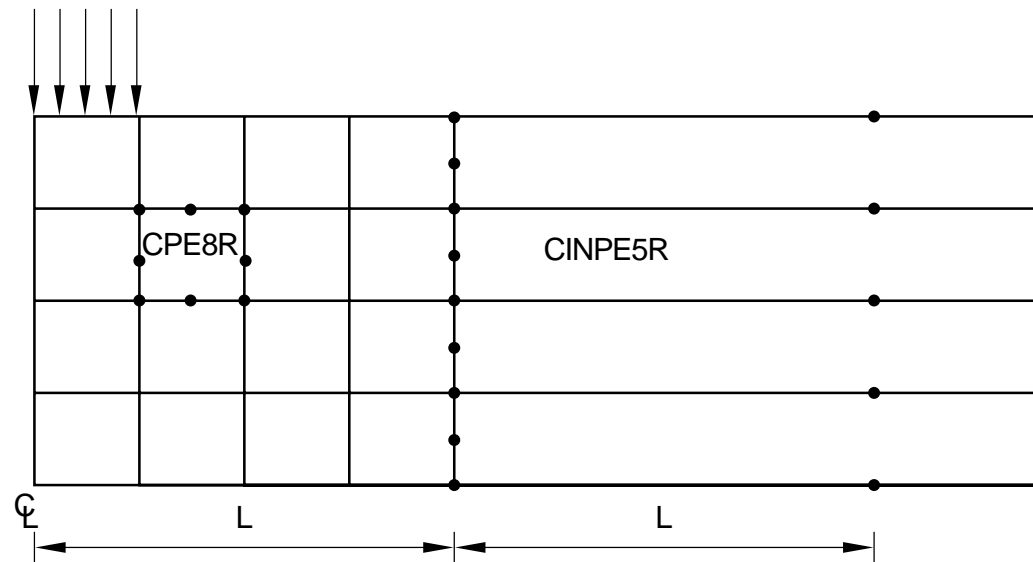


CIN3D18R

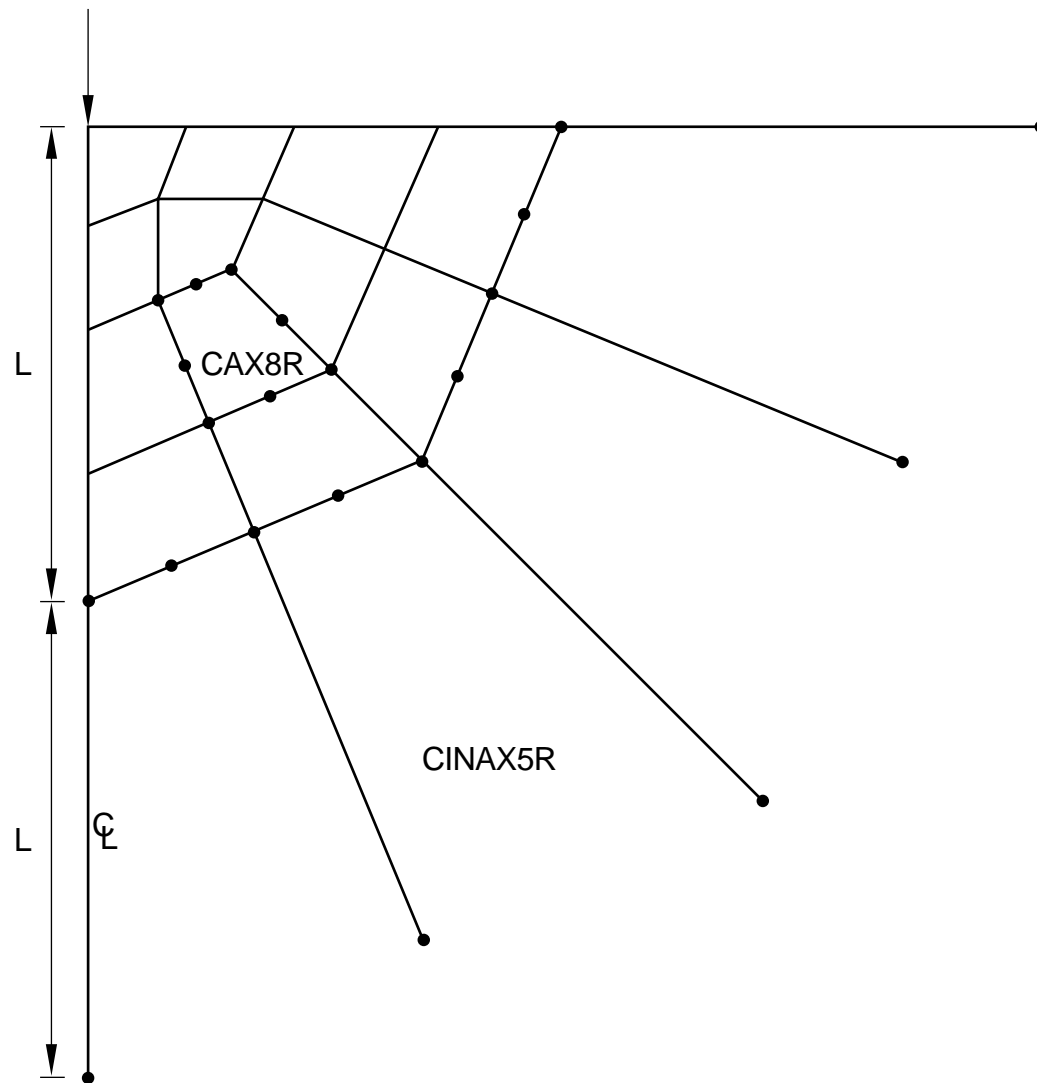
Standard finite elements are used to model the region of interest, with the infinite elements modeling the far-field region.

The solution in the far field is assumed to be linear, so only linear behavior is provided in the infinite elements.





The static behavior of the infinite elements is based on modeling the basic solution variable, u (in stress analysis u is a displacement component), with respect to spatial distance r measured from a “pole” of the solution, so that $u \rightarrow 0$ as $r \rightarrow \infty$, and $u \rightarrow \infty$ as $r \rightarrow 0$. The interpolation provides terms of order $1/r$, $1/r^2$. The far-field behavior of many common cases, such as a point load on a half-space, is thereby included.

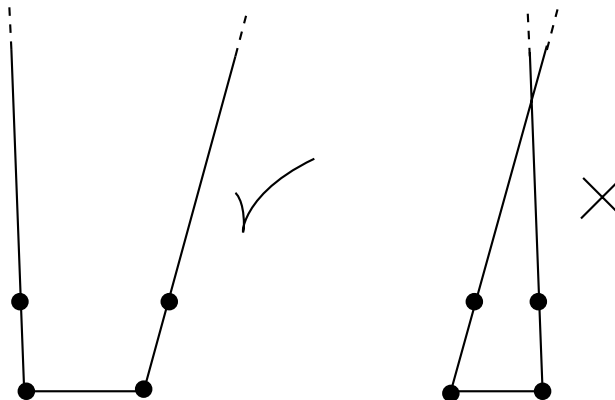


It is important to make an appropriate choice of the position of the nodes in the infinite direction with respect to the origin (“pole”) of the far-field solution.

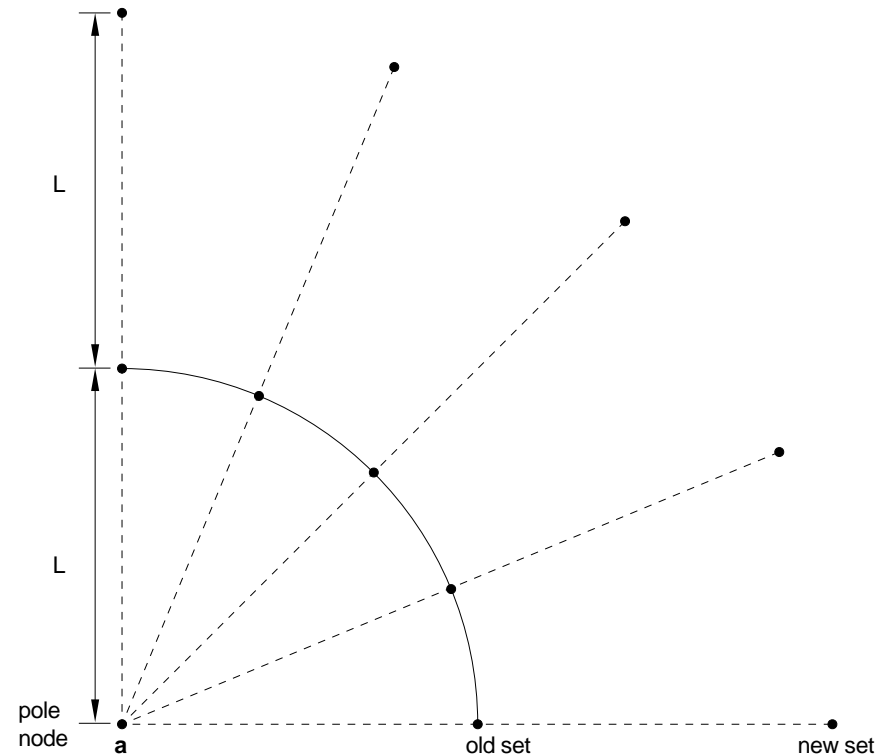
For example, the solution for a point load applied to the boundary of a half-space has its pole at the point of application of the load.

The second node along each infinite element edge pointing in the infinite direction must be positioned so that it is twice as far from the pole as the node on the same edge at the boundary between the finite and the infinite elements.

In addition, be careful when specifying the second nodes in the infinite direction so that the element edges in the infinite direction do not cross over.



The *NCOPY, POLE option provides a convenient way of defining these second nodes in the infinite direction.



*NCOPY, POLE option



In plane stress and plane strain problems in which the loading is not self-equilibrating, the far-field displacement solution is typically of the form $u = \ln(r)$. This implies the displacement approaches infinity as $r \rightarrow \infty$.

Infinite elements can still be used for such cases, provided the displacement results are treated as having an arbitrary reference value.

Thus, strain, stress, and *relative* displacements within the finite element part of the model will converge to unique values as the model is refined; the *total* displacements will depend on the size of the region modeled with finite elements.

If the loading is self-equilibrating, the total displacements will also converge on a unique solution.



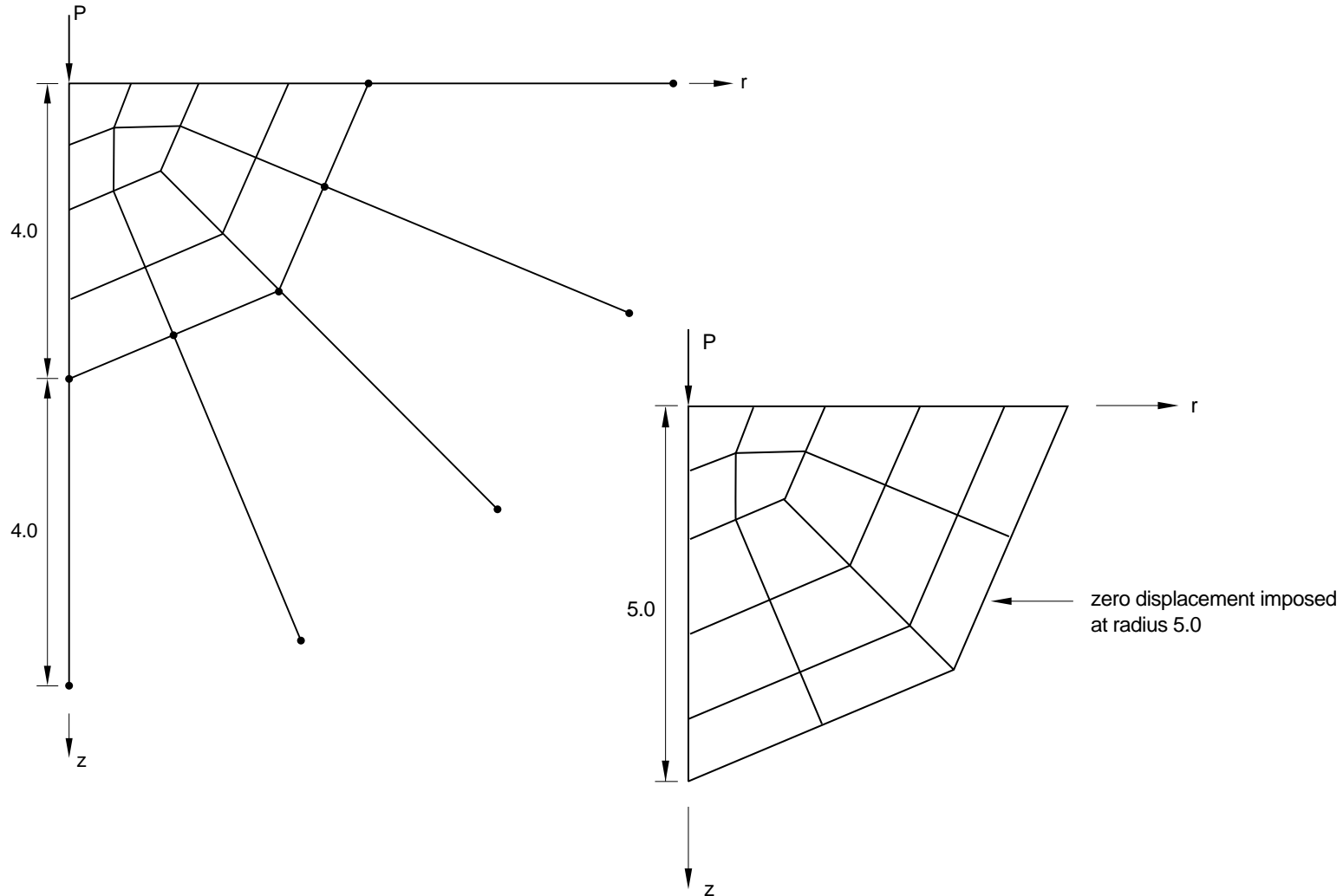
In many geotechnical problems, an initial stress field and a corresponding body force field must be defined.

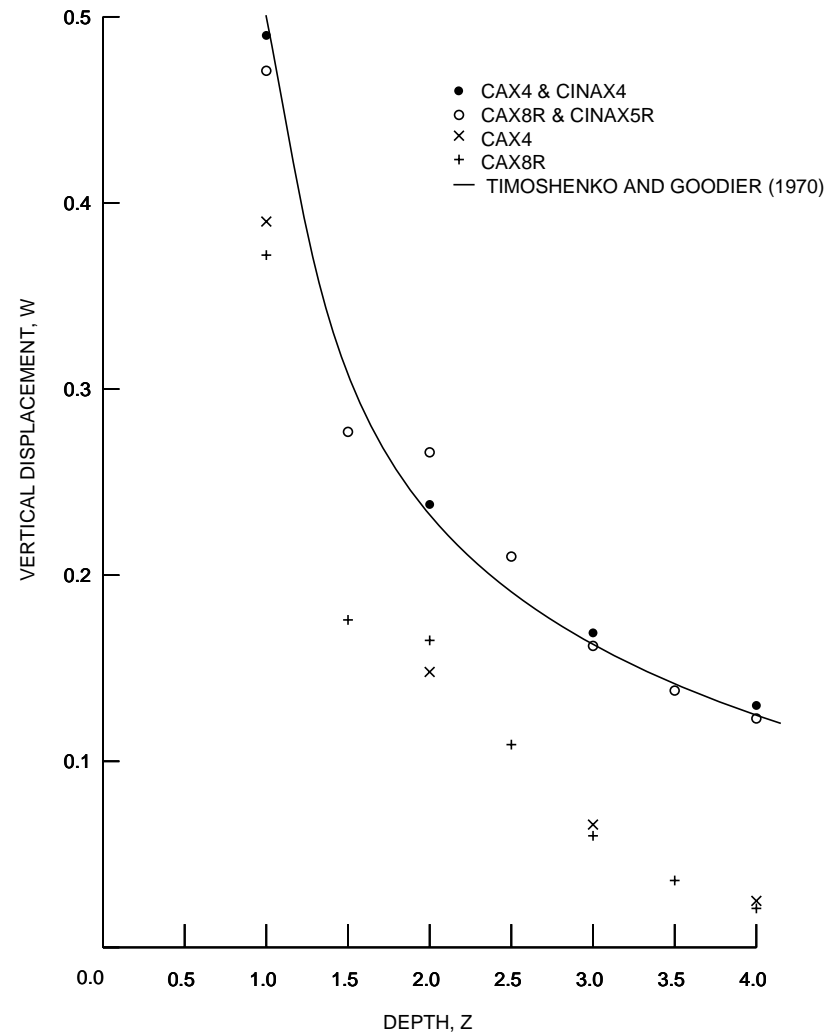
For standard elements, the initial stress field is given in `*INITIAL CONDITIONS, TYPE=STRESS`, and the corresponding body force in the `*DLOAD` option. ABAQUS checks for equilibrium in the initial state (`*GEOSTATIC` step) at the start of the analysis.

For infinite elements, the body force cannot be defined (the elements are infinite). Therefore, ABAQUS automatically inserts forces at the nodes of the infinite elements that cause those nodes to be in equilibrium at the start of the analysis. These forces remain constant throughout the analysis.

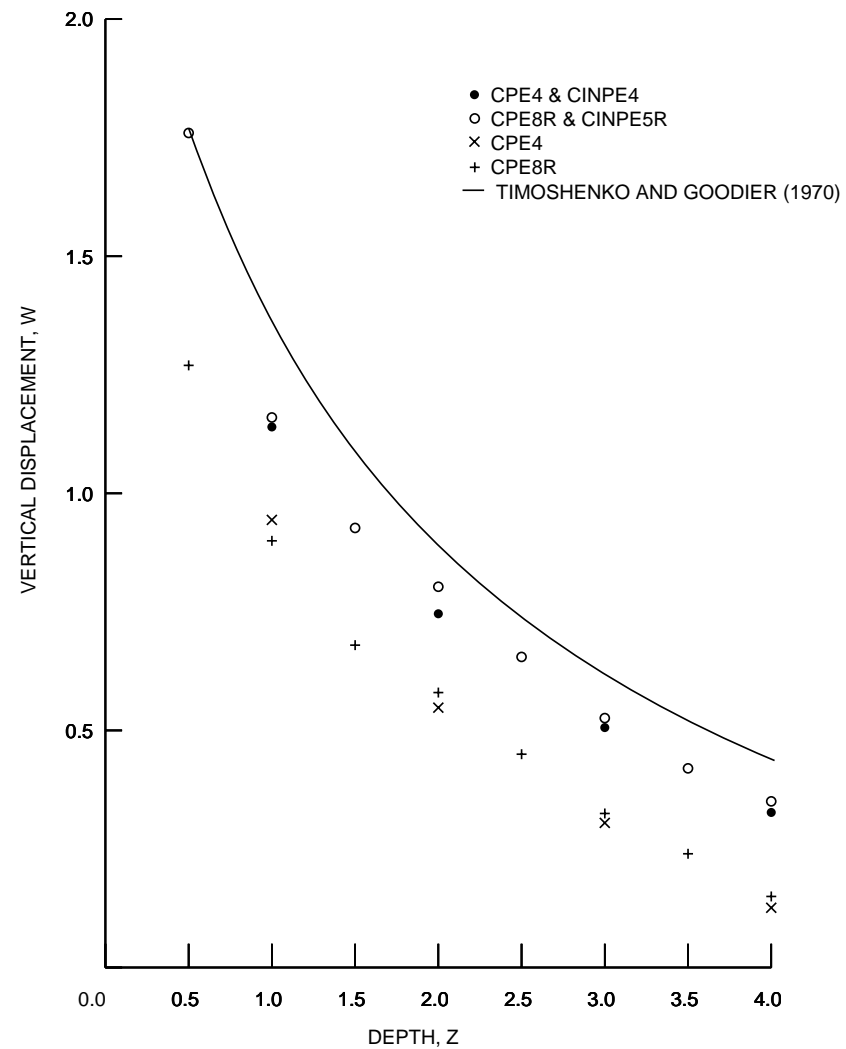
This allows the initial geostatic stress field to be defined in the infinite elements but provides no check on the reasonableness of that stress field. The user must ensure that, when infinite elements are used in conjunction with an initial stress condition, the first analysis step must be a `*GEOSTATIC` step.

The Boussinesq (point load on a half-space) and Flamant (line load on a half-space) problems:





Boussinesq Problem – Displacement Results (Benchmark Problem 2.2.2)



Flamant Problem – Displacement Results (Benchmark Problem 2.2.2)



Input Listing for Boussinesq Problem:

```
*HEADING
BOUSSINESQ PROBLEM, 12 CAX4 + 4 CINAX4
*NODE
1,0.,0.
4,0.,-1.
8,1.,0.
6,.75,-.75
21,0.,-2.
25,0.,-4.
101,2.,0.
105,4.,0.
61,1.5,-1.5
65,2.833333333,-2.833333333
*NGEN
21,25,2
61,65,2
101,105,2
21,61,20
23,63,20
25,65,20
```




```
61,101,20
63,103,20
65,105,20
*NSET,NSET=INTER,GENERATE
25,105,20
*NCOPY,OLD SET=INTER,CHANGE NUMBER=2,POLE,NEW SET=FAR
1
*NSET,NSET=LHS,GENERATE
1,4,3
21,27,2
*ELEMENT,TYPE=CAX4,ELSET=ALL
1,4,6,8,1
2,21,41,6,4
3,41,61,81,6
4,81,101,8,6
5,23,43,41,21
*ELGEN,ELSET=ALL
5,4,20,1,2,2,4
*ELEMENT,TYPE=CINAX4,ELSET=ALL
13,45,25,27,47
14,65,45,47,67
15,85,65,67,87
```



```
16,105,85,87,107
*SOLID SECTION,ELSET=ALL,MATERIAL=ONE
*MATERIAL,NAME=ONE
*ELASTIC
1.,.1
*BOUNDARY
LHS,1
*STEP
*STATIC
*CLOAD
1,2,-1.
*NODE FILE,NSET=LHS
U
*END STEP
```



In direct integration dynamic response analysis (*DYNAMIC) and in *STEADY STATE DYNAMICS, DIRECT frequency domain analysis, the elements provide “quiet” boundaries to the finite element model.

This means that they maintain the static force that was present at the start of the dynamic response analysis on the finite/infinite boundary.

As a consequence the far-field nodes in the infinite elements will not displace during the dynamic response (there is no dynamic response within the infinite elements).

The infinite elements will provide additional normal and shear tractions on the boundary, proportional to the normal and shear components of the velocity of the boundary.

The concept is simple. Consider one-dimensional wave propagation down the x -axis.

Equilibrium is

$$-\rho \ddot{u} + \frac{d\sigma}{dx} = 0.$$

The constitutive behavior is assumed to be linear elastic, and we also assume small deformation:

$$\sigma = E\varepsilon = E \frac{du}{dx}.$$

Combining,

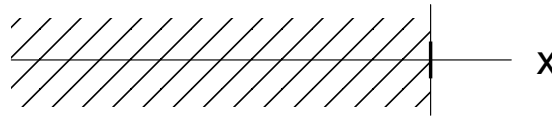
$$-\rho \ddot{u} + E \frac{d^2 u}{dx^2} = 0.$$

The general solution to this wave equation has the form

$$u = f(x \pm ct),$$

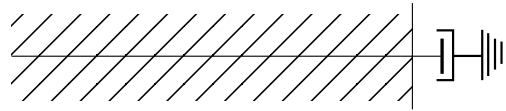
where $c = \sqrt{\frac{E}{\rho}}$ is the wave speed and f is any function. A wave traveling to the right (x increasing) has the form $u = f_1(x - ct)$; one traveling to the left is $f_2(x + ct)$.

Suppose we have a boundary to the right of the domain:



If an incident wave, $u_I = f_I(x - ct)$ approaches this boundary, we want no reflection, $u_R = f_R(x + ct)$, to occur.

For this purpose we introduce a dashpot at the boundary:



so that, at the boundary, $\sigma = -d\dot{u}$.

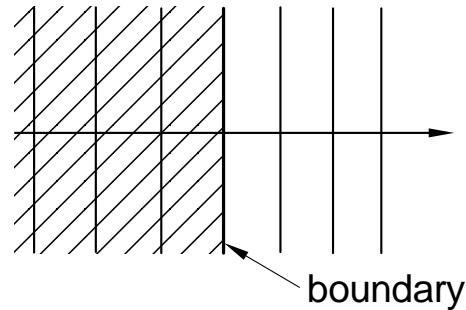
For both $u_I = f_I(x - ct)$ and $u_R = f_R(x + ct)$, at the boundary

$$\begin{aligned}\sigma &= E(f_I' + f_R') \text{ from elasticity} \\ &= d(-cf_I' + cf_R') \text{ for the dashpot.}\end{aligned}$$

Thus, $(E - dc)f_I' + (E + dc)f_R' = 0$. But, we want $f_R = 0$, so $f_R' = 0$.

This is always achieved if we choose $d = \frac{E}{c} = \rho c$.

This boundary damping is thus chosen to eliminate the reflection of wave energy back into the finite element mesh when plane waves cross the plane boundary:



Lysmer and Kuhlemeyer (1969) generalized this for 3-D cases, with damping of the normal velocity of the boundary:

$$d_p = \rho c_p = \rho \sqrt{\frac{\lambda + 2G}{\rho}},$$

and damping of the shear velocity:

$$d_s = \rho c_s = \rho \sqrt{\frac{G}{\rho}},$$

where c_p , c_s are the dilatational (pressure) and shear wave speeds, ρ is the mass density of the material, and λ , G are Lamé's constants:

$$\lambda = \frac{Ev}{(1 + \nu)(1 - 2\nu)}, \quad G = \frac{E}{2(1 + \nu)}.$$

This approach assumes that the material behavior close to the finite/infinite boundary is linear elastic (which is reasonable since the infinite elements are also assumed to be elastic).



Since, during dynamic analysis, the elements hold the static stress on the boundary constant but do not provide any stiffness, some rigid body motion of the region modeled will generally occur. This effect is usually small.

The elements are based on eliminating energy transmission for plane waves crossing a parallel plane boundary. Therefore, the ability of the elements to transmit energy out of the finite element mesh without trapping or reflecting it is optimized by making the finite/infinite boundary as close as possible to being orthogonal to the direction from which the waves will impinge on this boundary, and far enough from the detailed part of the mesh to be considered relatively plane.

Close to a free surface where Rayleigh waves may be important or to a material interface where Love waves may be important, the elements are most effective if they are orthogonal to this surface.

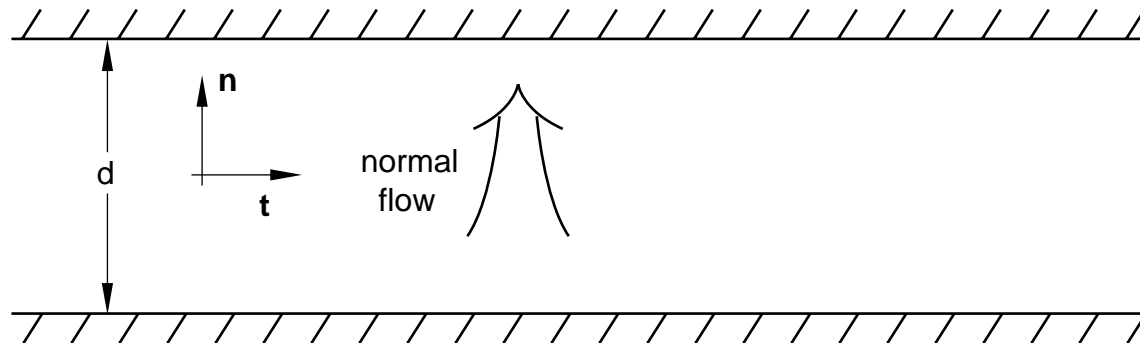
The elements do not provide any contribution to eigenmode-based analysis procedures.

A dynamic example is presented in **Dry Problems** (page L 6.3).

Pore Fluid Surface Interactions

The standard contact options offered in ABAQUS for stress analysis can be used for geotechnical applications. Their theory and usage is discussed in the Contact lecture notes.

The flow pattern is shown below:



Two configurations are possible:

1. Pore pressure continuum elements on either side of the interface.
2. Pore pressure elements on one side and “regular” elements on the other. This models fluid interaction with an impermeable surface.

The pore pressure is assumed to be continuous across the interface, regardless of whether the element is open or closed.

The contact condition is based on effective stress. Hence, contact points may open as the pore pressure increases (in a case where the total stress is constant and the effective stress decreases due to the pore pressure increase).

It is assumed that no fluid flow takes place tangential to the contact surface. In steady-state analysis, this implies that fluid that flows out of one side flows into the other side. In transient analysis, the flow into the interface is balanced with the rate of separation of the sides of the interface.

In a consolidation analysis fluid volume between the surfaces is considered when balancing the flow from each surface. The fluid in the interface is assumed incompressible.

Geostatic States of Stress

In most geotechnical problems, a nonzero state of stress exists in the medium. This typically consists of a vertical stress increasing linearly with depth, equilibrated by the weight of the material, and horizontal stresses caused by tectonic effects.

The active loading is applied on this initial stress state. Active loading could be the load on a foundation or the removal of material during an excavation.

It is clear that, except for purely linear analysis, with a different initial stress state, the response of the system would be different.

This well illustrates a point of nonlinear analysis: the response of a system to external loading depends on the state of the system when that loading sequence begins (and, by extension, to the sequence of loading). We can no longer think of superposing load cases as we do in linear analysis.

ABAQUS provides the *GEOSTATIC procedure to allow the user to establish the initial stress state.

The user will normally specify the initial effective stresses using *INITIAL CONDITIONS, TYPE=STRESS, GEOSTATIC and in the first step of analysis, apply the body (gravity) loads corresponding to the weight of the material.

Ideally, the loads and initial stresses should exactly equilibrate and produce zero deformations. However, in complex problems, it may be difficult to specify initial stresses and loads that exactly equilibrate.

The *GEOSTATIC procedure is used to reestablish initial equilibrium if the loads and initial stresses specified are not in equilibrium. It will also produce deformations while doing this.

If the deformations produced are significant compared to the deformations caused by subsequent loading, the definition of the initial state should be reexamined.

In a coupled deformation/flow analysis the *GEOSTATIC procedure is equivalent to the steady-state *SOILS procedure. In these problems it is important to establish initial stress equilibrium as well as steady-state flow conditions.

In fully or partially saturated flow problems, the initial void ratio, as well as the initial pore pressure and the initial effective stress, must be defined.

The initial conditions discussion that follows is based on the total pore pressure formulation (the magnitude and direction of the gravitational loading are defined by using the GRAV *DLOAD option).

Let us assume that the z -axis points vertically upwards. We assume that, in the geostatic state, the pore fluid is in hydrostatic equilibrium, so that

$$\frac{du_w}{dz} = -\gamma_w,$$

where γ_w is the specific weight of the pore fluid.

If we also take γ_w to be independent of z (which is usually the case, since the fluid is almost incompressible), this equation can be integrated:

$$u = \gamma_w(z_w^0 - z),$$

where z_w^0 is the height of the *phreatic surface*, at which $u = 0$ and above which $u < 0$ and the pore fluid is only partially saturated.

We usually assume that there are no significant shear stresses τ_{xz} , τ_{yz} .

Then vertical equilibrium gives

$$\frac{d\sigma_{zz}}{dz} = \rho g + sn^0 \gamma_w,$$

where ρ is the dry density of the porous solid material, g is the gravitational acceleration, n^0 is the initial porosity, and s is the saturation ($0 \leq s \leq 1.0$).

The *INITIAL CONDITIONS, TYPE=STRESS, GEOSTATIC option defines the initial value of the *effective stress*, $\bar{\sigma}$, as

$$\bar{\sigma} = \sigma + su\mathbf{I}.$$

Combining this definition with the equilibrium statement in the z -direction and hydrostatic equilibrium in the pore fluid gives

$$\frac{d\bar{\sigma}_{zz}}{dz} = \rho g - \gamma_w \left(s(1 - n^0) - \frac{ds}{dz}(z_w^0 - z) \right) ,$$

using the assumption that γ_w is independent of z .

In many cases s is constant. For example, in fully saturated flow $s = 1.0$ everywhere. If we further assume that the initial porosity, n^0 , and the dry density of the porous medium, ρ , are also constant, the above equation is readily integrated to give

$$\bar{\sigma}_{zz} = (\rho g - \gamma_w s (1 - n^0))(z - z^0) ,$$

where z^0 is the position of the surface of the medium.

In more complicated cases where s , n^0 and/or ρ vary with height, the equation must be integrated in the vertical direction to define the initial values of $\bar{\sigma}_{zz}(z)$.

In partially saturated cases the initial pore pressure and saturation values must lie on or between the absorption and exsorption curves.

In many geotechnical applications there is also horizontal stress. If the pore fluid is under hydrostatic equilibrium and $\tau_{xz} = \tau_{yz} = 0$, equilibrium in the horizontal directions requires that the horizontal components of effective stress do not vary with horizontal position: $\bar{\sigma}_h(z)$ only, where $\bar{\sigma}_h$ is any horizontal component of effective stress.

The horizontal stress is typically assumed to be a fraction of the vertical stress: those fractions are defined in the x - and y -directions with the `*INITIAL CONDITIONS, TYPE=STRESS, GEOSTATIC` option. If the horizontal stress is nonzero the boundary conditions on any nonhorizontal edges of the finite element model must be fixed in the horizontal direction, or infinite elements used, so that horizontal equilibrium is maintained.

Element Addition and Removal

Practical geotechnical excavations involve a sequence of steps, in each of which some part of the material mass is removed. Liners or retaining walls may be inserted during this process. Similar situations arise in the case of building an embankment.

Thus, geotechnical problems offer an interesting perspective on the need for generality in creating and using a finite element model: the model itself, and not just its response, changes with time—parts of the original model disappear, while other components that were not originally present are added.

The need for a close liaison between the analysis and geometric modeling is important.

The *MODEL CHANGE, REMOVE, ADD option is used to allow the user to remove or add elements to the model.

While elements are inactive, any distributed loads, fluxes, flows, and foundations specified for them are also inactive. A record of these loads is still kept, and continuation of loads across steps is not affected by removal, so on reactivation these loads are still present, unless they are removed by the user. Concentrated loads or fluxes are not removed. Therefore, the user must ensure that the concentrated loads or fluxes, which are carried by elements being removed, are also removed; otherwise, a solver problem will occur (a force is applied to a degree of freedom with zero stiffness).

The nodal variables are not changed by the ***MODEL CHANGE** option. However, the user can reset these variables by using the ***BOUNDARY** option while the elements are inactive. For example, if some elements that are removed are to be reintroduced with a different displacement, an intermediate step can be used in which the displacements for the nodes on these elements are reset by a ***BOUNDARY** that is removed when the elements are reactivated.

Elements can be reactivated either

- with strain (e.g., when simulating the refueling of a nuclear reactor, where the new fuel assembly must conform to the distortion of its old neighbors)

***MODEL CHANGE, ADD=WITH STRAIN**

- without strain (e.g., when simulating the addition of a new, strain-free layer to a strained construction)

***MODEL CHANGE, ADD=STRAIN FREE**

Example Problem 1.1.10 discusses the technique further.

Lecture 6

Example Problems

Overview

- Dry Problems
 - Limit Analysis of Foundation
 - Slope Stability Problem
 - A Dynamic Analysis
- Saturated Problems
 - Consolidation Problem (Transient)
 - Dam Problem (Steady-State)

- Partially Saturated Problems
 - Demand Wettability Problem (Uncoupled)
 - Desaturation of Soil Column (Transient)
 - Phreatic Surface Calculation (Steady-State)
- Excavation and Building Analysis
 - Tunneling Problem

Dry Problems

We present problems that involve the analysis of dry media: we solve the stress deformation equations only.

Limit Analysis of Foundation

This example presents solutions to limit load calculations for a strip of sand loaded by a rigid, perfectly rough footing (Benchmark Problem 1.14.4). It compares the results obtained with different parameters used in the modified Drucker-Prager model in ABAQUS, with and without a cap, matched to the classical Mohr-Coulomb model.

We may want to match the Drucker-Prager model to Mohr-Coulomb data for various reasons:

- Creep
- Rate dependence
- Compatibility with ABAQUS/Explicit

A mesh of finite/infinite elements is used to model the problem. In ABAQUS the infinite elements are always assumed to have linear elastic behavior; and, therefore, they are used beyond the region where plastic deformation takes place.

The elasticity is assumed to be linear, with $E = 30 \times 10^3$ psi and $\nu = 0.3$. Yield is governed by the Mohr-Coulomb surface, with $\phi = 20^\circ$ and $c = 10$ psi.

In **Stress Invariants and Spaces** (page L3.2) we showed alternative methods of converting these parameters to the parameters of the modified Drucker-Prager model. In this example we show results for the two standard conversions.

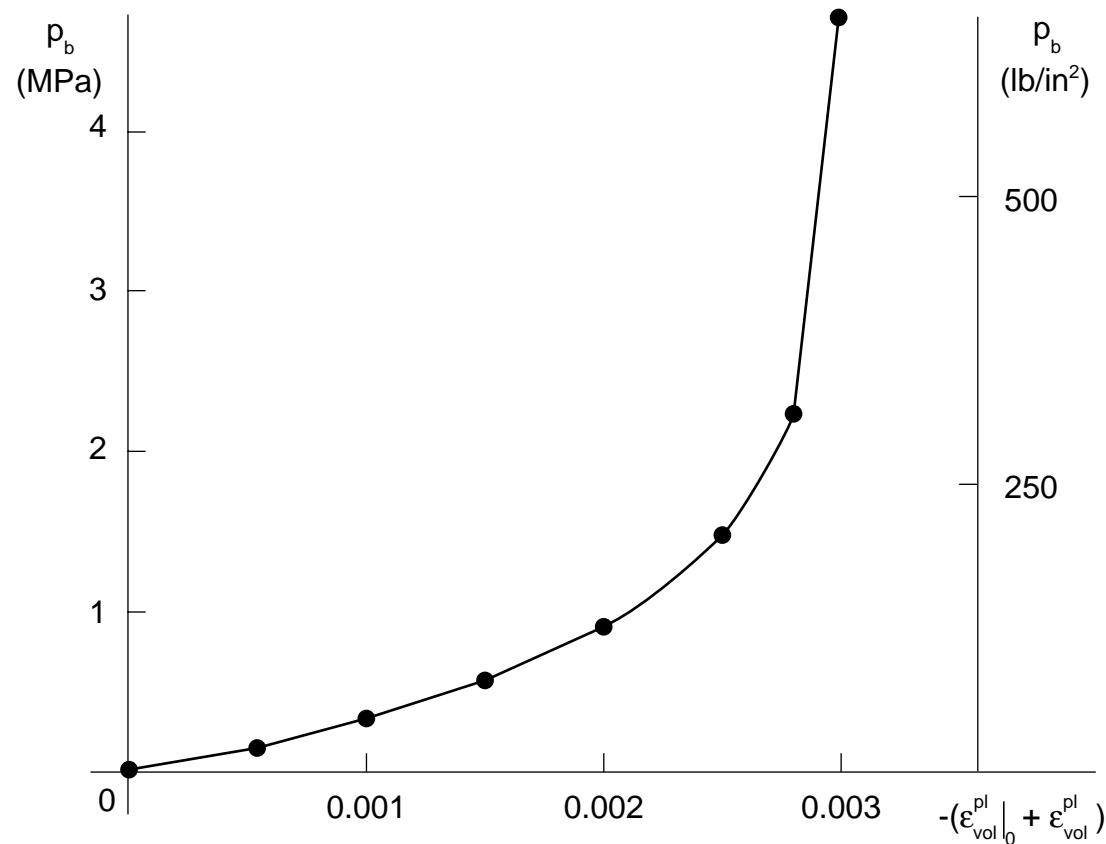
Matching the response of the models in triaxial compression and tension provides $\beta = 37.67^\circ$, $K = 0.795$, and $\sigma_c^0 = 28.56$ psi. The example is run for these parameter values with associated flow ($\psi = \beta$) and non-dilatant flow ($\psi = 0$).



Matching the limit load response of the models for plane strain provides $\beta = 30.16^\circ$ and $\sigma_c^0 = 19.8$ psi for associated flow; $\beta = 30.64^\circ$ and $\sigma_c^0 = 20.2$ psi for non-dilatant flow. The plane strain matching assumes that $K = 1$. The example is run using the associated flow parameters together with $\psi = \beta$ and using the non-dilatant flow parameters with $\psi = 0$.

The Drucker-Prager/Cap model is run using both the triaxial and the plane strain matching of the Mohr-Coulomb parameters. The additional material parameters required for the Cap model are adopted from Mizuno and Chen (1983).

The cap eccentricity parameter is chosen as $R = 0.1$, the initial cap position is taken as $\epsilon_{\text{vol}(0)}^{\text{pl}} = 0.00041$, and the cap hardening curve is shown below. The transition surface parameter $\alpha = 0.01$ is used.



The load-displacement responses are shown and compared to the limit analysis (slip line) Prandtl and Terzaghi solutions.

In this case the plane strain matching of the Mohr-Coulomb parameters provides significantly better predictions of the limit load than the triaxial compression/tension matching of the Mohr-Coulomb parameters.

This is attributable to the plane strain matching providing the same definition of plastic flow direction as well as of failure for plane strain. The triaxial matching only matches failure stress values under triaxial conditions.

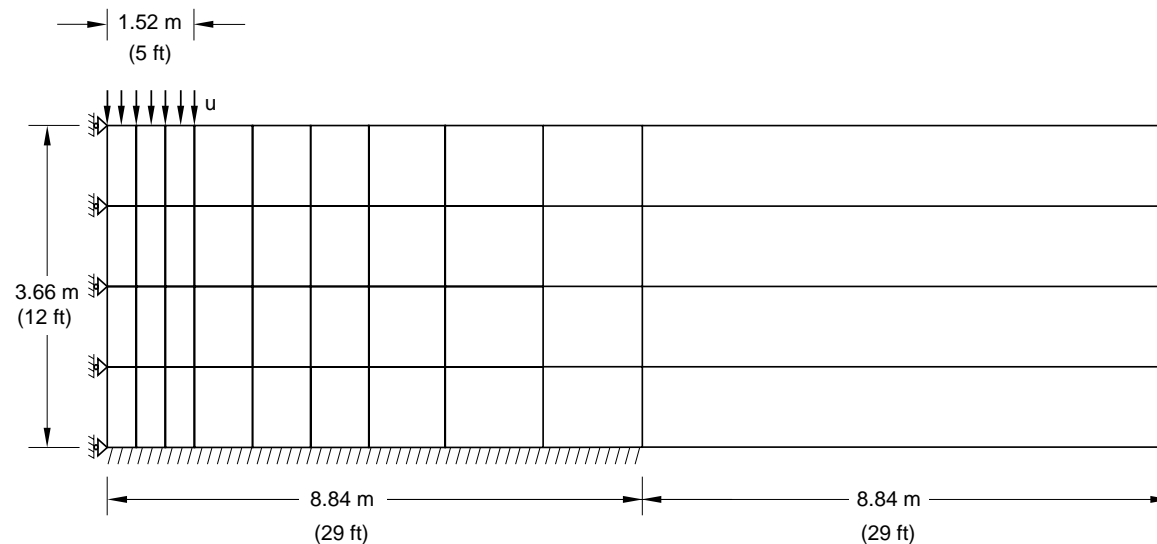
The non-dilatant Drucker-Prager models give a softer response and a lower limit load than the corresponding dilatant versions. The Cap model provides responses that are comparable to the corresponding Drucker-Prager non-dilatant responses.

This is due to the addition of the cap and the nonassociated flow in the failure region, which combine to reduce the dilation in the model and therefore approximate the Drucker-Prager non-dilatant flow model.

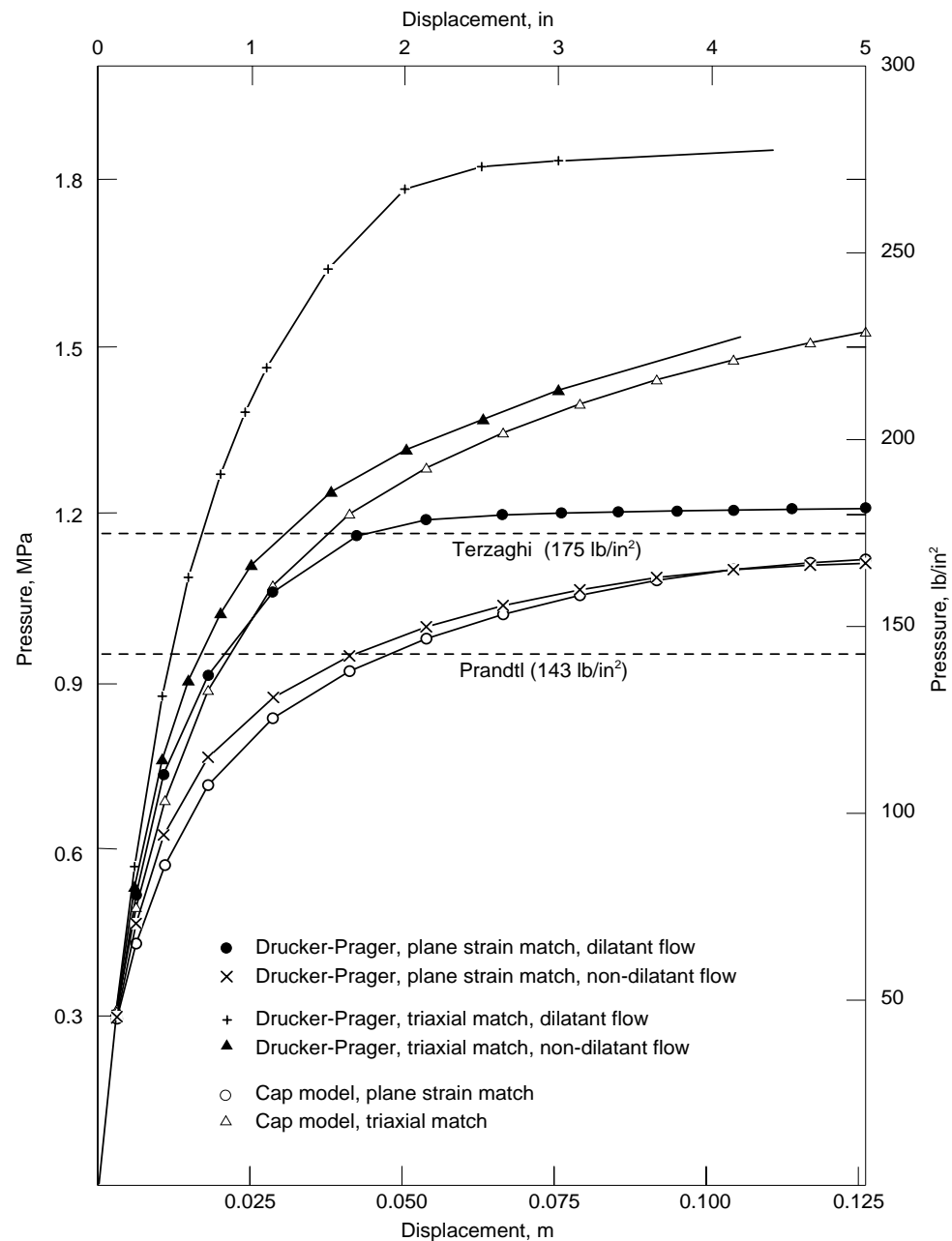
The closest comparisons to Mohr-Coulomb behavior are those obtained with the plane strain matching, non-dilatant, Drucker-Prager model, and the plane strain matching Cap model.

They provide almost identical limit loads, which fall between the Prandtl and Terzaghi solutions.

This conclusion can be extended to general geotechnical problems that are analyzed under plane strain or axisymmetric assumptions.



Finite/Infinite Element Model



Drucker-Prager and Cap Limit Load Results



Limit Analysis Problem File (Drucker-Prager):

***HEADING**

LIMIT LOAD STUDIES, DRUCKER PRAGER, PE, NON-DILATANT FLOW

***RESTART,WRITE,FREQUENCY=10**

***NODE**

1

7,60.

13,180.

15,228.

19,348.

801,,144.

807,60.,144.

813,180.,144.

815,228.,144.

819,348.,144.

20,696.

820,696.,144.

***NGEN,NSET=BASE**

1,7

7,13

13,15



```
15,19
*NSET,NSET=F1
801,
*NSET,NSET=F2,GENERATE
802,807
*NGEN,NSET=CENTER
1,801,100
*NGEN,NSET=TOP
801,807
807,813
813,815
815,819
*NFILL
BASE, TOP, 8, 100
*NGEN,NSET=FAR
20,820,200
*ELEMENT,TYPE=CPE8R
1,1,3,203,201,2,103,202,101
*ELGEN,ELSET=ALL
1,4,200,1,9,2,10
*ELSET,ELSET=PRINTELS
1,2,3,4
```



```
*SOLID SECTION,ELSET=ALL,MATERIAL=A1
*MATERIAL,NAME= A1
*ELASTIC
30000.,0.3
*DRUCKER PRAGER HARDENDING
20.2,0.
*DRUCKER PRAGER,SHEAR CRITERION=LINEAR
30.64,1.0,0.
*ELEMENT,TYPE=CINPE5R
101,219,19,20,220,119
*ELGEN,ELSET=FAR
101,4,200,1
*SOLID SECTION,ELSET=FAR,MATERIAL=A2
*MATERIAL,NAME= A2
*ELASTIC
30000.,0.3
*EQUATION
2
F2,2,1.,801,2,-1.
*BOUNDARY
CENTER,1
F2,1
```




```
BASE,1,2
*STEP,INC=50, UNSYMM=YES
  PRESCRIBE DISPLACEMENT
*STATIC
.025,1.,.,.1
*BOUNDARY
801,2.,.-5.0
*MONITOR,NODE=801,DOF=2
*CONTROLS,ANALYSIS=DISCONTINUOUS
*EL PRINT,ELSET=PRINTELS,FREQUENCY=10
S,E
SINV
ENER
E,IE
PE
*NODE PRINT,FREQUENCY=5
U,RF
*NODE PRINT,NSET=F1
U,RF
*EL FILE,ELSET=PRINTELS,FREQUENCY=10
S
SINV
```

```
ENER  
IE  
*NODE FILE,NSET=F1  
U,RF  
*END STEP
```



Limit Analysis Problem File (Cap Model):

***HEADING**

LIMIT LOAD STUDIES, CAP MODEL, TR, IE

***RESTART,WRITE,FREQUENCY=10**

***NODE**

1

7,60.

13,180.

15,228.

19,348.

801,,144.

807,60.,144.

813,180.,144.

815,228.,144.

819,348.,144.

20,696.

820,696.,144.

***NGEN,NSET=BASE**

1,7

7,13

13,15



```
15,19
*NSET,NSET=F1
801,
*NSET,NSET=F2,GENERATE
802,807
*NGEN,NSET=CENTER
1,801,100
*NGEN,NSET=TOP
801,807
807,813
813,815
815,819
*NFILL
BASE, TOP, 8, 100
*NGEN,NSET=FAR
20,820,200
*ELEMENT,TYPE=CPE8R
1,1,3,203,201,2,103,202,101
*ELGEN,ELSET=ALL
1,4,200,1,9,2,10
*ELSET,ELSET=PRINTELS
1,2,3,4
```



```
*SOLID SECTION,ELSET=ALL,MATERIAL=A1
*MATERIAL,NAME= A1
*ELASTIC
30000.,0.3
*CAP PLASTICITY
16.212,30.64,0.1,.00041,.01,1.0
*CAP HARDENING
2.15,0.
20.96,.0005
46.6,.001
79.67,.0015
126.28,.002
205.95,.0025
311.27,.0028
655.6,.00299
*ELEMENT,TYPE=CINPE5R
101,219,19,20,220,119
*ELGEN,ELSET=FAR
101,4,200,1
*SOLID SECTION,ELSET=FAR,MATERIAL=A2
*MATERIAL,NAME= A2
*ELASTIC
```



```
30000.,0.3
*EQUATION
2
F2,2,1.,801,2,-1.
*BOUNDARY
CENTER,1
F2,1
BASE,1,2
*STEP,INC=50, UNSYMM=YES
  PRESCRIBE DISPLACEMENT
*STATIC
.025,1.,,.1
*BOUNDARY
801,2,, -5.0
*MONITOR,NODE=801,DOF=2
*EL PRINT,ELSET=PRINTELS,FREQUENCY=10
S,E
SINV
ENER
E,IE
PE
PEQC
```



```
*NODE PRINT,FREQUENCY=5
U,RF
*NODE PRINT,NSET=F1
U,RF
*EL FILE,ELSET=PRINTELS,FREQUENCY=10
S
SINV
ENER
IE
PEQC
*NODE FILE,NSET=F1
U,RF
*END STEP
```

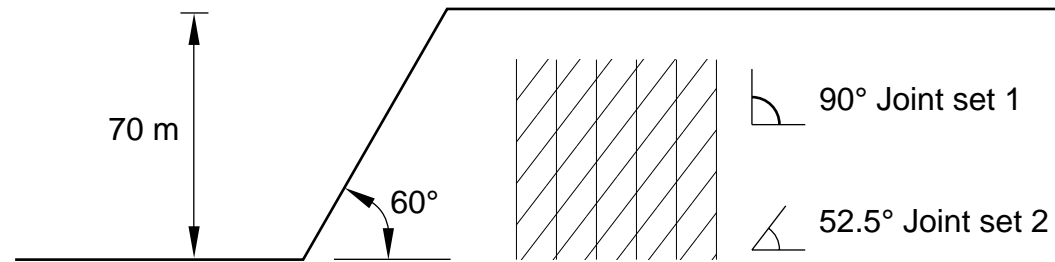
Slope Stability Problem

This is an illustration of the use of the jointed material model. We examine the stability of the excavation of part of a jointed rock mass, leaving a sloped embankment (Example Problem 1.1.6).

This problem has been studied previously by Barton (1971) and Hoek (1970), who used limit equilibrium methods, and by Zienkiewicz and Pande (1977), who used a finite element model.

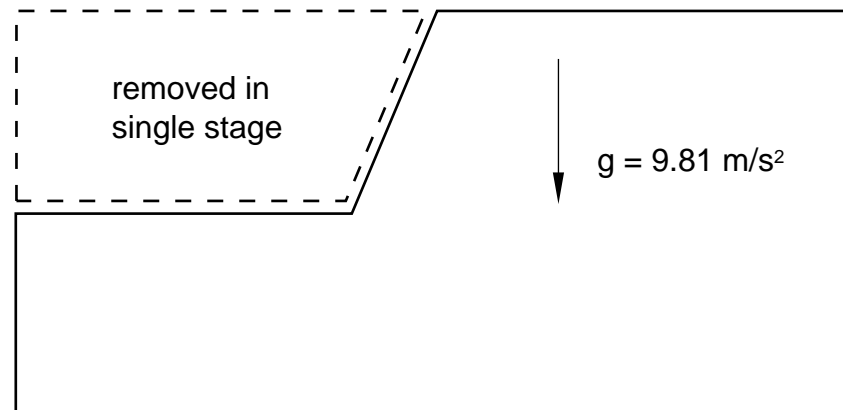
As in most geotechnical problems, we begin from a nonzero state of stress. The active “loading” in this case consists of removal of material to represent the excavation.

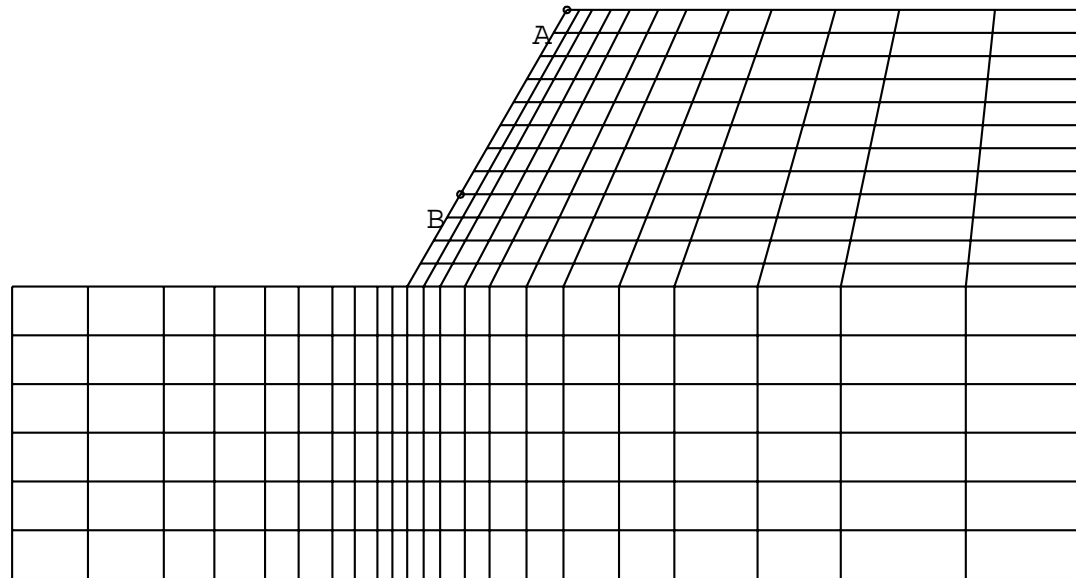
We examine the effect of joint cohesion on slope collapse through a sequence of solutions with different values of joint cohesion, with all other parameters kept fixed.



$E = 28 \text{ GPa}$
 $\nu = 0.2$
 $K_0 = 1/3$
 $\rho = 2500 \text{ kg/m}^3$

Joint sets : $\beta_a = 45^\circ$
 $d_a = \text{variable}$
 Bulk rock : $\beta_b = 45^\circ$
 $d_b = 5600 \text{ kPa}$





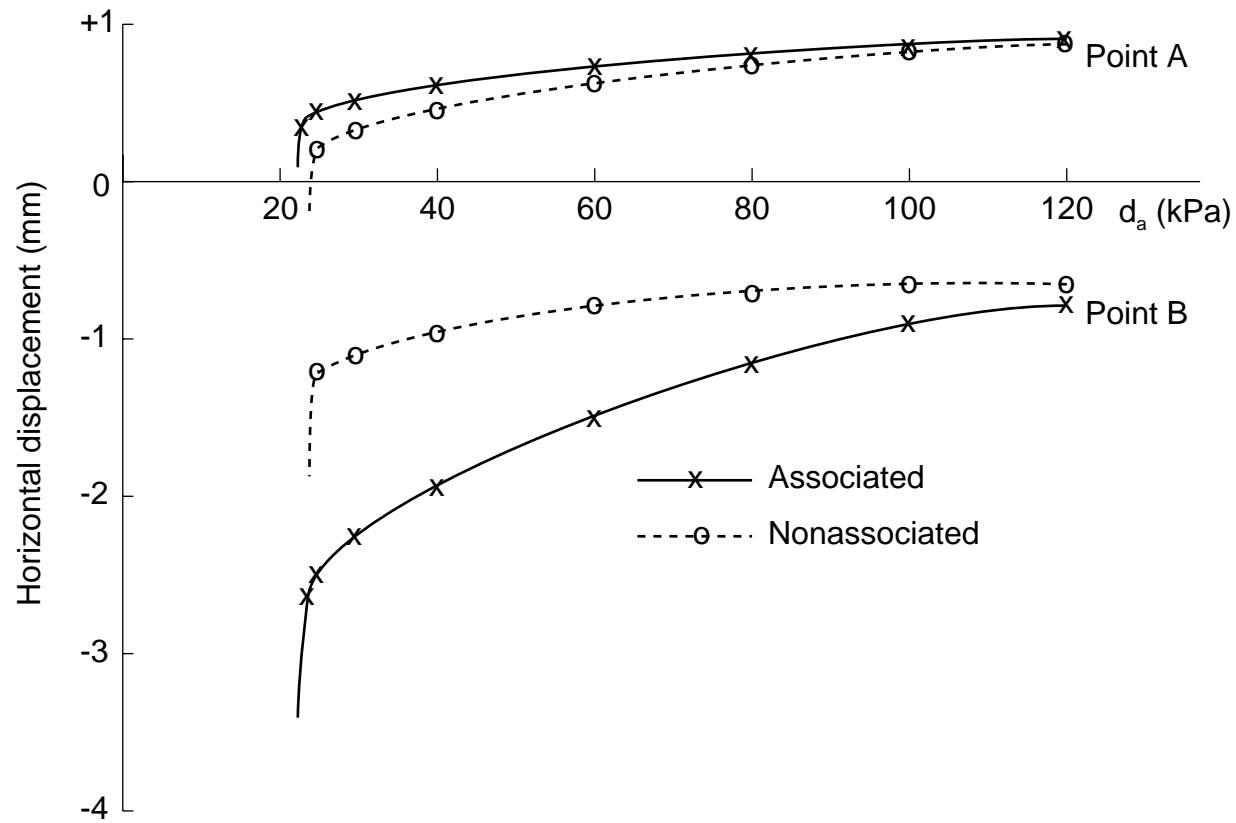
Jointed Rock Slope Problem

The displacement results show the variation of horizontal displacements as cohesion is reduced. They suggest that the slope collapses if the cohesion is less than 24 kPa for the case of associated flow or less than 26 kPa for the case of nondilatant flow.

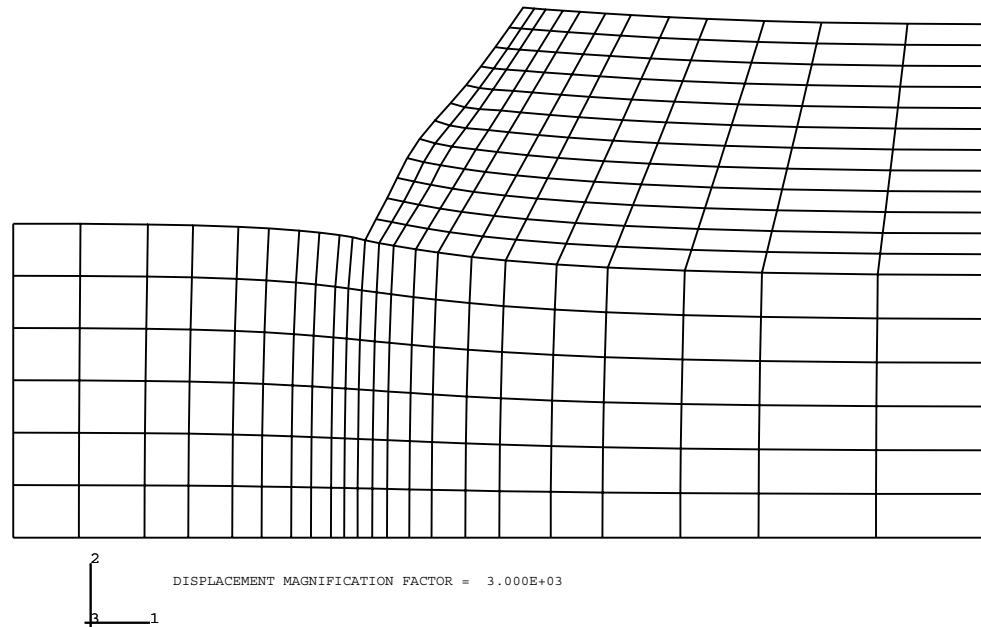
These values compare well with the value calculated by Barton (26 kPa) using a planar failure assumption in his limit equilibrium calculations. Barton's calculations also include “tension cracking” (akin to joint opening with no tension strength) as we do.

Hoek calculated a cohesion value of 24 kPa for collapse of the slope. Although he also makes the planar failure assumption, he does not include tension cracking. This may be why his calculated value is lower than Barton's.

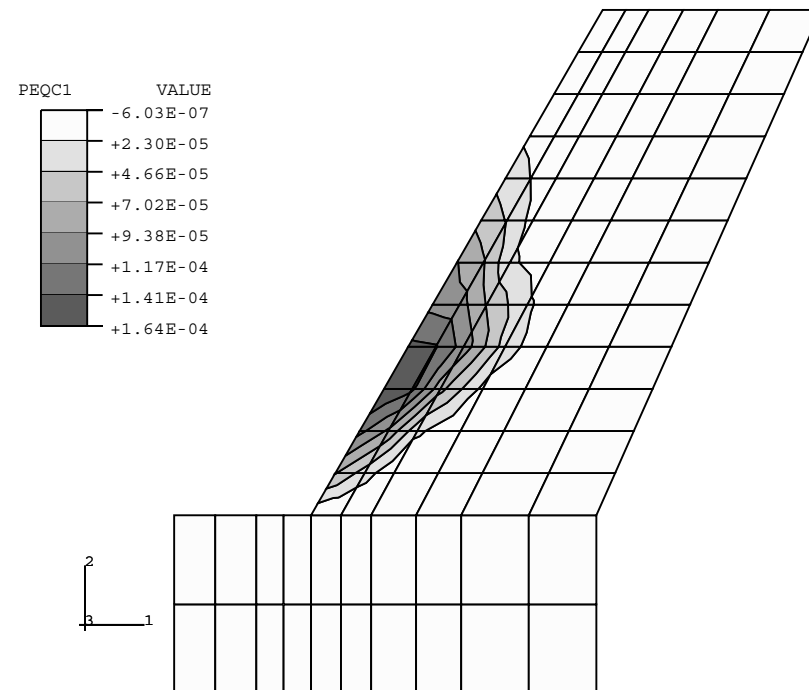
Zienkiewicz and Pande assume the joints have a tension strength of 1/10 of the cohesion and calculate the cohesion value necessary for collapse as 23 kPa for associated flow and 25 kPa for nondilatant flow.



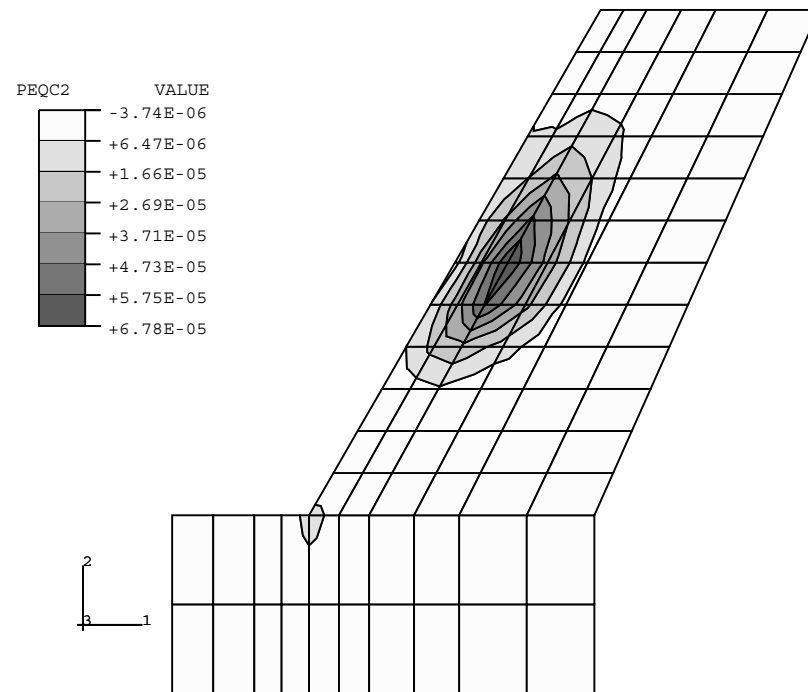
Displacement Results



Displaced Shape



Joint Set 1 (Vertical Joints) - Plastic Strains (Nonassociated Flow)



Joint Set 2 (Inclined Joints) - Plastic Strains (Nonassociated Flow)



Jointed Slope Stability Input File:

***HEADING**

**JOINTED ROCK SLOPE, 2 JOINTS, C=30, NONASSOC FLOW, .5 SH
RET**

***NODE**

1,0.,0.

11,100.,0.

23,272.9,0.

241,0.,74.

251,100.,74.

263,272.9,74.

731,140.4,144.

743,272.9,144.

***NGEN,NSET=BLHS**

1,241,40

***NGEN,NSET=BCEN**

11,251,40

***NGEN,NSET=BRHS**

23,263,40

***NGEN,NSET=TCEN**

251,731,40



```
*NGEN,NSET=TRHS
263,743,40
*NFILL,BIAS=1.5,TWO STEP
BLHS,BCEN,10
*NFILL,BIAS=.66666666,TWO STEP
BCEN,BRHS,12
*NFILL,BIAS=.66666666,TWO STEP
TCEN,TRHS,12
*NSET,NSET=SLHS,GENERATE
241,251
*NSET,NSET=SRHS,GENERATE
731,743
*NSET,NSET=BOT,GENERATE
1,23
*NSET,NSET=FILN
251,411,731
*ELEMENT,TYPE=CPE4
1,1,2,42,41
101,11,12,52,51
*ELGEN,ELSET=ALLE
1,6,40,1,10,1,10
101,18,40,1,12,1,20
```



```
*SOLID SECTION,ELSET=ALLE,MATERIAL=ALLE
*MATERIAL,NAME=ALLE
*ELASTIC
2.8E7,.2
*JOINTED MATERIAL,JOINT DIRECTION=JOINT1
45.,22.5,30.
*JOINTED MATERIAL,JOINT DIRECTION=JOINT2
45.,22.5,30.
*JOINTED MATERIAL,SHEAR RETENTION
.5
*ORIENTATION,NAME=JOINT1
1.,0.,0.,0.,1.,0.
*ORIENTATION,NAME=JOINT2
.7934,-.6088,0.,.6088,.7934,0.
*INITIAL CONDITIONS,TYPE=STRESS,GEOSTATIC
ALLE,0.,144.,-3600.,0.,.333333
*RESTART,WRITE,FREQUENCY=5
*STEP, UNSYMM=YES
*GEOSTATIC
1.,1.
*DLOAD
ALLE,BY,-25.
```



```
*BOUNDARY
BOT,2,2,0.
BLHS,1,1,0.
BRHS,1,1,0.
TRHS,1,1,0.
SLHS,1,2,0.
TCEN,1,2,0.
SRHS,1,2,0.
*EL PRINT
S,MISES,PRESS
E
PE
PEQC
*NODE PRINT
U,RF
*NODE FILE,NSET=FILN
U
*END STEP
*STEP,INC=20, UNSYMM=YES
*STATIC
.1,1.,.001,.1
*CONTROLS,ANALYSIS=DISCONTINUOUS
```



```
*BOUNDARY,OP=NEW  
BOT,2,2,0.  
BLHS,1,1,0.  
BRHS,1,1,0.  
TRHS,1,1,0.  
*MONITOR,NODE=411,DOF=1  
*END STEP
```

A Dynamic Analysis

This example shows the effectiveness of the infinite element quiet boundary formulation in a wave propagation problem (Benchmark Problem 2.2.1).

We compare the results obtained using a small mesh including infinite element quiet boundaries with an extended mesh of finite elements only.

Results obtained using the small mesh without the infinite element quiet boundaries are also given to show how the solution is affected by the reflection of the propagating waves.

The three plane strain meshes used for the infinite half-space problem excited by a vertical pulse line load are shown.

The finite element meshes are assumed to have free boundaries at the far field and will reflect the propagating waves.

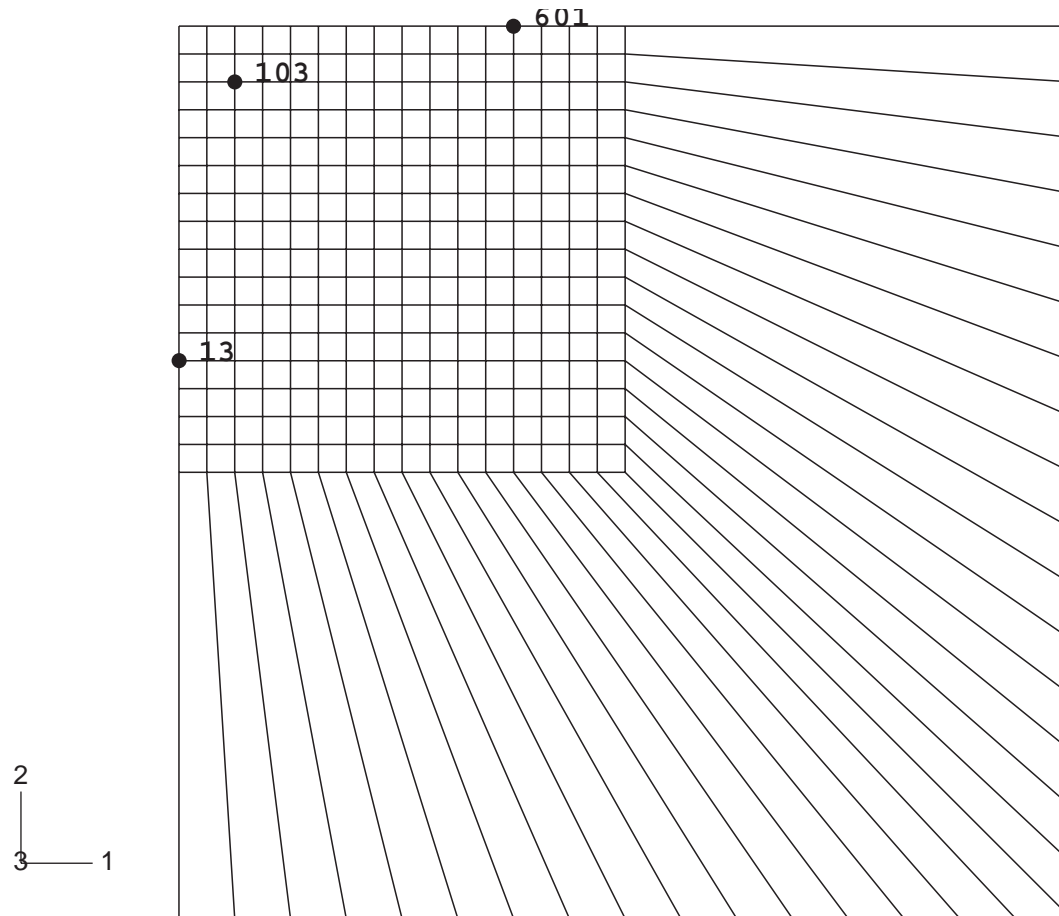
The material is elastic with $E = 73$ GPa, $\nu = 0.33$, and

$\rho = 2842 \text{ kg/m}^3$. Material damping is not included. The applied vertical pulse has a triangular amplitude variation with amplitude of $1.0\text{E}+9$.

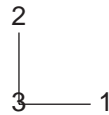
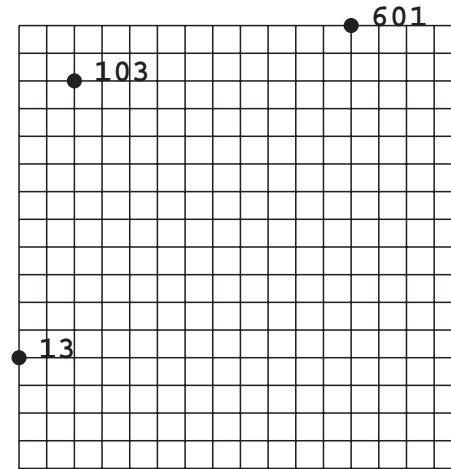
The speed of propagation of push waves in the material is approximately 6169 m/s and the speed of propagation of shear waves is approximately 3107 m/s.

The predominant push waves should reach the boundary of the small mesh in 0.324 μs and reach the boundary of the extended mesh in 0.97 μs . The analyses are run for 1.5 μs so the waves are allowed to reflect into the meshes.

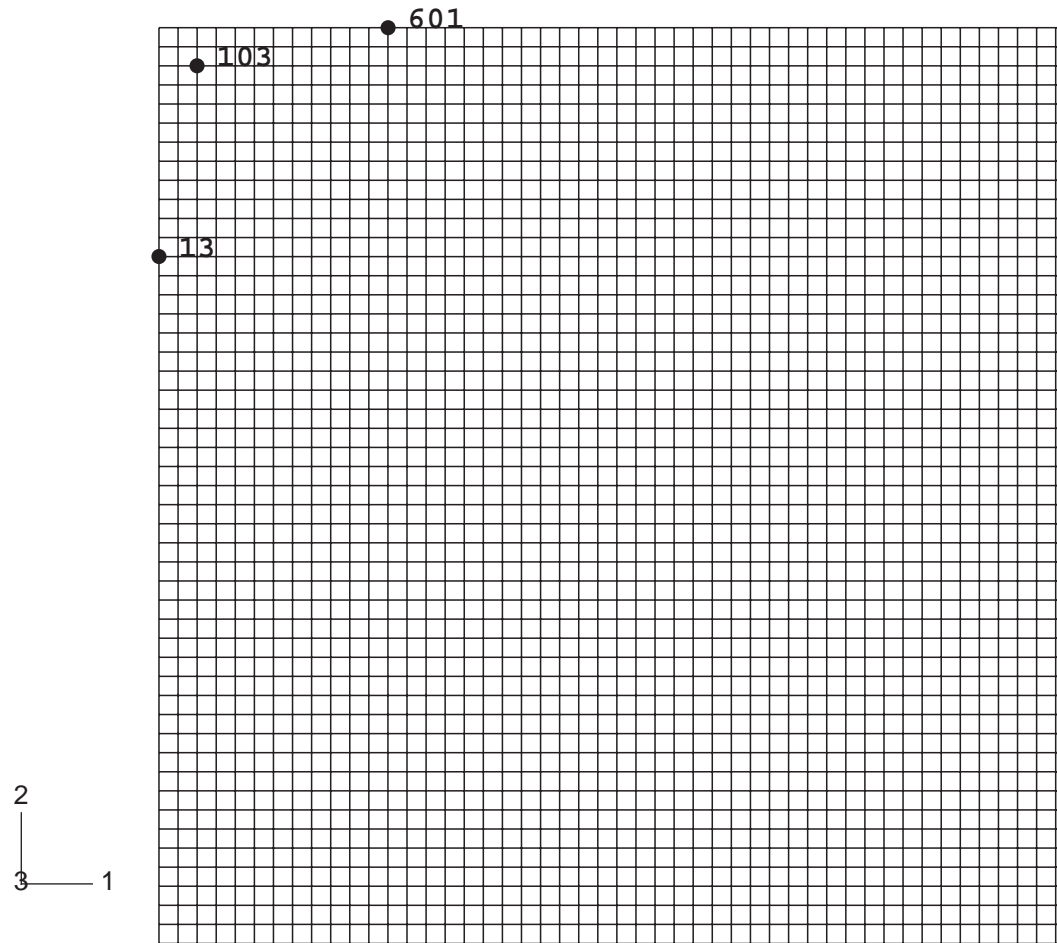
The results are shown as time histories of vertical displacements at nodes 13, 103, and 601. It is clear that the small finite/infinite element and the extended finite element meshes give very similar results. The small finite element mesh response is very different as soon as the waves have had time to reflect.



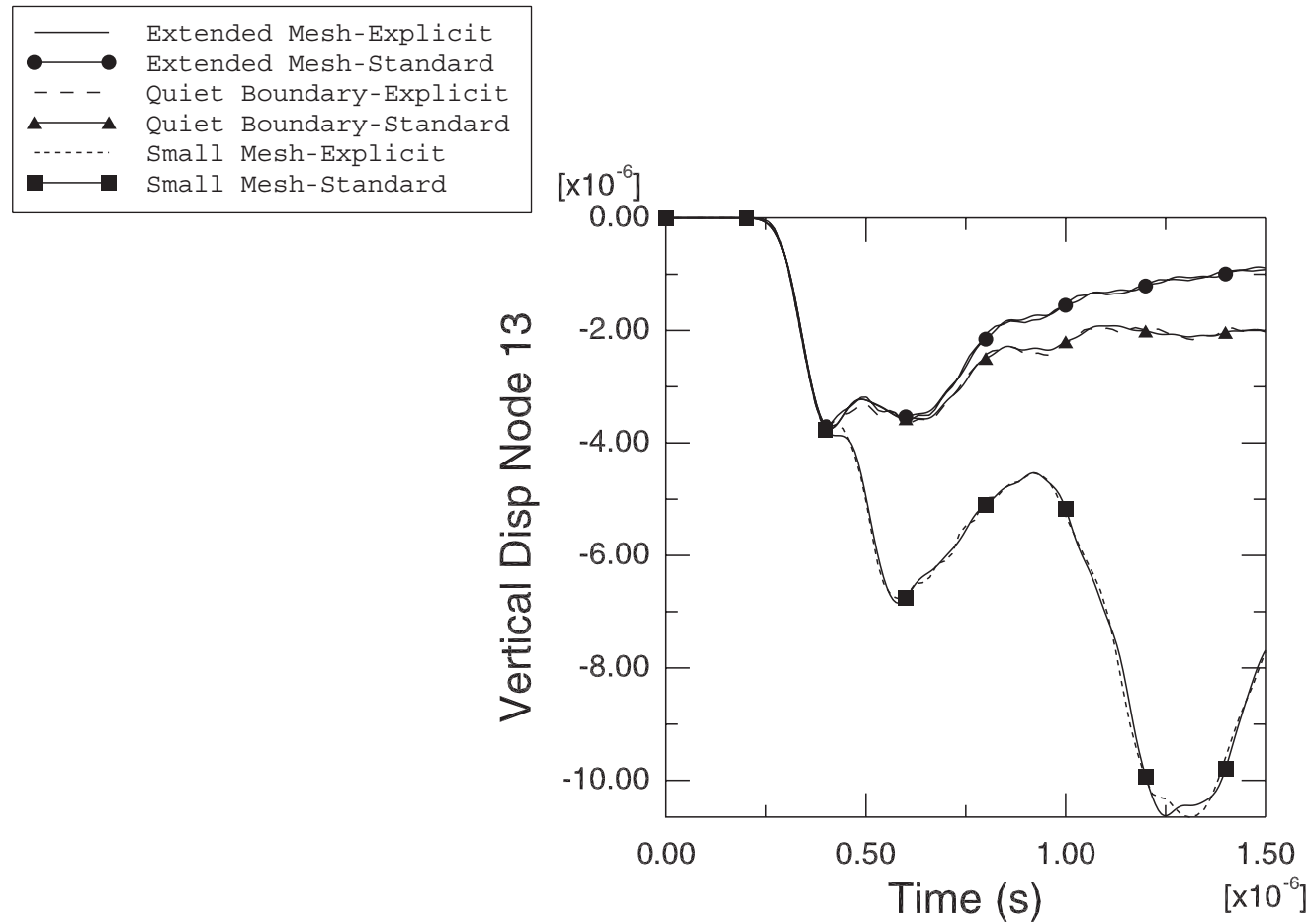
Infinite Element Quiet BoundaryMesh



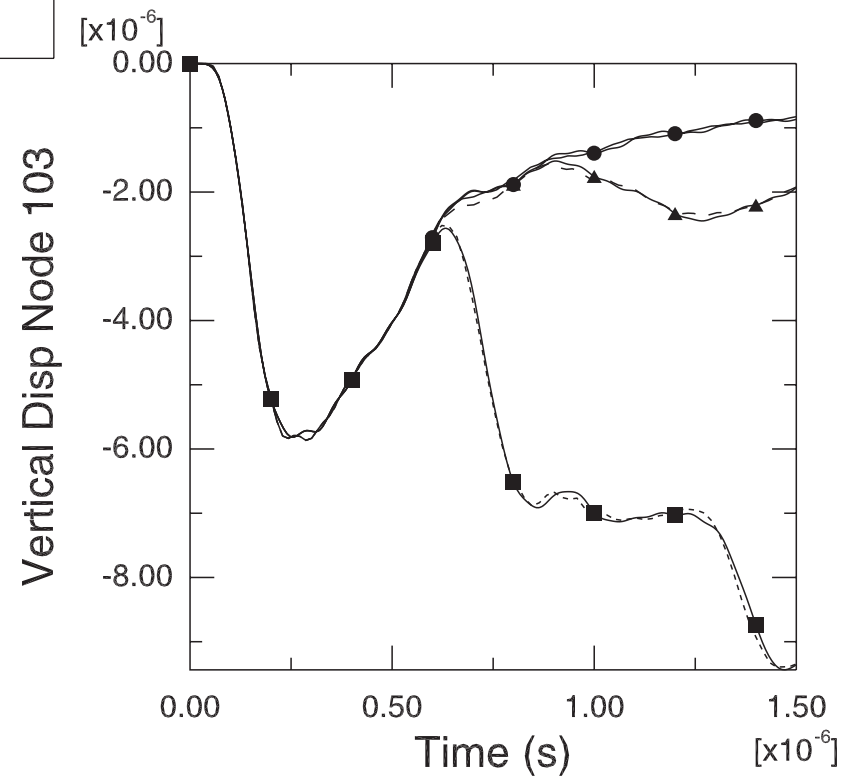
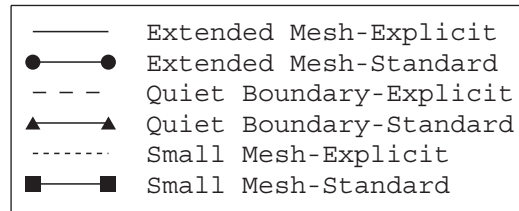
Small Finite Element Mesh



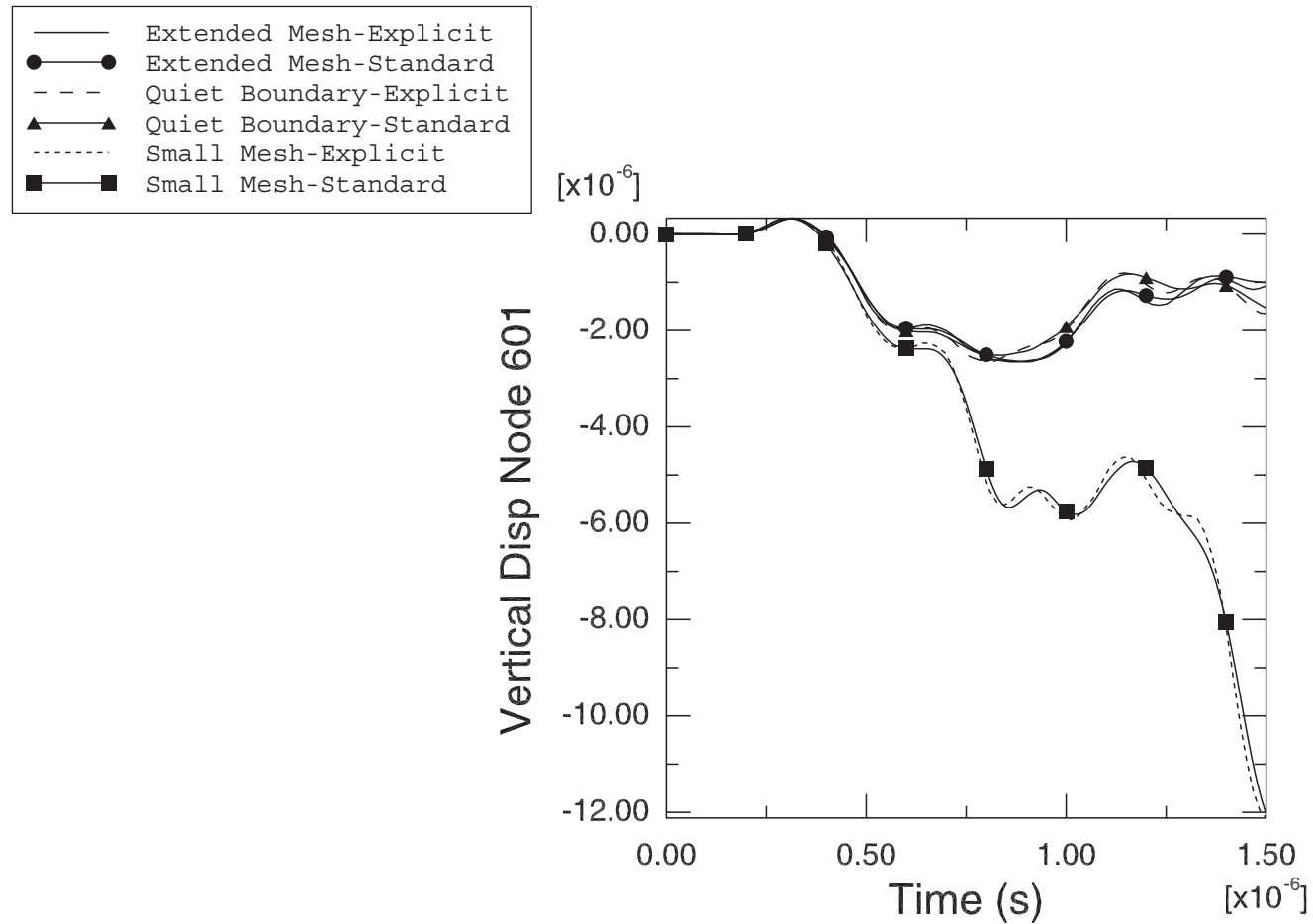
Extended Finite Element Mesh



Node 13 Vertical Displacement Response



Node 103 Vertical Displacement Response



Node 601 Vertical Displacement Response



Wave Propagation Problem Input File:

```
*HEADING
VERTICAL PULSE LOADING, QUIET BOUND, 16X16 CPE4R + 32
CINPE4
*NODE
1,0.,0.
801,2e-3,0.
17,0.,-2e-3
817,2e-3,-2e-3
*NGEN,NSET=LHS
1,17
*NGEN,NSET=RHS
801,817
*NFILL
LHS,RHS,16,50
*NSET,NSET=INTER1,GEN
17, 817, 50
*NSET, NSET=INTER2,GEN
801,816
*NSET, NSET=INTER
INTER1, INTER2
```



```
*NCOPY,OLD SET=INTER,CHANGE NUMBER=1000,POLE,NEW SET=FAR
1,
*NSET,NSET=FILEN
13, 103, 601
*ELEMENT,TYPE=CPE4R,ELSET=FE
1,2,52,51,1
*ELGEN,ELSET=FE
1,16,1,1,16,50,16
*SOLID SECTION,ELSET=FE,MATERIAL=MAT1
*ELEMENT,TYPE=CINPE4,ELSET=IE
257, 67,17,1017,1067
273, 816,817,1817,1816
*ELGEN, ELSET=IE
257, 16, 50, 1
273, 16, -1, 1
*ELSET, ELSET=LOAD,GEN
1,81,16
*SOLID SECTION,ELSET=IE,MATERIAL=MAT1
*MATERIAL,NAME=MAT1
*ELASTIC
7.3E10,.33
```



```
*DENSITY
2842.0,
*BOUNDARY
LHS,1
*AMPLITUDE,NAME=PULSE
0,0,1e-7,1,2e-7,0
**
*STEP,INC=400
*DYNAMIC,NOHAF
8e-9,1.5e-6
*DLOAD,AMPLITUDE=PULSE
LOAD,p3,1e+9
*OUTPUT,FIELD
*NODE OUTPUT
U,V,A
*OUTPUT,HISTORY
*NODE OUTPUT,NSET=FILEN
U,V,A
*NODE FILE, FREQUENCY=1000, NSET=FILEN
U
*END STEP
```

Saturated Problems

We present problems involving the analysis of saturated media: we solve stress/fluid flow coupled problems.

Consolidation Problem (Transient)

This example involves the large scale consolidation of a two-dimensional solid (Benchmark Problem 1.14.3).

Nonlinearities caused by the large geometry changes are considered, as well as the effects of the change in the voids ratio on the permeability of the material.

The model, material properties, and boundary conditions used are shown in the first figure.

The load is applied in two equal time increments of a first *SOILS, CONSOLIDATION step, and it is kept constant thereafter.

Practical consolidation analyses require solutions across several orders of magnitude of time, and the automatic time incrementation scheme is designed to generate cost effective solutions for such cases.



The algorithm is based on the user supplying a tolerance on the pore pressure change permitted in any increment, UTOL.

ABAQUS uses this value in the following manner: if the maximum change in pore pressure at any node is greater than UTOL, the increment is repeated with a proportionally reduced time increment.

If the maximum change in pore pressure at any node is consistently less than UTOL, the time increment size is proportionally increased.

In this case UTOL is set to 15 psi. This is about 3% of the maximum pore pressure in the model following application of the load.

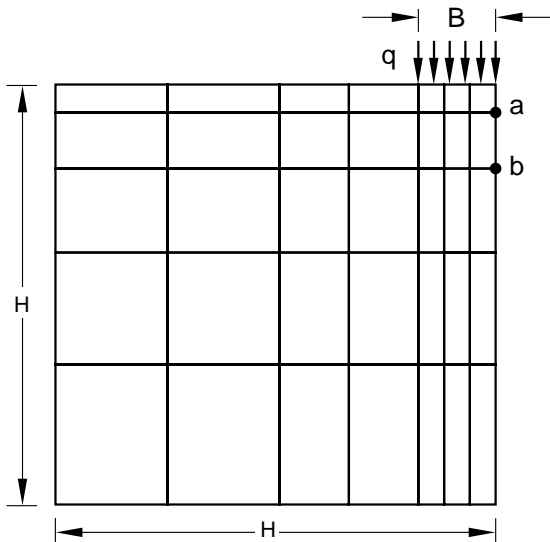
With this value the first time increment is 7.2 seconds and the final time increment is 1.266×10^4 seconds. This is quite typical of diffusion processes: at early times the time rates of pore pressure are significant and at later times these time rates are very low.

The first analysis considers finite-strain effects, and the soil permeability varies with void ratio. A small-strain analysis is also run, with constant permeability. The predictions of the midpoint settlement versus time are shown.



The two analyses predict large differences in the final consolidation: the small-strain result shows about 40% more deformation than the finite-strain case. This is consistent with results from the one-dimensional Terzaghi consolidation solutions.

Clearly, in cases where settlement magnitudes are significant, finite-strain effects are important.



$H = 1.524 \text{ m (60.0 in)}$

$B = 304.8 \text{ mm (12.0 in)}$

Material:

Young's modulus = $6.895 \text{ MPa (1.0 x 10}^3 \text{ lb/in}^2\text{)}$

Poisson's ratio = 0.0

Initial void ratio = 1.5

Permeability = $5.08 \times 10^{-7} \text{ m/s (2.0 x 10}^{-5} \text{ in/s)}$
at void ratio = 1.5

Permeability = $5.08 \times 10^{-8} \text{ m/s (2.0 x 10}^{-6} \text{ in/s)}$
at void ratio = 1.0

Loading:

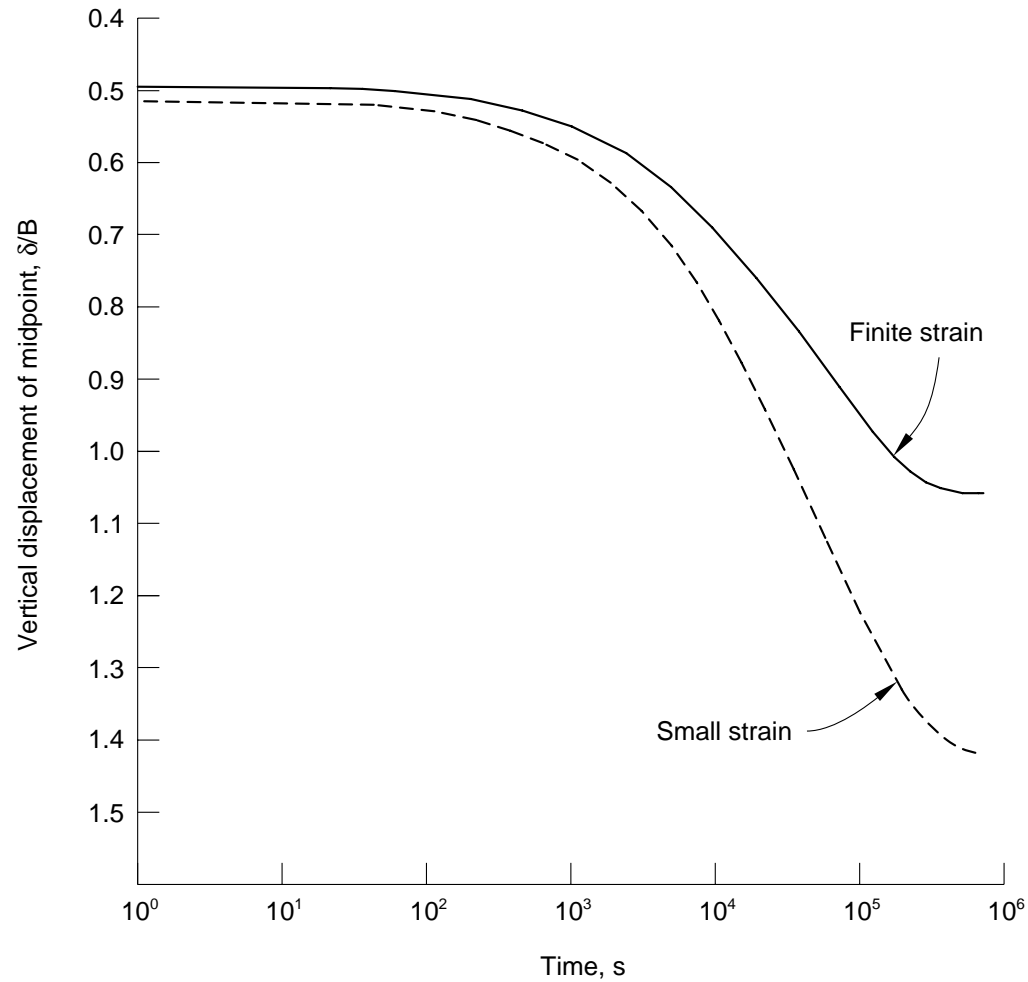
Pressure = $q = 3.4475 \text{ MPa (500.0 lb/in}^2\text{)}$

Boundary conditions:

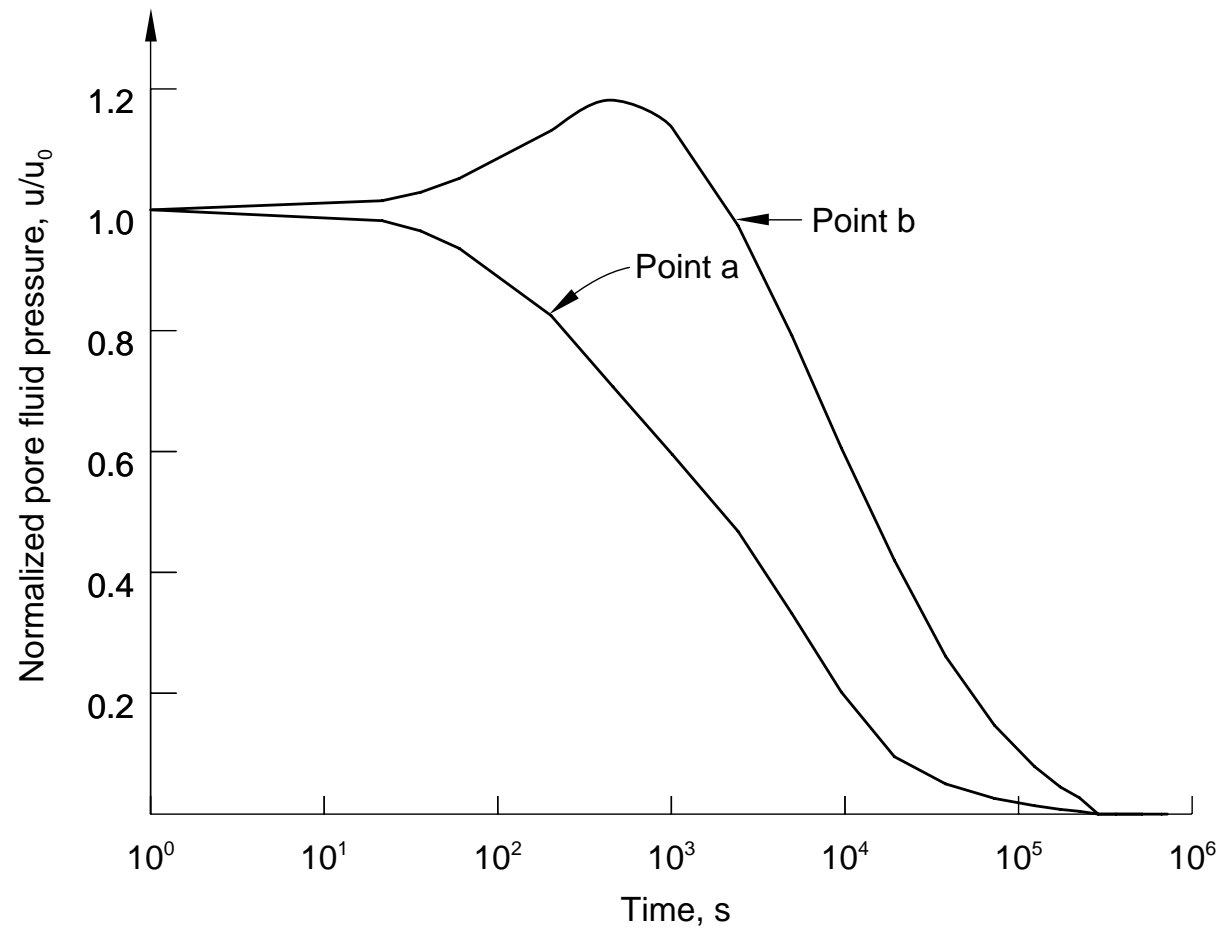
Free drainage across top surface

Other surfaces impermeable and smooth

Model and Properties



Deformation Histories



Pore Pressure Histories



2-D Finite-Strain Consolidation Input File:

```
*HEADING
  2-D CONSOLIDATION - FINITE STRAIN EXAMPLE
*NODE, INPUT=CONSOL.NOD, NSET=NODES
*NSET, NSET=CLINE, GENERATE
1, 11
*NSET, NSET=BOT, GENERATE
11, 1411, 100
*NSET, NSET=WALL, GENERATE
1401, 1411
*NSET, NSET=TOP, GENERATE
1, 1401, 200
*ELEMENT, TYPE=CPE8RP
101, 1, 201, 203, 3, 101, 202, 103, 2
*ELGEN, ELSET=SOIL
101, 7, 200, 100, 5, 2, 1
*SOLID SECTION, ELSET=SOIL, MATERIAL=A1
*MATERIAL, NAME=A1
*ELASTIC
1000.
*PERMEABILITY
```



```
2.E-6,1.
2.E-5,1.5
*BOUNDARY
CLINE,1
BOT,2
WALL,1
TOP,8
*INITIAL CONDITIONS,TYPE=RATIO
NODES,1.5
*RESTART,WRITE,FREQUENCY=25
*STEP,NLGEOM,AMPLITUDE=RAMP
SET UP INITIAL PORE PRESSURES
*SOILS,CONSOLIDATION
3.6,7.2
*DLOAD
101,P1,500.
201,P1,500.
301,P1,500.
*NODE PRINT,FREQUENCY=5,NSET=CLINE
U,RF,POR,RVT
***PRINT,RESIDUAL=NO,FREQUENCY=5
*EL PRINT,FREQUENCY=25,POSITION=CENTROID
```



```
S, MISES, E
*NODE FILE,NSET=CLINE,FREQUENCY=25
U
POR
*END STEP
*STEP,NLGEOM,INC=500
  CONSOLIDATE
*SOILS,CONSOLIDATION,UTOL=15.
7.2,7.2E5,7.2
*END STEP
```


Dam Problem (Steady-State)

This is a benchmark problem run on ABAQUS regarding the analysis of a concrete dam on a rock foundation. The original description of the benchmark problem provided by Dr. G. Pande of Swansea University formed the basis of the analysis.

The problem consists of a concrete dam on a rock foundation. The dam is 30 m high and the rock foundation extends to a depth of 30 m where an impervious boundary is assumed. The benchmark definition calls for a model of the foundation that extends horizontally 30 m on either side of the base of the dam. We assume that no horizontal displacements take place at the ends of the foundation model; we also assume zero vertical displacements at the bottom, impervious boundary of the rock foundation. The finite element mesh used in the analysis contains 110 CPE8RP elements.



The material comprising the rock foundation has a Young's modulus $E = 30000 \text{ MPa}$ and a Poisson's ratio $\nu = 0.2$. We assume the rock behaves as a Drucker-Prager material with nonassociated flow. The material constants used in the Drucker-Prager model are: cohesion of 0.1 MPa , friction angle of 40° , and dilation angle of 20° . The rock exhibits orthotropic permeability with $k_h = 0.0002 \text{ m/sec}$ and

$k_v = 0.00001 \text{ m/sec}$. The mass density of the rock is 2400 kg/m^3 . The concrete material that forms the dam wall has a Young's modulus of $E = 20000 \text{ MPa}$ and a Poisson's ratio $\nu = 0.25$. In addition, we have used the concrete model in ABAQUS where we assumed that the concrete cracks in tension at a stress of 0.15 MPa to simulate the requirement that the material should resist a minimal amount of tensile stress. This is a very low tensile strength, perhaps less than one tenth of the real tensile strength of the material. The permeability of the concrete is 0.00001 m/sec and its mass density is 2400 kg/m^3 .



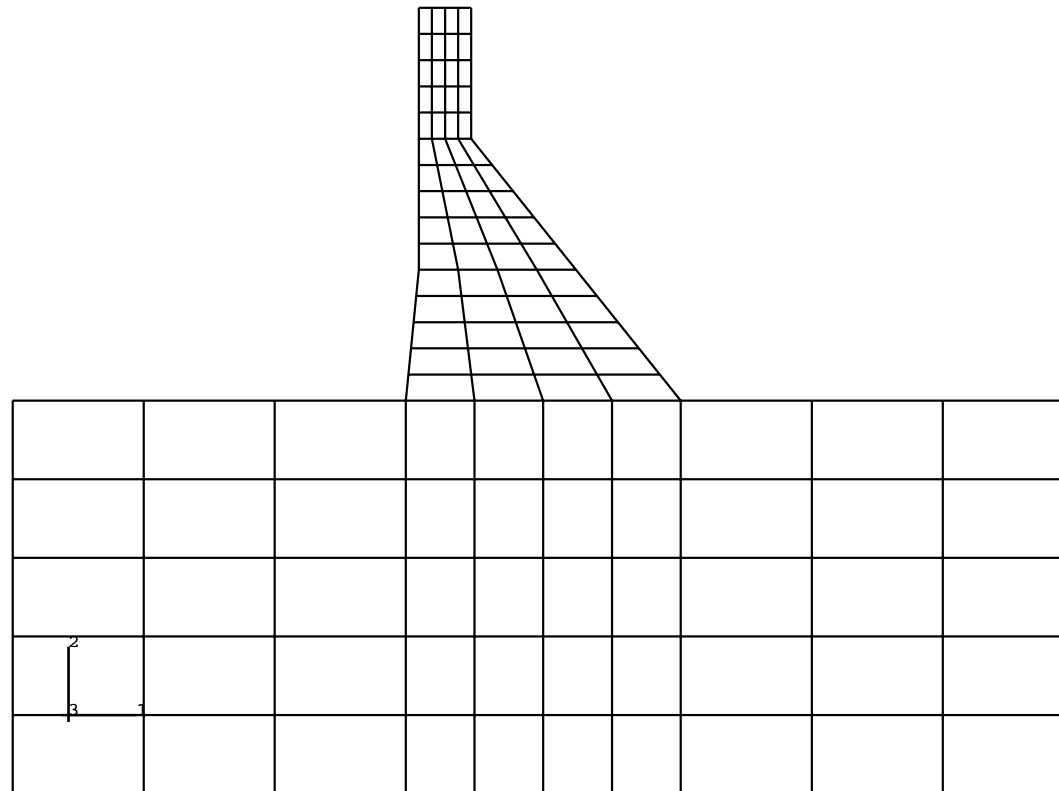
The problem is done in three stages.

In the first stage, we establish geostatic equilibrium where the in situ stresses balance the gravity loads in the rock. At this point, the rock has a vertical stress of zero at the surface increasing linearly to approximately -0.7 MPa at the impervious bottom boundary; the horizontal stresses are 0.6 times the vertical stress. The excess pore pressure in the rock is zero. This state of stress corresponds to the undeformed configuration of the rock mass.

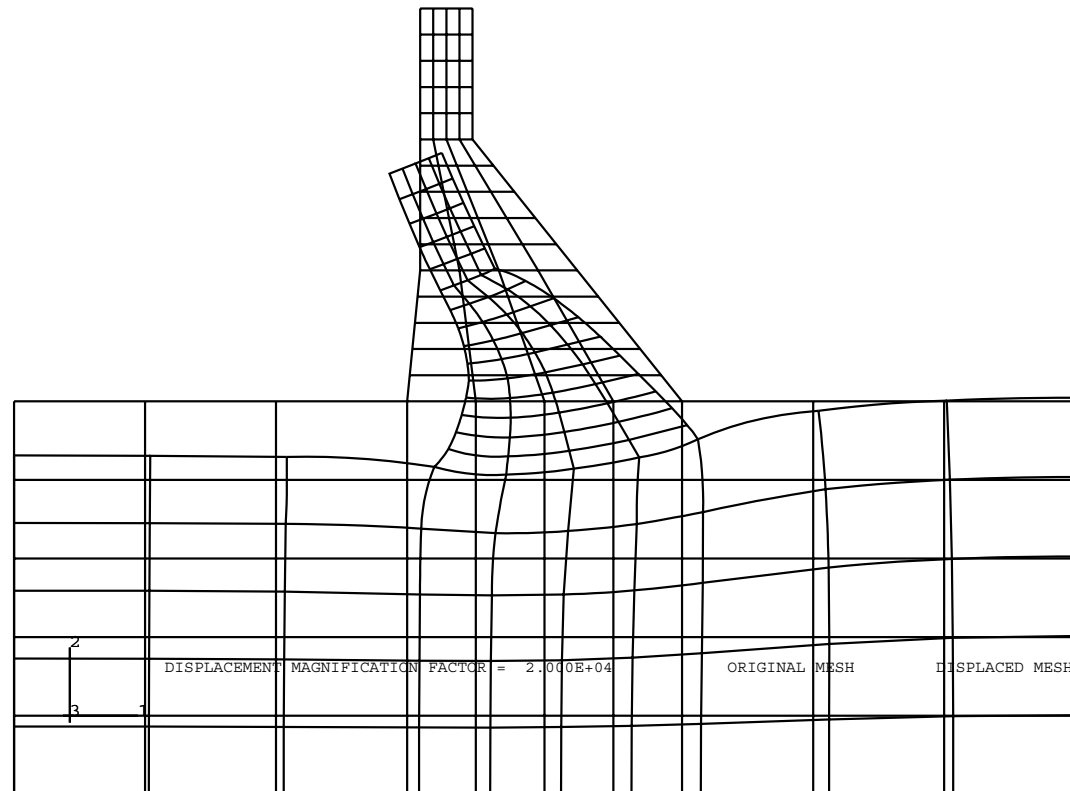
In the second stage of analysis, we apply the gravity loads due to the concrete dam construction and the pressure loads on the upstream face of the dam representing the filling of the reservoir. In this step of analysis we are concerned with the short-term behavior and assume that no pore pressures develop because the concrete and rock have very low permeabilities. We show the short-term results in the form of a deformed shape and contours of principal stresses and plastic strain.



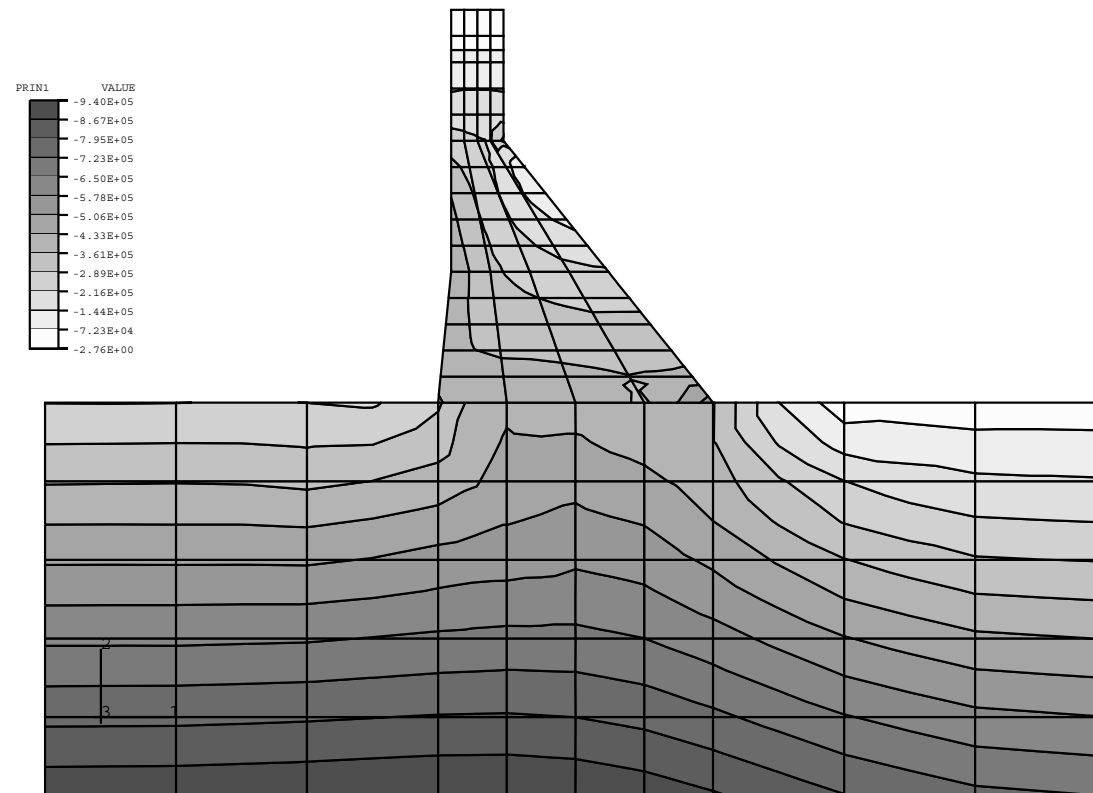
In the final stage of analysis, we perform a steady-state pore fluid diffusion/stress analysis to calculate the state of the structure 25 years after filling the reservoir. The boundary conditions on the seepage part of the problem consist of an impervious boundary at the bottom of the rock foundation, zero excess pore fluid pressure on the downstream boundary of the rock foundation, and nonzero excess pore pressures on the upstream face of the dam and foundation corresponding to the hydrostatic pressure caused by the head of water in the full reservoir. We also include a phreatic surface in the concrete dam wall. In this case the position of this zero pore pressure surface is assumed, the analysis is performed, and the validity of the assumption is checked; an iterative procedure can then be used to correct the location of the phreatic surface at steady state. Although not done in this case, ABAQUS is capable of calculating the phreatic surface automatically, as illustrated later in **Phreatic Surface Calculation (Steady-State)** (page L6.114). Steady-state results are shown.



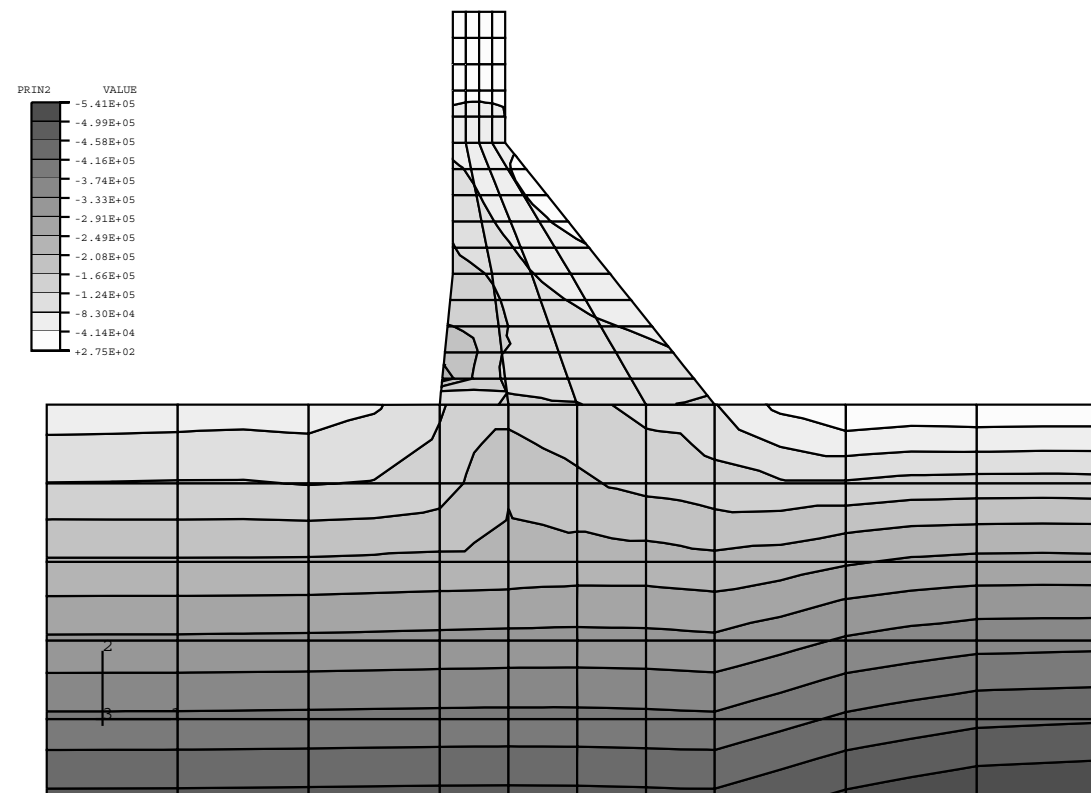
Finite Element Model



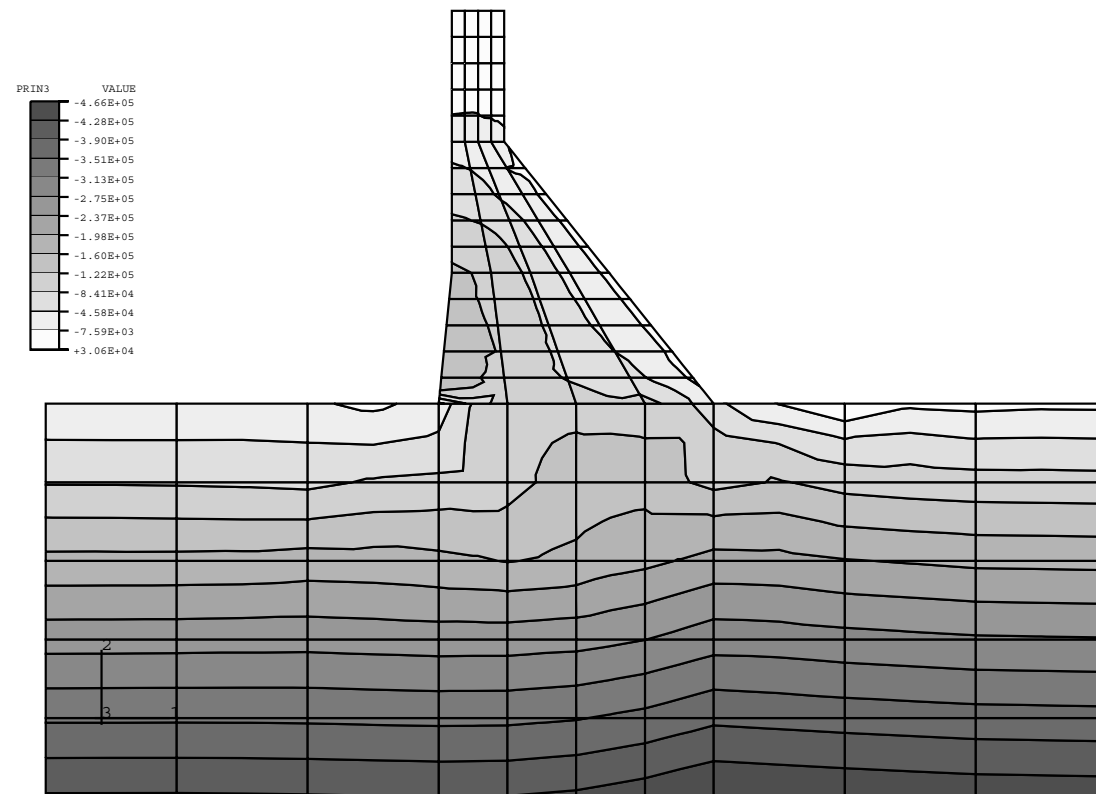
Short-Term Deformed Shape



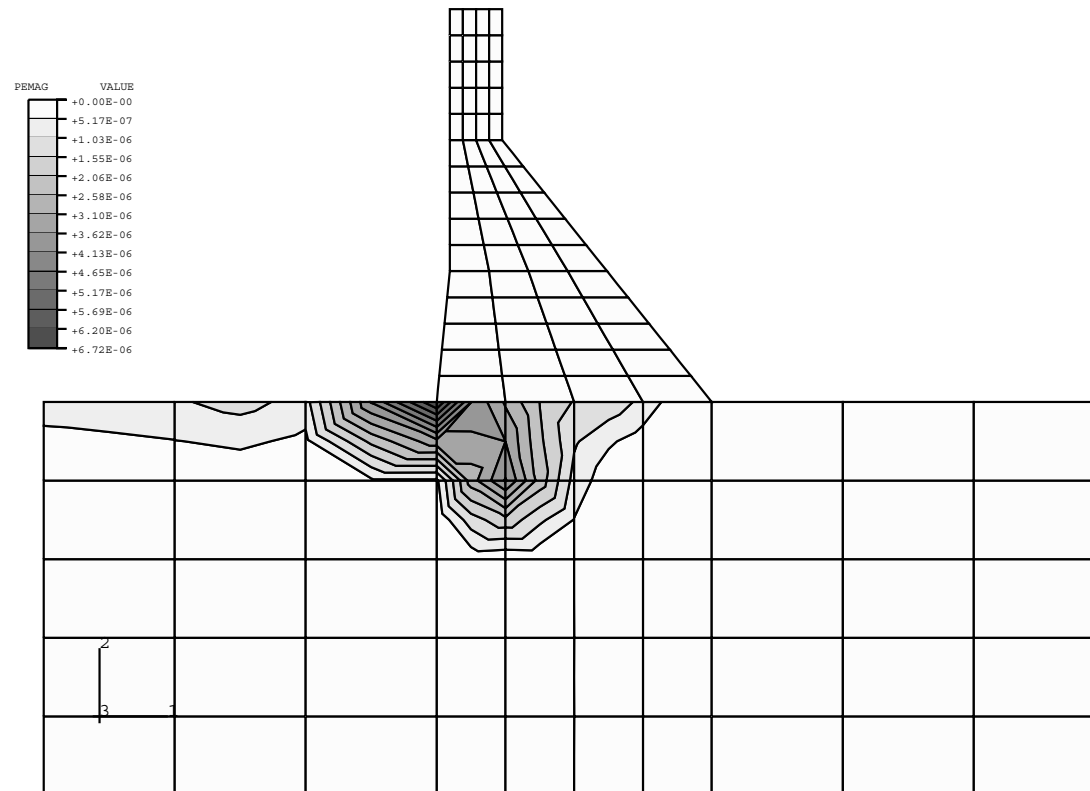
Short-Term Minimum Principal Stress



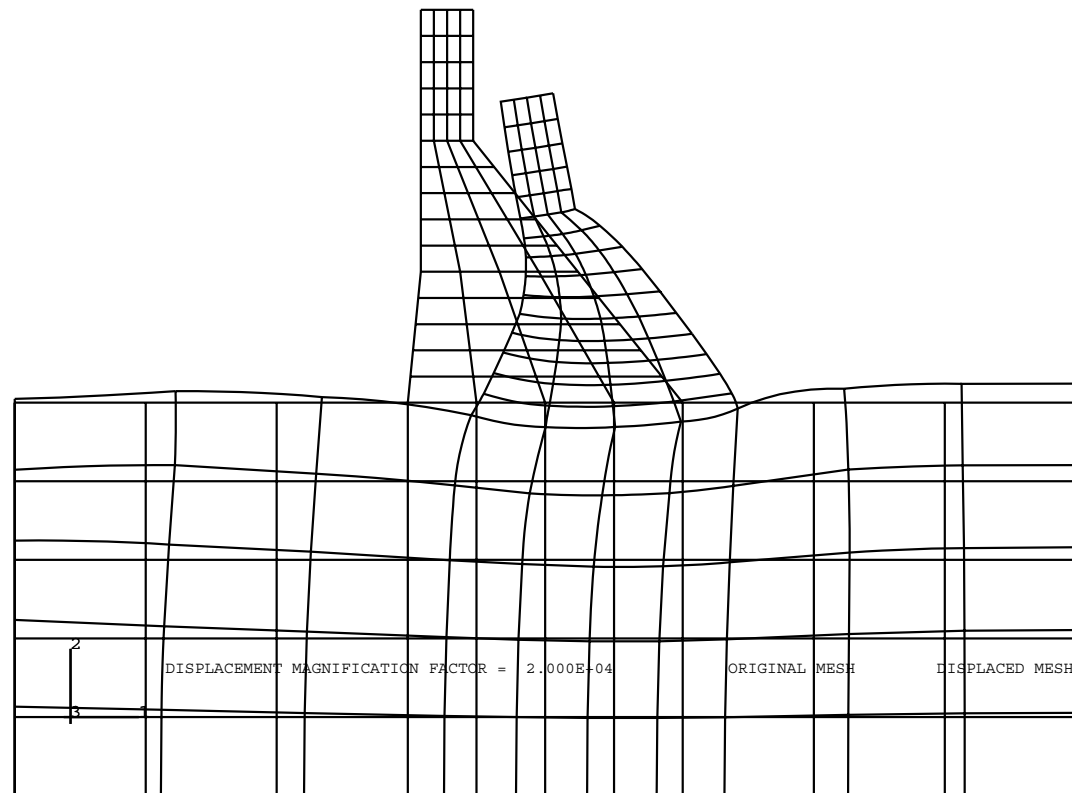
Short-Term Intermediate Principal Stress



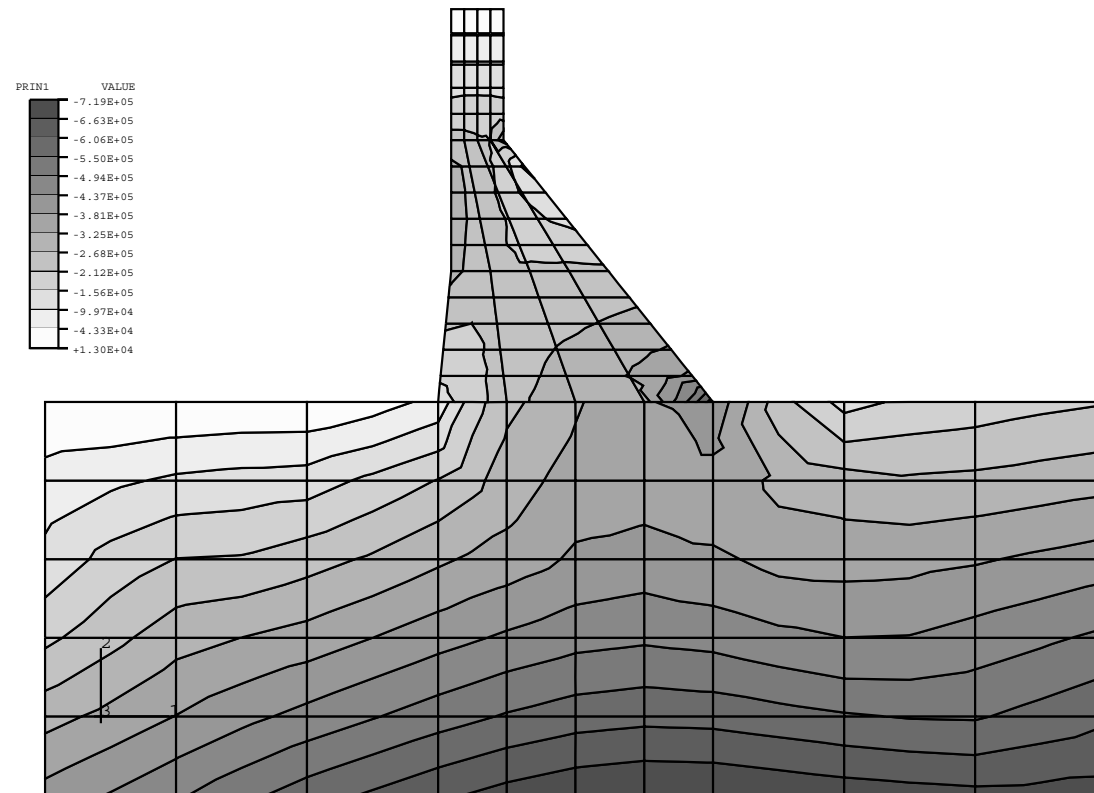
Short-Term Maximum Principal Stress



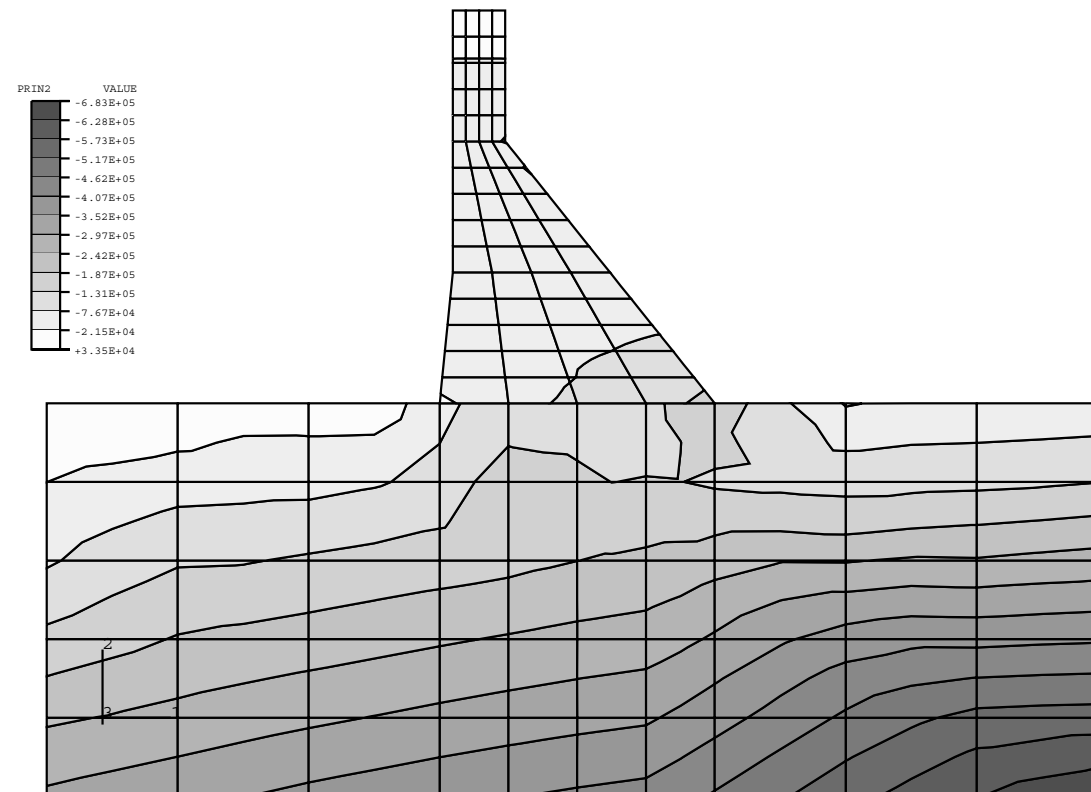
Short-Term Plastic Strain



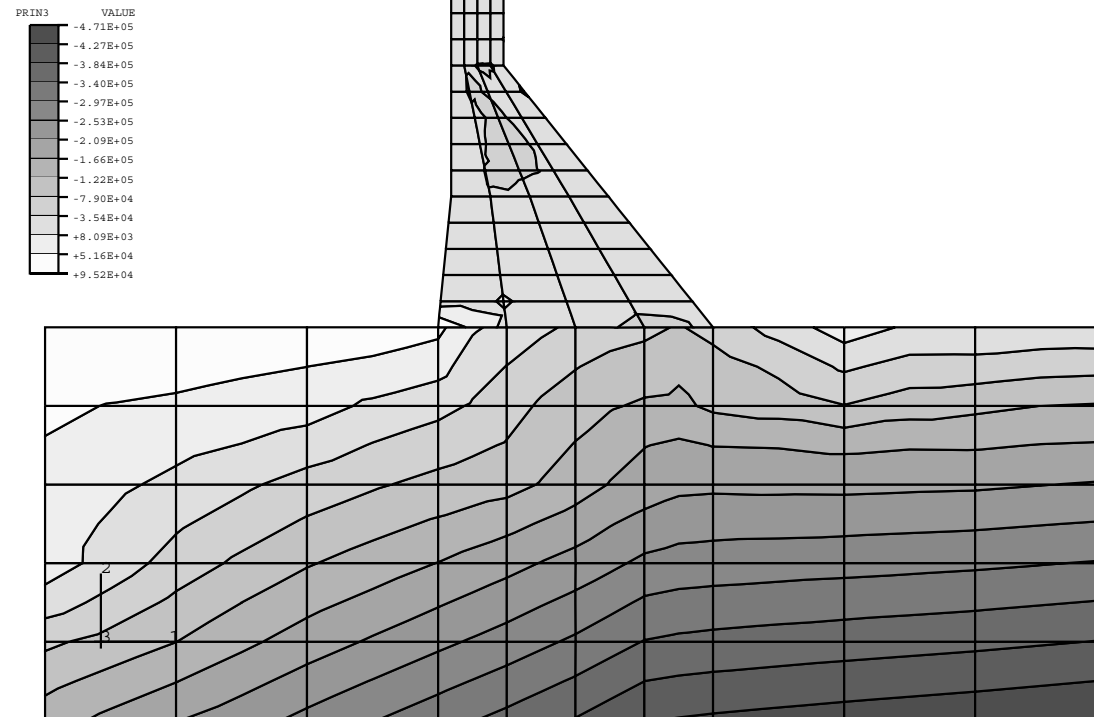
Long-Term Deformed Shape



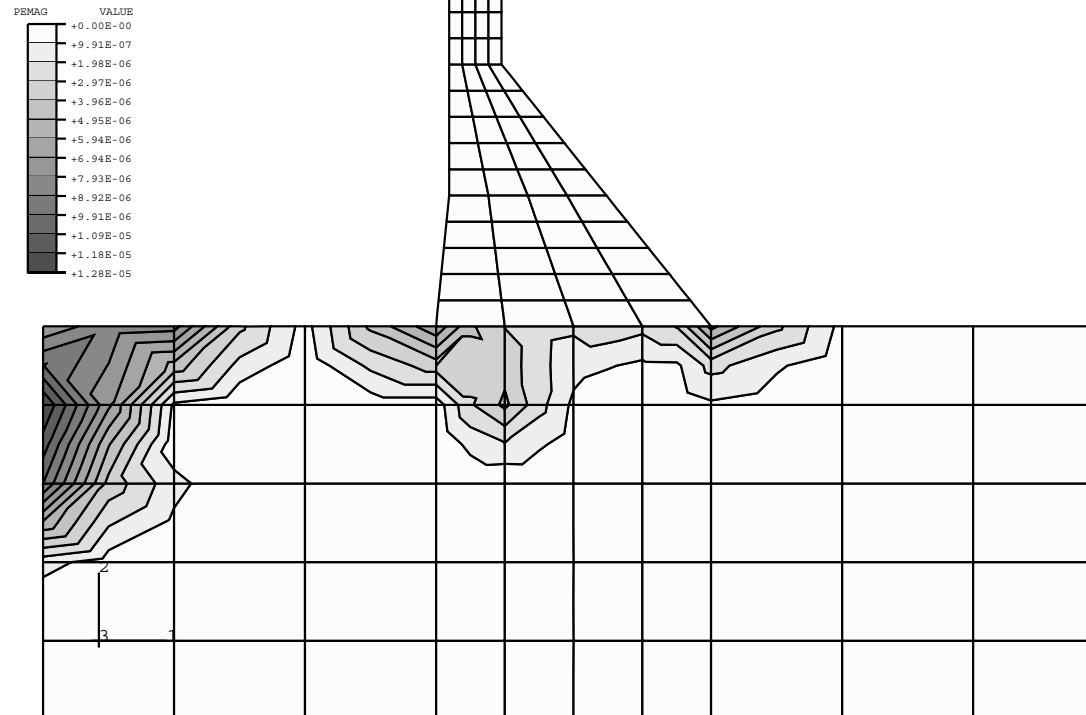
Long-Term Minimum Principal Stress



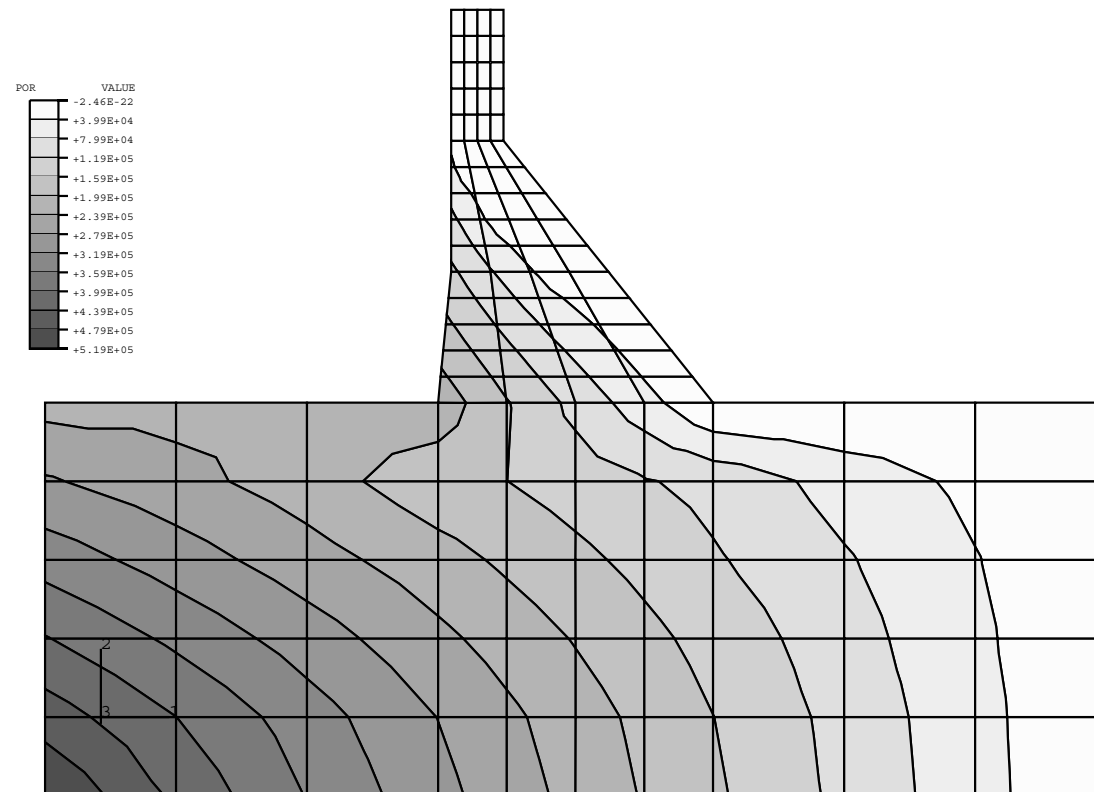
Long-Term Intermediate Principal Stress



Long-Term Maximum Principal Stress



Long-Term Plastic Strain



Long-Term Pore Pressure



Dam Problem Input File:

```
*HEADING
ABAQUS BENCHMARK FOR UNITED NATIONS DAM IN INDIA
*** SI UNITS (METER, KILOGRAM, SECOND)
*NODE,NSET=ALLN
1,0.,0.
7,30.,0.
15,51.,0.
21,81.,0.
401,0.,30.
407,30.,30.
415,51.,30.
421,81.,30.
807,31.,40.
1607,31.,60.
1215,35.,50.
1615,35.,60.
*NGEN,NSET=BOTF
1,7
7,15
15,21
```



```
*NGEN,NSET=TOPF
401,407
407,415
415,421
*NFILL,NSET=NODF
BOTF,TOPF,10,40
*NSET,NSET=LHSF,GEN
1,401,40
*NSET,NSET=RHSF,GEN
21,421,40
*NGEN,NSET=LHSD
407,807,40
807,1607,40
*NGEN,NSET=RHSD
415,1215,40
1215,1615,40
*NFILL,NSET=NODD
LHSD,RHSD,8,1
*NSET,NSET=DRAIN,GEN
21,421,80
415,421,2
415,1615,80
```



```
813,1613,80
971,1611,80
1129,1609,80
1287,1607,80
*NSET,NSET=ALLN
NODF,NODD
*ELEMENT,TYPE=CPE8RP
1,1,3,83,81,2,43,82,41
54,407,409,489,487,408,449,488,447
*ELGEN,ELSET=FOUND
1,10,2,1,5,80,10
*ELGEN,ELSET=DAM
54,4,2,1,15,80,10
*ELSET,ELSET=ALLE
FOUND,DAM
*ELSET,ELSET=OUTE,GEN
4,194,10
7,197,10
*SOLID SECTION,ELSET=FOUND,MATERIAL=ROCK
1.
*SOLID SECTION,ELSET=DAM,MATERIAL=CONCRETE
1.
```



```
*MATERIAL,NAME=ROCK
*ELASTIC
30000.E6,.2
*YIELD
.139E6
*DRUCKER PRAGER
40.,1.,20.
*DENSITY
2400.
*PERMEABILITY,SPECIFIC=9810.,TYPE=ORTHO
.0002,.00001,.0002
*MATERIAL,NAME=CONCRETE
*ELASTIC
20000.E6,.25
*CONCRETE
10.E6
20.E6,.001
*FAILURE RATIOS
1.16,.0075
*TENSION STIFFENING
1.,0.
0.,.5E-3
```



```
*SHEAR RETENTION
1.,1000.
*DENSITY
2400.
*PERMEABILITY,SPECIFIC=9810.
.00001
*BOUNDARY
BOTF,2
LHSF,1
RHSF,1
*INITIAL CONDITIONS,TYPE=RATIO
ALLN,.5
*INITIAL CONDITIONS,TYPE=STRESS,GEOSTATIC
FOUND,0.,30.,-706320.,0.,.6
*RESTART,WRITE,FREQ=10
*STEP
GEOSTATIC STATE OF STRESS IN FOUNDATION
*STATIC
1.,1.
*DLOAD
FOUND,BY,-23544.
*EL PRINT,ELSET=OUTE
```



```
S, PRESS, MISES, POR, E11, E22
PE
*EL PRINT, ELSET=DAM
CRACK
CONF
*NODE PRINT
U, RF, POR
*END STEP
*STEP
IMMEDIATLY AFTER FILLING:DAM GRAVITY LOADS+FULL RESERVOIR
LOADS
*STATIC
1., 1.
*DLOAD
DAM, BY, -23544.
41, P3, 215820.
42, P3, 215820.
43, P3, 215820.
54, P4, 215820.
64, P4, 196200.
74, P4, 176580.
84, P4, 156960.
```



```
94,P4,137340.
104,P4,117720.
114,P4,98100.
124,P4,78480.
134,P4,58860.
144,P4,39240.
154,P4,19620.
*END STEP
*STEP
25 YEARS AFTER FILLING:DAM GRAVITY LOADS+FULL RESERVOIR
LOADS
*SOILS
.7884E9,.7884E9
*BOUNDARY
DRAIN,8,8,0.
1,8,8,519930.
81,8,8,461070.
161,8,8,402210.
241,8,8,343350.
321,8,8,284490.
401,8,8,225630.
403,8,8,225630.
```



```
405,8,8,225630.  
407,8,8,225630.  
487,8,8,206010.  
567,8,8,186390.  
647,8,8,166770.  
727,8,8,147150.  
807,8,8,127530.  
887,8,8,107910.  
967,8,8,88290.  
1047,8,8,68670.  
1127,8,8,49050.  
1207,8,8,29430.  
*END STEP
```


Partially Saturated Problems

We present problems that involve the analysis of partially saturated media: we solve coupled and uncoupled problems.

Demand Wettability Problem (Uncoupled)

This example illustrates the ABAQUS capability to solve uncoupled partially saturated porous fluid flow problems (Benchmark Problem 1.8.1).

We consider a “constrained demand wettability” test. The demand wettability test is a common way of measuring the absorption properties of porous materials. In such a test, fluid is made available to the material at a certain location and the material is allowed to absorb as much fluid as it can.

We consider a square specimen of material and allow it to absorb fluid at its center. The quarter mesh of reduced-integration elements is shown.

We investigate two cases: one in which the material contains a large number of gel particles that entrap fluid and, as a result, enhance the fluid retention capability of the material, and the other in which the material does not contain gel. We also study the cyclic wetting behavior in the case of the sample containing gel particles.

The “loading” consists of prescribing a zero pore pressure (corresponding to full saturation) at the center of the sample (node 1). This pore pressure is held fixed for 600 seconds to model the fluid acquisition process.

Draining for 600 seconds is modeled by prescribing a pore pressure of -10000.0 at node 1; this corresponds to a saturation of 10%, which is the least saturation the sample can have once it has been wetted.

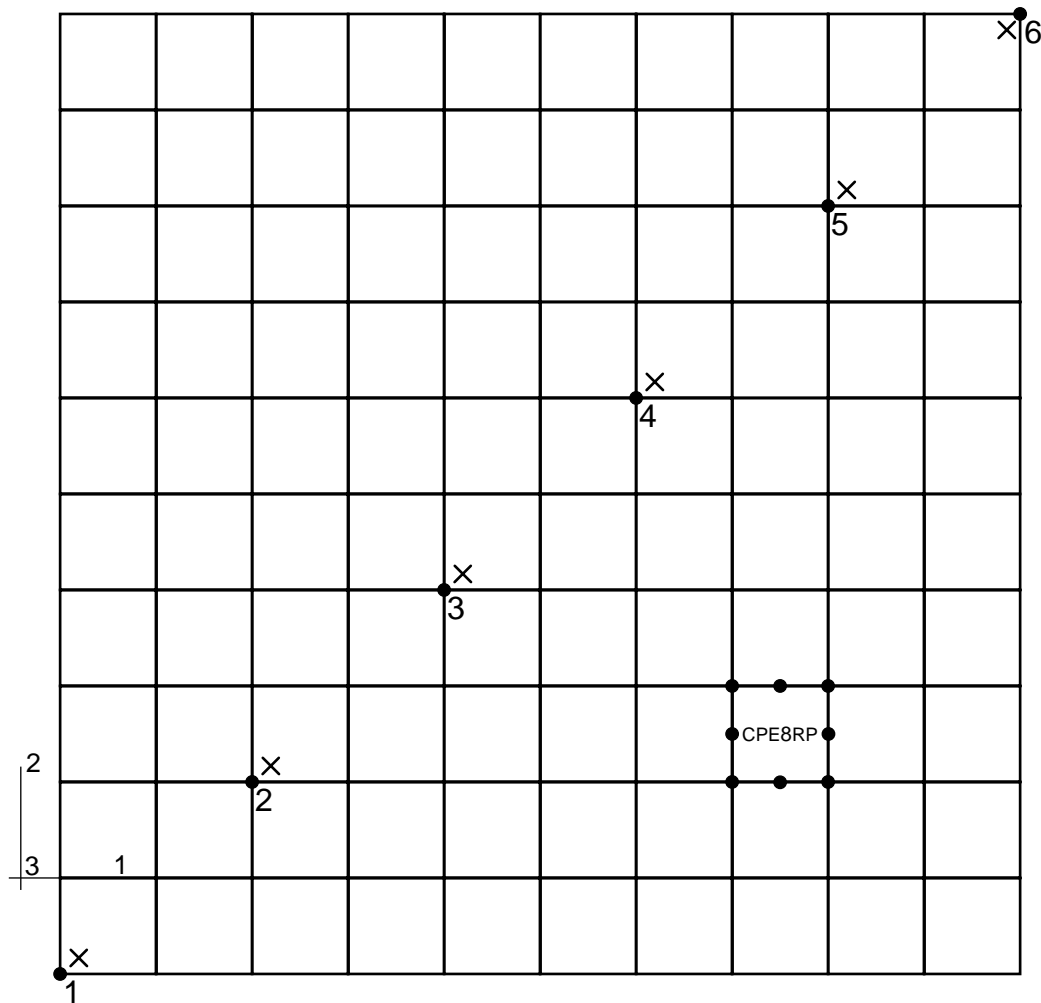
Finally, we model the rewetting process over a time period of 800 seconds in the third step, by once again prescribing a zero pressure corresponding to full saturation at the center of the sample.

The analysis is performed with the *SOILS, CONSOLIDATION procedure using automatic time incrementation. UTOL, the pore pressure tolerance that controls the automatic incrementation, is set to a large value since we expect the nonlinearity of the material to restrict the size of the time increments during the transient stages of the analysis.

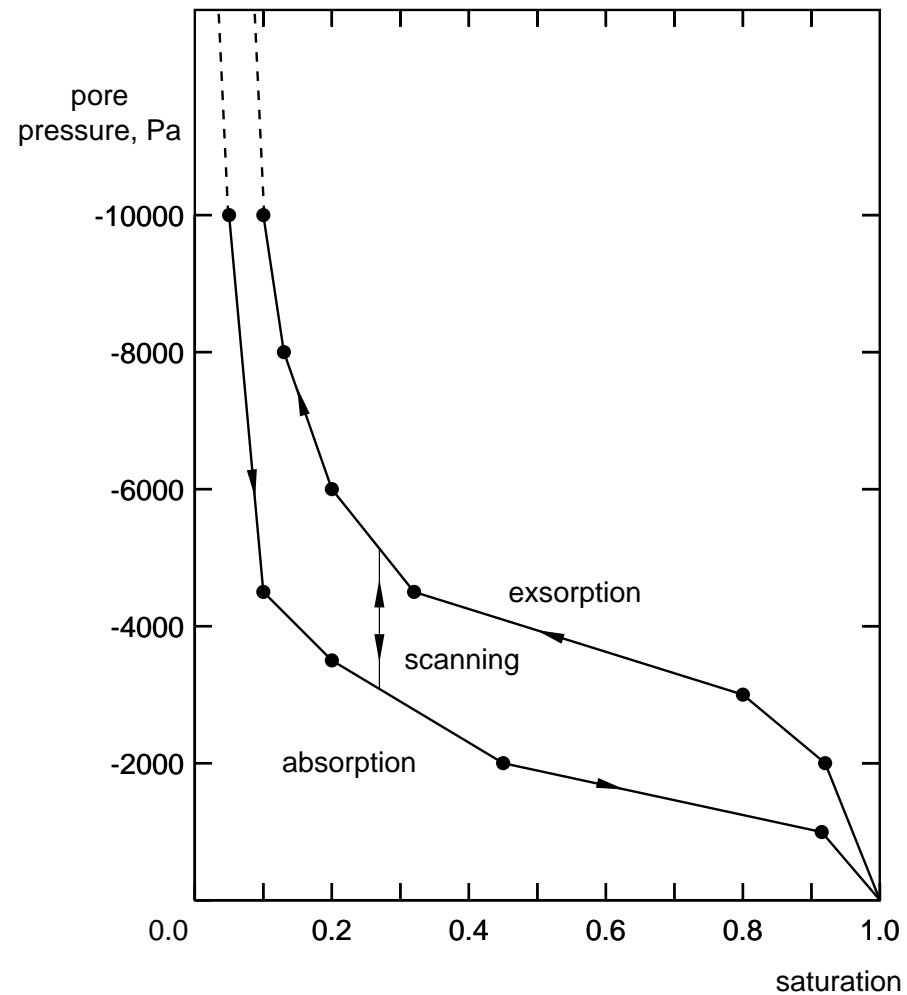
Since the volume occupied by the sample is fixed (all displacements have been constrained) we must expect the volume of fluid absorbed to be the same in the cases of the sample with and without gel particles. The difference will be in the proportions of the volume of the sample that will be occupied by free fluid and fluid trapped in the gel particles.

Time histories of the response at six nodes along the diagonal of the sample are shown.

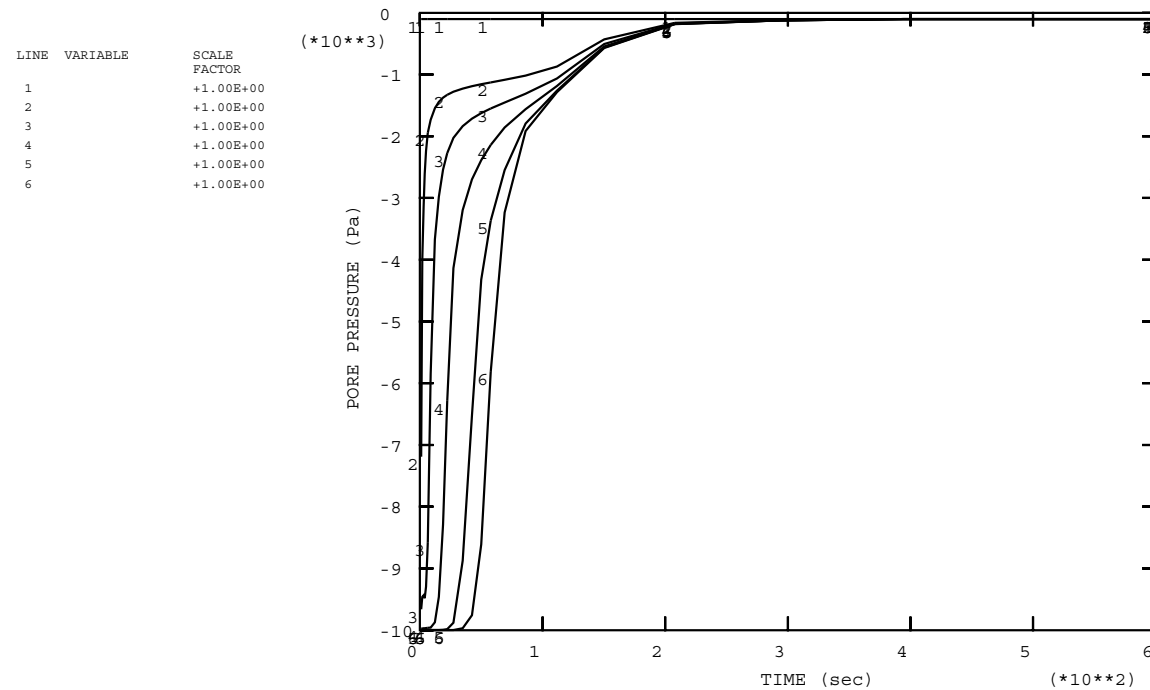
The cyclic wetting response of the sample is also shown.



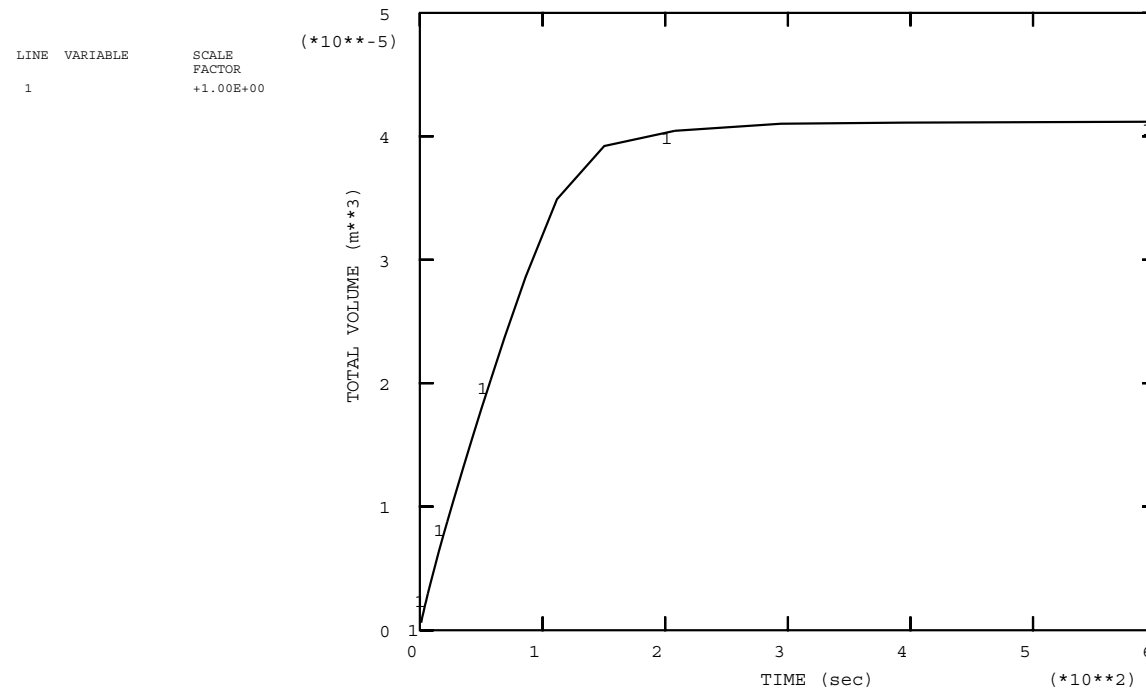
Finite Element Model



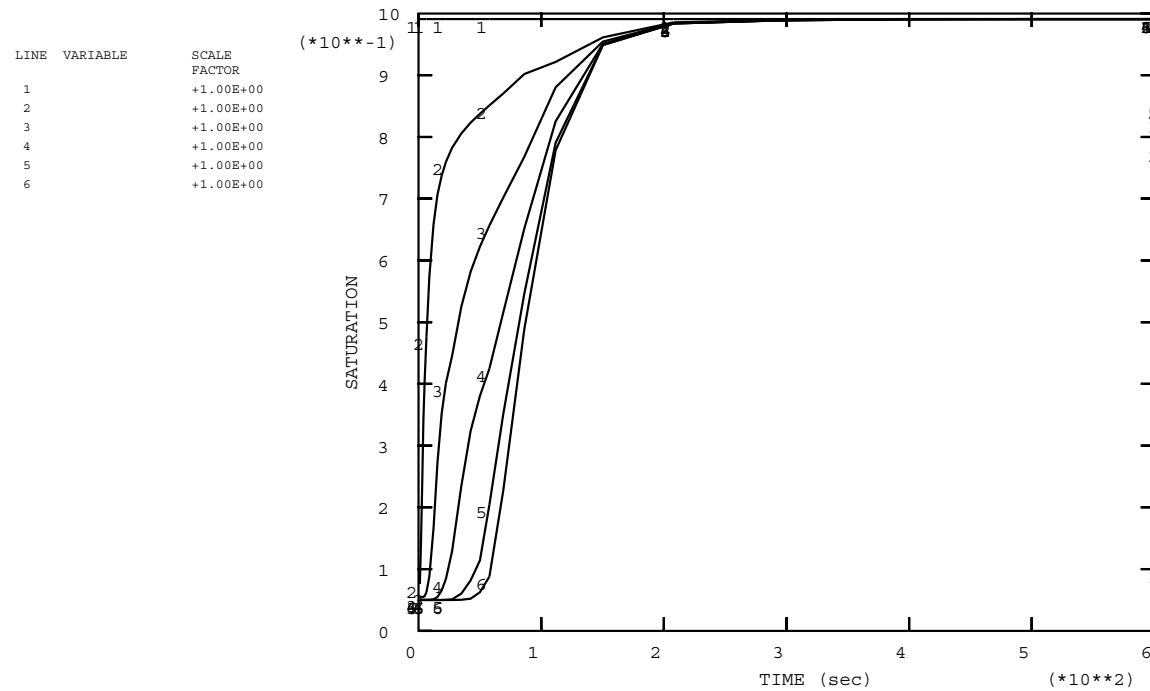
Absorption/Exsorption Curves



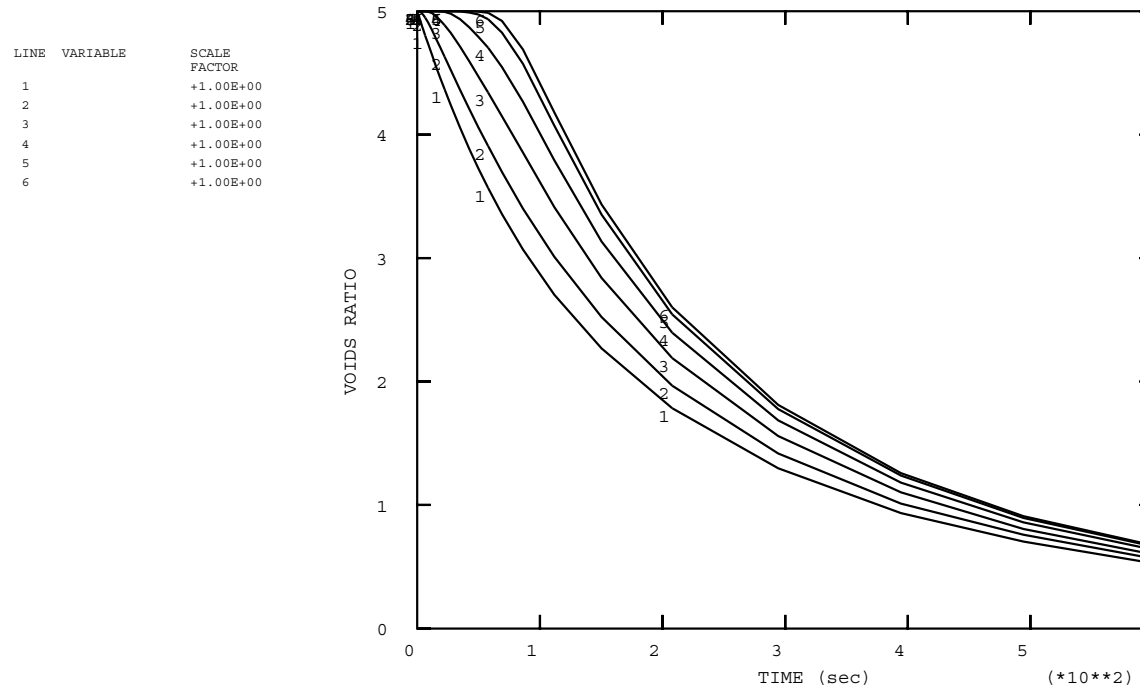
Pore Pressure for Samples With and Without Gel



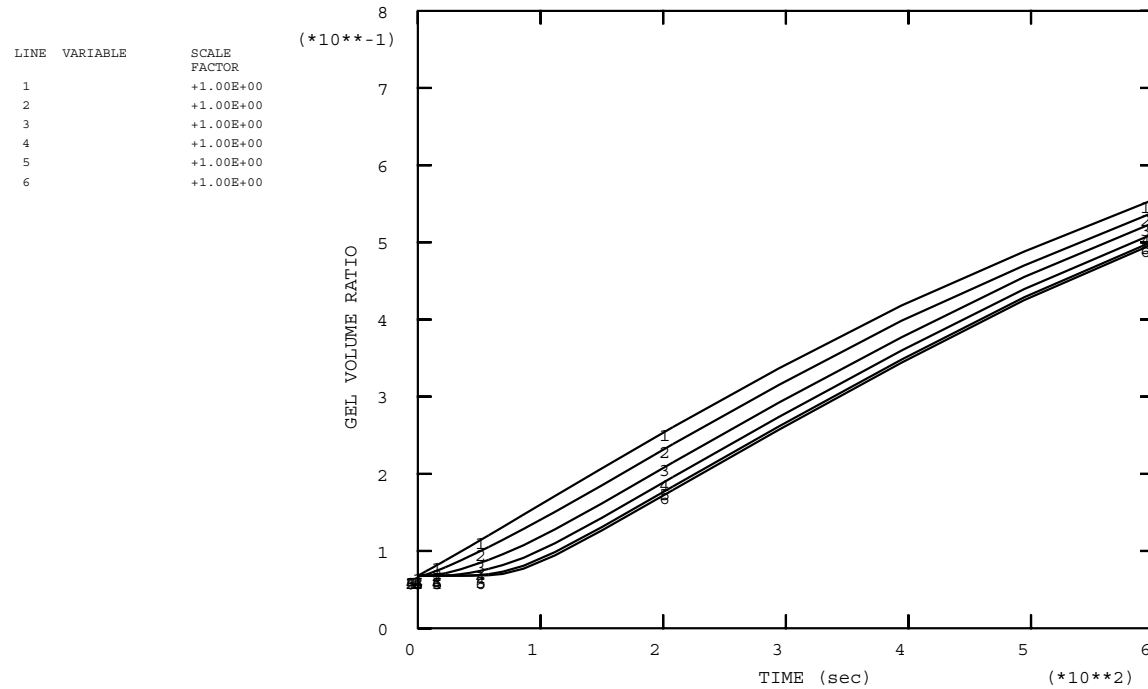
Fluid Volume Absorbed for Samples With and Without Gel



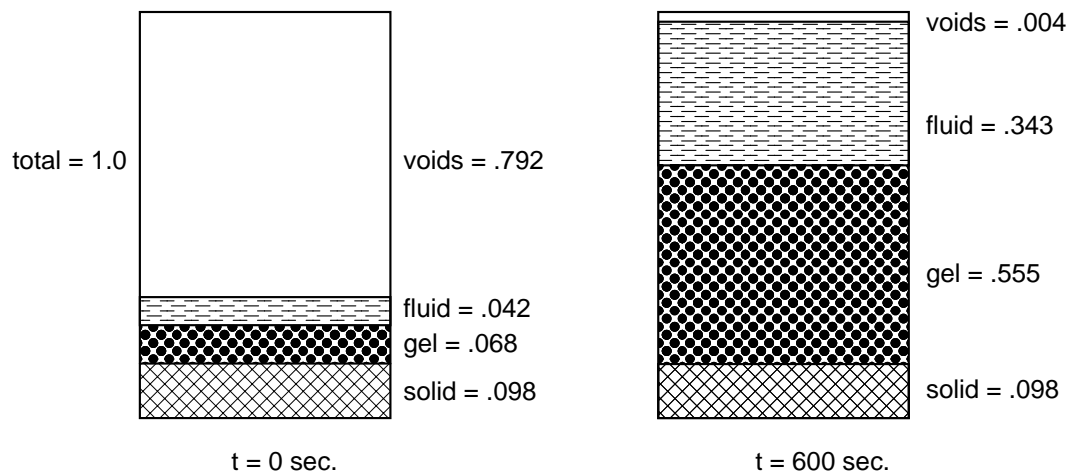
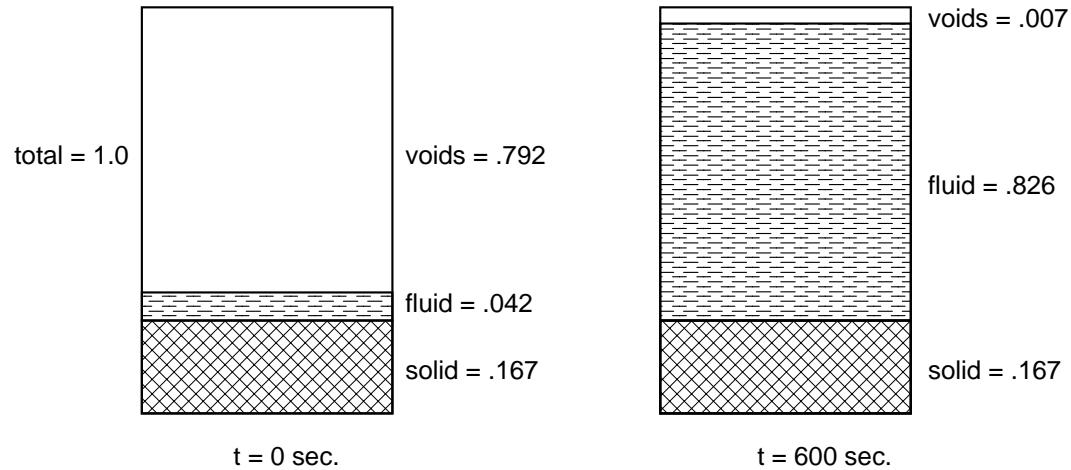
Saturation for Samples With and Without Gel

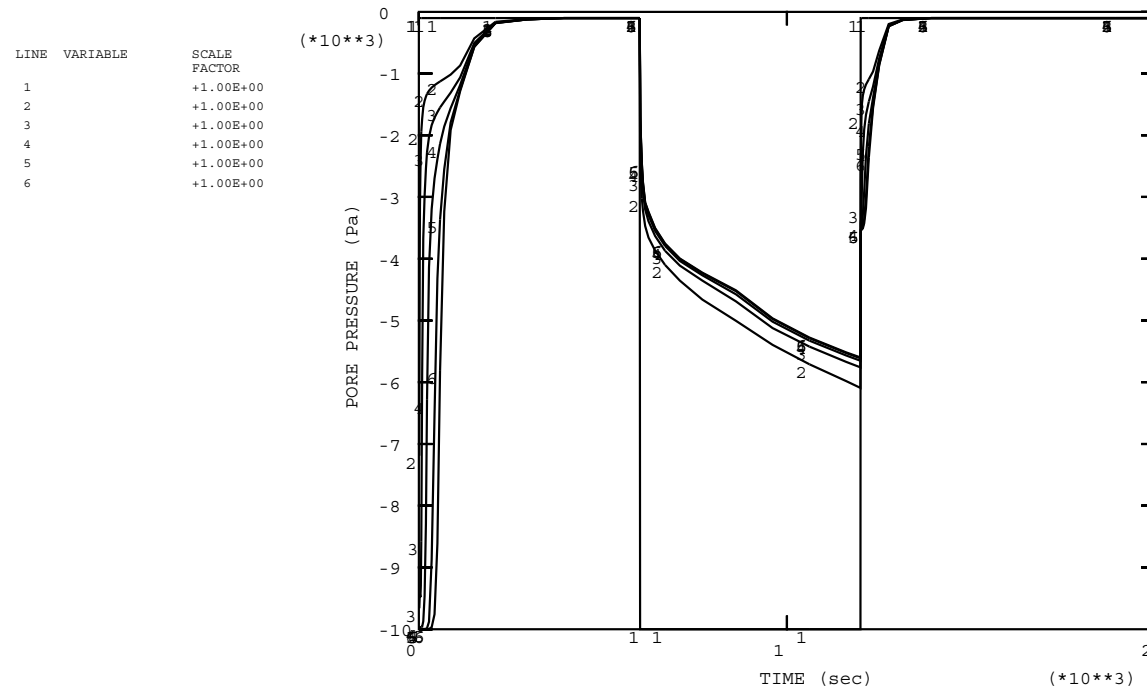


Void Ratio for Sample With Gel

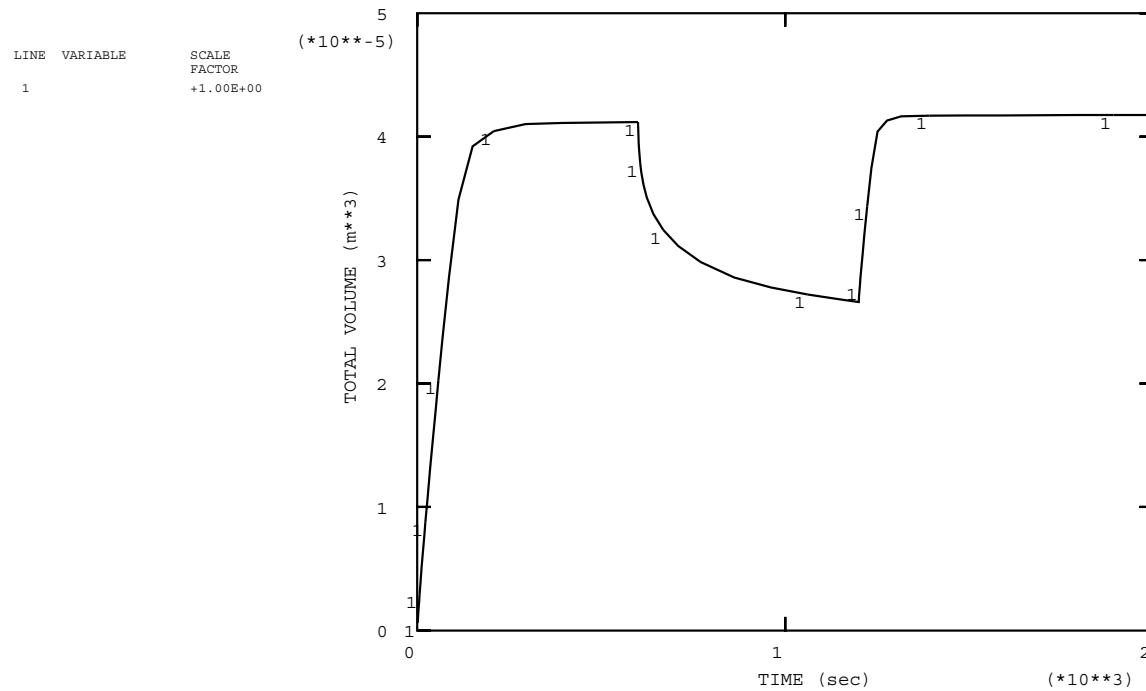


Gel Volume Ratio for Sample With Gel

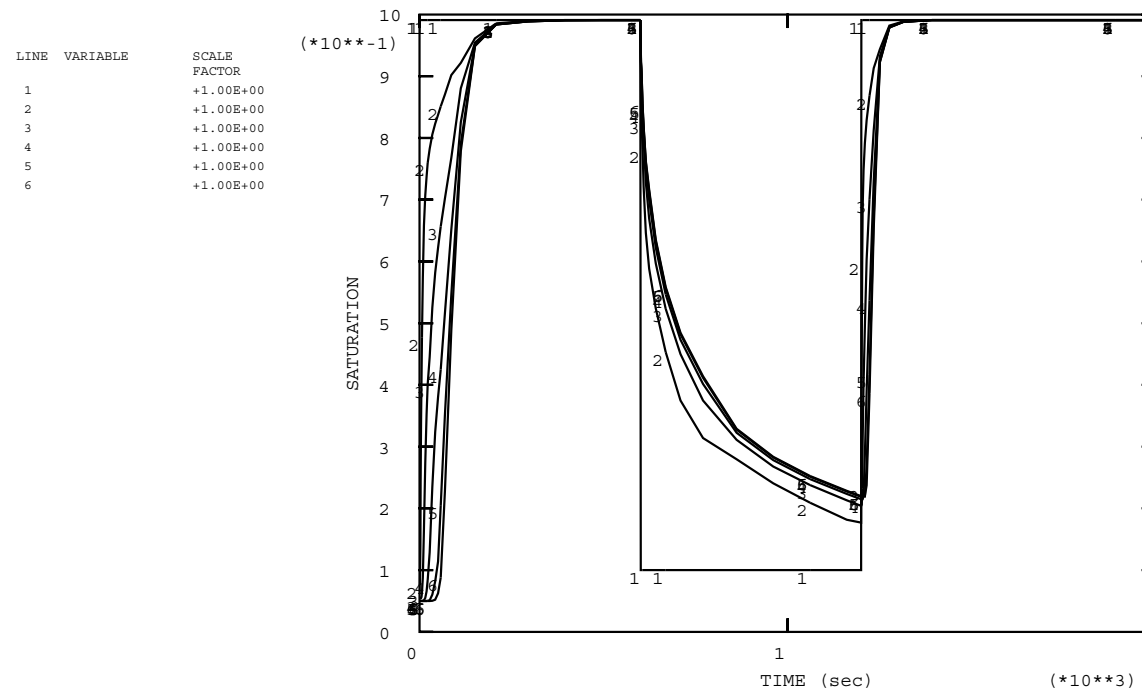




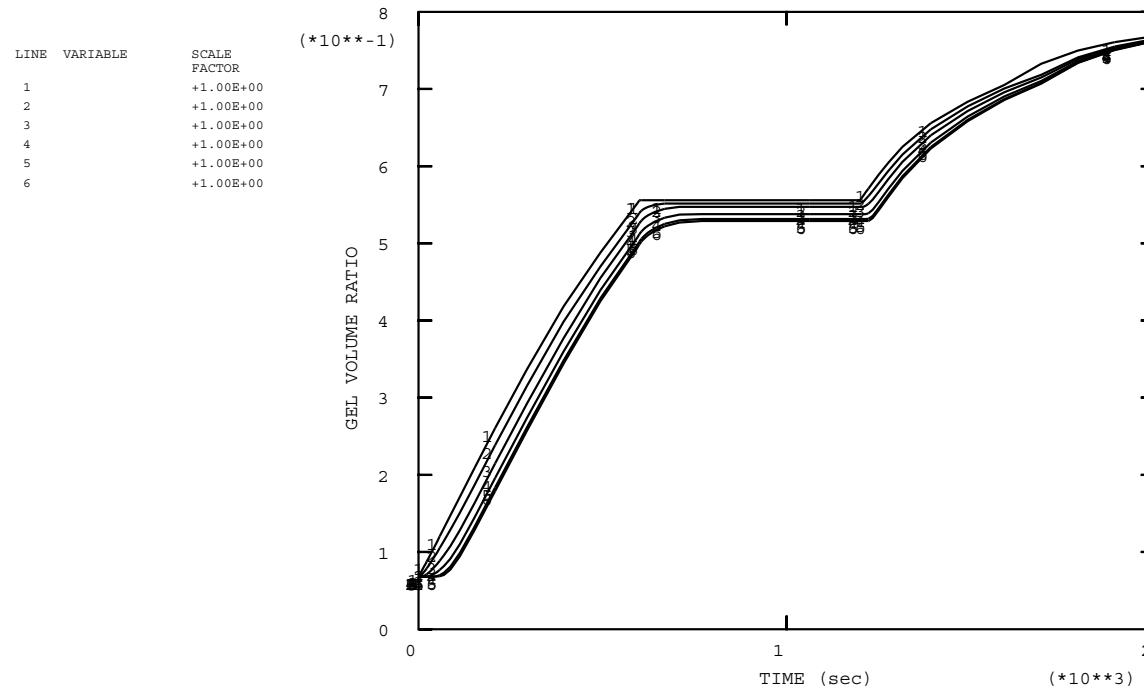
Pore Pressure in Cyclic Wettability Test



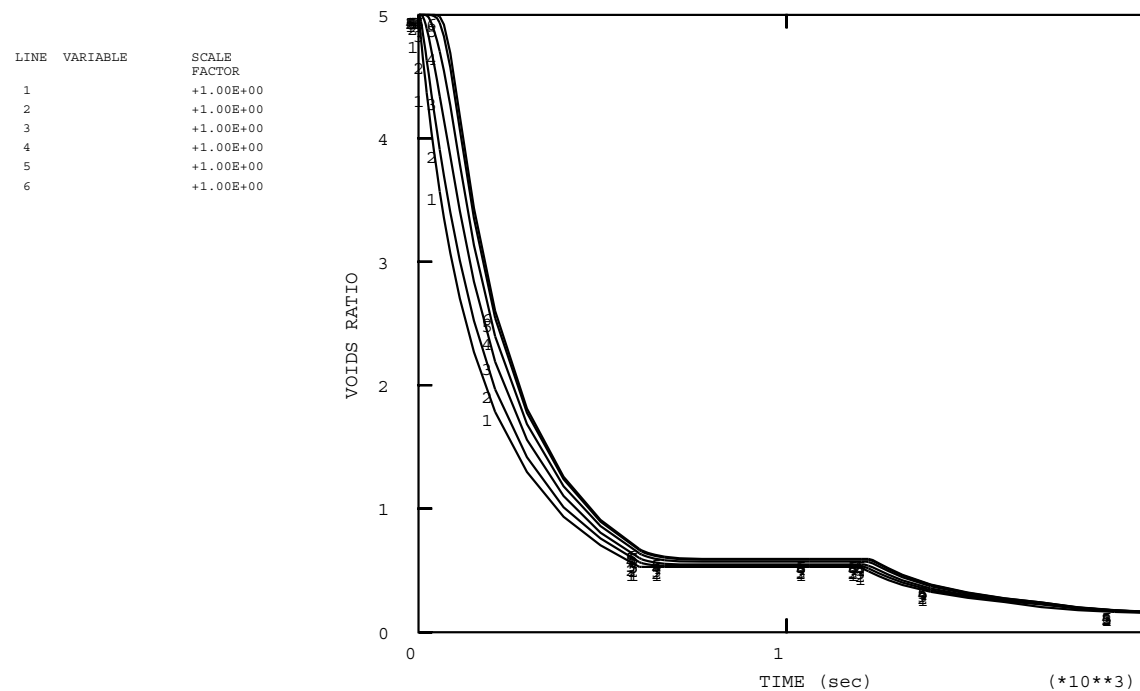
Fluid Volume Absorbed in Cyclic Test



Saturation in Cyclic Wettability Test



Gel Volume Ratio in Cyclic Wettability Test



Void Ratio in Cyclic Wettability Test

Cyclic Demand Wettability Test Input File:

```
*HEADING
2-D CYCLIC DEMAND WETTABILITY,WITH GEL
*** UNITS: M, SEC, NEWTON
*NODE,NSET=ALLN
1,0.,0.
21,.0508,0.
801,0.,.0508
821,.0508,.0508
*NGEN,NSET=BOT
1,21,1
*NGEN,NSET=TOP
801,821,1
*NFill,NSET=ALLN
BOT,TOP,20,40
*NSET,NSET=OUTN
1,165,329,493,657,821
*ELEMENT,TYPE=CPE8RP,ELSET=BLOCK
1,1,3,83,81,2,43,82,41
*ELGEN,ELSET=BLOCK
1,10,2,1,10,80,10
```



```
*ELSET, ELSET=OUTE
1, 23, 45, 67, 89, 100
*SOLID SECTION, ELSET=BLOCK, MATERIAL=CORE
.02
*MATERIAL, NAME=CORE
*PERMEABILITY, SPECIFIC WEIGHT=10000.
3.7E-4
*SORPTION
-100000., .04
-10000., .05
-4500., .1
-3500., .18
-2000., .45
-1000., .91
0., 1.
*SORPTION, TYPE=EXSORPTION
-100000., .09
-10000., .1
-8000., .11
-6000., .18
-4500., .33
-3000., .79
```



```
-2000.,.91
0.,1.
*POROUS BULK MODULI
,100000000.
*GEL
.0005,.0015,1.E8,500.
*INITIAL CONDITIONS,TYPE=SATURATION
ALLN,.05
*NSET,NSET=NPOR,GENERATE
1,21,2
81,101,2
161,181,2
241,261,2
321,341,2
401,421,2
481,501,2
561,581,2
641,661,2
721,741,2
801,821,2
*INITIAL CONDITIONS,TYPE=PORE PRESSURE
NPOR,-10000.
```



```
*INITIAL CONDITIONS,TYPE=RATIO
ALLN,5.
*RESTART,WRITE,FREQUENCY=10
*STEP,INC=50,AMPLITUDE=STEP
*SOILS,CONSOLIDATION,UTOL=10000.
1.,600.,,100.0
*BOUNDARY
ALLN,PINNED
1,8,, -100.
*CONTROLS,PARAMETERS=FIELD,FIELD=PORE FLUID PRESSURE
.01,1.,,1.E-6
*CONTROLS,ANALYSIS=DISCONTINUOUS
*NODE PRINT,FREQUENCY=10,NSET=NPOR
POR,RVF,RVT
*EL PRINT,FREQUENCY=10
SAT,POR,VOIDR,GELVR
*NODE FILE,FREQUENCY=1,NSET=OUTN
POR,RVF,RVT
*EL FILE,FREQUENCY=1,ELSET=OUTE
SAT,POR,VOIDR,GELVR
*END STEP
*STEP,INC=20,AMPLITUDE=STEP
```



```
*SOILS, CONSOLIDATION, UTOL=10000.  
1., 600., , 100.0  
*BOUNDARY  
ALLN, PINNED  
1, 8, , -10000.  
*END STEP  
*STEP, INC=20, AMPLITUDE=STEP  
*SOILS, CONSOLIDATION, UTOL=10000.  
1., 800., , 100.0  
*BOUNDARY  
ALLN, PINNED  
1, 8, , -100.  
*END STEP
```

Desaturation of Soil Column (Transient)

This example validates the ABAQUS capability to solve coupled fluid flow problems in partially saturated porous media where the effects of gravity are important (Benchmark Problem 1.8.4).

We compare ABAQUS results with the experimental work of Liakopoulos (1965). The Liakopoulos experiment consists of the drainage of water from a vertical column of sand. A column is filled with sand and instrumented to measure the moisture pressure through its height.

Prior to the start of the experiment, water is added continually at the top and allowed to drain freely at the bottom. The flow is regulated until zero pore pressure readings are obtained throughout the column.

At this point flow is stopped and the experiment starts: the top of the column is made impermeable and the water is allowed to drain out of the column, under gravity. Pore pressures are measured.

We investigate two cases: one in which the column is not allowed to deform (uncoupled flow problem), and the other in which we consider the deformation of the sand (coupled problem).

The weight is applied by GRAV loading. In the case of the deforming column, an initial step of *GEOSTATIC analysis is performed to establish the initial equilibrium state.

The initial conditions exactly balance the weight of the fluid and dry material so that no deformation takes place, while the zero pore pressure boundary conditions enforce the initial steady state of fluid flow.

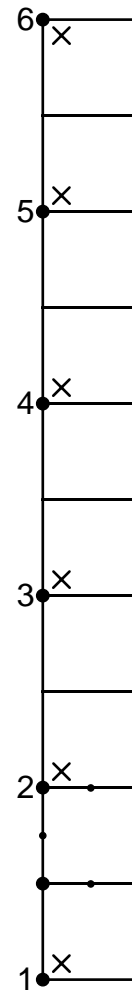
Then the fluid is allowed to drain through the bottom of the column, by prescribing zero pore pressures at these nodes, during a *SOILS, CONSOLIDATION step. The fluid will drain until the pressure gradient is equal to the weight of the fluid, at which time equilibrium is established.

The transient analysis is performed using automatic time incrementation. UTOL, the pore pressure tolerance that controls the automatic incrementation, is set to a large value since we expect the nonlinearity of the material to restrict the time increment size.

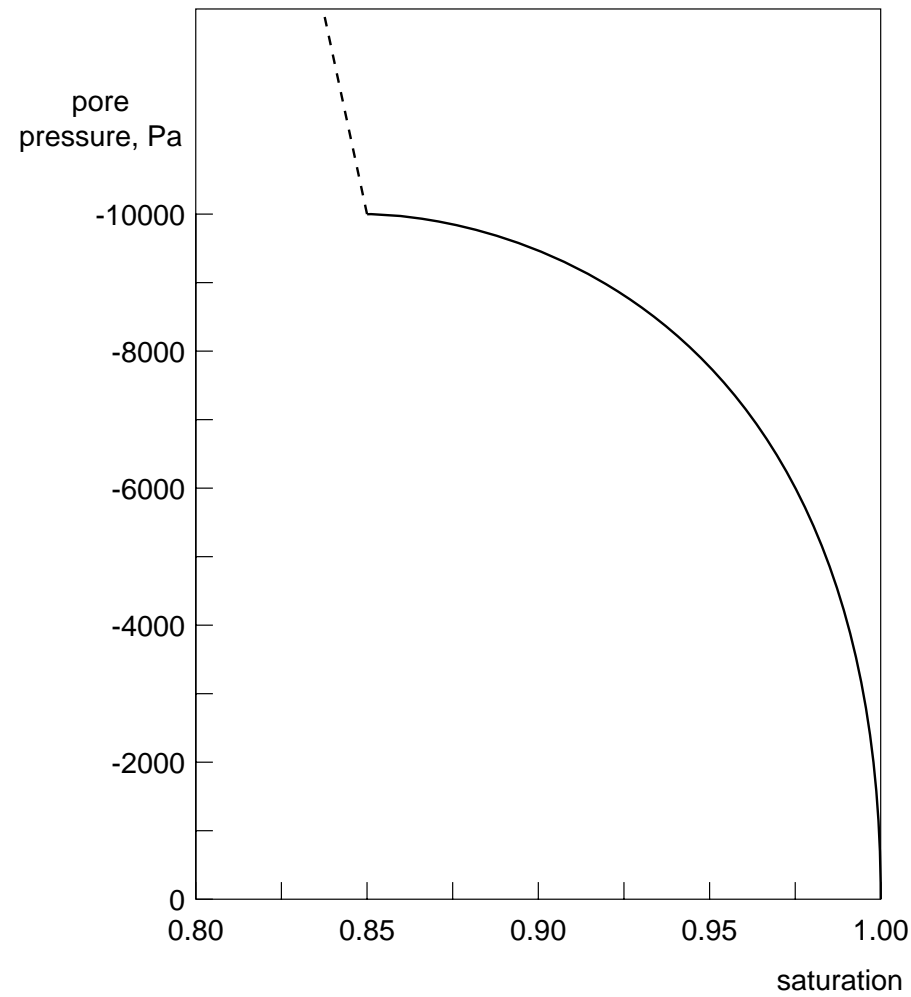
The pore pressure results of the coupled analysis are closer to the experiment than those of the uncoupled analysis; the uncoupled analysis overestimates the pore pressures in the early stages of the transient. It suggests that the coupled analysis is a better approximation of reality, as we would expect.

As the transient continues, the material deformation slows (see the displacement histories of six points along the height of the column) and therefore the rigid column assumption becomes closer to reality; as steady state is approached both numerical solutions are in good agreement with the experiment.

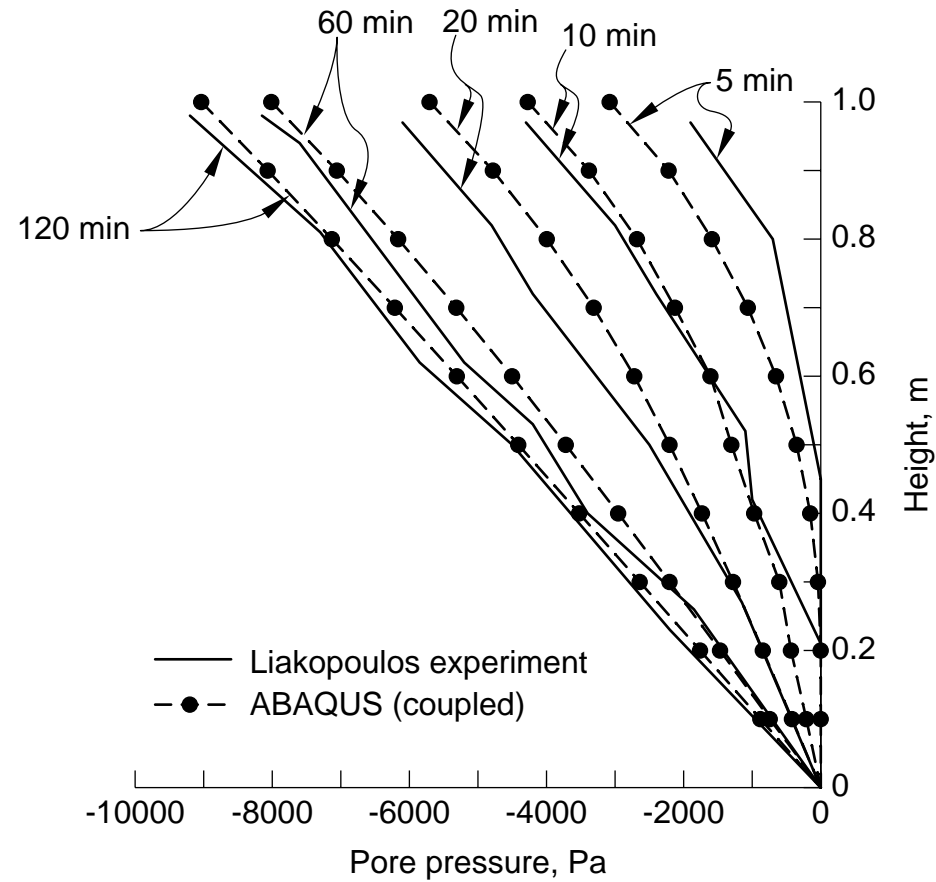
At steady state, the pore pressure gradient equals the fluid weight density as required by Darcy's law.



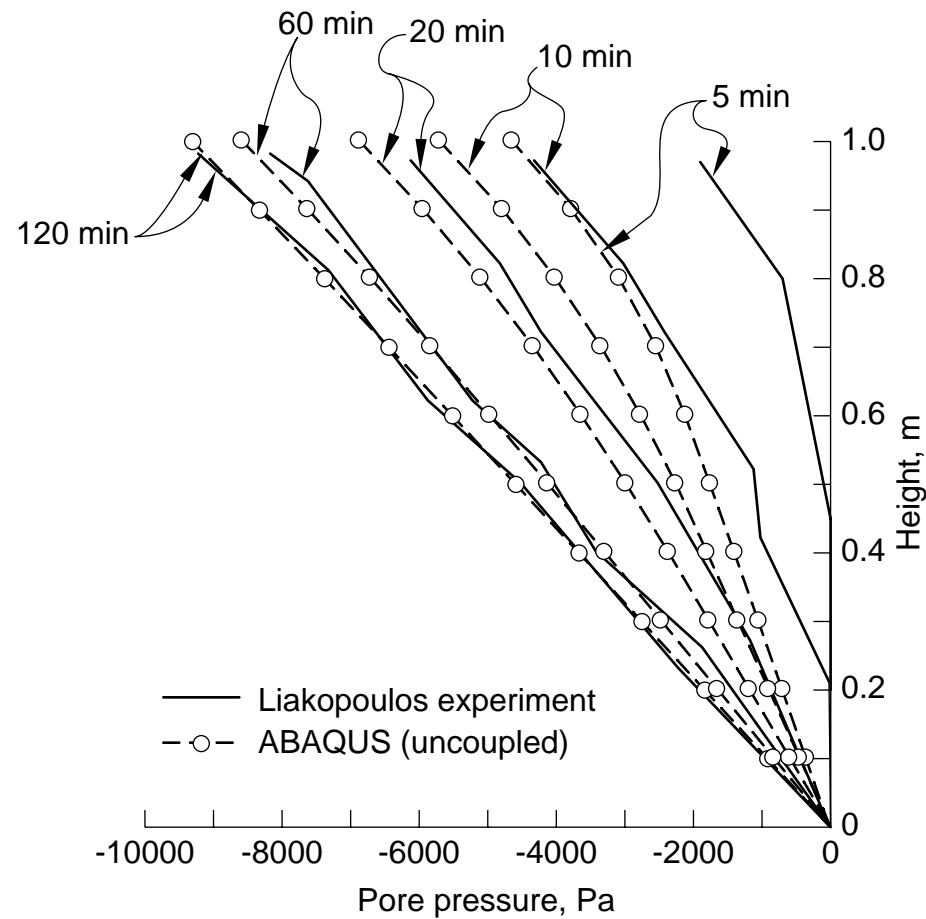
Finite Element Model



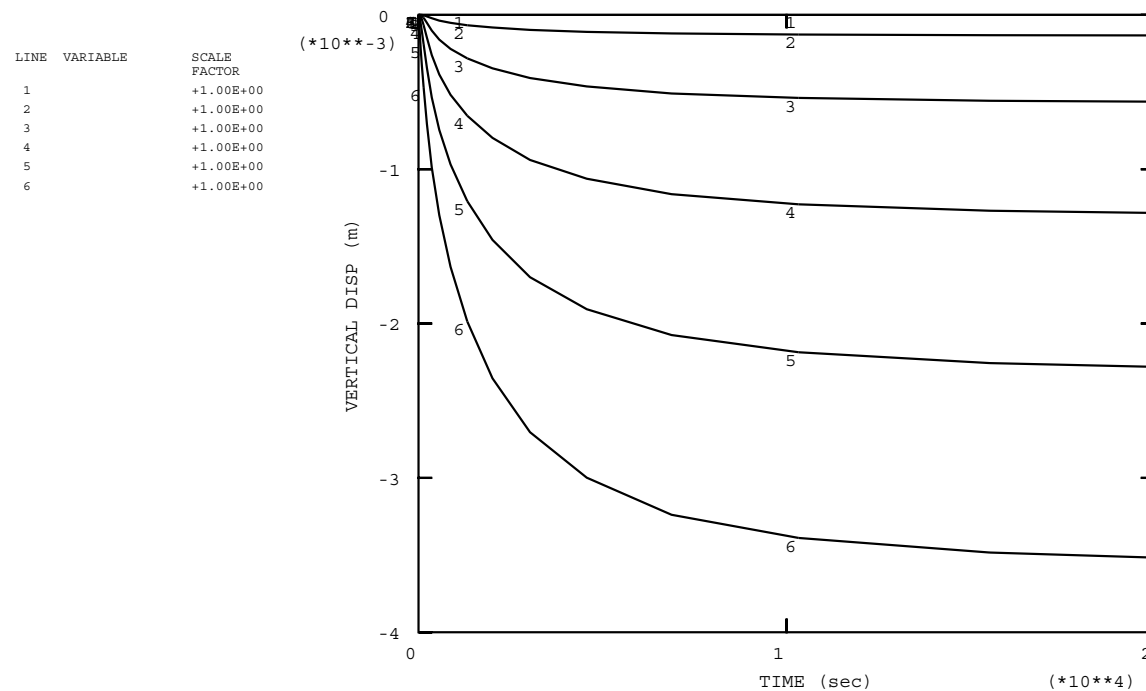
Absorption/Exsorption Curve



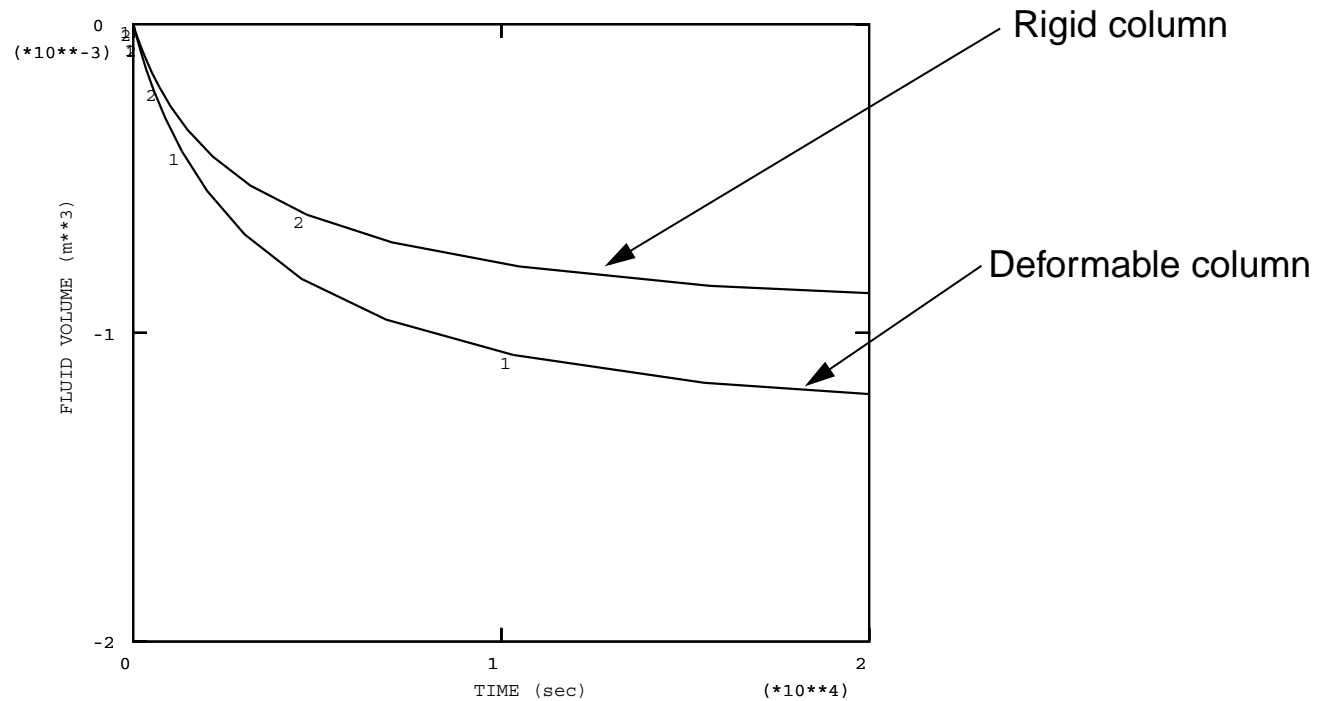
Pore Pressure Profiles (Deformable Column)



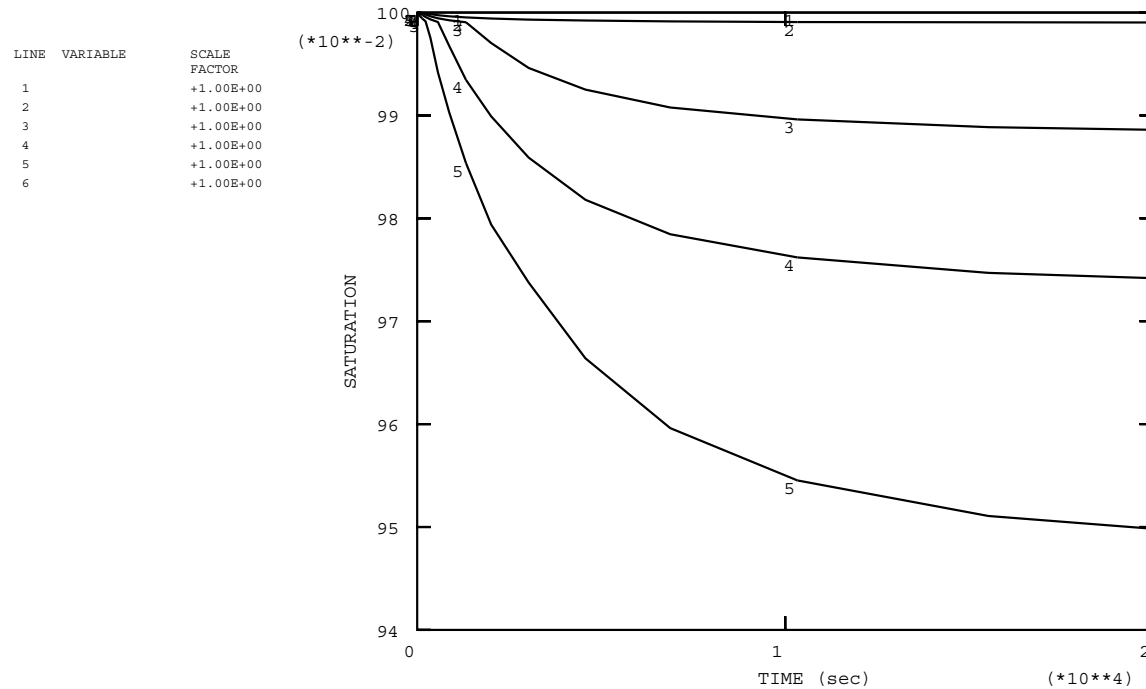
Pore Pressure Profiles (Rigid Column)



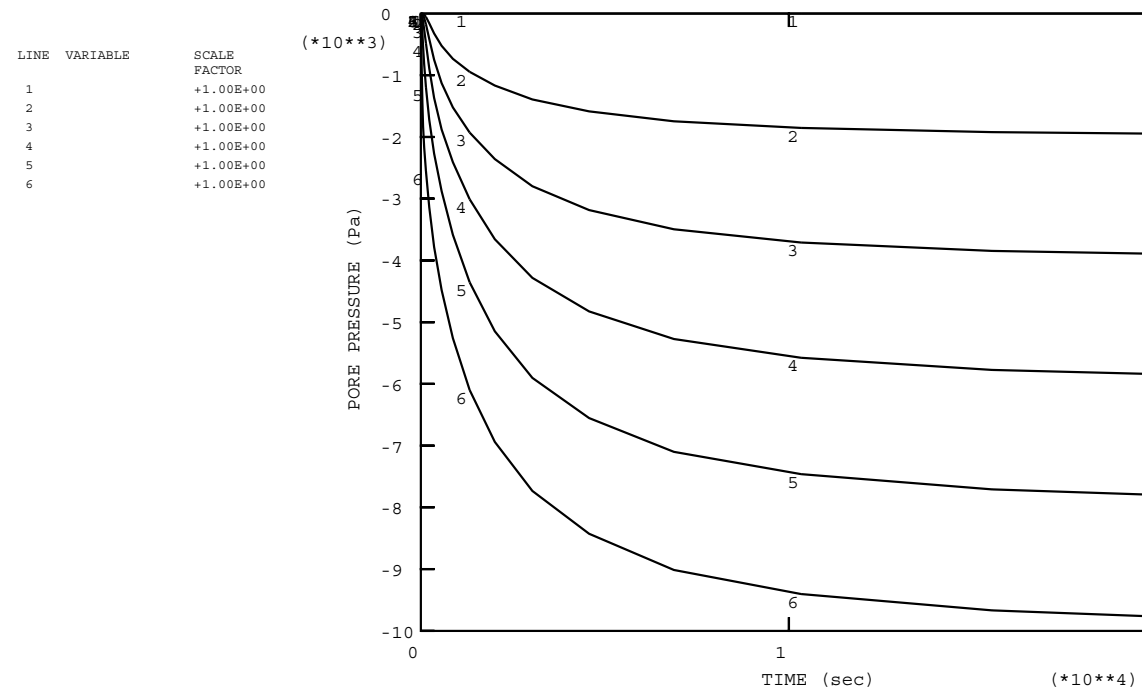
Displacement Histories (Deformable Column)



Fluid Volume Lost (Deformable and Rigid Columns)



Saturation Histories



Pore Pressure Histories

Desaturation Example Input File:

```
*HEADING
ONE DIMENSIONAL DESATURATION PROBLEM, COUPLED
*** UNITS: M, TON, SEC, KN
*NODE,NSET=ALLN
1,0.,0.
3,.1,0.
101,0.,1.
103,.1,1.
*NGEN,NSET=BOT
1,3,1
*NGEN,NSET=TOP
101,103,1
*NFILL,NSET=ALLN
BOT,TOP,20,5
*NSET,NSET=LHS,GENERATE
1,101,5
*NSET,NSET=RHS,GENERATE
3,103,5
*ELEMENT,TYPE=CPE8RP,ELSET=BLOCK
1,1,3,13,11,2,8,12,6
```



```
*ELGEN, ELSET=BLOCK
1,10,10,1
*ELSET, ELSET=OUTE
1,3,5,7,9
*SOLID SECTION, ELSET=BLOCK, MATERIAL=CORE
*MATERIAL, NAME=CORE
*ELASTIC
1.3E3, 0.
*DENSITY
1.5
*POROUS BULK MODULI
, 2.E6
*PERMEABILITY, SPECIFIC WEIGHT=10.
4.5E-6
*PERMEABILITY, TYPE=SATURATION
.666666, .85
1., 1.
*SORPTION
-100., .8
-10., .85
-9.5, .9
-9., .922
```



```
-8.,.947
-7.,.961
-6.,.973
-4.,.988
-2.,.999
0.,1.
*SORPTION,TYPE=EXSORPTION
-100.,.8
-10.,.85
-9.5,.9
-9.,.922
-8.,.947
-7.,.961
-6.,.973
-4.,.988
-2.,.999
0.,1.
*INITIAL CONDITIONS,TYPE=SATURATION
ALLN,1.
*NSET,NSET=NPOR,GENERATE
1,101,10
3,103,10
```



```
*INITIAL CONDITIONS,TYPE=PORE PRESSURE
NPOR,0.
*INITIAL CONDITIONS,TYPE=RATIO
ALLN,.4235
*INITIAL CONDITIONS,TYPE=STRESS,GEOSTATIC
BLOCK,0.,1.,-17.9750615,0.,0.,0.
*EQUATION
2
3,8,1.,1,8,-1.
*BOUNDARY
ALLN,1
BOT,2
*RESTART,WRITE,FREQUENCY=10
*STEP,INC=1
*GEOSTATIC
1.E-6,1.E-6
*DLOAD
BLOCK,GRAV,10.,0.,-1.,0.
*BOUNDARY
NPOR,8,,0.
*NODE PRINT,FREQUENCY=5,NSET=LHS
U,RF,POR,RVT
```



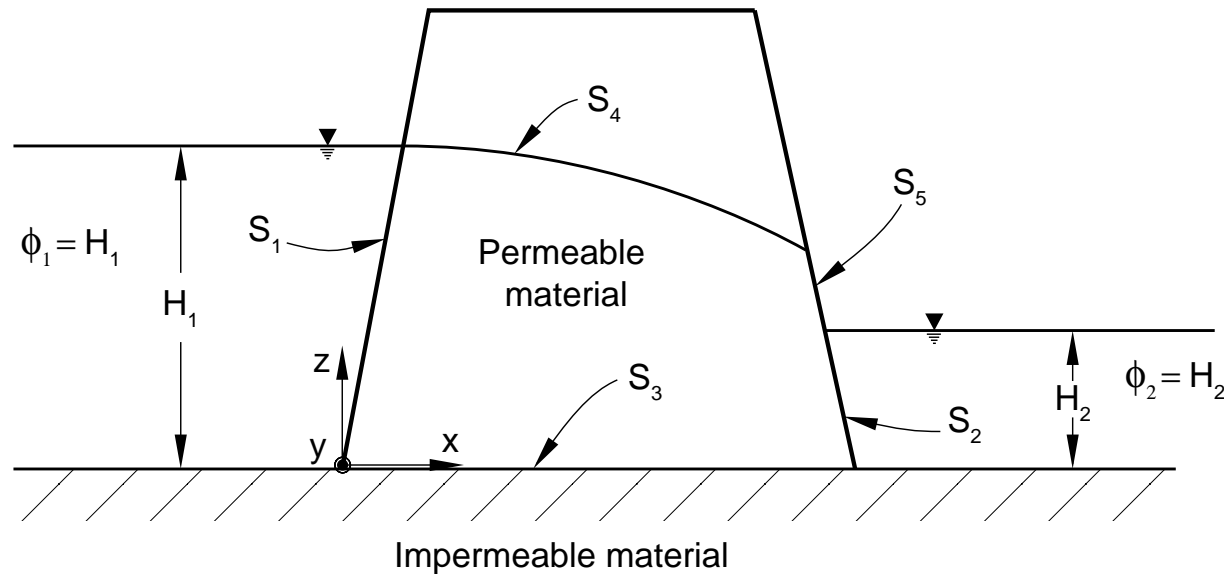
```
*EL PRINT,FREQUENCY=5,ELSET=OUTE  
S,E  
SAT,POR,VOIDR  
*NODE FILE,FREQUENCY=10,NSET=LHS  
U,RF,POR,RVT  
*EL FILE,FREQUENCY=10,ELSET=OUTE  
S,E  
SAT,POR,VOIDR  
*END STEP  
*STEP,INC=100  
*SOILS,CONSOLIDATION,UTOL=10.  
20.,50000.  
*BOUNDARY,OP=NEW  
1,8,,0.  
ALLN,1,,0.  
BOT,2,,0.  
*CONTROLS,ANALYSIS=DISCONTINUOUS  
*END STEP
```

Phreatic Surface Calculation (Steady-State)

This example (Example Problem 8.1.2) illustrates the use of ABAQUS to solve for the flow through a porous medium in which fluid flow is occurring in a gravity field and only part of the region is fully saturated, so that the location of the phreatic surface is a part of the solution. Such problems are common in hydrology. An example is the well draw-down problem, where the phreatic surface of an aquifer must be located, based on pumping rates at particular well locations.

The basic approach takes advantage of the ABAQUS capability to perform partially and fully saturated analysis: the phreatic surface is located as the boundary of the fully saturated part of the model. This approach has the advantage that the capillary zone, just above the phreatic surface, is also identified.

We consider fluid flow only: deformation is ignored.

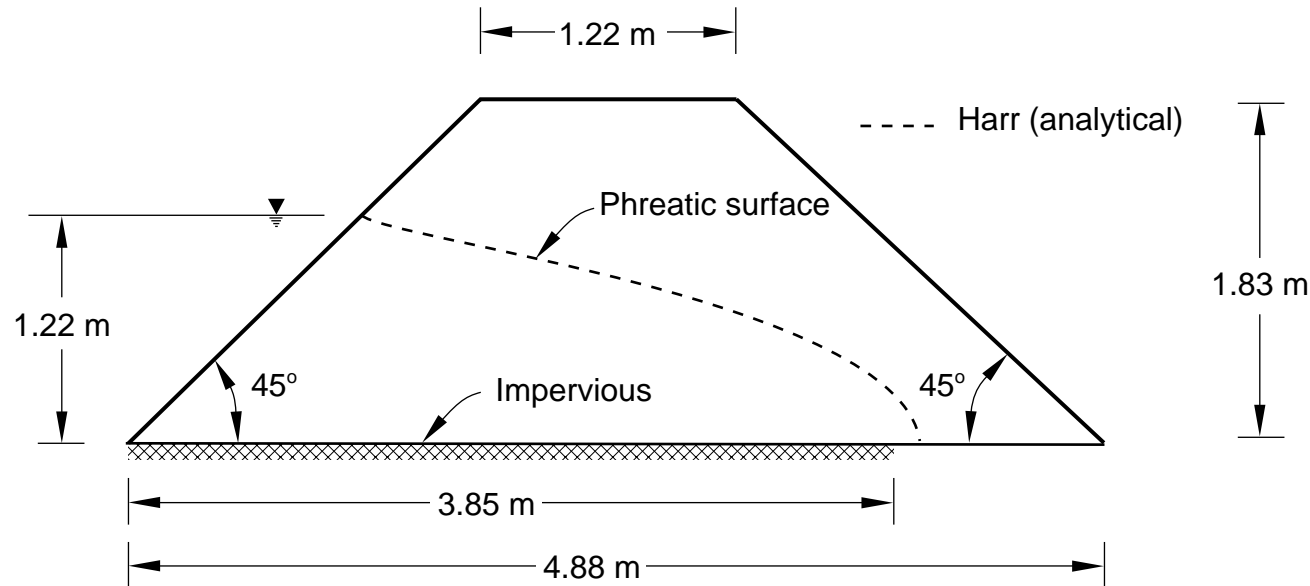


The upstream face of the dam (surface S_1) is exposed to water in the reservoir behind the dam. Since ABAQUS uses a total pore pressure formulation, the pore pressure on this face must be prescribed to be $u_w = (H_1 - z)g\rho_w$. Likewise, on the downstream face of the dam (surface S_2), $u_w = (H_2 - z)g\rho_w$.

The bottom of the dam (surface S_3) is assumed to rest on an impermeable foundation. Since the natural boundary condition in the pore fluid flow formulation provides no flow of fluid across a surface of the model, no further specification is needed on this surface.

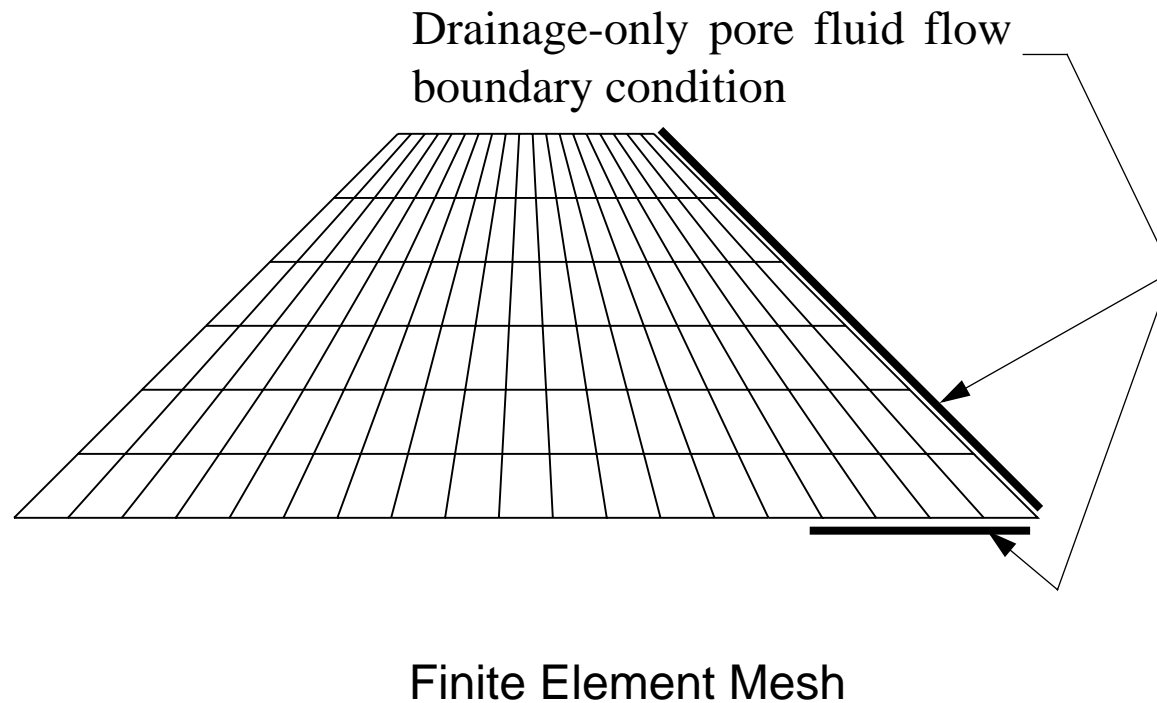
The phreatic surface in the dam, S_4 , is found as the locus of points at which the pore fluid pressure, u_w , is zero. Above this surface the pore fluid pressure is negative, representing capillary tension causing the fluid to rise against the gravitational force and thus creating a capillary zone. The saturation associated with particular values of capillary pressure is given by the absorption/exsorption curves.

A special boundary condition is needed if the phreatic surface reaches an open, freely draining surface, as indicated on surface S_5 . In such a case the pore fluid can drain freely down the face of the dam, so that $u_w = 0$ at all points on this surface below its intersection with the phreatic surface. Above this point $u_w < 0$, with its particular value depending on the solution.



Earth Dam and Analytical Phreatic Surface

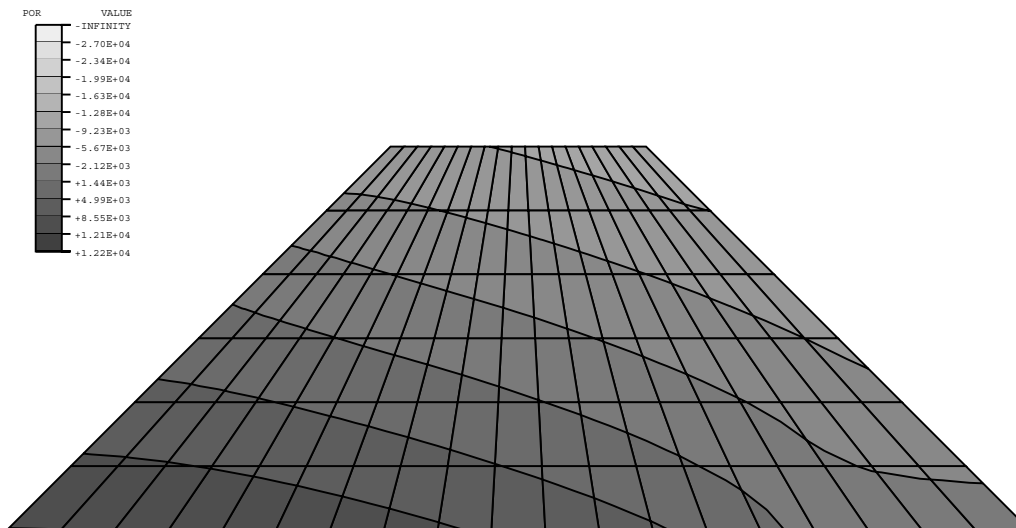
This example is specifically chosen to include this effect, to illustrate the use of the ABAQUS drainage-only flow boundary condition (*FLOW with the drainage-only flow type label QnD).



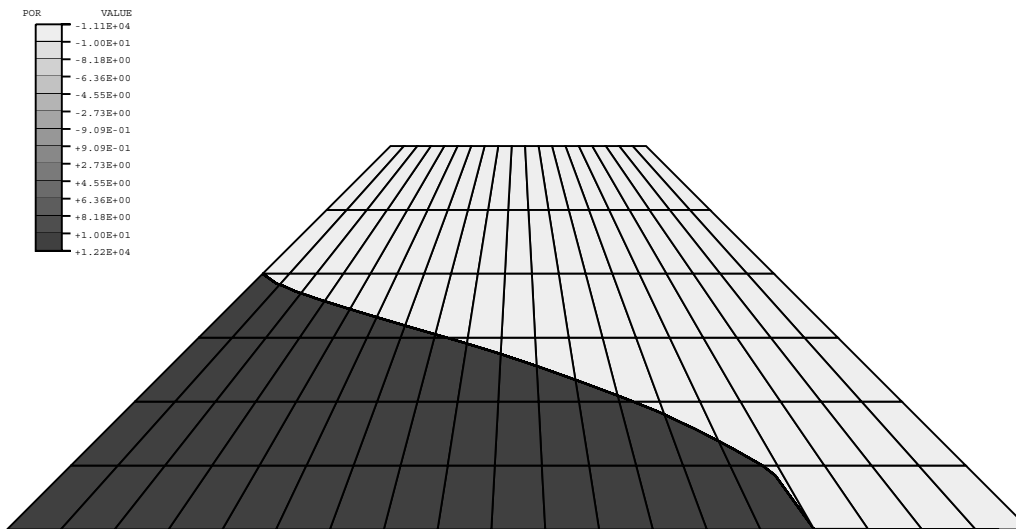
The finite element model shows the element edges where the drainage-only boundary condition is applied. On these edges, the pore fluid pressure, u_w , is constrained by a penalty method to be less than or equal to zero, thus enforcing the proper drainage-only behavior.

The weight of the water is applied by GRAV loading and the upstream and downstream pore pressures are prescribed as discussed above. A steady-state *SOILS analysis is performed in five increments to allow ABAQUS to resolve the high degree of nonlinearity.

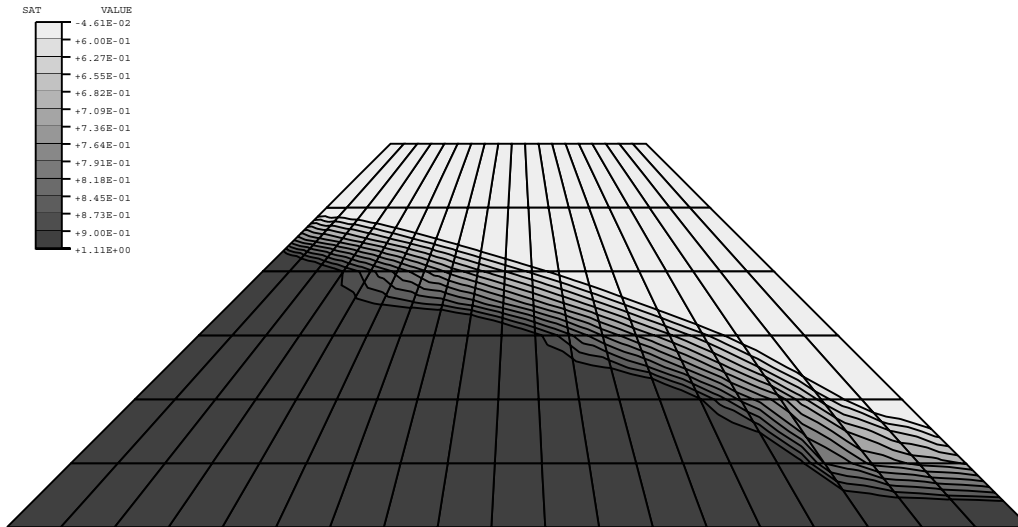
Examining the steady-state contours of pore pressure we see that the upper right part of the dam shows negative pore pressures, indicating that it is partly saturated or dry.



The phreatic surface is best shown when we draw the contours in the vicinity of zero pore pressure. This surface compares well with the analytical phreatic surface calculated by Harr (1962).



Phreatic Surface



The contours of saturation show a fully saturated region under the phreatic surface and decreasing saturation in and above the phreatic zone.

Phreatic Surface Calculation Input File:

```
*HEADING
EARTH DAM - STEADY STATE FREE SURFACE SEEPAGE
*** UNITS: M, KG, SEC, NEWTON
*NODE,NSET=ALLN
1,0.,0.
39,4.8768,0.
601,1.8288,1.8288
639,3.048,1.8288
*NGEN,NSET=BOT
1,39,1
*NGEN,NSET=TOP
601,639,1
*NFILL,NSET=ALLN
BOT,TOP,12,50
*NSET,NSET=POR0,GENERATE
1,39,2
*NSET,NSET=POR1,GENERATE
101,139,2
*NSET,NSET=POR2,GENERATE
201,239,2
```



```
*NSET,NSET=POR3,GENERATE
301,339,2
*NSET,NSET=POR4,GENERATE
401,439,2
*NSET,NSET=POR5,GENERATE
501,539,2
*NSET,NSET=POR6,GENERATE
601,639,2
*NSET,NSET=POR
  POR0, POR1, POR2, POR3
*NSET,NSET=OUTN,GENERATE
1,601,100
21,621,100
*ELEMENT,TYPE=CPE8RP,ELSET=DAM
1,1,3,103,101,2,53,102,51
*ELGEN,ELSET=DAM
1,19,2,1,6,100,20
*ELSET,ELSET=FSIDE,GENERATE
19,119,20
*ELSET,ELSET=FBOT,GENERATE
16,19
*ELSET,ELSET=OUTE,GENERATE
11,111,20
```



```
*SOLID SECTION,ELSET=DAM,MATERIAL=FILL
*MATERIAL,NAME=FILL
*ELASTIC
1000.,
*DENSITY
2000.,
*PERMEABILITY,SPECIFIC=10000.
2.1167E-4,
*SORPTION
-100000.,.04
-10000.,.05
0.,1.
*INITIAL CONDITIONS,TYPE=SATURATION
ALLN,1.
*INITIAL CONDITIONS,TYPE=PORE PRESSURE
POR, 12192.0, 0.0, 0.0, 1.2192
POR4,0.
POR5,0.
POR6,0.
*INITIAL CONDITIONS,TYPE=RATIO
ALLN,1.
```




```
*BOUNDARY
ALLN,1
ALLN,2
*RESTART,WRITE,FREQUENCY=10
*STEP,INC=5
*SOILS
.2,1.
*DLOAD
DAM,GRAV,10.,0.,-1.,0.
*BOUNDARY
1,8,,12192.
101,8,,9144.
201,8,,6096.
301,8,,3048.
401,8,,0.
*FLOW
FSIDE,Q2D,0.1
FBOT,Q1D,0.1
*CONTROLS,ANALYSIS=DISCONTINUOUS
*NODE PRINT,FREQUENCY=10,NSET=OUTN
POR,
```



```
*EL PRINT,FREQUENCY=10,ELSET=OUTE  
SAT,POR  
*NODE FILE,FREQUENCY=10,NSET=OUTN  
POR,  
*EL FILE,FREQUENCY=10,ELSET=OUTE  
SAT,POR  
*END STEP
```

Excavation and Building Analysis

Many geotechnical applications involve a sequence of steps, in each of which some material is removed or added.

Thus, geotechnical problems offer an interesting perspective on the need for generality in creating and using a finite element model: the model itself, and not just its response, changes with time.

The need for close liaison between the analysis and geometric modeling is important.

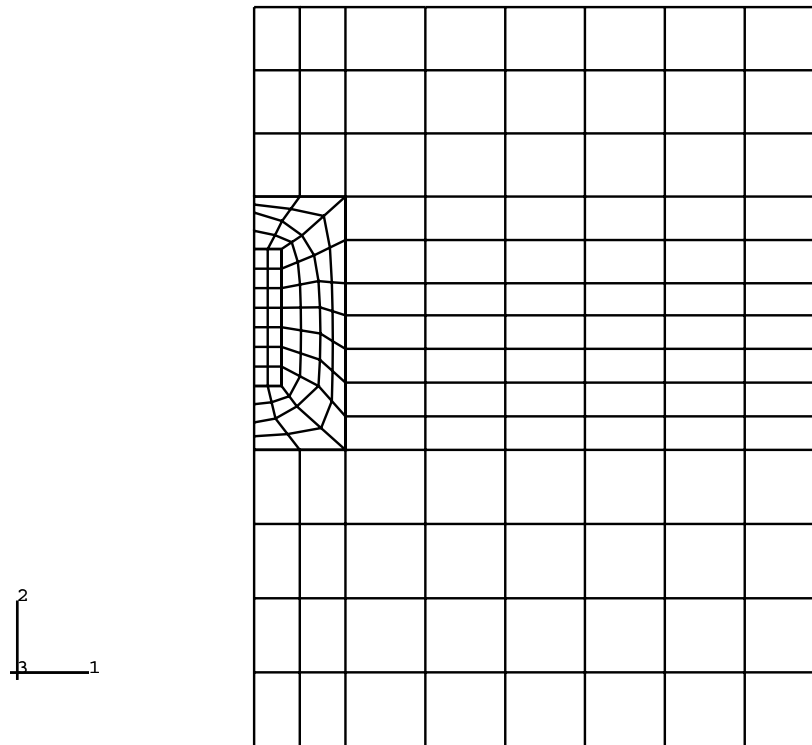
The *MODEL CHANGE option provides a convenient way of modeling the addition and/or removal of elements.

In this section, we present an example of such a problem.

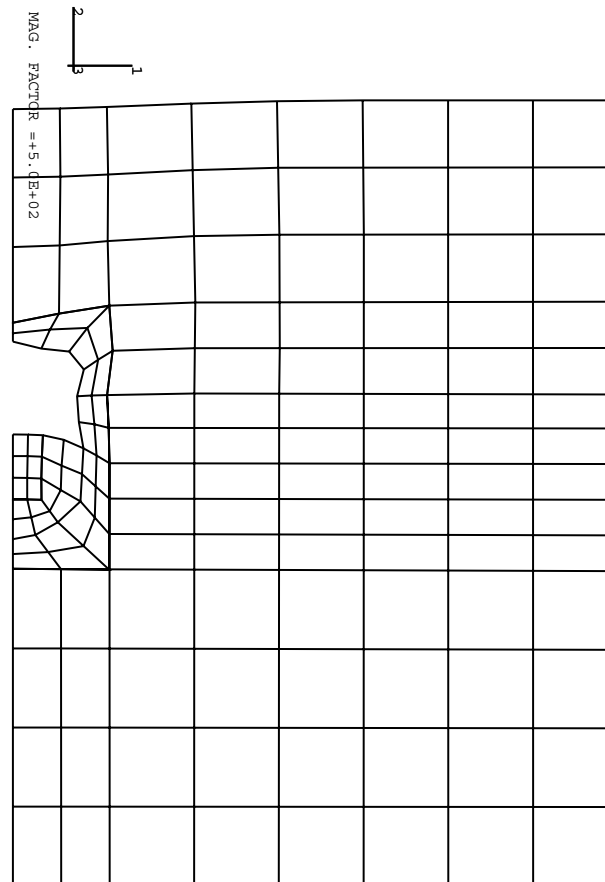
Tunneling Problem

This tunneling example was provided by Sauer Corporation. It deals with the sequential excavation of a tunnel designed according to the principles of the New Austrian Tunneling Method. The excavation is done in steps and shotcrete is used as the initial liner. The problem geometry given in the first figure shows the cross-section of a tunnel (shaded area) to be excavated in layered rock. The tunnel is to be lined with shotcrete and some concrete is to be cast at the bottom of the tunnel after excavation. The finite element model is quite coarse (164 CPE4 rock and concrete elements and 15 B21 lining elements) and serves only for illustration purposes. The rock is modeled with the modified Drucker-Prager model where the elastic properties are made dependent on a predefined field variable so that the stiffness can be degraded during the excavation process as called for in the design procedure. The concrete and the shotcrete are modeled as linear elastic.

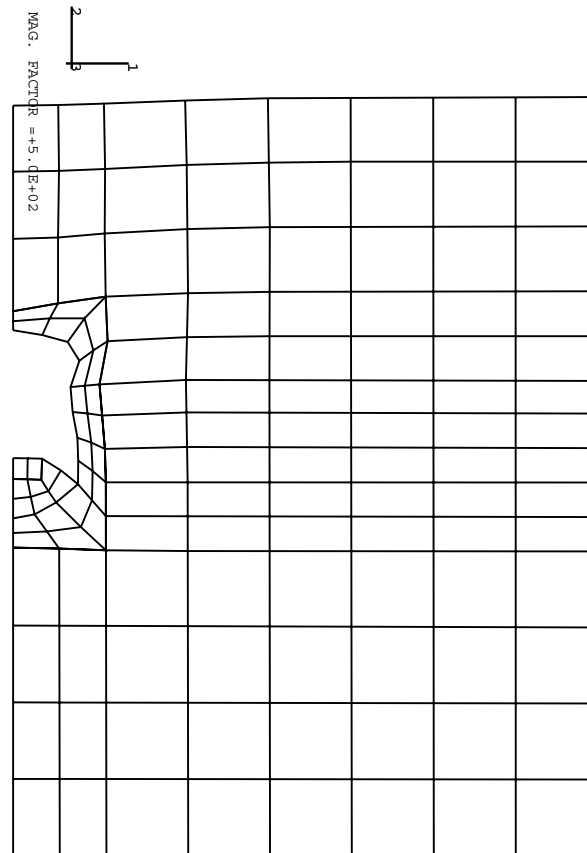
In the first step of analysis we remove the lining elements (*MODEL CHANGE, REMOVE) since they have to be included in the original mesh but are not in place at the start of the operation. In the second step we apply the gravity loads that equilibrate the virgin stress state in the rock—this causes no deformation. In Step 3 we degrade the stiffness of the top heading of the tunnel, which is excavated in Step 4 by removing the corresponding elements. In Step 4 we also activate (strain free) the shotcrete lining elements on the excavated surface (*MODEL CHANGE, ADD=STRAIN FREE). Steps 5–8 are repetitions of the previous sequence, leading to the excavation of the bench and invert parts of the tunnel and their respective lining. Finally, in Step 9 concrete is cast in place at the bottom of the tunnel.



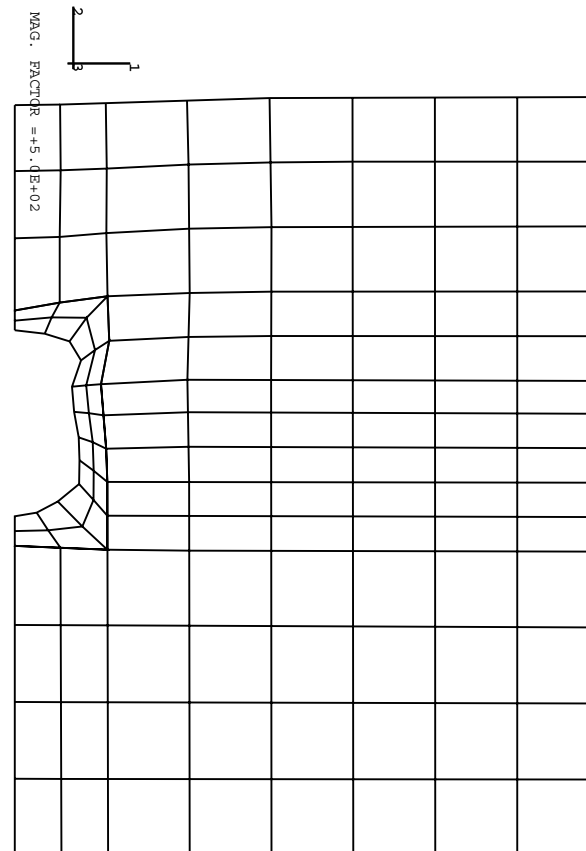
Finite Element Model



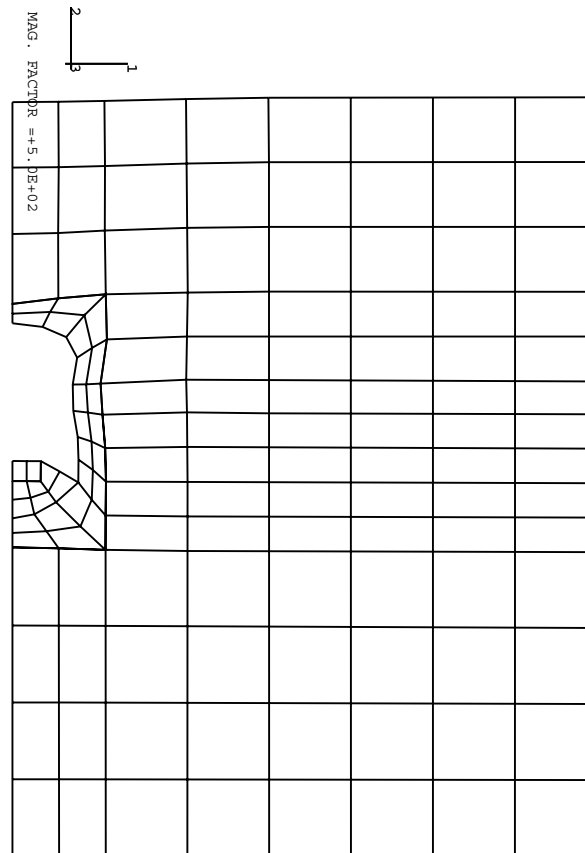
Displacement After Top Heading Excavation/Lining



Displacement After Bench Excavation/Lining



Displacement After Invert Excavation/Lining



Final Displacement After Concrete Casting

Tunneling Problem Input File:

```
*HEADING
COARSE MESH OF TEST TUNNEL, CPE4, COMPLETE SIMULATION
*NODE
1,0.,32.4
3,4.,32.4
9,25.,32.4
31,0.,24.1
33,4.,24.1
39,25.,24.1
101,0.,13.
103,4.,13.
109,25.,13.
141,0.,0.
143,4.,0.
149,25.,0.
53,4.,20.3
59,25.,20.3
63,4.,18.9
69,25.,18.9
```

```
*NGEN,NSET=LTOP
1,31,10
*NGEN,NSET=MTOP
3,33,10
*NGEN,NSET=LBOT
101,141,10
*NGEN,NSET=MBOT
103,143,10
*NGEN,NSET=MCEN
33,53,10
63,103,10
*NGEN,NSET=RTOP
9,39,10
*NGEN,NSET=RCEN
39,59,10
69,109,10
*NGEN,NSET=RBOT
109,149,10
*NFILL,NSET=TOP
LTOP,MTOP,2
MTOP,RTOP,6
*NFILL,NSET=CEN
MCEN,RCEN,6
```

```
*NFILL,NSET=BOT
LBOT,MBOT,2
MBOT,RBOT,6
*ELEMENT,TYPE=CPE4
1,11,12,2,1
33,43,44,34,33
101,111,112,102,101
*ELGEN,ELSET=OUTERE
1,8,1,1,3,10,10
33,6,1,1,7,10,10
101,8,1,1,4,10,10
***
*NODE
205,0.,24.1
225,4.,24.1
245,4.,20.3
255,4.,18.9
315,0.,13.
295,4.,13.
201,0.,21.8
```

```
221,1.2,21.8
291,1.2,15.8
311,0.,15.8
203,0.,23.4
243,2.816,20.4
283,2.816,15.8
313,0.,14.2
*NGEN,NSET=MIDOUT
205,225,10
225,245,10
255,295,10
295,315,10
*NGEN,NSET=MIDIN
201,221,10
221,291,10
291,311,10
*NGEN,NSET=MIDMID,LINE=P
203,243,10,,2.1,22.4,0.
243,283,10,,2.9,18.1,0.
283,313,10,,1.408,14.6,0.
*NFILL,NSET=TUNBOU
MIDIN,MIDMID,2
MIDMID,MIDOUT,2
```



```
*ELEMENT, TYPE=CPE4
201,211,212,202,201
*ELGEN, ELSET=MIDE
201,4,1,1,11,10,10
***
*NODE
401,0.,21.8
403,1.2,21.8
471,0.,15.8
473,1.2,15.8
*NGEN
401,471,10
403,473,10
401,403,1
471,473,1
402,472,10
*ELEMENT, TYPE=CPE4
401,411,412,402,401
*ELGEN, ELSET=CENE
401,2,1,1,7,10,10
**
**-----DEFINITIONS LINING ELEMENTS-----
**
```

```
*ELEMENT, TYPE=B21
1001, 203, 213
1002, 213, 223
1003, 223, 233
1004, 233, 243
1005, 243, 253
1006, 253, 263
2001, 263, 273
2002, 273, 283
3001, 283, 293
3002, 293, 303
3003, 303, 313
**
**-----DEFINITIONS OF ELSETS FOR HISTORY-----
**
*ELSET, ELSET=MT11, GENERATE
101, 138, 1
*ELSET, ELSET=MT12, GENERATE
63, 98, 1
*ELSET, ELSET=MT13
253, 254, 263, 264, 273, 274, 283, 284, 293, 294, 303, 304
```



```
*ELSET,ELSET=MAT1
MT11,MT12,MT13
**
*ELSET,ELSET=MT21,GENERATE
53,58,1
*ELSET,ELSET=MT22
243,244
*ELSET,ELSET=MAT2
MT21,MT22
**
*ELSET,ELSET=MT31,GENERATE
33,38,1
*ELSET,ELSET=MT32,GENERATE
43,48,1
*ELSET,ELSET=MT33
203,204,213,214,223,224,233,234
*ELSET,ELSET=MAT3
MT31,MT32,MT33
**
*ELSET,ELSET=MAT4,GENERATE
1,28,1
**
```

```
*ELSET,ELSET=TOPH1
202,212,222,232,201,211,221,231,401,402,411,412
**
*ELSET,ELSET=TOPH2
421,422,241,242
**
*ELSET,ELSET=TOPH3
431,432,251,252
**
*ELSET,ELSET=BENCH
441,442,451,452,261,262,271,272
**
*ELSET,ELSET=INVER
461,462,281,282,291,292,301,302
**
*ELCOPY,OLDSET=INVER,NEWSET=CINV,ELEMENT SHIFT=10000,SHIFT
NODES=0
**
*ELSET,ELSET=M3TH1
MAT3,TOPH1
*ELSET,ELSET=M2TH2
MAT2,TOPH2
```

```
*ELSET,ELSET=M1TBI
MAT1, TOPH3, BENCH, INVER
**
*ELSET,ELSET=SHHEA, GENERATE
1001,1006,1
*ELSET,ELSET=SHBEN
2001,2002
*ELSET,ELSET=SHINV
3001,3002,3003
*ELSET,ELSET=ALLSH
SHHEA, SHBEN, SHINV
**
*ELCOPY, OLDSET=SHHEA, NEWSET=CLIN1, ELEMENT SHIFT=1000, SHIFT
NODES=0
*ELCOPY, OLDSET=SHBEN, NEWSET=CLIN2, ELEMENT SHIFT=1000, SHIFT
NODES=0
*ELSET,ELSET=CLIN
CLIN1, CLIN2
*ELSET,ELSET=CLIN36, GEN
2003,2006,1
**
*ELSET,ELSET=ALGEO
MAT4, M3TH1, M2TH2, M1TBI
```

```
*ELSET,ELSET=ALLEL,GENERATE
1,500,1
**
**-----DEFINITION OF NODESETS FOR TEMP AND BOUND-----
**
*NSET,NSET=SYMM1
1,11,21,111,121,131,141,205,204,203,202,401,411
*NSET,NSET=SYMM2
421,431,441,451,461,471,312,313,314,315
*NSET,NSET=SYMM
SYMM1,SYMM2
*NSET,NSET=BOTT,GENERATE
141,149,1
*NSET,NSET=EDGE,GENERATE
9,149,10
*NSET,NSET=ALNOD,GENERATE
1,1000,1
**
**-----DEFINITIONS MATERIAL PROPERTIES-----
**
**-----MATERIAL 1-----
**
```

```
*SOLID SECTION,ELSET=MAT1,MATERIAL=M1
*MATERIAL,NAME=M1
*ELASTIC,TYPE=ISOTROPIC
2414.,.27
*DRUCKER PRAGER
54.82, 1, 54.82
*DRUCKER PRAGER HARDENING
2.15
*DENSITY
.0247
**
**-----MATERIAL 2-----
**
*SOLID SECTION,ELSET=MAT2,MATERIAL=M2
*MATERIAL,NAME=M2
*ELASTIC,TYPE=ISOTROPIC
690.,.30
*DRUCKER PRAGER
50.19, 1, 50.19
*DRUCKER PRAGER HARDENING
1.
*DENSITY
.021
```

```
**
**-----MATERIAL 3-----
**
*SOLID SECTION,ELSET=MAT3,MATERIAL=M3
*MATERIAL,NAME=M3
*ELASTIC,TYPE=ISOTROPIC
60.,.325
*DRUCKER PRAGER
44.53, 1, 44.53
*DRUCKER PRAGER HARDENING
.146
*DENSITY
.019
**
**-----MATERIAL 4-----
**
*SOLID SECTION,ELSET=MAT4,MATERIAL=M4
*MATERIAL,NAME=M4
*ELASTIC,TYPE=ISOTROPIC
60.,.375
*DRUCKER PRAGER
43.26, 1, 43.26
*DRUCKER PRAGER HARDENING
.205
*DENSITY
.019
```

```
**
**-----MATERIAL MTOPH1-----
**
*SOLID SECTION,ELSET=TOPH1,MATERIAL=MTOPH1
*MATERIAL,NAME=MTOPH1
*ELASTIC,TYPE=ISOTROPIC
60.,.325,0.
24.,.325,1.
24.,.325,8.
*DRUCKER PRAGER
44.53, 1, 44.53
*DRUCKER PRAGER HARDENING
.146
*DENSITY
.019
**
**-----MATERIAL MTOPH2-----
**
*SOLID SECTION,ELSET=TOPH2,MATERIAL=MTOPH2
*MATERIAL,NAME=MTOPH2
*ELASTIC,TYPE=ISOTROPIC
690.,.3,0.
276.,.3,1.
276.,.3,8.
```

```
*DRUCKER PRAGER
50.19, 1, 50.19
*DRUCKER PRAGER HARDENING
1.
*DENSITY
.021
**
**-----MATERIAL MTOPH3-----
**
*SOLID SECTION,ELSET=TOPH3,MATERIAL=MTOPH3
*MATERIAL,NAME=MTOPH3
*ELASTIC,TYPE=ISOTROPIC
2414.,.27,0.
965.6,.27,1.
965.6,.27,8.
*DRUCKER PRAGER
54.82, 1, 54.82
*DRUCKER PRAGER HARDENING
.464
*DENSITY
.0247
```



```
**
**-----MATERIAL MBENCH-----
**
*SOLID SECTION,ELSET=BENCH,MATERIAL=MBENCH
*MATERIAL,NAME=MBENCH
*ELASTIC,TYPE=ISOTROPIC
2414.,.27,0.
2414.,.27,1.
965.6,.27,2.
965.6,.27,8.
*DRUCKER PRAGER
54.82, 1, 54.82
*DRUCKER PRAGER HARDENING
.464
*DENSITY
.0247
```

```
**
**-----MATERIAL MINVER-----
**
*SOLID SECTION,ELSET=INVER,MATERIAL=MINVER
*MATERIAL,NAME=MINVER
*ELASTIC,TYPE=ISOTROPIC
2414.,.27,0.
2414.,.27,2.
965.6,.27,3.
965.6,.27,8.
*DRUCKER PRAGER
54.82, 1, 54.82
*DRUCKER PRAGER HARDENING
.464
*DENSITY
.0247
**
```

```
**-----MATERIAL SHOTCRETE-----  
**  
*BEAM SECTION,SECTION=RECT,ELSET=ALLSH,MATERIAL=SHOCR  
1.,.2  
*MATERIAL,NAME=SHOCR  
*ELASTIC,TYPE=ISOTROPIC  
15000.,.17  
*DENSITY  
.025  
**  
**-----MATERIAL CONCRETE-----  
**  
*BEAM SECTION,SECTION=RECT,ELSET=CLIN,MATERIAL=CONCR  
1.,.2  
*SOLID SECTION,ELSET=CINV,MATERIAL=CONCR  
*MATERIAL,NAME=CONCR  
*ELASTIC,TYPE=ISOTROPIC  
27000.,.17  
*DENSITY  
.025  
*SOLID SECTION,ELSET=CINV,MATERIAL=CONCR
```

```
**-----MPCS AND BOUNDARY-----  
*MPC  
TIE,201,401  
TIE,211,402  
TIE,221,403  
TIE,231,413  
TIE,241,423  
TIE,251,433  
TIE,261,443  
TIE,271,453  
TIE,281,463  
TIE,291,473  
TIE,301,472  
TIE,311,471  
***  
TIE,31,205  
TIE,32,215  
TIE,33,225  
TIE,43,235  
TIE,53,245  
TIE,63,255  
TIE,73,265  
TIE,83,275
```

```
TIE,93,285
TIE,103,295
TIE,102,305
TIE,101,315
**
*BOUNDARY
SYMM,1
BOTT,2
EDGE,1
202,6
313,6
**
**-----HISTORY-----
**
*RESTART, WRITE, FREQUENCY=5
*INITIAL CONDITIONS, TYPE=STRESS, GEOSTATIC
MAT4,0.,32.4,-.1589,24.1,.8
M3TH1,-.1589,24.1,-.2313,20.3,.45
M2TH2,-.2313,20.3,-.26,18.9,.45
M1TBI,-.26,18.9,-.727,0.0,.4
**
*INITIAL CONDITIONS,TYPE=TEMPERATURE
ALNOD,0.
**
```

```
**----- REMOVE ALL LINING ELEMENTS -----  
**  
*STEP, AMPLITUDE=RAMP  
*STATIC  
*MODEL CHANGE, REMOVE  
ALLSH,CLIN,CINV  
*END STEP  
**  
**----- GRAVITY LOADING -----  
**  
*STEP, AMPLITUDE=RAMP  
*STATIC  
*DLOAD  
ALLEL, GRAV, 1., , -1.  
*EL PRINT, FREQUENCY=10  
S, MISES, PRESS  
E  
PE  
*NODE PRINT, FREQUENCY=10  
U  
RF  
*END STEP
```

```
**-----EXCAVATION TOPHEADING ( 1 / 2.5 )-----  
**  
*STEP, AMPLITUDE=RAMP  
*STATIC  
*TEMPERATURE  
ALNOD,1.  
*END STEP  
**-----SHOTCRETE TOP HEADING -----  
**  
*STEP, AMPLITUDE=RAMP  
*STATIC  
*TEMPERATURE  
ALNOD,1.  
*MODEL CHANGE,ADD=STRAIN FREE  
SHHEA  
*EL PRINT,FREQUENCY=10  
S,MISES,PRESS  
E  
PE  
SF  
*END STEP  
**
```

```
*STEP, AMPLITUDE=RAMP
*STATIC
*TEMPERATURE
ALNOD,1.
*MODEL CHANGE,REMOVE
TOPH1,TOPH2,TOPH3
*END STEP
**-----EXCAVATION BENCH ( 1 / 2.5 )-----
**
*STEP, AMPLITUDE=RAMP
*STATIC
*TEMPERATURE
ALNOD,2.
*END STEP
**-----SHOTCRETE BENCH -----
*STEP, AMPLITUDE=RAMP
*STATIC
*TEMPERATURE
ALNOD,2.
*MODEL CHANGE,ADD=STRAIN FREE
SHBEN
*END STEP
```



```
*STEP, AMPLITUDE=RAMP
*STATIC
*TEMPERATURE
ALNOD, 2.
*MODEL CHANGE, REMOVE
BENCH
*END STEP
**-----EXCAVATION INVERT ( 1 / 2.5 )-----
**
*STEP, AMPLITUDE=RAMP
*STATIC
*TEMPERATURE
ALNOD, 3.
*END STEP
**-----SHOTCRETE INVERT -----
*STEP, AMPLITUDE=RAMP
*STATIC
*TEMPERATURE
ALNOD, 3.
*MODEL CHANGE, ADD=STRAIN FREE
SHINV
*END STEP
```

```
*STEP, AMPLITUDE=RAMP
*STATIC
*TEMPERATURE
ALNOD, 3.
*MODEL CHANGE, REMOVE
INVER
*END STEP
**
**-----CAST IN PLACE CONCRETE -----
**
*STEP, AMPLITUDE=RAMP
*STATIC
*TEMPERATURE
ALNOD, 3.
*MODEL CHANGE, ADD=STRAIN FREE
CLIN36, CINV
*END STEP
```

Note that the last step does not change the results from the previous step; its presence, however, would impact subsequent steps.

Appendix A

Stress Equilibrium and Fluid Continuity Equations

To study the different couplings and nonlinearities of the coupled problem, we can write the resulting Newton equations at a node as

$$\begin{bmatrix} \mathbf{K}_{dd} & \mathbf{K}_{du} \\ \mathbf{K}_{ud} & K_{uu} \end{bmatrix} \begin{bmatrix} \mathbf{d}_c \\ u_c \end{bmatrix} = \begin{bmatrix} \mathbf{F}_r \\ \Delta V_r \end{bmatrix}$$

where \mathbf{d}_c represents the vector of displacement corrections, \mathbf{F}_r are the force residuals conjugate to the displacements, u_c is the pore pressure correction, and ΔV_r is the residual change in fluid volume over the time increment conjugate to the pore pressure.

Special cases of the fully and partly saturated problems are presented in the following sections.

Fully Saturated Fluid Flow

\mathbf{K}_{dd} , \mathbf{K}_{du} , \mathbf{K}_{ud} , \mathbf{K}_{uu} have the following components:

$$\mathbf{K}_{dd} = \mathbf{K}_s(\bar{\sigma}, \mathbf{d}) + \mathbf{L}(\mathbf{d}, \mathbf{u}) + \mathbf{K}_{gd}(\mathbf{d})$$

$$\mathbf{K}_s = \int_V \beta : \bar{\mathbf{D}} : \beta \, dV$$

$$\mathbf{L} = - \int_V \beta : \mathbf{I} \, \mathbf{u} \, \mathbf{I} : \beta \, dV$$

$$\mathbf{K}_{gd} = - \int_V \mathbf{N} : \mathbf{g} \, f_1 \, \mathbf{I} : \beta \, dV$$

$$\mathbf{K}_{du} = \mathbf{B}(\mathbf{d}) + \mathbf{K}_{sg}(\bar{\sigma}, \mathbf{d})$$

$$\mathbf{B} = - \int_V \beta : \mathbf{I} \, dV$$

$$\mathbf{K}_{sg} = \int_V \frac{1}{3K_g} \beta : \bar{\mathbf{D}} : \mathbf{I} \, dV$$

$$\mathbf{K}_{ud} = \mathbf{B}^T(\mathbf{d}) + \mathbf{K}_{sg}^T(\bar{\boldsymbol{\sigma}}, \mathbf{d}) + \Delta t \mathbf{L}_c(\mathbf{d}, \mathbf{e}) + \Delta t \mathbf{k}_{ec}(\bar{\boldsymbol{\sigma}}, \mathbf{d}, \mathbf{e})$$

$$\mathbf{B}^T = - \int_V \mathbf{I} : \beta \, dV$$

$$\mathbf{K}_{sg}^T = \int_V \frac{1}{3K_g} \mathbf{I} : \bar{\mathbf{D}} : \beta \, dV$$

$$\mathbf{L}_c = - \int_V \frac{\partial \delta u}{\partial \mathbf{x}} \cdot \mathbf{k}^* \cdot \left(\frac{\partial u}{\partial \mathbf{x}} - \rho_w \mathbf{g} \right) \mathbf{I} : \beta \, dV$$

$$\mathbf{k}_{ec} = \int_V \frac{\partial \delta u}{\partial \mathbf{x}} \cdot \frac{d\mathbf{k}^*}{de} \cdot \left(\frac{\partial u}{\partial \mathbf{x}} - \rho_w \mathbf{g} \right) \frac{1}{(1-n)^2} \left[\frac{\mathbf{I} : \bar{\mathbf{D}}}{3K_g} - \frac{1-n^0}{JK_g} \mathbf{I} \right] : \beta \, dV$$

$$K_{uu} = \Delta t k(\mathbf{d}, e) + K_{sg}^*(\bar{\boldsymbol{\sigma}}) + K_g^*(\mathbf{d}) + K_w^*(\mathbf{d}) + \Delta t k_e(\bar{\boldsymbol{\sigma}}, \mathbf{d}, e)$$

$$k = - \int_V \frac{\partial \delta u}{\partial \mathbf{x}} \cdot \mathbf{k}^* \cdot \frac{\partial u}{\partial \mathbf{x}} dV$$

$$K_{sg}^* = \int_V \frac{1}{9K_g^2} \mathbf{I} : \bar{\mathbf{D}} : \mathbf{I} dV$$

$$K_g^* = - \int_V \frac{1 - n^0}{J K_g} dV$$

$$K_w^* = \int_V \frac{1 - n^0}{J K_w} - \frac{1}{K_w} dV$$

$$k_e = \int_V \frac{\partial \delta u}{\partial \mathbf{x}} \cdot \frac{d\mathbf{k}^*}{de} \cdot \left(\frac{\partial u}{\partial \mathbf{x}} - \rho_w \mathbf{g} \right) \frac{1}{(1 - n)^2} \left[\frac{\mathbf{I} : \bar{\mathbf{D}} : \mathbf{I}}{9K_g^2} - \frac{1 - n^0}{J K_g} \right] dV$$

where β is the strain-displacement matrix, $\bar{\mathbf{D}}$ is the constitutive matrix, \mathbf{N} is the interpolator, K_g and K_w are the solid grains and fluid bulk moduli.

Special Cases

To facilitate the understanding of the coupled equations, let us consider some special cases of the **transient** problem *without fluid gravity* effects:

- Linear material, small strain, incompressible grains and fluid, constant permeability:

$$\begin{bmatrix} \mathbf{K}_s & \mathbf{B} \\ \mathbf{B}^T & \Delta t \mathbf{k} \end{bmatrix}$$

where \mathbf{K}_s is the usual stress stiffness; \mathbf{B} , \mathbf{B}^T are the stress/pore pressure coupling terms; and $\Delta t \mathbf{k}$ is the porous medium permeability term. The resulting system of equations is linear and symmetric.

- Nonlinear material, large strain, incompressible grains and fluid, nonlinear permeability:

$$\begin{bmatrix} \mathbf{K}_s(\bar{\sigma}, \mathbf{d}) + \mathbf{L}(\mathbf{d}, \mathbf{u}) & \mathbf{B}(\mathbf{d}) \\ \mathbf{B}^T(\mathbf{d}) + \Delta t \mathbf{L}_c(\mathbf{d}, \mathbf{e}) & \Delta t k(\mathbf{d}, \mathbf{e}) \end{bmatrix}$$

where $\mathbf{K}_s(\bar{\sigma}, \mathbf{d})$ is the stress stiffness term with material and geometric nonlinearities; $\mathbf{L}(\mathbf{d}, \mathbf{u})$ is a large volume change term; $\mathbf{B}(\mathbf{d})$, $\mathbf{B}^T(\mathbf{d})$ are the stress/pore pressure coupling terms with geometric nonlinearity; $\Delta t \mathbf{L}_c(\mathbf{d}, \mathbf{e})$ is a large-strain coupling term with nonlinear permeability; and $\Delta t k(\mathbf{d}, \mathbf{e})$ is the permeability term with geometric and permeability nonlinearities. The problem now becomes nonlinear and unsymmetric. The loss of symmetry is due to the inclusion of finite strains.

- Linear material, small strain, compressible grains and fluid, constant permeability:

$$\begin{bmatrix} \mathbf{K}_S & \mathbf{B} + \mathbf{K}_{sg} \\ \mathbf{B}^T + \mathbf{K}_{sg}^T & \Delta t \, k + \mathbf{K}_{sg}^* + \mathbf{K}_g^* + \mathbf{K}_w^* \end{bmatrix}$$

where \mathbf{K}_S is the usual stress stiffness; \mathbf{B} , \mathbf{B}^T are the stress/pore pressure coupling terms; \mathbf{K}_{sg} , \mathbf{K}_{sg}^T , \mathbf{K}_{sg}^* , \mathbf{K}_g^* are grain compressibility terms; \mathbf{K}_w^* is a fluid compressibility term; and $\Delta t \, k$ is the porous medium permeability term. The resulting system of equations is linear and symmetric.

- Nonlinear material, large strain, compressible grains and fluid, nonlinear permeability:

$$\left[\begin{array}{c|c} \mathbf{K}_s(\bar{\sigma}, \mathbf{d}) + \mathbf{L}(\mathbf{d}, \mathbf{u}) & \mathbf{B}(\mathbf{d}) + \mathbf{K}_{sg}(\bar{\sigma}, \mathbf{d}) \\ \hline \mathbf{B}^T(\mathbf{d}) + \mathbf{K}_{sg}^T(\bar{\sigma}, \mathbf{d}) + \Delta t \mathbf{L}_C(\mathbf{d}, \mathbf{e}) + \Delta t \mathbf{k}_{ec}(\bar{\sigma}, \mathbf{d}, \mathbf{e}) & \Delta t \mathbf{k}(\mathbf{d}, \mathbf{e}) + \mathbf{K}_{sg}^*(\bar{\sigma}) + \mathbf{K}_g^*(\mathbf{d}) + \mathbf{K}_w^*(\mathbf{d}) + \Delta t \mathbf{k}_e(\bar{\sigma}, \mathbf{d}, \mathbf{e}) \end{array} \right]$$

where $\Delta t \mathbf{k}_{ec}(\bar{\sigma}, \mathbf{d}, \mathbf{e})$, $\Delta t \mathbf{k}_e(\bar{\sigma}, \mathbf{d}, \mathbf{e})$ are additional nonlinear grain compressibility terms with large-strain effects. This most general problem is nonlinear and unsymmetric. The loss of symmetry is now due to two reasons: finite strains and nonlinear permeability.

Consider now the **steady-state** problem *without fluid gravity* effects. In its simplest case (linear material, small strain, incompressible grains and fluid, constant permeability), it is only one way coupled:

$$\begin{bmatrix} \mathbf{K}_s & \mathbf{B} \\ \mathbf{0} & \mathbf{k} \end{bmatrix}$$

The equations are clearly unsymmetric.

The steady-state problem becomes fully coupled if large strains and/or nonlinear permeability are considered. However, the equations retain their unsymmetric characteristic for these cases.

In ABAQUS the steady-state equations are always solved directly in the coupled form for all cases.

The porous media coupled analysis capability can provide solutions either in terms of total or of *excess* pore pressure. The excess pore pressure at a point is the pore pressure in excess of the hydrostatic pressure required to support the weight of pore fluid above the elevation of the material point.

[Total pore pressure solutions are provided when the GRAV distributed load type is used to define the gravity load on the model. Excess pore pressure solutions are provided in all other cases (for example, when gravity loading is defined with distributed load types BX, BY, or BZ)].

One important aspect arising from the inclusion of pore fluid gravity (in total pore pressure analyses) is that it generates a Newton method Jacobian term that is always unsymmetric:

$$\mathbf{K}_{gd} = - \int_V \mathbf{N} : \mathbf{g} f_1 \mathbf{I} : \beta \, dV. (\mathbf{K}_{dd})$$

Partially Saturated Fluid Flow

\mathbf{K}_{dd} , \mathbf{K}_{du} , \mathbf{K}_{ud} , \mathbf{K}_{uu} have the following components:

$$\mathbf{K}_{dd} = \mathbf{K}_s(\bar{\sigma}, \mathbf{d}) + \mathbf{L}(\mathbf{d}, u) + \mathbf{K}_{gd}(\mathbf{d})$$

$$\mathbf{K}_s = \int_V \beta : \bar{\mathbf{D}} : \beta \, dV$$

$$\mathbf{L} = - \int_V \beta : \mathbf{I} \, s u \, \mathbf{I} : \beta \, dV$$

$$\mathbf{K}_{gd} = - \int_V \mathbf{N} : \mathbf{g} \, s f_1 \, \mathbf{I} : \beta \, dV$$

$$\mathbf{K}_{du} = \mathbf{B}(\mathbf{d}) + \mathbf{B}_s(\mathbf{d}, u) + \mathbf{K}_{sg}(\bar{\sigma}, \mathbf{d}) + \mathbf{K}_{sgs}(\bar{\sigma}, \mathbf{d}, u) + \mathbf{K}_{gu}(\mathbf{d})$$

$$\mathbf{B} = - \int_V s \, \beta : \mathbf{I} \, dV$$

$$\mathbf{B}_s = - \int_V u \frac{ds}{du} \boldsymbol{\beta} : \mathbf{I} dV$$

$$\mathbf{K}_{sg} = \int_V \frac{s}{3K_g} \boldsymbol{\beta} : \bar{\mathbf{D}} : \mathbf{I} dV$$

$$\mathbf{K}_{sgs} = \int_V \frac{u}{3K_g} \frac{ds}{du} \boldsymbol{\beta} : \bar{\mathbf{D}} : \mathbf{I} dV$$

$$\mathbf{K}_{gu} = - \int_V \mathbf{N} : \mathbf{g} f_2 \frac{ds}{du} dV$$

$$\mathbf{K}_{ud} = \mathbf{B}^T(\mathbf{d}) + \mathbf{K}_{sg}^T(\bar{\boldsymbol{\sigma}}, \mathbf{d}) + \Delta t \mathbf{L}_c(\mathbf{d}, \mathbf{e}) + \Delta t \mathbf{k}_{ec}(\bar{\boldsymbol{\sigma}}, \mathbf{d}, \mathbf{e})$$

$$\mathbf{B}^T = - \int_V s \mathbf{I} : \boldsymbol{\beta} dV$$

$$\mathbf{K}_{sg}^T = \int_V \frac{s}{3K_g} \mathbf{I} : \bar{\mathbf{D}} : \beta \, dV$$

$$\mathbf{L}_c = - \int_V s \frac{\partial \delta u}{\partial \mathbf{x}} \cdot \mathbf{k}^* \cdot \left(\frac{\partial u}{\partial \mathbf{x}} - \rho_w \mathbf{g} \right) \mathbf{I} : \beta \, dV$$

$$\mathbf{k}_{ec} = \int_V \frac{\partial \delta u}{\partial \mathbf{x}} \cdot \frac{d\mathbf{k}^*}{de} \cdot \left(\frac{\partial u}{\partial \mathbf{x}} - \rho_w \mathbf{g} \right) \frac{s}{(1-n)^2} \left[\frac{\mathbf{I} : \bar{\mathbf{D}}}{3K_g} - \frac{1-n^0}{JK_g} \mathbf{I} \right] : \beta \, dV$$

$$K_{uu} = \Delta t k(\mathbf{d}, e) + K_{sg}^*(\bar{\sigma}) + K_g^*(\mathbf{d}) + K_w^*(\mathbf{d}) + K_s^*(\mathbf{d})$$

$$+ \Delta t k_e(\bar{\sigma}, \mathbf{d}, e) + \Delta t k_{es}(\mathbf{d}, e)$$

$$k = - \int_V s \frac{\partial \delta u}{\partial \mathbf{x}} \cdot \mathbf{k}^* \cdot \frac{\partial u}{\partial \mathbf{x}} \, dV$$

$$K_{sg}^* = \int_V \frac{s}{9K_g^2} \mathbf{I} : \bar{\mathbf{D}} : \mathbf{I} \, dV$$

$$K_g^* = - \int_V s \frac{1 - n^0}{J K_g} dV$$

$$K_w^* = \int_V s \left(\frac{1 - n^0}{J K_w} - \frac{1}{K_w} \right) dV$$

$$K_s^* = - \int_V \frac{ds}{du} \left(1 - \frac{1 - n^0}{J} \right) dV$$

$$k_e = \int_V \frac{\partial \delta u}{\partial \mathbf{x}} \cdot \frac{d\mathbf{k}^*}{de} \cdot \left(\frac{\partial u}{\partial \mathbf{x}} - \rho_w \mathbf{g} \right) \frac{s}{(1 - n)^2} \left[\frac{\mathbf{I} : \bar{\mathbf{D}} : \mathbf{I}}{9 K_g^2} - \frac{1 - n^0}{J K_g} \right] dV$$

$$k_{es} = - \int_V \frac{s}{k_s} \frac{ds}{du} \frac{\partial \delta u}{\partial \mathbf{x}} \cdot \mathbf{k}^* \cdot \left(\frac{\partial u}{\partial \mathbf{x}} - \rho_w \mathbf{g} \right) dV$$

where β is the strain-displacement matrix, $\bar{\mathbf{D}}$ is the constitutive matrix, \mathbf{N} is the interpolator, K_g and K_w are the solid grains and fluid bulk moduli.

Special Cases

To facilitate the understanding of the coupled equations, let us consider some special cases of the **transient** problem *without fluid gravity* effects:

- Linear material, small strain, incompressible grains and fluid, constant permeability:

$$\begin{bmatrix} \mathbf{K}_s & \mathbf{B} + \mathbf{B}_s \\ \mathbf{B}^T & \Delta t \, k + \Delta t \, k_{es} + K_s^* \end{bmatrix}$$

where \mathbf{K}_s is the usual stress stiffness; \mathbf{B} , \mathbf{B}^T are stress/pore pressure coupling terms; \mathbf{B}_s is a partially saturated coupling term; $\Delta t \, k$ is the permeability term; and $\Delta t \, k_{es}$, K_s^* are partially saturated permeability terms.

The resulting system of equations is unsymmetric.

- Nonlinear material, large strain, incompressible grains and fluid, nonlinear permeability:

$$\left[\begin{array}{c|c} \mathbf{K}_s(\bar{\sigma}, \mathbf{d}) + \mathbf{L}(\mathbf{d}, \mathbf{u}) & \mathbf{B}(\mathbf{d}) + \mathbf{B}_s(\mathbf{d}, \mathbf{u}) \\ \hline \mathbf{B}^T(\mathbf{d}) + \Delta t \mathbf{L}_c(\mathbf{d}, \mathbf{e}) & \Delta t k(\mathbf{d}, \mathbf{e}) + \Delta t k_{es}(\mathbf{d}, \mathbf{e}) + K_s^*(\mathbf{d}) \end{array} \right]$$

where $\mathbf{K}_s(\bar{\sigma}, \mathbf{d})$ is the stress stiffness term with material and geometric nonlinearities; $\mathbf{L}(\mathbf{d}, \mathbf{u})$ is a large volume change term; $\mathbf{B}(\mathbf{d})$, $\mathbf{B}^T(\mathbf{d})$ are coupling terms with geometric nonlinearity; $\mathbf{B}_s(\mathbf{d}, \mathbf{u})$ is a partially saturated coupling term with geometric nonlinearity; $\Delta t \mathbf{L}_c(\mathbf{d}, \mathbf{e})$ is a large-strain coupling term with nonlinear permeability; $\Delta t k(\mathbf{d}, \mathbf{e})$ is the permeability term with geometric and permeability nonlinearities; and $\Delta t k_{es}(\mathbf{d}, \mathbf{e})$, $K_s^*(\mathbf{d})$ are partially saturated permeability terms with geometric and permeability nonlinearities.

The problem remains unsymmetric.

- Linear material, small strain, compressible grains and fluid, constant permeability:

$$\begin{bmatrix} \mathbf{K}_s & \mathbf{B} + \mathbf{B}_s + \mathbf{K}_{sg} + \mathbf{K}_{sgs} \\ \mathbf{B}^T + \mathbf{K}_{sg}^T & \Delta t k + \Delta t k_{es} + \mathbf{K}_s^* + \mathbf{K}_{sg}^* + \mathbf{K}_g^* + \mathbf{K}_w^* \end{bmatrix}$$

where \mathbf{K}_s is the usual stress stiffness; \mathbf{B} , \mathbf{B}^T are stress/pore pressure coupling terms; \mathbf{B}_s is a partially saturated coupling term; \mathbf{K}_{sg} , \mathbf{K}_{sg}^T , \mathbf{K}_{sgs} , \mathbf{K}_{sg}^* , \mathbf{K}_g^* are grain compressibility terms; \mathbf{K}_w^* is a fluid compressibility term; $\Delta t k$ is the porous medium permeability term; and $\Delta t k_{es}$, \mathbf{K}_s^* are partially saturated permeability terms.

The resulting system of equations is unsymmetric.

- Nonlinear material, large strain, compressible grains and fluid, nonlinear permeability:

$$\begin{array}{c|c}
 \mathbf{K}_s(\bar{\sigma}, \mathbf{d}) + \mathbf{L}(\mathbf{d}, \mathbf{u}) & \mathbf{B}(\mathbf{d}) + \mathbf{B}_s(\mathbf{d}, \mathbf{u}) + \mathbf{K}_{sg}(\bar{\sigma}, \mathbf{d}) \\
 & + \mathbf{K}_{sgs}(\bar{\sigma}, \mathbf{d}, \mathbf{u}) \\
 \hline
 \mathbf{B}^T(\mathbf{d}) + \mathbf{K}_{sg}^T(\bar{\sigma}, \mathbf{d}) + \Delta t \mathbf{L}_C(\mathbf{d}, \mathbf{e}) & \Delta t k(\mathbf{d}, \mathbf{e}) + \Delta t k_{es}(\mathbf{d}, \mathbf{e}) \\
 + \Delta t \mathbf{k}_{ec}(\bar{\sigma}, \mathbf{d}, \mathbf{e}) & + K_s^*(\mathbf{d}) + K_{sg}^*(\bar{\sigma}) + K_g^*(\mathbf{d}) \\
 & + K_w^*(\mathbf{d}) + \Delta t k_e(\bar{\sigma}, \mathbf{d}, \mathbf{e})
 \end{array}$$

where $\Delta t \mathbf{k}_{ec}(\bar{\sigma}, \mathbf{d}, \mathbf{e})$, $\Delta t k_e(\bar{\sigma}, \mathbf{d}, \mathbf{e})$ are additional nonlinear grain compressibility terms with large-strain effects.

This most general problem is unsymmetric.

In conclusion, the transient partially saturated flow problem is always unsymmetric.

Consider now the **steady-state** problem *without fluid gravity* effects. In its simplest case (linear material, small strain, incompressible grains and fluid, constant permeability), it is only one way coupled:

$$\begin{bmatrix} \mathbf{K}_s & \mathbf{B} + \mathbf{B}_s \\ 0 & k + k_{es} \end{bmatrix}$$

The equations are unsymmetric.

The steady-state problem becomes fully coupled if large strains and/or nonlinear permeability are considered. The equations retain their unsymmetric characteristic for these cases.

In ABAQUS the steady-state equations are always solved directly in the coupled form for all cases.

The porous media coupled analysis capability can provide solutions either in terms of total or of *excess* pore pressure.

[Total pore pressure solutions are provided when the GRAV distributed load type is used to define the gravity load on the model. Excess pore pressure solutions are provided in all other cases (for example, when gravity loading is defined with distributed load types BX, BY, or BZ)].

One important aspect arising from the inclusion of pore fluid gravity (in total pore pressure analyses) is that it generates Newton method Jacobian terms that are always unsymmetric:

$$\mathbf{K}_{gd} = - \int_V \mathbf{N} : \mathbf{g} \, sf_1 \, \mathbf{I} : \beta \, dV \quad \text{in } \mathbf{K}_{dd}$$

$$\mathbf{K}_{gu} = - \int_V \mathbf{N} : \mathbf{g} \, f_2 \, \frac{ds}{du} \, dV \quad \text{in } \mathbf{K}_{du}$$

Appendix B

Bibliography of Geotechnical Example Problems

The following is a list of ABAQUS Example and Benchmark Problems that show the use of capabilities for geotechnical modeling:

Example problems:

- 1.1.6: Jointed rock slope stability
- 1.1.10: Stress-free element reactivation

- 8.1.1: Plane strain consolidation
- 8.1.2: Calculation of phreatic surface in an earth dam
- 8.1.3: Axisymmetric simulation of an oil well
- 8.1.4 Analysis of a pipeline buried in soil

Benchmark problems:

- 1.1.10: Concrete slump test

- 1.8.1: Partially saturated flow in porous media
- 1.8.2: Demand wettability of a porous medium: coupled analysis
- 1.8.3: Wicking in a partially saturated porous medium
- 1.8.4: Desaturation in a column of porous material

- 1.14.1: The Terzaghi consolidation problem
- 1.14.2: Consolidation of triaxial test specimen
- 1.14.3: Finite-strain consolidation of a two-dimensional solid
- 1.14.4: Limit load calculations with granular materials
- 1.14.5: Finite deformation of an elastic-plastic granular material

- 2.2.1: Wave propagation in an infinite medium
- 2.2.2: Infinite elements: the Boussinesq and Flamant problems
- 2.2.3: Infinite elements: circular load on half-space
- 2.2.4: Spherical cavity in an infinite medium

- 3.2.4: Triaxial tests on a saturated clay
- 3.2.5: Uniaxial tests on jointed material
- 3.2.6: Verification of creep integration